ABSTRACT

Title of Document: A SUBSET OF 3′ TO 5′ EXORIBONUCLEASES ARE THE PRIMARY ENZYMES RESPONSIBLE FOR THE DEGRADATION OF PGPG IN CYCLIC DI-GMP SIGNALING

Mona Wu Orr, Doctor of Philosophy, 2016

Directed By: Associate Professor Vincent T. Lee, Department of Cell Biology and Molecular Genetics

Bis-(3′-5′)-cyclic dimeric guanosine monophosphate, or cyclic di-GMP (c-di-GMP) is a ubiquitous bacterial second messenger that regulates processes such biofilm formation, motility, and virulence. C-di-GMP is synthesized by diguanylate cyclases (DGCs), while phosphodiesterases (PDE-As) end signaling by linearizing c-di-GMP to 5′-phosphoguanylyl-(3′,5′)-guanosine (pGpG), which is then hydrolyzed to two GMPs by previously unidentified enzymes termed PDE-Bs. To identify the PDE-B responsible for pGpG turnover, a screen for pGpG binding proteins in a *Vibrio cholerae* open reading frame library was conducted to identify potential pGpG binding proteins. This screen led to identification of oligoribonuclease (Orn). Purified Orn binds to pGpG and can cleave pGpG to GMP in vitro. A deletion mutant of *orn* in *Pseudomonas aeruginosa* was highly defective in pGpG turnover and accumulated pGpG. Deletion of *orn* also resulted in accumulation c-di-GMP, likely through

pGpG-mediated inhibition of the PDE-As, causing an increase in c-di-GMP-governed auto-aggregation and biofilm. Thus, we found that Orn serves as the primary PDE-B enzyme in *P. aeruginosa* that removes pGpG, which is necessary to complete the final step in the c-di-GMP degradation pathway. However, not all bacteria that utilize c-di-GMP signaling also have an ortholog of *orn*, suggesting that other PDE-Bs must be present. Therefore, we asked whether RNases that cleave small oligoribonucleotides in other species could also act as PDE-Bs. NrnA, NrnB, and NrnC can rapidly degrade pGpG to GMP. Furthermore, they can reduce the elevated aggregation and biofilm formation in *P. aeruginosa* Δ*orn*. Together, these results indicate that rather than having a single dedicated PDE-B, different bacteria utilize distinct RNases to cleave pGpG and complete c-di-GMP signaling. The Δ*orn* strain also has a growth defect, indicating changes in other regulatory processes that could be due to pGpG accumulation, c-di-GMP accumulation, or another effect due to loss of Orn. We sought to investigate the genetic pathways responsible for these growth defect phenotypes by use of a transposon suppressor screen, and also investigated transcriptional changes using RNA-Seq. This work identifies that c-di-GMP degradation intersects with RNA degradation at the point of the Orn and the functionally related RNases.

A SUBSET OF 3′ TO 5′ EXORIBONUCLEASES ARE THE PRIMARY ENZYMES RESPONSIBLE FOR THE DEGRADATION OF PGPG IN CYCLIC DI-GMP SIGNALING

By

Mona Wu Orr

Dissertation submitted to the Faculty of the Graduate School of the
University of Maryland, College Park, in partial fulfillment
of the requirements for the degree of
Doctor of Philosophy
2016

Advisory Committee:
Associate Professor Vincent T. Lee, Chair
Associate Professor Wade C. Winkler
Associate Professor Richard C. Stewart
Professor Kevin S. McIver
Associate Professor Jason D. Kahn

Dedication

This dissertation is dedicated to my family: Gina Wu, Michael Wu, Diana S. Wu, David Molter Orr, and Samuel Wu Orr. Without their encouragement and love I would not be here today.

Acknowledgements

First, I thank my advisor Dr. Vincent T. Lee. His mentorship has been invaluable to my development as a scientist. Every moment in lab from Monday morning coffee to Friday afternoon wine has been nothing if not interesting.

I am grateful to my committee members Drs. Kevin S. McIver, Wade C. Winkler, and Richard C. Stewart for our scientific discussions, their input on experimental design and their advice on career decisions. I thank Dr. Kahn for stepping in as Deans' Representative in my committee. I also especially wish to thank Dr. Winkler for the secondhand baby and toddler toys.

I thank the people whose work has contributed to this dissertation: Kevin G. Roelofs for construction of the ORFeome, Gregory P. Donaldson for pGpG inhibition, Dr. Christopher C. Waters and Geoffrey B. Severin for detecting cellular nucleotides, Xiaoran Shang for help with the transposon suppressor screen, Dr. Stephanie J. Cole and Jonathan Goodson for RNA-Seq work, and Cordelia A. Weiss for microscopy imaging of bacterial strains.

I thank the many members of the Lee, Winkler, and McIver laboratories who have provided useful tips and a sympathetic ear. The innumerable coffee runs, candies, desserts, and mugs of alcohol we've shared helped smooth the path in this difficult journey. Kayla M. Valdes deserves my particular gratitude for always remembering departmental deadlines so I didn't have to.

Finally, I thank Sylvia J. Zhu for that one time she brought a cold leftover pizza to the BRB for me to devour in the elevator back up to lab. This dissertation would not have happened without you.

Table of Contents

List of Tables

List of Figures

Chapter 1: Introduction

1.1 Bacterial nucleotide second messengers

In order to survive, bacteria need to respond to changes in their environment and enact suitable responses. In a process called signal transduction, an extracellular event is transduced across the cell surface to the interior of the cell. Signal transduction is typically a three step process in which the extracellular signal is detected, a cellular response is triggered, and then the response is terminated and the system returns to its initial state. One widely utilized method of signal transduction is the regulated production and turnover of nucleotide second messengers. In this mechanism, detection of an extracellular signal results in the activation of an intracellular synthase that produces a unique diffusible intracellular nucleotide signaling molecule. This molecule then binds to effector molecules to allosterically regulate their function, and these effector molecules go on to interact with other intracellular molecules to effect a change in phenotype. Finally, signaling is terminated by the activity of inactivating enzymes that break down the signaling molecule.

One of the earliest discovered bacterial second messenger was cyclic AMP (cAMP). In the classical *Escherichia coli* bacterial model, cAMP is a key regulator in carbon catabolite repression (see (1) for review). In response to low concentrations of extracellular glucose and thus reduced glucose import, adenylate cyclase is activated to synthesize cAMP, which binds to the cAMP receptor protein (CRP) to activate its

DNA-binding domain. The cAMP-CRP complex binds promoters of many genes involved in alternate sugar utilization pathways. In combination with other transcriptional regulators, the cAMP-CRP complex modulates gene expression (2, 3). Signal termination occurs by conversion of the cAMP molecule to AMP by cAMP-specific phosphodiesterases. The AMP is rephosphorylated and recycled into the free cellular nucleotide pool. The protein products of genes regulated by cAMP-CRP must then be removed or inactivated to fully terminate the process initiated upon cAMP synthesis. Besides cAMP, bacteria utilize a number of other different nucleotide signaling molecules to regulate a variety of phenotypes. To date, those reported include cyclic GMP (cGMP), (p)ppGpp, cyclic di-GMP (c-di-GMP), cyclic di-AMP (c-di-AMP), and cyclic AMP-GMP (cAG). (See (4) for review of cAMP, (p)ppGpp, and c-di-GMP, (5) for a review of c-di-GMP, (6) for c-di-AMP, and (7) for a review of cGMP.) Nucleotide second messengers can also target additional processes downstream of transcription. One of the most prolifically studied signaling nucleotides after cAMP is c-di-GMP, which has been shown to regulate behavior by affecting transcription, translation, and post-translational protein activity.

1.2 Cyclic di-GMP synthesis, turnover, and signaling

C-di-GMP was originally described in 1987 by the Benziman lab as an allosteric activator of cellulose synthase in *Acetobacter xylinum* (since renamed *Komagataeibacter xylinus*) (8). In their initial report, the Benziman lab demonstrated that c-di-GMP is synthesized from two GTP molecules by enzymes with diguanylate cyclase (DGC) activity, linearized to pGpG by enzymes with phosphodiesterase A (PDE-A) activity, and then further hydrolyzed to two GMPs with enzymes with

phosphodiesterase B (PDE-B) activity (8). The Benziman lab later identified the genetic loci responsible for synthesizing and linearizing c-di-GMP, suggesting that proteins containing the GGDEF and EAL domains (so named for conserved residues) are involved in c-di-GMP synthesis and turnover (9). Work from multiple labs later confirmed the GGDEF domains are responsible for DGC activity (10-12) and EAL domains are responsible for PDE-A activity (11, 13, 14). Several years later, the HD-GYP domain enzymes were shown to also be able to hydrolyze c-di-GMP to pGpG (15). See Fig. 1 for diagram of protein domains involved in c-di-GMP synthesis and degradation.

The advent of genomic sequencing in the late 1990s revealed these domains to be widely distributed across bacterial phyla, suggesting that c-di-GMP signaling is common in prokaryotes (16). This genetic analysis also revealed that the genomes of many bacterial species encode multiple proteins containing domains associated with c-di-GMP signaling (16). For example, the genome of *V. cholerae* encodes 31 GGDEF, 12 EAL, 10 dual GGDEF and EAL, and 8 HD-GYP domains proteins, while *Pseudomonas aeruginosa* encodes 17 GGDEF, 6 EAL, 16 dual GGDEF and EAL, and 2 HD-GYP domain proteins. The multiplicity of c-di-GMP synthesizing and degrading enzymes suggested that c-di-GMP signaling is highly complex.

In the years following its discovery, studies have shown that c-di-GMP is utilized by diverse bacterial species to regulate numerous phenotypes. Identification of the c-di-GMP governed phenotypes has generally been achieved via overexpression of the DGCs that synthesize c-di-GMP or deletion of the PDE-As that

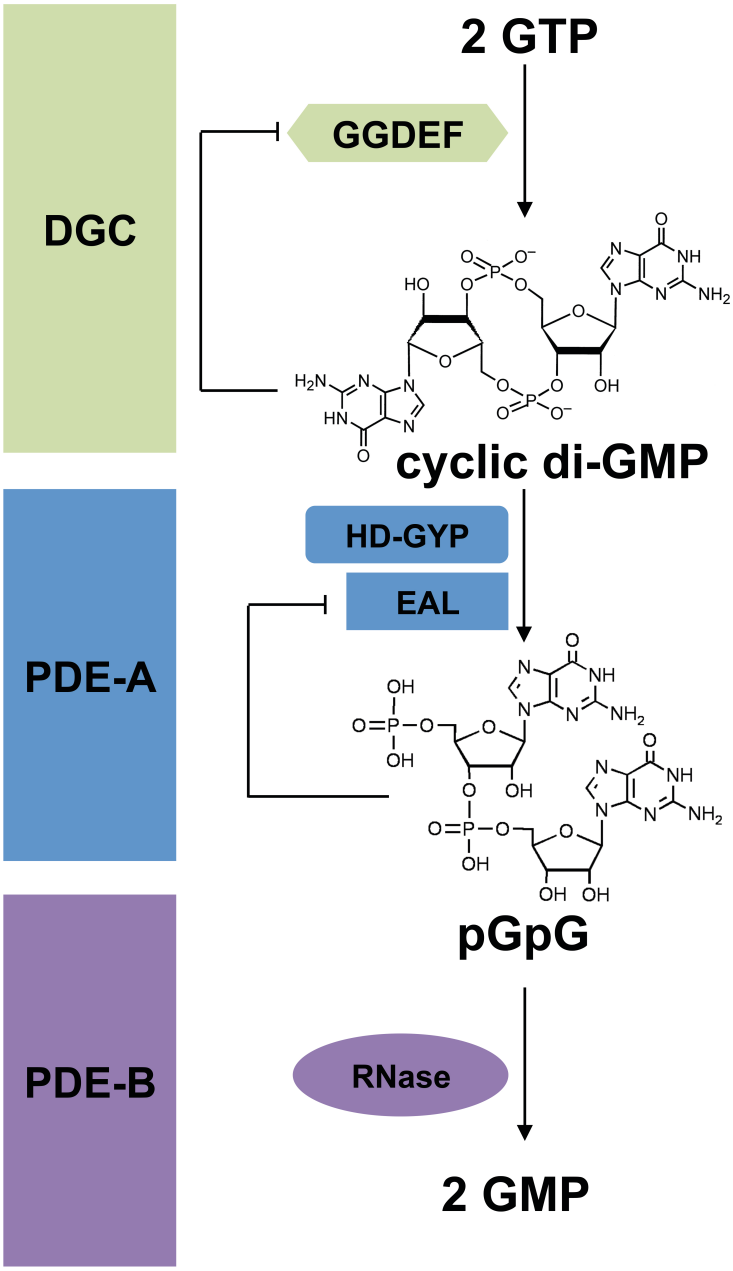

Figure 1. C-di-GMP synthesis and degradation. A diagram showing the protein domains involved in c-di-GMP synthesis and turnover. The diguanylate cyclases (DGC) consist of GGDEF domains enzymes that cyclize two GTP molecules to generate c-di-GMP. C-di-GMP can bind the I-site in GGDEF domains to allosterically inhibit its own production. The phosphodiesterase As (PDE-A) consist of EAL or HD-GYP domain enzymes that can hydrolyze c-di-GMP to pGpG. Data from this dissertation suggests that phosphodiesterase Bs (PDE-B) for pGpG cleavage are RNases.

linearize it. The results of these studies revealed that c-di-GMP governs biofilm formation, motility, virulence, differentiation, and cell cycle progression, making it a crucial regulator in bacterial lifestyle decisions. In general, high levels of c-di-GMP promote the sessile, biofilm forming lifestyle while low levels of c-di-GMP promote a motile, planktonic lifestyle (see (5) for a comprehensive review of c-di-GMP signaling).

C-di-GMP can regulate these processes by binding to and allosterically altering the activity of many different kinds of effector proteins. The first of these c-di-GMP effector proteins to be identified were the PilZ domain proteins. They were predicted based on bioinformatic analysis to be likely c-di-GMP receptors (17) and were indeed later proven to be a class of c-di-GMP binding proteins ((18) and reviewed in (5, 19, 20)). Another class of c-di-GMP receptors includes proteins with catalytically inactive GGDEF and EAL domains. The GGDEF domain contains an I-site with an RxxD motif that allows for allosteric inhibition of cyclase activity. In degenerate GGDEF domain receptors, such as the PopA regulator of cell cycle progression in *Caulobacter crescentus* (21), the diguanylate cyclase activity is lost, but the RxxD domain still binds c-di-GMP to regulate protein function. The degenerate EAL domain proteins can bind c-di-GMP at the EAL domain, but cannot cleave it to pGpG. Instead, binding at the degenerate EAL domain allows for control of protein function. These proteins include LapD (22), which promotes cell adhesion when bound to c-di-GMP, and FimX, which undergoes a large conformational change upon c-di-GMP binding to regulate type IV pilus production (23, 24). Other effector proteins including PelD from *P. aeruginosa* (25) and FlrA from *V. cholerae* (26)

contain unique binding sites that could not be bioinformatically predicted. Finally, another class of effectors are transcription factors with novel binding sites such as FleQ from *P. aeruginosa* (27, 28), BldD from *Streptomyces coelicolor* (29), the CRP-homolog Clp from *Xanthomonas* species (30-32), and Vps from *V. cholerae* (33). In addition to binding proteins, c-di-GMP has been shown to interact with two different types of riboswitches to affect gene expression (34, 35), indicating yet another mechanism by which c-di-GMP can control bacterial processes.

Despite the progress made in understanding c-di-GMP regulation, there is still much to be discovered. C-di-GMP effectors have not been identified for all processes known to be affected by elevated c-di-GMP. Additionally, despite nearly three decades of research on c-di-GMP, the identity of the PDE-B responsible for the hydrolysis of pGpG to GMP had not yet been identified at the outset of this project. The identification of several pGpG-binding proteins suggests that pGpG could have regulatory activities that have been previously overlooked. Because pGpG is a product of c-di-GMP, any pGpG-controlled phenotypes would have been attributed to the effects of elevated c-di-GMP (Fig. 1).

1.3 The cellular sources and fate of pGpG

In addition to being derived from c-di-GMP linearization, there are other potential sources of cellular pGpG. Since pGpG is a two-nucleotide RNA molecule, the degradation of longer RNAs or abortive transcription initiation can yield short RNA fragments that could include pGpG. In *E. coli*, the endonuclease RNase E cleaves long RNA transcripts to yield short fragments, which are then further degraded by 3′ to 5′ exonucleases to yield short RNAs between two nucleotides

(2mer) to five nucleotides long (5mer) (see (36) for review). In abortive transcription initiation, the RNA polymerase stutters at the start of initiation and synthesizes very short RNAs before proceeding to engage and synthesize the full transcript (37).

It was unknown whether pGpG was merely an inactive intermediate or whether it had any signaling potential of its own. That two classes of structurally and functionally distinct c-di-GMP specific PDE-As exist has led to speculation that pGpG production may be important (38), but no research into a physiological role of pGpG has been conducted. Very short RNAs have been shown to prime transcription in vivo, leading to changes in transcript levels (39-41). This leads to the possibility that pGpG could act by priming transcription in vivo. Furthermore, high levels of pGpG were shown to inhibit the ability of an EAL domain PDE-A, YfgF, from *E. coli* to cleave c-di-GMP in vitro (42). This inhibition was also observed in our lab for the EAL domain PDE-A, RocR, *P. aeruginosa*. These observations suggest a potential for pGpG-mediated inhibition of c-di-GMP turnover. Additionally, pGpG could bind to other protein targets to regulate their function.

After it is generated, pGpG is hydrolyzed into two molecules of GMP. Although the existence of an enzyme with this activity, termed PDE-B, has been known since the initial report of c-di-GMP (8), its identity remained undetermined. Given that pGpG is a short dinucleotide, it is possible that general RNases are capable of turning over pGpG. Alternatively, there could be pGpG-specific degradation enzymes. This motivated a screen to identify pGpG-binding proteins, which would represent pGpG receptors or the PDE-Bs responsible for hydrolyzing pGpG.

1.4 A DRaCALA-based screen for pGpG binding partners

Our lab recently developed a binding screen that allows for systematic identification of protein-ligand binding from a bacterial genome. This screen is based on the Differential Radial Capillary Action of Ligand Assay (DRaCALA) (43). DRaCALA relies on the differential movement of a radiolabeled nucleotide and protein on nitrocellulose (43). For this assay, a small volume of protein mixed with radiolabeled ligand in a binding buffer is applied to dry nitrocellulose. The protein remains bound to the nitrocellulose at the point of application, while the free ligand will be mobilized by capillary action with the liquid phase. These DRaCALA spots can be quantified by calculating the fraction bound: the intensity of the radiation detected from protein-sequestered ligand over the total radiation of the spot (43). DRaCALA can be used to detect interactions without the need to purify from an *E. coli* overexpression strain lysate under three conditions: first, the protein is expressed to a level such that its concentration is above the dissociation constant; second, the ligand is not naturally abundant in the overexpression strain to compete for radioactively labeled ligand binding; and third, heterologous expression of the single protein is sufficient for binding.

The DRaCALA screen takes advantage of available Gateway-compatible open reading frame libraries (ORFeome) to query each predicted ORF of an entire genome individually for ligand binding. The ORF is recombined into Gateway compatible destination expression plasmids and transformed into the *E. coli* T7Iq expression strain, which is then grown, induced for protein expression, and lysed all in a 96-well plate format. Each well in the expression library contains a lysate overexpressing a

single ORF. Radiolabeled ligand is then added via a liquid dispenser. This lysate-ligand mix is then transferred to a nitrocellulose sheet using a 96-pin tool and exposed for quantification. ORFs that increase binding above the average background binding seen for the expression library are considered positive hits. These candidate binding proteins can then be purified and assayed for confirmation of binding (Fig. 2 for process overview).

This method has been successfully used to identify novel c-di-AMP binding proteins in a *Staphylococcus aureus* open reading frame library (ORFeome) screen (44) and novel c-di-GMP binding proteins from a *V. cholerae* ORFeome screen (45) and an *E. coli* ORFeome screen (46). We expected to detect pGpG-binding proteins in this ORFeome screen because *V. cholerae* has an extensive c-di-GMP network (16, 47), the *V. cholerae* El Tor N16961 ORF library (ORFeome) contains high coverage of the predicted OFRs (48), and this library was successfully used to identify c-di-GMP binding proteins (45). Since the PDE-B must first bind pGpG to degrade it, it is expected that this screen will also reveal the PDE-B responsible for pGpG hydrolysis.

In this dissertation, I sought to identify the PDE-B(s) responsible for pGpG turnover and determine whether pGpG has a role as a signaling molecule. To identify PDE-Bs and pGpG receptors, a DRaCALA-based screen was used to probe the *V. cholerae* ORFeome for pGpG binding proteins. The screen identified seventeen potential pGpG binding proteins. One of the enzymes identified was an oligoribonuclease (Orn) homolog. Experiments confirmed that Orn from *V. cholerae* and *P. aeruginosa* are pGpG binding proteins that can rapidly convert pGpG to GMP in vitro. Lysates of a *P. aeruginosa* PA14 Δ*orn* strain were highly defective in pGpG

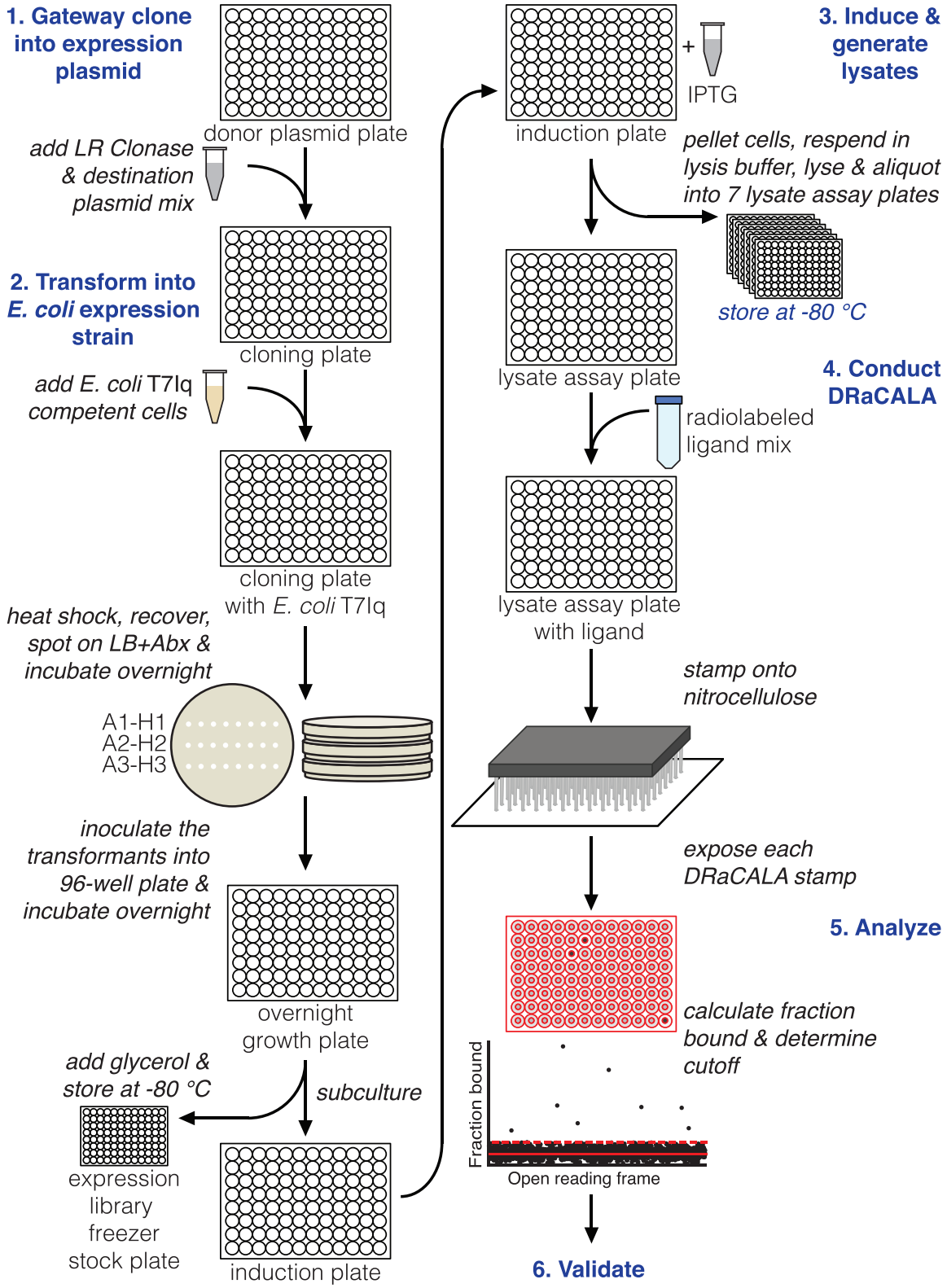

Figure 2. Schematic of high-throughput DRaCALA ORFeome screen. Diagram showing each step of the DRaCALA ORFeome screen. Each of the plates has a designated name, shown below the plate, which is used in the accompanying text. The general procedural steps are indicated by text on the side of each arrow.

hydrolysis and accumulated pGpG. Thus, Orn likely is the primary PDE-B enzyme in *P. aeruginosa*. Not all bacteria that utilize c-di-GMP signaling have an identifiable ortholog of *orn*, indicating that other proteins must provide PDE-B activity. Because Orn is an RNase that specializes in cleaving short oligoribonucleotides, other RNases that can also cleave short oligoribonucleotides could also act as PDE-Bs.

1.5 NanoRNases as PDE-Bs for pGpG

Orn was first isolated from *E. coli* and demonstrated to be capable of degrading short (5mer and shorter) poly-adenosine (poly(A)) oligoribonucleotides in 1975 (49, 50). The *orn* gene was identified and cloned over two decades later (51), and was shown to be essential as inactivation of the gene resulted in cessation of growth in *E. coli* (52). A temperature-dependent mutant was generated by introducing a chromosomal interruption in the *orn* locus while supplying *orn* on a temperature-sensitive plasmid (52). Upon growth of this temperature-dependent *orn* mutant *E. coli* in non permissive conditions, the strain was shown to accumulate oligoribonucleotides of RNA that are 2mer-5mer long (52), indicating that Orn is the major enzyme responsible for degrading this RNAs of this size in *E. coli*.

Homologs for *orn* are not found in the genome sequences of all bacterial classes, such as the Alphaproteobacteria or the Firmicutes, leading researchers to hypothesize that other enzymes filled this role in other bacterial species. Because the Danchin lab discovered that Orn could bind pAp (53), they used a pulldown for pAp-binding proteins in the Firmicute *B. subtilis* to attempt to identify other RNases with Orn-like activity. Using the method, the Danchin lab identified YtqI from *B. subtilis*, a 3´ to 5´ exonuclease that was able to degrade 5mer and shorter oligoribonucleotides

down to monomers but had little activity against 24mer RNAs in vitro (54). The discovery prompted those authors to propose the new terms “nanoRNA” and “nanoRNase” to describe these very short oligoribonucleotides and the RNases that preferentially degrade them. While this choice in terminology could be confused for the International System of Units designation of the prefix “nano-” to refer to 10^{-9}, it is instead in homage to the naming of microRNAs (55-57). The three groups simultaneously reporting the discovery of these ~ 20-nucleotide-long regulatory RNAs in *Caenorhabditis elegans* agreed to the designation “microRNA”, as “micro-” is derived from the Greek *mikros*, meaning small (55-57). Thus the Danchin lab selected “nano” from the Greek *nanos*, meaning dwarf, to indicate that these RNAs are smaller than microRNAs. YtqI was renamed nanoRNase A (NrnA).

A screen of a genetic library of *B. subtilis* revealed another RNase, named NrnB, could fully rescue growth in an *E. coli orn* conditional mutant (58) and a screen of a genetic library from the Alphaproteobacteria *B. birtlesii* (59) in the same system identified another RNase, named NrnC. Like NrnA, NrnB and NrnC were shown to be able to cleave 5mer and shorter oligoribonucleotides to monomers and displayed far higher rates (>1000x) of in vitro activity against 5mers compared to 24mers, suggesting that they are specific for shorter substrates (54, 58, 59). Two other previously identified RNases that have activity against longer substrates, YhaM and RNase J1, were also shown to partially rescue growth of the *E. coli orn* conditional mutant (58). Figure 3 shows a Venn diagram of the currently known exoribonucleases from the Gammaproteobacteria *E. coli* and *P. aeruginosa*, the Firmicute *B. subtilis*, and the Alphaproteobacteria *B. birtlesii*. The only RNases that could rescue growth in

the *E. coli* conditional *orn* mutant were the RNases unique to *B. subtilis* and *B. birtlesii*. Together, these studies strongly suggest that the ability to degrade very short RNAs, or "nanoRNAs" is specific to a subset of RNases. However, although proposed to be grouped as "nanoRNases", these proteins belong in different domain families. NrnA and NrnB to the DHH/DHHA1 domain family, named for the four conserved acidic residues and a conserved DHH-assoaciated motif (DHHA1) (54, 58, 60). NrnC is a member of the DEDDy domain family, so named for the conserved residues (59, 61). Thus, the term "nanoRNase" groups these RNases by their proposed activity against very short RNAs rather than by shared homology of structure or active site residues.

NrnA, NrnB, NrnC, RNase J1 and YhaM were shown to cleave short oligoribonucleotides in vitro. The presence of NrnA, NrnB, and NrnC could fully rescue and RNase J1 and YhaM could partially rescue an *E. coli orn* mutant. Therefore, we hypothesized that these RNases could also be the major PDE-B for c-di-GMP in bacteria lacking an *orn* ortholog and should be able to restore the behavior of the *P. aeruginos*a Δ*orn* strain to wild type. Experiments here determined that NrnA, NrnB and NrnC can rapidly degrade pGpG to GMP in vitro and can restore the ability of *P. aeruginosa* Δ*orn* pGpG degradation. Taken together, these data indicate that a subset of RNases serve as the final processing enzyme to terminate c-di-GMP signaling instead of a dedicated PDE-B.

1.6 Other phenotypes in PA14 Δ*orn* and the essentiality of *orn*

Finally, the work in this dissertation sought to determine the cause of the phenotypes observed in the *P. aeruginosa* PA14 Δ*orn* strain. These include increased

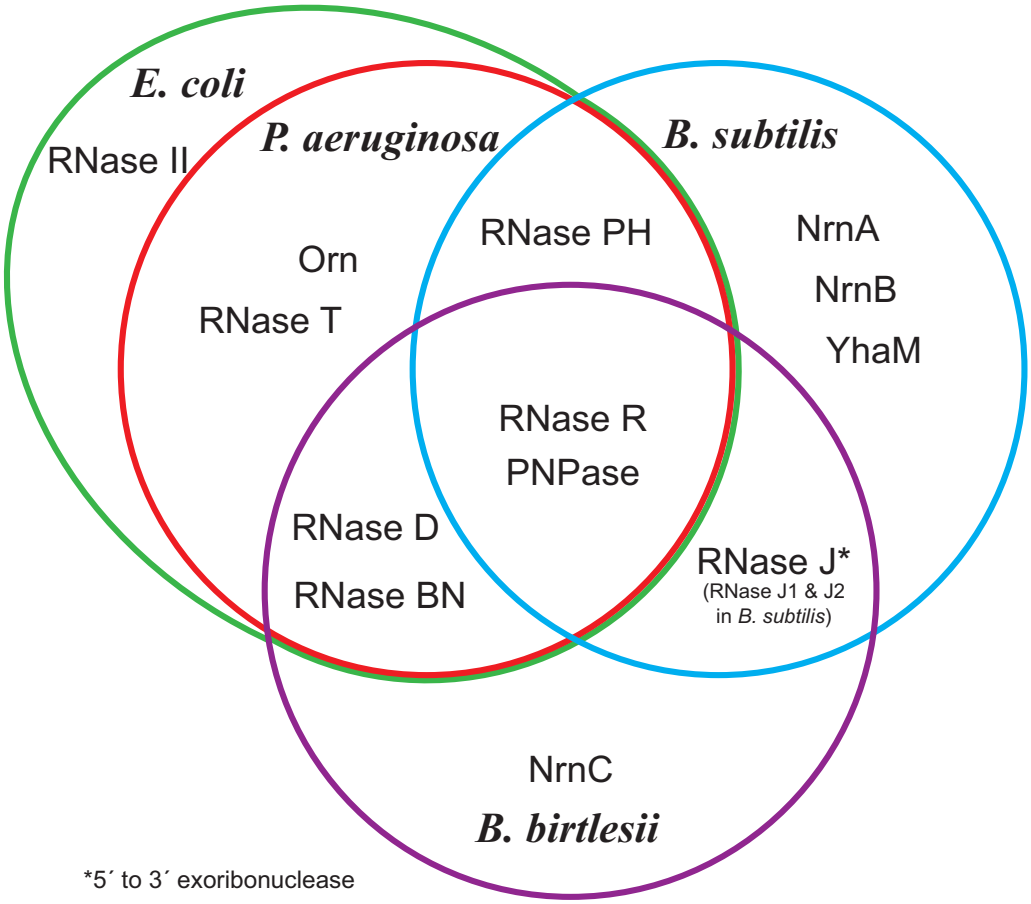

Figure 3. Exoribonucleases in *E. coli*, *P. aeruginosa*, *B. subtilis*, and *B. birtlesii*. A Venn diagram showing exoribonucleases found in *E coli* (green), *P. aeruginosa* (red), *B. subtilis* (blue) and *B. birtlesii* (purple). All are 3´ to 5´ except RNase J, which is 5´ to 3´. RNases were identified based on presence in the COG database, sequence homology by NCBI protein BLAST, or report in literature.

biofilm formation and aggregation and a growth defect that resulted in the mutant forming much smaller colonies than wild type PA14 on agar plates. Work here demonstrates that this biofilm and aggregate formation are dependent on the *pel* operon, which encodes the enzymes and other machinery responsible for producing and assembling the PEL exopolysaccharide (62). PEL production is dependent on c-di-GMP (25, 27), indicating that enhanced biofilm and aggregation observed with the Δ*orn* mutant were most likely due to elevated c-di-GMP signaling. The Δ*orn* mutant showed higher concentrations of c-di-GMP, likely due to pGpG-mediated inhibition of the PDE-As responsible for cleaving c-di-GMP. However, the growth phenotype was not *pel* dependent, suggesting changes in other regulatory processes that are not c-di-GMP related.

The loss of *orn* is deleterious in bacteria. In *E. coli*, for example, an inactivating insertional mutant could not be generated (52), indicating that *orn* is an essential gene. Similarly, a transposon mutant could not be recovered in *V. cholerae* (63). In *Pseudomonas* species, *orn* is not essential, but mutants do have a growth defect (64, 65). This led to an investigation of why the loss of *orn* causes reduced growth rate or loss of viability. To identify the processes disregulated in an *orn* mutant, a transposon suppressor screen was utilized to identify mutants that restored colony size for the Δ*orn* mutant of *P. aeruginosa*. These suppressing mutations are likely to occur in pathways that are inappropriately activated in the *orn* mutant, so identifying the site of the suppressor mutations could lead to the identification of processes regulated by Orn. Additionally, RNA-Seq experiments have revealed changes in gene expression in the Δ*orn* strain to identify the transcriptional changes

that could lead to growth rate defects. Finally, Tn-Seq experiments are planned to identify additional mutants that can rescue growth rate. This approach could identify suppressor mutations that were missed by the visual colony size screen. It may also identify synthetic lethal mutants which could represent RNase genes in *P. aeruginosa* that have a redundant function to *orn*, which could explain why *orn* mutants are viable in *P. aeruginosa* but not *E. coli*.

In summary, findings from this dissertation demonstrate that Orn and nanoRNases are the PDE-Bs responsible for cleaving pGpG and also suggest additional roles for Orn-mediated bacterial regulation.

Chapter 2: Oligoribonuclease is the primary degradative enzyme for pGpG in *Pseudomonas aeruginosa* that is required for cyclic-di-GMP turnover

2.1 Copyright notice

Author Contributions: Orr, M.W., Donaldson, G.P., Severin, G.B. performed research; Wang, J. and Dr. Sintim, H.O. contributed new reagents; Orr, M.W., Donaldson, G.P., Severin, G.B., Dr. Waters, C.M. and Dr. Lee, V.T. analyzed data; and Orr, M.W., Severin, G.B., Dr. Waters, C.M. and Dr. Lee, V.T. wrote the paper.

Data gathered by Donaldson, G.P. are in Figs. 4 & 5 and by Severin, G.B., are in Table 2.

2.2 Introduction

Cyclic-di-GMP (c-di-GMP) is a phylogenetically widely used bacterial second messenger (5). C-di-GMP is synthesized by diguanylate cyclase enzymes (DGC) that contain the GGDEF domain (9, 10). Once synthesized, the c-di-GMP binds to intracellular receptors to decrease motility and increase biofilm formation, contributing to the virulence of several pathogens (5, 19, 66-68). C-di-GMP signaling is terminated by phosphodiesterases (PDE-A) that linearize it into pGpG, which is

then hydrolyzed into GMP by an unknown phosphodiesterase termed "PDE-B" (9). Bacteria encode two structurally unrelated PDE-As; one containing the EAL domain (11, 13, 14) and a second containing the HD-GYP domain (15). The overexpression of GGDEF domain DGCs elevates c-di-GMP and c-di-GMP-regulated processes (11, 69); conversely, overexpression of the EAL and HD-GYP domain PDE-As decreases c-di-GMP and c-di-GMP regulated processes (11, 70-72). These c-di-GMP synthesizing and degrading domains are commonly linked to sensory and signal transduction domains (5, 20), thereby allowing synthesis and degradation of c-di-GMP in response to environmental changes.

In addition to regulation by extracellular signals, c-di-GMP homeostasis is subject to feedback inhibition. Crystal structures of the DGCs PleD *from C. crescentus* and WspR from *P. aeruginosa* show that c-di-GMP binds to an RxxD domain I-site to inhibit c-di-GMP synthesis (73, 74). Additionally, the *X. campestris* XCC4471 DGC lacking an RxxD motif can also be inhibited by excess c-di-GMP through c-di-GMP binding to and occluding the active site (75). The linearized c-di-GMP hydrolysis product, pGpG, also plays an active role in nucleotide turnover. Purified YfgF from *E coli*, a PDE-A, is inhibited by excess pGpG through an unknown mechanism (42). Here, we show that the EAL domain PDE-A RocR from *P. aeruginosa* PA14 strain is also inhibited by excess pGpG via direct competition with c-di-GMP binding in the active site. Accordingly, the addition of excess pGpG results in an increased c-di-GMP half-life in vitro, suggesting that removal of pGpG is required for terminating c-di-GMP signaling.

To elucidate the mechanism of c-di-GMP signal termination, we sought to identify the PDE-B(s) responsible for cleaving pGpG. Previously, HD-GYP domain-containing proteins were proposed to be the PDE-Bs involved in pGpG hydrolysis because they bind pGpG with higher affinity than c-di-GMP (76). However, HD-GYP domain proteins are missing in some genomes that contain other c-di-GMP signaling machinery (5), suggesting that other enzymes must be responsible for PDE-B activity. To identify PDE-B(s), we used a screen based on the Differential Radial Capillary Action of Ligand Assay (DRaCALA) (43, 44) to probe an open reading frame library of *V. cholerae* El Tor N16961 (48) for proteins that bind pGpG. This screen identified oligoribonuclease (Orn) as a protein that binds pGpG, but not c-di-GMP. Orn is an exoribonuclease that cleaves two to five nucleotide long RNA molecules (51). We found that purified Orn from both *V. cholerae* and *P. aeruginosa* bound and cleaved pGpG. To determine whether Orn is the primary PDE-B in bacteria, we show that whole cell lysates of an *orn* transposon mutant (*orn*::tn) from the *P. aeruginosa* PA14 Non-Redundant Transposon Insertion Mutant Library (64) and an in frame deletion mutant of *orn* (Δ*orn*) were decreased in pGpG cleaving activity by 25-fold as compared to the parental strain. Complementation with wild type *orn,* but not active site point mutants, restored pGpG hydrolysis in cell lysates. Thus, loss of *orn* is expected to increase pGpG concentration in vivo, and may inhibit PDE-A activity to also elevate c-di-GMP concentrations in the Δ*orn* strain. In support of elevated c-di-GMP in the Δ*orn* strain, we observed three times more activity from the c-di-GMP-responsive *pel* promoter FleQ (27). We also demonstrate that two c-di-GMP governed phenotypes, biofilm formation (77) and aggregation (78), are

enhanced in the Δ*orn* strain, and are dependent on the c-di-GMP-regulated PEL exopolysaccharides (25). Using LC/MS-MS, we directly detect higher levels of both pGpG and c-di-GMP in extracts of the Δ*orn* strain compared to wild type. Taken together, these results indicate that Orn is the primary PDE-B responsible for degrading pGpG in *P. aeruginosa*.

2.3 pGpG inhibits phosphodiesterase activity by binding to the active site

PDE-A YfgF from *E. coli* is inhibited by the addition of 100 μM of pGpG (42). We asked whether PDE-A inhibition by pGpG is a generalizable phenomenon. The RocR PDE-A from *P. aeruginosa* PA14 was used to determine inhibition by pGpG. In the absence of competitor (Fig. 4A), RocR rapidly converts 89% of the radiolabeled c-di-GMP to pGpG within five minutes as measured after separation by thin layer chromatography. The addition of 100-fold excess of pGpG nearly completely inhibited c-di-GMP linearization (Fig. 4A). These results demonstrate that pGpG inhibits PDE-A activity. To determine if pGpG is competing with c-di-GMP for active site binding in RocR, we performed experiments in which binding of radiolabeled c-di-GMP to purified RocR was assessed in the presence of different unlabeled nucleotide competitors. RocR binds c-di-GMP with a fraction bound of 0.54 ± 0.03 in the absence of competitor, while the addition of 50 μM unlabeled pGpG reduced fraction bound to 0.022 ± 0.005, $p < 0.001$, indicating that pGpG competes for c-di-GMP binding (Fig. 4B, black bars). To see if binding is mutually exclusive, RocR was incubated with radiolabeled pGpG in the presence of the same panel of unlabeled nucleotide competitors (Fig. 4B, white bars). The addition of 50 μM c-di-GMP reduced fraction bound from 0.48 ± 0.01 to 0.13 ± 0.03, $p < 0.001$,

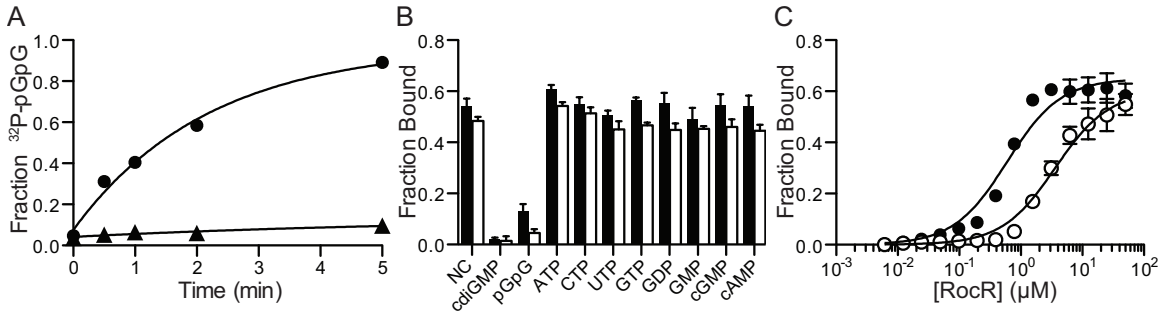

Figure 4. pGpG inhibits RocR phosphodiesterase activity by competing for c-di-GMP binding in the active site. (A) The rate of ^{32}P-pGpG formation from ^{32}P-c-di-GMP hydrolysis by RocR in the absence of competitor (NC, circle) or 500 μM pGpG competitor (triangle). (B) The fraction bound of ^{32}P-c-di-GMP (black) or ^{32}P-pGpG (white) to RocR (10 μM) was quantified by DRaCALA in the presence of no competitor (NC) or 500 μM excess unlabeled nucleotide competitor. (C) The dissociation constants (K_d) for RocR binding to ^{32}P-c-di-GMP (black) and ^{32}P-pGpG (white) as determined by DRaCALA. All data shown represent the average and SD of triplicate independent experiments.

indicating that c-di-GMP is also able to prevent pGpG binding. No other nucleotide had a significant effect on fraction of pGpG or c-di-GMP bound to RocR (Fig. 4B). Thus, RocR binding to pGpG and c-di-GMP is specific and mutually exclusive.

Crystal structures of another EAL domain PDE-A FimX show that pGpG binds in the active site where c-di-GMP cleavage occurs (79). Since the binding is occurring at the same site, the relative affinity of RocR binding to pGpG and c-di-GMP is important to determine if pGpG competition of c-di-GMP binding could occur in physiological conditions. The dissociation constant (K_d) of RocR binding to pGpG and c-di-GMP were found to be 3.6 ± 0.4 μM and 0.60 ± 0.07 μM respectively (Fig. 4C). The c-di-GMP concentration in the cell has been reported to be 11 μM – 30 μM (80). Therefore, rapid turnover of c-di-GMP can yield pGpG concentrations that exceed the K_d for RocR if pGpG is not also quickly removed from the cell.

2.4 Excess pGpG extends c-di-GMP half-life in vitro

Inhibition of RocR by pGpG should effectively increase the half-life of c-di-GMP. To test this in vitro, a coupled DGC and PDE-A reaction was performed to trace the synthesis and linearization of c-di-GMP in the presence of different intermediates in the c-di-GMP biosynthesis and degradation pathways. Specifically, the DGC WspR and PDE-A RocR from *P. aeruginosa* PA14 were incubated with radiolabeled α-^{32}P-GTP in the presence of either: A) no competitor, B) GMP, C) c-di-GMP, or D) pGpG. The reactions were stopped at different times by the addition of the divalent metal chelator EDTA and heat inactivation. The reaction products were separated by TLC and intensities of radiolabeled GTP, c-di-GMP, and pGpG were quantified (Fig. 5). In the absence of any competitor, the α-^{32}P-GTP is converted to c-

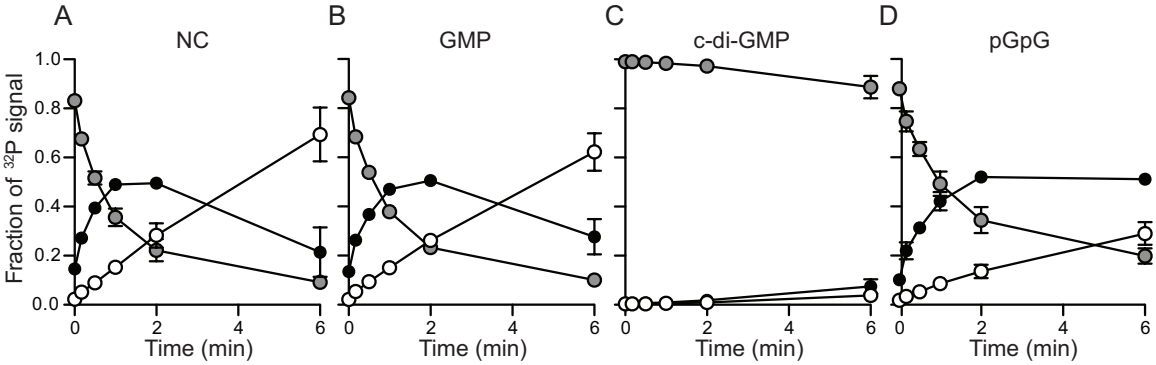

Figure 5. Excess pGpG extends the half-life of c-di-GMP in an in vitro diguanylate cyclase and phosphodiesterase activity assay. TLC-based quantification of the conversion of ^{32}P-GTP (gray) to ^{32}P-c-di-GMP (black) and ^{32}P-pGpG (white) in a coupled WspR and RocR reaction in (A) the absence of competitor (NC), (B) 300 μM GMP, (C) 300 μM c-di-GMP, or (D) 300 μM pGpG. All data shown represent the average and SD of triplicate independent experiments.

di-GMP, which is then linearized to pGpG. Adding 100-fold excess GMP shows no effect on enzymatic activity, as expected (Fig. 5A, 5B). Addition of excess c-di-GMP inhibited the ability of WspR to convert α-^{32}P-GTP to c-di-GMP, which is consistent with inhibition through binding to the I-site (Fig. 5C) (73, 74). Most importantly, the addition of excess pGpG reduced the turnover c-di-GMP (Fig. 5D), supporting our hypothesis that elevated concentrations of pGpG can increase the half-life of c-di-GMP by reducing PDE-A activity.

2.5 Identification of pGpG binding proteins from the *V. cholerae* ORFeome

Based on the above results, the PDE-B responsible for hydrolyzing pGpG is critical for completing the c-di-GMP degradation pathway. To identify this enzyme, we utilized a high throughput DRaCALA-based screen to interrogate pGpG binding to a library of open reading frames (ORFs) (43, 44). The *V. cholerae* El Tor N16961 complete genome ORF library (ORFeome) was used because 97% of the ORFs are represented (48) and *V. cholerae* utilizes c-di-GMP signaling extensively(16, 47). Each ORF was recombined into two destination vectors with an IPTG inducible T7 promoter, one containing a 10x histidine N-terminal tag and a second containing a 10x histidine-maltose binding protein (MBP) N-terminal tag. These two libraries were individually introduced into an *E. coli* T7Iq expression strain and arrayed in 96-well plates. Following IPTG induction, whole cell lysates were generated and assayed for binding to pGpG using DRaCALA. The fraction bounds for each ORF tested are listed in Table 8 (see Appendices). Positive hits were defined as three standard deviations above the mean fraction bound of the entire library. For validation, each positive hit was re-picked from the expression library and new were re-generated and

re-assayed for pGpG binding. The fraction bound of each ORF to pGpG is shown for both ORFeomes with validated hits in color (Fig. 6). A list of hits and their known or predicted functions is provided in Table 1.

Table 1. pGpG-binding screen results from *V. cholerae* ORFeome libraries.

VC Number	Protein Function*	Evidence
VC0341	Oligoribonuclease	Predicted by homology
VC0371‡	Replicative DNA helicase	Predicted by homology
VC0419†	RNase G	Predicted by homology
VC0653	GGDEF-EAL domain phosphodiesterase	(71)
VC0658	GGDEF-EAL domain phosphodiesterase	(81)
VC1592	EAL domain phosphodiesterase	(82)
VC1641	EAL domain protein	Predicted by homology
VC1652†	EAL domain phosphodiesterase	(13)
VC1710	EAL domain protein	Predicted by homology
VC2174	5´-nucleotidase	Predicted by homology
VC2459†	DNA repair protein RecO	Predicted by homology
VC2708	Guanylate kinase	Predicted by homology
VC2750	GGDEF-EAL domain protein	Predicted by homology
VCA0080	GGDEF-EAL domain protein	Predicted by homology
VCA0593	hypothetical protein with RecJ domain	N/A
VCA0681	HD-GYP domain phosphodiesterase	(83)
VCA0931	HD-GYP domain phosphodiesterase	(83)

*Predicted protein function identified based on UniProt search
†Only identified in the His-tagged ORFeome library
‡Only identified in the His-MBP-tagged ORFeome library

The *V. cholerae* ORFeome library includes known c-di-GMP binding proteins: 28 out of 31 GGDEF domain proteins (16), all five PilZ domain proteins (84), and all three c-di-GMP-binding transcription factors (26, 33, 85). None of these proteins were identified in this screen, indicating that the assay is specific for pGpG-binding proteins. We expected to identify EAL domain and HD-GYP domain proteins, both of which have been shown to bind pGpG (76, 79). The *V. cholerae* ORFeome library includes eleven out of twelve EAL domain proteins encoded in the genome, nine out of ten dual GGDEF-EAL domain proteins, and all nine HD-GYP domain proteins (16). Of these, four EAL-domain containing proteins: VC1592, VC1641, VC1652 and VC1710 (Fig. 6, blue dots); four GGDEF-EAL domain

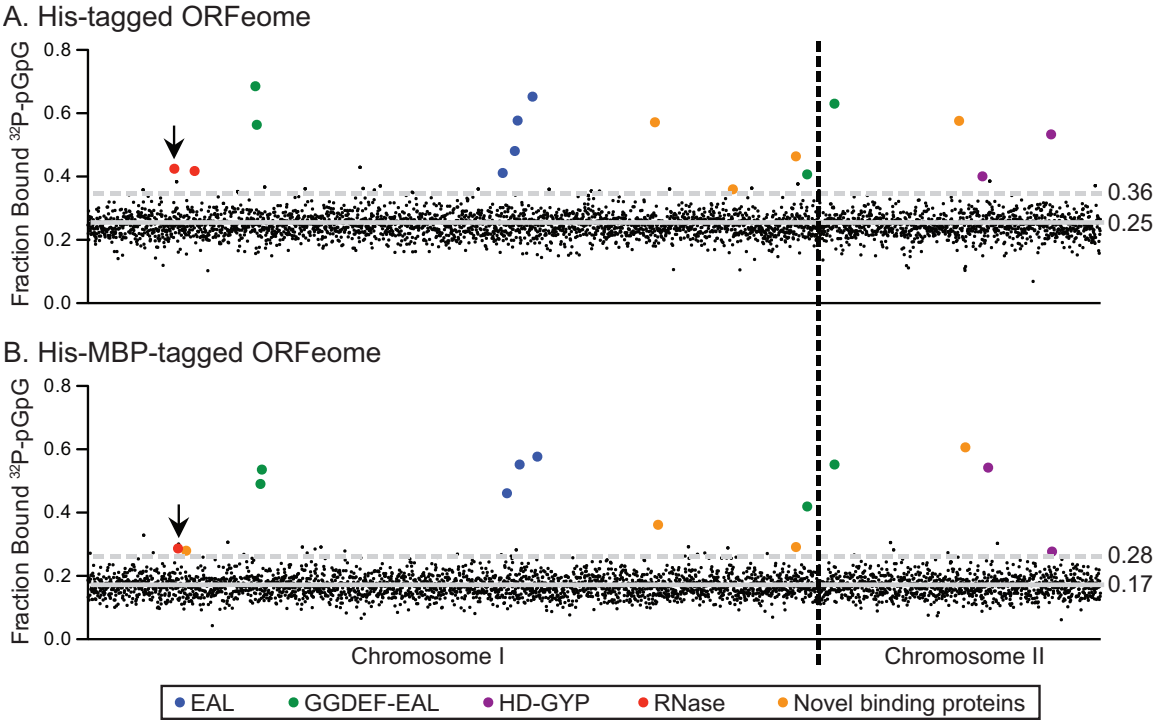

Figure 6. A high-throughput DRaCALA screen to identify pGpG binding proteins from *V. cholerae*. The fraction bounds of ^{32}P-pGpG to each ORF from the *V. cholerae* (A) His-tagged or (B) His-MBP–tagged expression libraries. The ORFs are arranged in ascending numerical order by chromosome. The average fraction bound calculated for each library (solid gray line), and 3 SDs above the average (dotted gray line) are noted. Orn is marked by the black arrows. ORFs with fraction bounds below the cutoff or which were not validated are shown in small black circles. Colored circles indicate validated hits.

containing proteins: VC0653, VC0658, VC2750 and VCA0080 (Fig. 6, green dots); and two HD-GYP domain containing proteins: VCA0681 and VCA0931 (Fig. 6, purple dots) bound pGpG in the screen. Not all EAL or HD-GYP domain ORF lysates showed binding in this system, which could reflect either genuine inability to bind pGpG or low protein expression in *E. coli,* resulting in concentrations below the K_d.

Since pGpG is a two-nucleotide-long RNA, we expected ribonucleases (RNases) to bind as well. The ORFeome library included all fifteen annotated RNases from the *V. cholerae* genome, of which two were found to bind pGpG: VC0210 and VC0341 (Fig. 6, red dots). Additionally, the screen identified five ORFs that were not previously known to interact with pGpG: VC0371, VC2147, VC2459, VC2708 and VCA0593 (Fig. 6, orange dots). Sequence homology predictions indicate that four out of these five proteins are predicted to interact with nucleic acids or nucleotides, while VCA0593 has no predicted function (Table 1). VC0341 is a homologue of oligoribonuclease (Orn), which is a known exoribonuclease that cleaves two to five nucleotide-long RNAs (51). Because VC0341 was shown to bind in both the His-tagged and the His-MBP-tagged ORFeomes it was chosen for further study.

2.6 Oligoribonuclease binds to pGpG specifically and can cleave it into GMP

To fully validate the interaction between Orn and pGpG observed in cell lysates, Orn from *P. aeruginosa* PA14 and *V. cholerae* were His-MBP-tagged, purified and assayed for pGpG binding by DRaCALA. pGpG bound both *P. aeruginosa* and *V. cholerae* Orn with fraction bounds of 0.32 ± 0.02 and 0.27 ± 0.01 in the absence of competitor (NC) (Fig. 7A, 7C). Addition of excess unlabeled pGpG

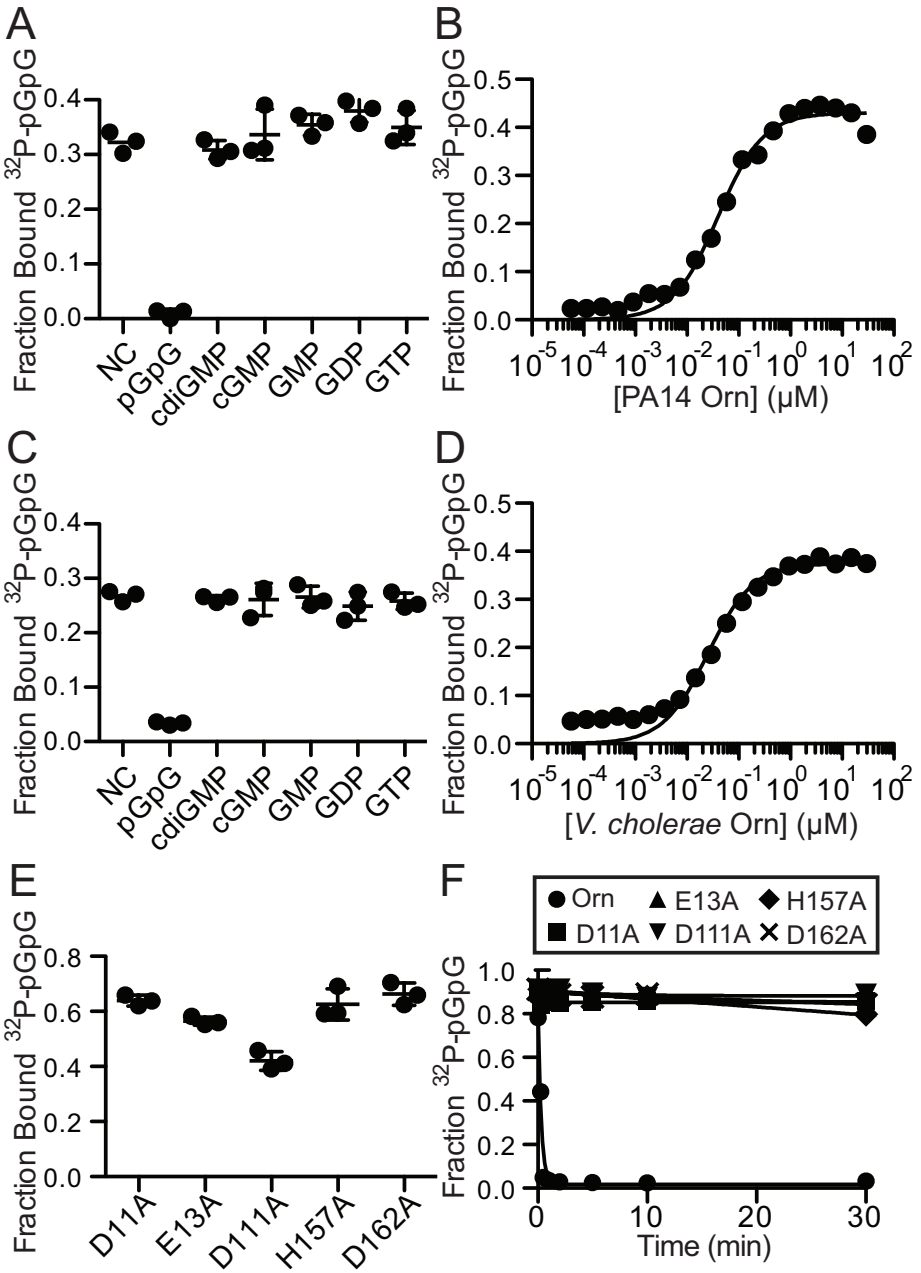

Figure 7. Orn binds and hydrolyzes pGpG. Quantification of fraction bound of ^{32}P-pGpG to Orn from (A) *P. aeruginosa* PA14 or (C) *V. cholerae* in the presence of indicated competitors (250 μM). The dissociation constants (K_d) of ^{32}P- pGpG binding to Orn from (B) *P. aeruginosa* PA14 and (*D*) *V. cholerae* as determined by DRaCALA. (E) Quantification of the fraction bound of ^{32}P-pGpG to purified *P. aeruginosa* Orn active site mutants D11A, E13A, D111A, H157A, and D162A. (F) The rate of ^{32}P-pGpG hydrolysis by purified wild type Orn and active site mutants of *P. aeruginosa* Orn: D11A, E13A, D111A, H157A, and D162A. All data shown represent the average and SD of at least three independent experiments.

effectively competed radiolabeled pGpG binding, reducing the fraction bounds to0.009 ± 0.008 and 0.03 ± 0.003 for *P. aeruginosa* and *V. cholerae* Orn ($p < 0.05$) (Fig. 7A, 7C). However, Orn binding to pGpG was not affected by the addition of excess c-di-GMP or any other guanine-containing nucleotides tested, indicating that Orn binds pGpG specifically (Fig. 7A, 7C). Finally, Orn from *P. aeruginosa* and *V. cholerae* bound to pGpG with high affinity, with K_d of 40 ± 2 nM and 25 ± 2 nM, respectively (Fig. 7B, 6D).

Having demonstrated specific and high-affinity binding, we then investigated the ability of Orn to hydrolyze pGpG. Purified *P. aeruginosa* His-MBP-Orn degraded pGpG (Fig. 7F) into GMP within ten seconds at room temperature. Orn belongs to the DEDDh sub-family of 3′ to 5′ exoribonucleases that have a highly conserved active site motif (61). The location of the DEDDh active site residues was shown in the solved crystal structure of *X. campestris* Orn (86) and an alignment of *P. aeruginosa* PA14 Orn with *X. campestris* Orn revealed the active site residues D11, E13, D111, H157, and D162 (Fig. 8). Single alanine point mutants in the signature motif of another DEDDh RNase, RNase T of *E. coli*, had significantly reduced catalytic activity (87). Therefore, we introduced single alanine substitutions into each residue of the DEDDh motif (D11A, E13A, D111A, H157A, and D162A) of *P. aeruginosa* Orn to assay for pGpG binding and degradation. All of the Orn variants bound pGpG (Fig. 7E), but failed to cleave pGpG (Fig. 7F). Taken together, these results demonstrate that purified Orn binds pGpG with nanomolar affinity and requires an intact active site for pGpG hydrolysis activity.

```
Q02F67|P. aeruginosa   1 ----MQNPQNLIWIDLEMTGLDPDRDVIIEMATIVTDSDLNTLAEGPVIAIHQPEEILAG 56
Q8P8S1|X. campestris   1 MADNVAGNDRLIWIDLEMTGLDTDRDSIIEIATIVTDAQLNVLAEGPELAIAHSLETLEA 60

Q02F67|P. aeruginosa  57 MDEWNTRQHGQSGLTQRVRESTVSMAEAEAQTLAFLEQWVPKRSSPICGNSICQDRRFLY 116
Q8P8S1|X. campestris  61 MDEWNRNQHRRSGLWQRVLDSQVTHAQAEAQTVAFLSEWIRAGASPMCGNSICQDRRFLH 120

Q02F67|P. aeruginosa 117 RHMPRLEGYFHYRNLDVSTLKELAARWAPQVRESFKKGNTHLALDDIRESIAELRHYRDH 176
Q8P8S1|X. campestris 121 RQMSRLERYFHYRNLDVSTIKELARRWAPAVASGFAKSSAHTALSDVRDSIDELRHYRQF 180

Q02F67|P. aeruginosa 177 FIKL---------- 180
Q8P8S1|X. campestris 181 MGTLGGDNGGGVQN 194
```

Figure 8. Alignment of the oligoribonuclease protein sequences from *P. aeruginosa* and *X. campestris*. The *P. aeruginosa* PA14 Orn and the *X. campestris* Orn protein sequences were aligned using ClustalW. The DEDDh active site residues previously reported for the *X. campestris* Orn crystal structure (D15, E17, D115, H161, and D166) and the corresponding amino acids in the *P. aeruginosa* Orn sequence (D11, E13, D111, H157, and D162) are shown in red. These residues were selected for mutagenesis in this study

2.7 Oligoribonuclease is the primary enzyme responsible for pGpG degradation

Our results led us to ask whether Orn is the primary PDE-B responsible for turnover of pGpG in *P. aeruginosa*. An *orn* transposon mutant (*orn*::tn) and a control strain *cat*::tn (chloramphenicol acetyltransferase, which is not expected to affect pGpG hydrolysis) from the PA14 Transposon Library (64) were grown to mid-log, lysed, and assayed for the ability to degrade radiolabeled pGpG. Lysates of the control *cat*::tn strain rapidly degraded pGpG (Fig. 9A). In contrast, the *orn*::tn strain showed a 10-fold reduced rate in pGpG cleaving ability, indicating that Orn is the primary enzyme involved in degradation (Fig. 9A). The *orn* mutant extracts still converted a small fraction of pGpG into GMP, indicating that there are additional proteins with PDE-B activity. Because purified HD-GYP domain phosphodiesterases from *P. aeruginosa* were shown to bind pGpG with higher affinity than c-di-GMP (76), we tested also pGpG degradation in cell lysates of transposon mutants of the two HD-GYP genes from *P. aeruginosa*. Lysates from PA4108::tn and PA4781::tn, showed no reduction in rates of pGpG cleavage compared to *cat*::tn (Fig. 9A), so their individual contribution to pGpG turnover in vivo is less than Orn. To further validate the defect of the *orn*::tn strain, an in-frame deletion of *orn* was generated in *P. aeruginosa* PA14 and the cell lysate was analyzed for pGpG degradation. The Δ*orn* strain showed a 25-fold reduced pGpG cleavage rate compared to the parental strain, consistent with the pGpG hydrolysis defect seen in the *orn*::tn strain (Fig. 9B, 9A). Complementation with wild type *orn* on an IPTG-inducible plasmid restored the ability to hydrolyze pGpG, while complementation with the catalytically inactive *orn* alleles did not (Fig. 9C). Addition of purified wild type Orn from PA14 to the Δ*orn*

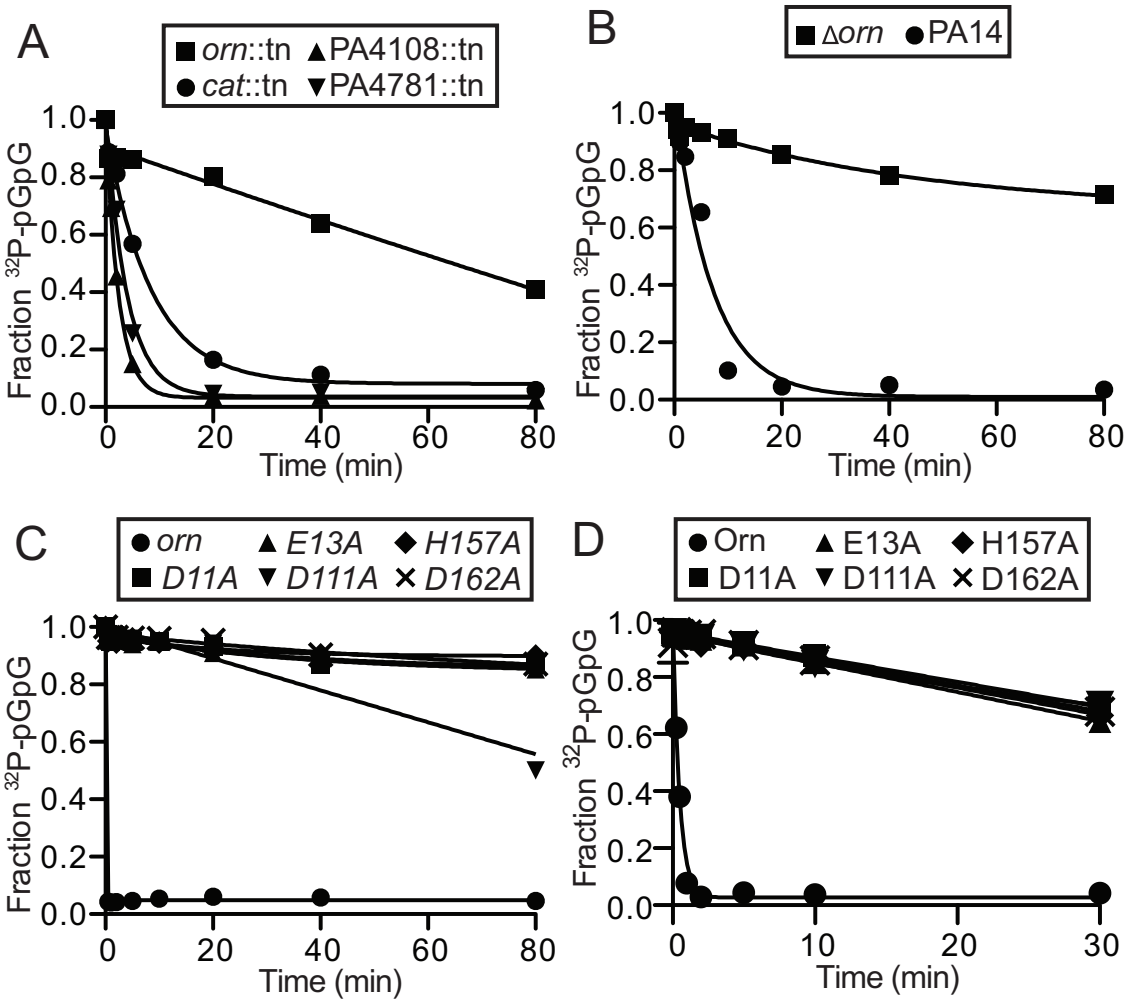

Figure 9. PA14 *orn* mutants are defective in hydrolyzing pGpG. The rate of ^{32}P-pGpG cleavage by (A) whole cell lysates of *P. aeruginosa* PA14 transposon insertion strains *cat::tn*, *orn::tn*, *PA4108::tn*, or *PA4781::tn*, (B) whole cell lysates of *P. aeruginosa* PA14 or Δ*orn* in-frame deletion mutant, (C) whole cell lysates of *P. aeruginosa* Δ*orn* mutant complemented with wild type or mutant alleles of *orn*, or (D) whole cell lysates of *P. aeruginosa* Δ*orn* with 100 nM of the indicated purified protein added. All data shown represent the average of triplicate independent experiments.

lysate restored hydrolysis activity, while addition of the purified catalytically inactive proteins (D11A, E13A, D111A, H157A, and D162A) had no effect (Fig. 9D). Taken together, these results demonstrate that Orn is the primary enzyme responsible for removing pGpG in *P. aeruginosa*.

2.8 Aggregation and biofilm are increased in Δ*orn* and *pel*-dependent

We assayed the Δ*orn* strain for two phenotypes positively regulated by c-di-GMP: auto-aggregation (78) and biofilm formation (77). The auto-aggregation assay measures the ability of bacterial aggregates to settle. Wild type *P. aeruginosa* PA14 cultures remain in suspension, while the Δ*orn* strain formed larger aggregates that settled to the bottom of the culture tube (Fig. 10A). Complementation of Δ*orn* with active *orn* on a plasmid abolished aggregate formation while complementation with catalytically inactive alleles did not (Fig. 10B). In a crystal violet microtiter plate assay for biofilm formation (88), cultures of wild type *P. aeruginosa* PA14 formed less biofilm than Δ*orn*, with A_{595} readings of 0.84 ± 0.37 and 1.98 ± 0.73, respectively ($p < 0.05$) (Fig. 10C).

In PA14, extracellular matrix products such as PEL exopolysaccharides are required for biofilm formation (62). Cyclic di-GMP elevates the production of the PEL exopolysaccharides (77) by increasing transcription of the *pel* operon (27) and activating biosynthesis (25). Therefore, we generated a Δ*orn*Δ*pel* double deletion mutant to asked whether PEL is required for the increased aggregation and biofilm formation we observe in the Δ*orn* mutant. The Δ*orn*Δ*pel* double mutant remained in suspension like the wild type and the Δ*pel* single mutant cultures (Fig. 10A), indicating that PEL is required for the aggregation observed in the Δ*orn* strain. The

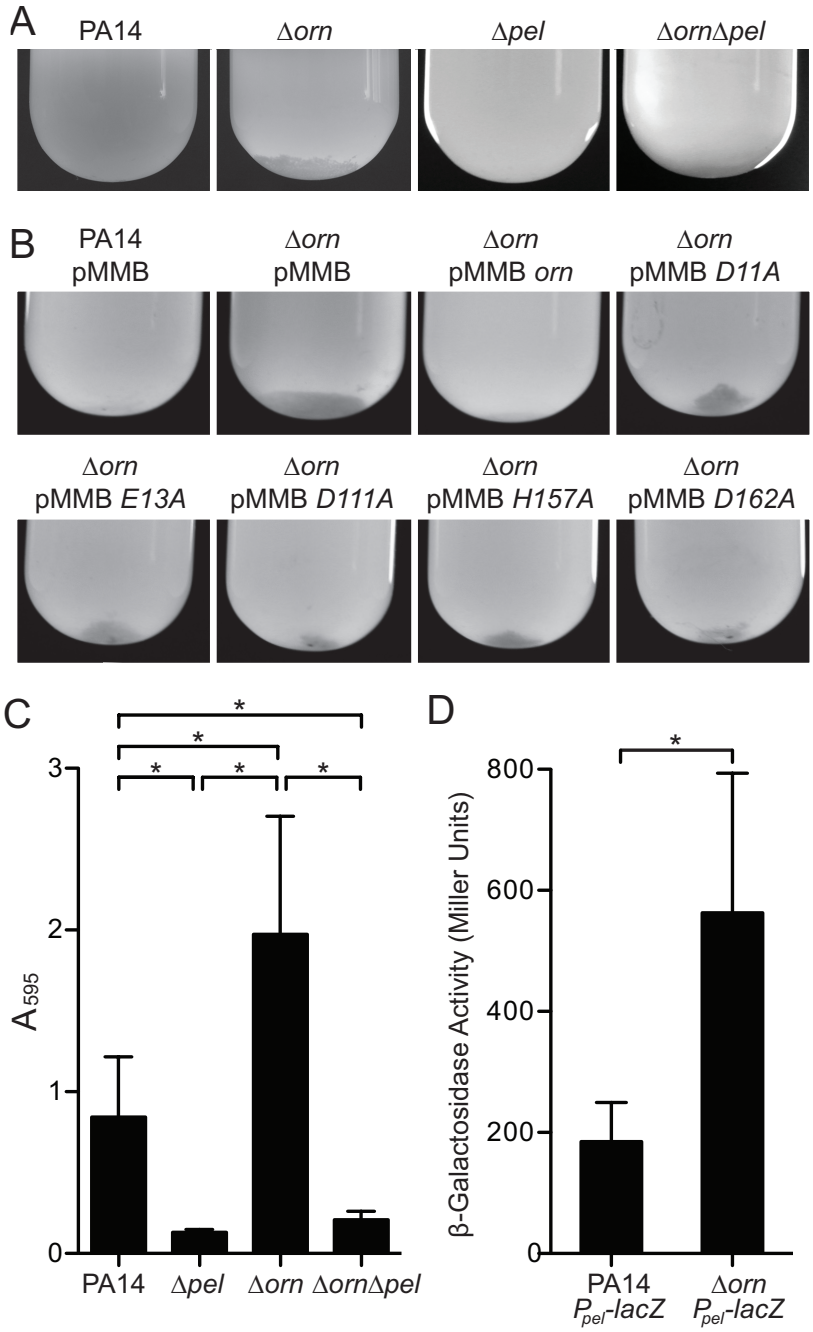

Figure 10. Increased aggregation and biofilm formation in the *orn* mutant is PEL dependent. (A) Photograph of auto-aggregation assays of PA14, Δ*orn*, Δ*pel*, and Δ*orn*Δ*pel* mutants. (B) Photograph of auto-aggregation assays of PA14 and the Δ*orn* strain complemented with WT *orn* and active site mutant alleles. (C) Quantification of the biofilm formed after 24 h of static culture by the crystal violet assay by determining absorbance at 595 nm (A_{595}). A_{595} values results show the average and SD of triplicate independent experiments. (D) Miller assay showing β-galactosidase activity of WT and Δ*orn* strains containing a single copy of the *pel* promoter *lacZ* (P_{pel}-*lacZ*) reporter on the chromosome. * indicates $p < 0.05$ by Students' unpaired two-tailed *t*-test assuming equal variance for C and D.

pel operon is also known to be required for in vitro pellicle biofilm formation in *P. aeruginosa* PA14 (62). As expected, the Δ*pel* mutant was unable to form biofilm in a microtiter plate assay, with a crystal violet A_{595} reading of 0.13 ± 0.02 compared to 0.84 ± 0.37 for wild type ($p < 0.05$) (Fig. 10C). The ability to form biofilm is also lost in the Δ*orn*Δ*pel* double deletion strain, which had an A_{595} reading of 0.21 ± 0.05 ($p < 0.05$ compared to wild type) (Fig. 10C). These data indicate that the increased aggregation and biofilm formation seen in the Δ*orn* strain is PEL-dependent. Another measure of elevated c-di-GMP levels is through the activity of the transcription factor FleQ, which leads to increased transcription from the *pel* promoter when bound to c-di-GMP (27). The *pel* promoter fused to *lacZ* (P_{pel}-*lacZ*) was integrated into the chromosome of both *P. aeruginosa* PA14 wild type and Δ*orn* strains. These strains were grown to mid-log and assayed for β-galactosidase activity. Approximately 3-fold increase in β-galactosidase activity was observed in the Δ*orn* strain compared to wild type, with 563 ± 230 Miller units compared to 185 ± 64 Miller units, respectively ($p < 0.05$) (Fig. 10D). Together, our results support the hypothesis that the loss of *orn* elevates c-di-GMP to promote c-di-GMP-regulated biofilms.

In additional support for the role of c-di-GMP in aggregation, overexpression of enzymes that either make or linearize c-di-GMP have opposing effects on aggregation in the Δ*orn* strain. Elevating c-di-GMP via overexpression of the DGCs *PA1107* and *wspR* increased aggregation. Conversely, decreasing c-di-GMP via expression of the PDE-As *PA2133* and *rocR* was unable to completely reverse bacterial aggregation (Fig. 11). These results indicate that because the Δ*orn* mutant

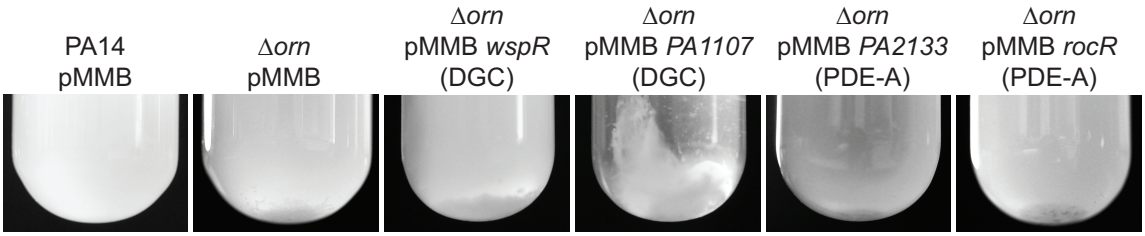

Figure 11. Aggregation assay of the orn mutant overexpressing diguanylate cyclases and EAL domain phospohodiesterase-As. Photograph of auto-aggregation assay of overnight cultures of WT harboring empty vector (pMMB), Δorn harboring either empty vector or vector-born copies of two known active diguanylate cyclases (DGCs) or two known active EAL domain phosphodiesterases (PDE-A).

lacks the ability to rapidly hydrolyze pGpG, it cannot complete degradation of c-di-GMP even when overexpressing EAL PDE-As.

2.9 Intracellular pGpG and c-di-GMP are elevated in Δ*orn*

To confirm the presence of increased c-di-GMP and pGpG in the PA14 Δ*orn* strain, both nucleotides were directly detected by LC-MS/MS. Wild type and *Δorn* cultures were grown mid-log (OD_{600} = 0.6) and late-log (OD_{600} = 2.0), and the nucleotides were extracted for analysis. Both c-di-GMP and pGpG were detected in the PA14 wild type and *Δorn* mutant strains. At mid-log, the *Δorn* strain had 5.9-fold increased c-di-GMP compared with PA14, with 2.86 ± 0.67 vs. 0.49 ± 0.08 μM, respectively ($p < 0.001$; Table 2). We also detect 6.6-fold more pGpG in the *Δorn* strain than PA14 in mid-log (70.8 ± 1.6 vs. 10.8 ± 1.4 μM; $p < 0.001$; Table 2). Lower concentrations of c-di-GMP and pGpG were detected from both strains at late-log, although both nucleotides remained higher in the *Δorn* strain. At late-log, the *Δorn* strain had 8.1-fold increased c-di-GMP compared with PA14 (0.65 ± 0.20 vs. 0.08 ± 0.01 μM, respectively; $p < 0.05$) and 6.6-fold increased pGpG compared with PA14 (26.3 ± 3.6 vs. 4.0 ± 1.0 μM, respectively, $p < 0.005$; Table 2). The above data confirm that pGpG and c-di-GMP are both elevated in orn mutants at both growth phases. All together, our results show that in addition to its known role degrading oligoribonucleotides (51), Orn is the major PDE-B that hydrolyzes pGpG in *P. aeruginosa*.

Table 2. Quantification of c-di-GMP and pGpG in PA14 wild type and Δ*orn*

	μM c-di-GMP			
	PA14	Δ*orn*	Δ*orn*/PA14	p-value
OD_{600} = 0.6	0.49 ± 0.08	2.86 ± 0.67	5.86	0.007
OD_{600} = 2	0.08 ± 0.01	0.65 ± 0.20	8.13	0.02
	μM pGpG			
	PA14	Δ*orn*	Δ*orn*/PA14	p-value
OD_{600} = 0.6	10.8 ± 1.4	70.8 ± 1.6	6.56	2.4×10^{-6}
OD_{600} = 2	4.0 ± 1.0	26.3 ± 3.6	6.62	1.3×10^{-3}

Data shown are mean ± standard deviation of three independent samples.

2.10 Discussion

2.10.1 Oligoribonucleases as PDE-Bs

Early characterization of c-di-GMP from the Benziman lab identified that c-di-GMP is linearized by PDE-As into pGpG, which is then degraded into two GMPs through the action of a presumed PDE-B (8). Through nearly three decades of c-di-GMP research that followed, the identity of the PDE-B remained unknown. We demonstrate here that the 3´-5´exoribonuclease Orn is the primary PDE-B in *P. aeruginosa*. The linearized product of c-di-GMP hydrolysis by PDE-As, pGpG, is a two-nucleotide-long RNA that matches the known substrates of Orn. We present several lines of evidence indicate that Orn is the primary PDE-B for c-di-GMP in *P. aeruginosa*: 1. Orn binds pGpG and not c-di-GMP, 2. Orn rapidly degrades pGpG in vitro, 3. lysates of *P. aeruginosa orn* mutants are greatly reduced for PDE-B activity, 4. DEDDh catalytic residues used to degrade oligonucleotides are required for pGpG cleavage, and 5. loss of *orn* results in enhanced intracellular pGpG and c-di-GMP. This additional role for Orn is important because we demonstrate that the loss of Orn results in increased c-di-GMP and c-di-GMP governed phenotypes, likely due to accumulated pGpG inhibiting PDE-As as shown in our model (Fig. 12A).

B

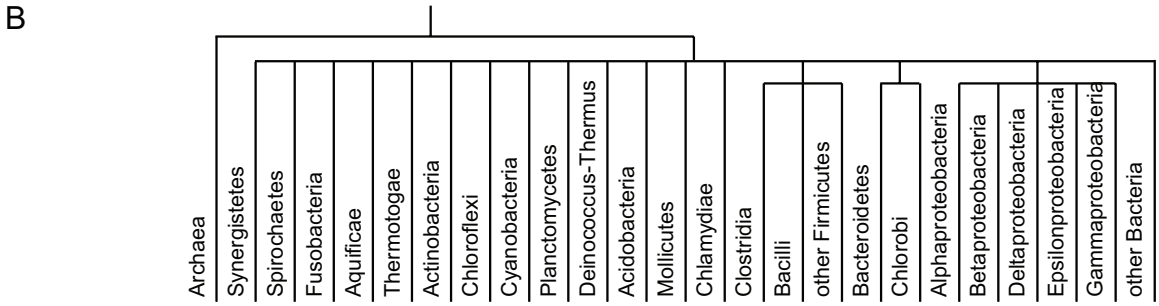

	Archaea	Synergistetes	Spirochaetes	Fusobacteria	Aquificae	Thermotogae	Actinobacteria	Chloroflexi	Cyanobacteria	Planctomycetes	Deinococcus-Thermus	Acidobacteria	Mollicutes	Chlamydiae	Clostridia	Bacilli	other Firmicutes	Bacteroidetes	Chlorobi	Alphaproteobacteria	Betaproteobacteria	Deltaproteobacteria	Epsilonproteobacteria	Gammaproteobacteria	other Bacteria
Total	83	5	7	5	8	7	74	9	31	6	6	6	10	6	49	33	6	55	5	75	52	28	11	103	31
Orn COG1949	0	0	0	0	0	0	64	0	0	0	0	0	0	0	0	0	0	0	0	0	47	8	0	101	4
NrnA COG0618	65	4	6	5	8	7	35	7	29	6	6	5	10	1	48	33	6	53	5	2	0	25	9	5	27
NrnB COG2404	52	4	0	1	3	0	0	0	2	0	0	1	0	0	2	5	0	0	1	3	12	4	10	5	6
GGDEF domain COG2199, COG2199	14	5	7	1	8	7	51	8	30	6	6	6	1	2	44	24	3	30	5	68	43	28	10	78	23
DisA domain COG1623, COG1624	42	5	7	5	8	7	50	7	31	6	6	3	7	6	48	33	6	46	1	0	0	27	0	0	25

Figure 12. The distribution of RNases, GGDEF domain proteins, and diadenylate cyclase domain proteins. (A) A model showing the synthesis and degradation of c-di-GMP with the inclusion of pGpG-mediated feedback inhibition of EAL-domain PDE-As and Orn as a PDE-B. (B) A simplified phylogenetic tree of prokyaryotic and archaeal species from the COG database and a table showing the number of species from each class that encodes the following proteins: Orn, NrnA, NrnB, GGDEF domains, and diadenylate cyclase (DisA) domains. The number of species were determined by a COG database search: Orn = COG1949; NrnA = COG0618; NrnB = COG2404; GGDEF = COG2199, COG3706; DisA = COG1623, COG1624.

Orn degrades short oligoribonucleotides regardless of sequence (49), raising the interesting possibility that it could degrade all linearized bacterial cyclic dinucleotides. In addition to c-di-GMP, two other cyclic dinucleotide signaling molecules have so far been identified in bacteria. Cyclic di-AMP (c-di-AMP) is synthesized by diadenylate cyclases which are widely distributed among bacterial species (6), and a hybrid cyclic AMP-GMP is synthesized by DncV in *V. cholerae* (89) and an unknown cyclase in *Geobacter sulfurreducens* (90). C-di-AMP is linearized into pApA by HD domain and DHH-DHHA-1 domain phosphodiesterases (91, 92), and cAMP-GMP is linearized by HD-GYP proteins in *V. cholerae* (93). The linearized cyclic di-nucleotides could also be hydrolyzed by Orn. However, not all species that utilize cyclic dinucleotides posses an Orn homolog. In a search of the COG database, only Actinobacteria, Fibrobacteres, Betaproteobacteria, Deltaproteobacteria, Gammaproteobacteria, and a few unclassified species are predicted to encode Orn (94) (Fig. 12B). *Bacillus subtilis* has both c-di-GMP (95) and c-di-AMP signaling systems (96, 97), but lacks *orn*. Nevertheless, *B. subtilis* is capable of degrading two to five nucleotide long RNAs using the potential Orn functional homologs NrnA, NrnB, YhaM, and RNase J1. All of these enzymes have oligoribonuclease activity and were able to partially rescue an *E. coli orn* conditional mutant (54, 58). NrnA homologs are found in many bacteria that lack Orn (54). Additionally, another RNase with oligoribonuclease activity, NrnC, was recently identified in *Bartonella birtlesii* and is widely found in Alphaproteobacteria (59). Nearly all bacteria that encode diguanylate and diadenylate cyclases encode at least one RNase capable of degrading short oligoribonucleotides. Based on this genomic

distribution, we predict these RNases are likely the primary PDE-Bs for hydrolyzing linearized cyclic dinucleotides into mononucleotides. Our observation that residual PDE-B activity is present in mutants lacking *orn* indicates that other proteins can cleave pGpG. Proposed PDE-B candidates include the HD-GYP domain proteins, which were shown to bind pGpG with higher affinity than c-di-GMP in vitro and were capable of degrading pGpG (76). However single transposon mutants in both of the HD-GYP domain proteins of *P. aeruginosa* PA14 did not show a defect in pGpG removal in our system, in contrast to the large defect observed for the *orn* mutant. Despite being shown to be essential in *E. coli* (52), *orn* mutants in *P. aeruginosa* are viable (64, 98), suggesting some functional redundancy. However, *P. aeruginosa* PA14 has no homologs of NrnA (54), NrnB (58), YhaM (expect value > 1 in a protein BLAST search), RNase J1 (99), or NrnC (59). Other RNases may possess oligoribonuclease activity that partially compensates for the loss of *orn*. Our DRaCALA screen identified one other RNase, VC0419 (predicted based on homology to be RNase G), but purified VC0419 did not hydrolyze pGpG (data not shown). Purified N-terminal His- and His-MBP-tagged RNase G from *E. coli* have been shown to be active in vitro against longer RNA substrates (≥10 nucleotides) (100-102). RNase G has a 5′ monophosphosphate sensor pocket that binds 5′ monophosphorylated RNAs and is distinct from the active site (103, 104). It is possible that pGpG, which has a 5′ monophosphate, is bound by the 5′ sensor of VC0419, but cannot be accessed by the active site due to its short length. Other PDE-Bs responsible for residual pGpG cleavage may have been missed in our ORFeome binding screen. The screen is limited by the exogenous expression of targets in *E.*

coli. For example, RNase E (VC2030) is structurally similar to RNase G and possesses a 5´ sensor pocket (104) and thus would be expected to bind pGpG, but SDS-PAGE analysis of the RNase E whole cell lysates from the ORFeome libraries showed the protein was poorly expressed. Another limitation of assaying whole cell lysates is that pGpG could be degraded by endogenous PDE-Bs from *E. coli*. Although Orn can rapidly degrade pGpG in whole cell lysates, we were able to detect binding in our DRaCALA screen because the buffer contained Ca^{2+} rather than Mn^{2+} or Mg^{2+}, which is required for Orn activity (50). Future studies with a *P. aeruginosa* ORFeome library will seek to identify other RNases responsible for the residual non-Orn PDE-B activity.

2.10.2 Intracellular concentration of pGpG and c-di-GMP

We were able to detect pGpG in both PA14 and the Δ*orn* mutant by LC-MS/MS. As expected, the level of pGpG in the Δ*orn* mutant was elevated compared with wild type. The levels of pGpG detected in the Δ*orn* strain at both mid- and late-log are well above the K_d of RocR binding to pGpG. As a consequence, pGpG can compete for c-di-GMP binding to inhibit RocR activity, leading to the observed increase in c-di-GMP concentration. There are two potential sources of pGpG in the cell: linearization of c-di-GMP and normal RNA processing and turnover (105). Future studies will determine the relative contribution of each source. The detection of pGpG in the PA14 indicates a potential physiological role for pGpG in *P. aeruginosa* during normal growth conditions. Other positive hits from the ORFeome screen represent potential cellular receptors for other pGpG-regulated processes.

A previous study reported ~ 11 μM of c-di-GMP *in P. aeruginosa PAO1* grown to mid-log in rich media (80). We detect ~ 0.5 μM c-di-GMP for PA14 grown at mid-log phase. The difference in c-di-GMP levels is likely due to differences between strains and estimations of cell size. The concentration of c-di-GMP for PA14 we detect is below the reported dissociation constants for *P. aeruginosa* c-di-GMP receptors, which are in the low micromolar range (Alg44 K_d = 5.6 μM (106), PelD K_d = 1 μM (25), and FleQ K_d = 15 - 25 μM (27)). This level of c-di-GMP is consistent with PA14 cells behaving as motile, planktonic cells at mid-log phase, which is indicative of reduced c-di-GMP signaling. However, the c-di-GMP concentration detected for the Δ*orn* mutant strain at mid-log is ~ 3 μM. The level of c-di-GMP in the Δorn mutant is sufficient to drive PelD activation, which is consistent with the requirement of the *pel* operon for biofilm formation and aggregation.

2.10.3 C-di-GMP phenotypes in *orn* mutants

The Δ*orn* strain formed more PEL-dependent biofilm and aggregates and had higher levels of pGpG and c-di-GMP. The connection between pGpG and elevated c-di-GMP is through pGpG inhibition of the PDE-As. The pGpG inhibition of PDE-A activity has also been observed for YfgF from *E. coli* (42). YfgF and RocR EAL domains are linked to different sensor domains and have different oligomer states (42, 107, 108) yet are both inhibited by pGpG. From our DRaCALA-based ORFeome screen, several other EAL and HD-GYP proteins also bind pGpG, suggesting that product inhibition by pGpG may be a general phenomenon. As a consequence, pGpG generated from c-di-GMP hydrolysis will act to extend c-di-GMP signaling unless a PDE-B is active to reduce the pGpG pool. As expected, deletion of the primary PDE-

B (*orn*) in *P. aeruginosa* resulted in the accumulation of c-di-GMP and increased biofilm formation and auto-aggregation. These observations will likely extend to other bacteria that use Orn homologs to degrade pGpG.

Orn may also be involved in other phenotypes regulated by c-di-GMP. Cystic fibrosis patients are chronically infected with mucoid strains of *P. aeruginosa*, leading to poor patient prognosis (109). The mucoid phenotype is due to high production of the alginate polysaccharide, which is synthesized by components of the *alg* operon (110). C-di-GMP regulates production post-transcriptionally by binding to the PilZ domain of Alg44 to activate alginate biosynthesis (106). Overexpression of the diguanylate cyclase PA1107 significantly enhanced alginate production in *P. aeruginosa* (106). In addition, transcription of the operon is regulated by several proteins, including the activator AlgB (111). A mucoid cystic fibrosis isolate FRD of *P. aeruginosa* becomes non-mucoid upon deletion of *algB*, although the strain is still able to produce low levels of alginate (111). A genetic screen for suppressor mutants that restored alginate production of the *algB* mutant identified six transposon insertion mutants. Two of these insertions were in the *orn* gene (98). A possible explanation based on our model (Fig. 12A) is that the loss of *orn* resulted in pGpG accumulation, inhibition of PDE-A, and thus elevated c-di-GMP to allow for increased Alg44 activation and enhanced mucoidy. These observations indicate that the PDE-B must be present and highly active during c-di-GMP signaling termination in order to prevent pGpG-mediated PDE-A inhibition.

2.11 Materials and Methods

2.11.1 *V. cholerae* ORFeome library pGpG binding screen

Gateway destination vectors were generated from pET-19-derived expression vectors pVL791 (N-terminal His_{10} tag, carbenecillin resistance) and pVL847 (N-terminal His_{10}-MBP tag, gentamycin resistance). The Gateway destination cassette was amplified from pRFA and cloned in frame with the N-terminal tags to produce the gateway adapted vectors pVL791 GW and pVL847 GW. The *V. cholerae O1 biovar El Tor str. N16961* pDONR221 library was obtained from BEI Resources. The library was grown in 1.5 mL lysogeny broth (LB) in 2-mL, 96-well plates (Greiner) with kanamycin (50 mg/mL) selection, and the plasmids were isolated using the 96-well $MultiScreen_{HTS}$ Kit (Millipore). The ORFs were moved into the expression vector using LR-clonase enzyme II (Invitrogen) and introduced into chemically competent *E. coli* strain T7Iq (NEB) following the manufacturer's protocols. Recombinants were selected on LB agar plates containing either carbenecillin (50 mg/mL) or gentamycin (15 mg/mL). Multiple colonies from individual transformations were inoculated in LB M9-rich media in 96-well plate format and grown overnight with shaking at 30 °C with the appropriate antibiotic and then resuspended in 20% volume:volume (vol:vol) glycerol and frozen at -80 °C.

E. coli T7Iq containing the *V. cholerae* ORFs were inoculated from frozen stocks in LB M9 rich media with the appropriate antibiotic in 96-well plate format, grown overnight with shaking at 30 °C, subcultured 1:50 into 1.5-mL fresh LB M9 media with antibiotic, and grown for 4 h at 30 °C with shaking; 1 mM IPTG was added to induce protein expression and cultures were grown for an additional 4 h. The

induced culture was pelleted, and cells were resuspended in 1/10th volume of binding buffer (10 mM Tris, pH 8.0, 100 mM NaCl, 5 mM $CaCl_2$), as well as 10 μg/mL DNase, 250 μg/mL lysozyme, and 10 mM phenylmethane sulfonyl fluoride or phenylmethylsulfonyl fluoride (PMSF). Cells were lysed by three freeze/thaw cycles at -80 °C/21 °C. ORFeome whole cell lysates were stored at -80 °C until analysis by DRaCALA.

Binding of radiolabeled ligand to the ORFeome whole cell lysates was determined by DRaCALA as previously described (43, 44). Briefly, 16 pM ^{32}P-pGpG was added to the ORFeome whole cell lysate 96-well plates using a Multiflo Microplate Dispenser (BioTek) and then applied to nitrocellulose sheets (GE Healthcare) using a 96-well pin tool (V&P Scientific). The nitrocellulose was air dried and imaged using a Fujifilm FLA-7000 phosphorimager (GE), and the intensity of the DRaCALA spots was quantified using Fujifilm Multi Gauge software v3.0, and the fraction bounds were quantified (43). To confirm that positive hits were not due to cross-contamination between plate wells, each positive hit was repicked from the expression library, and eight replicate single colonies were used to generate eight new whole cell lysates. These replicate lysates were compared with empty vector lysates for ^{32}P-pGpG binding by DRaCALA.

2.11.2 Synthesis of ^{32}P-c-di-GMP and ^{32}P-pGpG

^{32}P-c-di-GMP was synthesized by incubating α-^{32}P-GTP (0.33 μM) (Perkin Elmer) with WspR D70E (4 μM) in a 100 μL reaction in 10 mM Tris, pH 8, 100 mM NaCl, and 5 mM $MgCl_2$ at 37 °C for 16 h. ^{32}P-pGpG was synthesized from ^{32}P-c-di-GMP by incubating ^{32}P-c-di-GMP (0.167 μM) with RocR (20 μM) in a 80 μL

reaction in 10 mM Tris, pH 8, 100 mM NaCl, and 5 mM $MgCl_2$ at room temperature for 1 h. The reactions were stopped by heating at 98 °C for 10 min and the protein removed with a 3 kDa cutoff spin column (Millipore). The reaction product was assayed for purity by TLC. Samples were spotted on polyethyleneimine-cellulose TLC plates (EMD Chemicals), dried, and developed in mobile phase consisting of 1:1.5 (vol:vol) saturated NH_4SO_4 and 1.5 M KH_2PO_4, pH 3.60. The TLC plate was dried and imaged using Fujifilm FLA-7000 phosphorimager (GE). The intensity of the radiolabeled nucleotides was quantified using Fujifilm Multi Gauge software v3.0. The radiolabeled c-di-GMP and pGpG nucleotides synthesized were used for experimentation if determined to be ≥ 95% pure.

2.11.3 Strains and culture conditions

The primers, plasmids, and strains used in this study are listed in Tables 5, 6, and 7, respectively in the Appendices. The in-frame deletion of *orn* was generated in *P. aeruginosa* PA14 using a Flp-*FRT* recombination system (112). The ~1-kb region upstream and downstream were PCR amplified and restriction digested to introduced these fragments into a pEX-Gn-based plasmid for making in-frame deletions as previously described (112). Deletions were verified by PCR. The *pel* promoter-*lacZ* fusion on a pCTX plasmid was incorporated into the genomic *att* site as previously described (113).

The alanine point mutations were generated by QuikChange using the primers listed in Table 4. Silent mutations resulting in addition or removal of a restriction site were introduced to facilitate mutagenesis: these were the addition of an AfeI site in D11A and H157A, addition of an MscI site in D111A, and removal of EcoRV in

D162A. The *orn* alleles from *P. aeruginosa* PA14 were cloned into pVL847 for purification and pMMB for complementation. The pMMB and pVL847 plasmids were maintained with gentamycin (15 mg/mL) and induced with 1 mM IPTG. Transposon mutants from the PA14 Non-Redundant Transposon Insertion Mutant Library (64) were maintained with gentamycin (15 mg/mL).

2.11.4 Protein expression and purification

His-MBP-RocR, His-MBP-Orn from *V. cholerae*, and His-MBP-Orn and His-MBP-Orn variants from *P. aeruginosa* were purified as previously described (43). Briefly, *E. coli* T7Iq strains or *E. coli* BL21 (DE3) containing expression plasmids were grown overnight, subcultured in fresh media, and grown to OD_{600}~1.0 when expression was induced with 1 mM IPTG. Induced bacteria were pelleted and resuspended in 10 mM Tris, pH 8, 100 mM NaCl, and 25 mM imidazole and frozen at -80 °C until purification. Proteins were purified over a Ni-NTA column followed by anion exchange on a Q-Sepharose column. Purified proteins were dialyzed twice against 10 mM Tris, pH 8, 100 mM NaCl, and 25% (vol:vol) glycerol, aliquoted, and frozen at -80 °C until use.

2.11.5 Whole cell lysate generation

Overnight cultures of *P. aeruginosa* PA14 parental, mutant, or complemented strains were subcultured 1:50 into fresh LB media with appropriate antibiotic and IPTG conditions, grown to OD_{600} = 0.4 at 37 °C with shaking, resuspended in 1/10th volume of reaction buffer (10 mM Tris, pH 8, 100 mM NaCl, 5 mM $MgCl_2$), 10 µg/mL DNase, 250 µg/mL of lysozyme, and 10 mM PMSF, and lysed by sonication.

DRaCALA Measurement of Ligand Binding, Nucleotide Competition, and Dissociation Constant.

The use of DRaCALA to probe protein-ligand interactions has been previously described (43). To assay binding, pure protein in binding buffer (10 mM Tris, pH 8.0, 100 mM NaCl, 5 mM $CaCl_2$) was mixed with radiolabeled ligand (4 pM ^{32}P-c-di-GMP or ^{32}P-pGpG), applied to nitrocellulose sheets, dried, imaged, and the fraction bound quantified (43). For competition assays, excess of unlabeled nucleotides were added to radiolabeled ligand and purified protein before analysis by DRaCALA (43). To measure K_d, twofold serial dilutions of purified His-MBP-Orn from either *P. aeruginosa* or *V. cholerae* were made in binding buffer (10 mM Tris, pH 8, 100 mM NaCl, 5 mM $CaCl_2$) and mixed with radiolabeled ligand and the fraction bound, and K_d was calculated as previously described (43).

2.11.6 Cell lysate and protein activity assays

The activity of whole cell lysates and purified proteins against ^{32}P-labeled substrates was measured by monitoring the appearance of ^{32}P-labeled products on TLC. The reactions were carried out at 37 °C in reaction buffer (10 mM Tris, pH 8, 100 mM NaCl, and 5 mM $MgCl_2$). At appropriate times, aliquots were removed and the reaction stopped by adding an equal volume of 0.2 M EDTA, pH 8, and heated at 98 °C for 10 min. (See 2.11.2 for TLC conditions.)

2.11.7 Aggregation assay

Cultures of *P. aeruginosa* strains were grown in 10 mL LB with appropriate antibiotic and IPTG conditions for 24 h at 37 °C with shaking. Cultures were imaged after 30 min of aggregate settling at room temperature.

2.11.8 Microtiter plate biofilm assay

P. aeruginosa PA14 wild type and mutant strains were grown overnight in LB at 37 °C with shaking. Overnight cultures were diluted 1:100 in LB and grown as static cultures in a 96-well polystyrene plate (Greiner) at 30 °C inside a humidified chamber for 24 h. The cultures were washed of planktonic cells and stained with crystal violet as previously described (88). The A_{595} was measured on a SpectraMax M5 spectrophotometer (Molecular Devices).

2.11.9 β-galactosidase reporter assay

P. aeruginosa strains containing the reporter were grown overnight in LB at 37 °C with shaking. Overnight cultures were subcultured in LB and grown at 37 °C with shaking to mid-log (OD_{600} = 0.5). The β-galactosidase activity was measured according to previously published methods (114).

2.11.10 Quantification of intracellular c-di-GMP and pGpG.

P. aeruginosa PA14 wild type and Δ*orn* strains were grown overnight in LB at 37 °C with shaking, subcultured 1:100 in 20 mL LB, and grown at 37 °C with shaking to mid-log (OD_{600} = 0.6) and late-log (OD_{600} = 2); 15 mL was pelleted by centrifugation, resuspended with 100 µL ice-cold extraction buffer, 40:40:20 (vol:vol:vol) MeOH, acetonitrile, and water with 0.1 N formic acid, incubated 30 min

at -20 °C for lysis, and neutralized after a 30-min incubation with 4 µL 15% (weight/vol) NH_4NCO_3. Cellular debris was pelleted, and the supernatant was removed for desiccation by a Savant SpeedVac Concentrator (Thermo Scientific). Desiccated samples were suspended in 100 µL ultra-pure water, and insoluble material was pelleted at 21,000 × *g* using a table-top microcentrifuge at room temperature for 5 min. The resulting supernatant was filtered through a Titan syringe filter (PVDF, 0.45 µm, 4 mm) before quantification of c-di-GMP and pGpG. Quantification of c-di-GMP and pGpG in cellular extracts was performed using LC-MS/MS on a Quattro Premier XE mass spectrometer (Waters) coupled with an Acquity Ultra Performance LC system (Waters). Cyclic-di-GMP was detected in 10-µL injections of filtered extracts using previously described HPLC and MS parameters (115). For the detection of pGpG, filtered extracts were diluted 1:100 in ultra-pure water, and 10-µL injections of the diluted extracts were then analyzed with electrospray ionization multiple reaction monitoring in positive-ion mode at *m/z* 709.31 → 152.26. The MS parameters were as follows: capillary voltage, 2.8 kV; cone voltage, 34 V; collision energy, 40 V; source temperature, 120 °C; desolvation temperature, 350 °C; cone gas flow (nitrogen), 0 L/h; desolvation gas flow (nitrogen), 800 L/h; and collision gas flow (nitrogen), 0.2 mL/min. Chromatography separation was normal phase using a Waters BEH Amide 1.7 µm, 2.1 × 100-mm column with the following flow rates and gradient of solvent B (acetonitrile) to solvent A (50 mM ammonium acetate in ultra-pure water, pH 9.28): t = 0.00 min; 0.200 mL/min and A-1%:B-99%, t = 1.00 min; 0.300 mL/min and A-1%:B-99%, t = 2.00 min; 0.300 mL/min and A-10%:B-90%, t = 4.00 min; 0.400 mL/min and A-25%:B-75%, t = 5.01

min; 0.400 mL/min and A-99%:B-1%, t = 5.50 min; 0.400 mL/min and A-99%:B-1%, t = 5.51 min; 0.500 mL/min and A-99%:B-1%, t = 13.00 min; 0.500 mL/min and A-99%:B-1%, t = 13.01 min; 0.200 mL/min and A-1%:B-99%, t = 15.00 min; 0.200 mL/min and A-1%:B-99% (end of gradient). Standard curves for calculating c-di-GMP and pGpG concentrations in cellular extracts were generated by dissolving chemically synthesized c-di-GMP (Axxora) in water at concentrations of 250, 125, 62.5, 31.25, 15.62, 7.81, 3.91, and 1.95 nM and dissolving chemically synthesized pGpG (Axxora) in water at concentrations of 125, 62.5, 31.25, 15.62, and 7.81 nM. The intracellular concentrations of c-di-GMP and pGpG were determined by first calculating the total number of colony-forming units in each sample and multiplying this value by the intracellular volume of a single bacterium. The number of cells per sample were enumerated at OD_{600} = 0.6 and 2.0 for each strain by plating serial dilutions. The volume of one bacterium was estimated to be 4.3×10^{-1} fL, assuming the bacterium to be cylindrical in shape with spherical poles having an average length of 1.5 and 0.65 μm in diameter based on scanning electron microscopy image analysis (116). The total c-di-GMP and pGpG extracted in each sample were then divided by the total intracellular volume of the cells in the sample to provide the intracellular concentration of each analyte.

Chapter 3: A subset of exoribonucleases are the PDE-Bs for cyclic di-nucleotides

3.1 Introduction

The cyclic di-nucleotide signaling molecule c-di-GMP regulates a wide range of bacterial processes such as biofilm formation. Once it is no longer needed, it is linearized into pGpG, which is then further degraded to two GMPs to be recycled back into the pool of free cellular nucleotides. The enzyme responsible for the cleavage of pGpG was previously unknown. We demonstrated that the oligoribonuclease (Orn) is the main PDE-B in *P. aeruginosa* and demonstrated that accumulated pGpG inhibits c-di-GMP turnover via inhibition of PDE-A function. Thus, the activity of the PDE-B is crucial for c-di-GMP signal termination. However, not all bacteria that encode cyclic di-nucleotide synthesizing enzymes also encode *orn*, suggesting that other enzymes must be acting as PDE-Bs in these species. Although *orn* homologs are not found in all bacteria, other RNases, termed "nanoRNases" have recently been described to fill the same role in turnover of two to five nucleotide long RNAs. Therefore, we hypothesized that these RNases could also be the major PDE-B for c-di-GMP in bacteria lacking *orn*.

NrnA from *B. subtilis* (54), NrnB from *B. subtilis* (58) and NrnC from *B. birtlesii* (59) have been shown to be able to cleave short oligoribonucleotides and can restore growth to an *orn* mutant in E. coli. Although now all classified as "nanoRNases" and shown to have 3′ to 5′ exoribonuclease activity against very short RNAs, they are not all structurally related and do not have the same substrate

specificity or divalent cation requirements. NrnA and NrnB are both members of the DHH/DHHA1 phosphoesterase family (60) while Orn and NrnC are members of the DEDDh and DEDDy family exonucleases (61), respectively. Both Orn and NrnC are inhibited by pAp (53, 59), while NrnA can act as a pAp phosphatase to degrade pAp to AMP (53) but NrnB cannot (58). Furthermore, in these in vitro experiments, different nanoRNAses had different substrate preferences. NrnA rapidly degraded a cytosine 5mer and an adenine 5mer to mononucleotides, while Orn, NrnB, and NrnC accumulated 2mers (although this may have been an artifact of the assay, which had a the 5´ cyanine dye on the 5mer). Finally, these enzymes appear to have different divalent cation preferences: NrnA was only active in the presence of Mn^{2+} and not Mg^{2+}, Zn^{2+} and Ca^{2+} (54), NrnB was active in Mn^{2+} and Co^{2+} and partially active in Mg^{2+} (58), and NrnC was equally active in Mn^{2+} and Mg^{2+}, less active in Co^{2+}, and not active in Ca^{2+} (59). Similar to NrnC, Orn was shown to be active in Mn^{2+} and Mg^{2+}, but not active in Ca^{2+} (50). Due to these differences from Orn and the fact that the previous in vitro experiments assayed activity against 5´Cy5-AAAAA and 5´Cy5-CCCCC (54, 58, 59), the ability of these enzymes ability to degrade pGpG is uncertain. In addition to these nanoRNases, the 3´ to 5´ exoribonuclease YhaM (117) and the 5´ to 3´ exoribonuclease RNase J1 (118) were also shown to have some in vitro activity against 5mer cytosine and adenine nanoRNAs (58). However YhaM showed far more rapid turnover of DNA than RNA and RNase J1 had very little activity against 5mers (58). Expression of both YhaM and RNase J1 could also only partially suppress the slow growth phenotype of the *E. coli* conditional *orn* deletion

mutant, suggesting that these two enzymes do not predominately function as nanoRNases in the cell (58).

Due to the ability of these enzymes to cleave nanoRNAs in vivo, we tested whether NrnA, NrnB, NrnC, YhaM and RNase J1 have PDE-B activity to degrade pGpG to GMP. We then also determined whether these NanoRNases can rescue the *orn* mutant phenotypes of *P. aeruginosa* PA14 associated with elevated c-di-GMP. Experiments are underway to determine whether loss of these enzymes also elevates c-di-GMP signaling in two other species that utilize c-di-GMP signaling and encode a non-Orn nanoRNase: *B. subtilis,* which has genes encoding the two putative nanoRNases *nrnA* and *nrnB*, and *C. crescentus*, which encodes *nrnC*. If these deletion mutants are also deficient in pGpG hydrolysis, then these nanoRNases are likely to be the major PDE-Bs for pGpG hydrolysis across bacterial species.

3.2 NanoRNases can bind pGpG

We initially identified Orn as a PDE-B by a screen conducted to identify pGpG binding proteins (119). To begin to determine whether any of these RNases have function as PDE-Bs, we cloned *nrnA*, *nrnB*, *yhaM* and *rnjA* from *B. subtilis* 168 and *nrnC* from *C. crescentus* CB15 into expression vectors. N-terminal 10x-His tagged NrnA, NrnB, NrnC, YhaM, and RNase J1 were purified and their ability to bind pGpG was measured using DRaCALA (43) and quantified (Fig. 13A, 13B). NrnA, NrnB and NrnC could increase fraction bound to pGpG above the no protein control ($p < 0.05$), while RNase J1 and YhaM could not (Fig. 13B). NrnB showed less pGpG binding by DRaCALA compared to NrnA and NrnC, however this is likely because binding was assayed in a buffer condition in which NrnB is active (10

mM Tris, pH 8.0, 100 mM NaCl, 5 mM $CaCl_2$), resulting in partially degraded probe and loss of detectable binding (data not shown).

3.3 NanoRNases can degrade pGpG

The ability of NrnA, NrnB, NrnC, RNase J1 and YhaM to hydrolyze pGpG was tested in vitro. NrnA, NrnB, and NrnC were highly active against pGpG, with 0.1 μM of protein able to rapidly hydrolyze 100 μM pGpG (Fig. 13C). The half-life of pGpG was 0.6 minutes for NrnA and NrnC and 3.5 minutes for NrnB. Because NrnB is able to cleave pGpG, it is able to bind it and the low binding observed by DRaCALA was indeed due to NrnB hydrolysis of the ^{32}P-pGpG probe. As expected of an enzyme unable to bind pGpG, 10 μM RNase J1 also could not hydrolyze 100 μM pGpG to GMP in vitro, with no change in ^{32}P-pGpG levels over the activity assay period. Although we could detect YhaM-mediated pGpG hydrolysis, it was only observed at 100x higher protein concentration than NrnA, NrnB or NrnC (10 μM YhaM vs. 0.1 μM). Therefore, we expect that only NrnA, NrnB, and NrnC are truly capable of catalyzing pGpG hydrolysis. However, the inability of purified protein to bind and cleave pGpG in an in vitro experiment does not necessarily indicate the lack of activity in vivo. Purified proteins may have lost activity during the purification process or the N-terminal His-tag utilized for purification may have interfered with cleavage. Therefore, we asked whether these enzymes could rescue the pGpG hydrolysis defect of the PA14 Δ*orn* cell lysates reported in Chapter 2 (Fig. 9).

3.4 NanoRNases can restore the pGpG hydrolysis of a PA14 Δ*orn* cell lysate

Each RNase was expressed off an IPTG inducible plasmid in the PA14 Δ*orn*

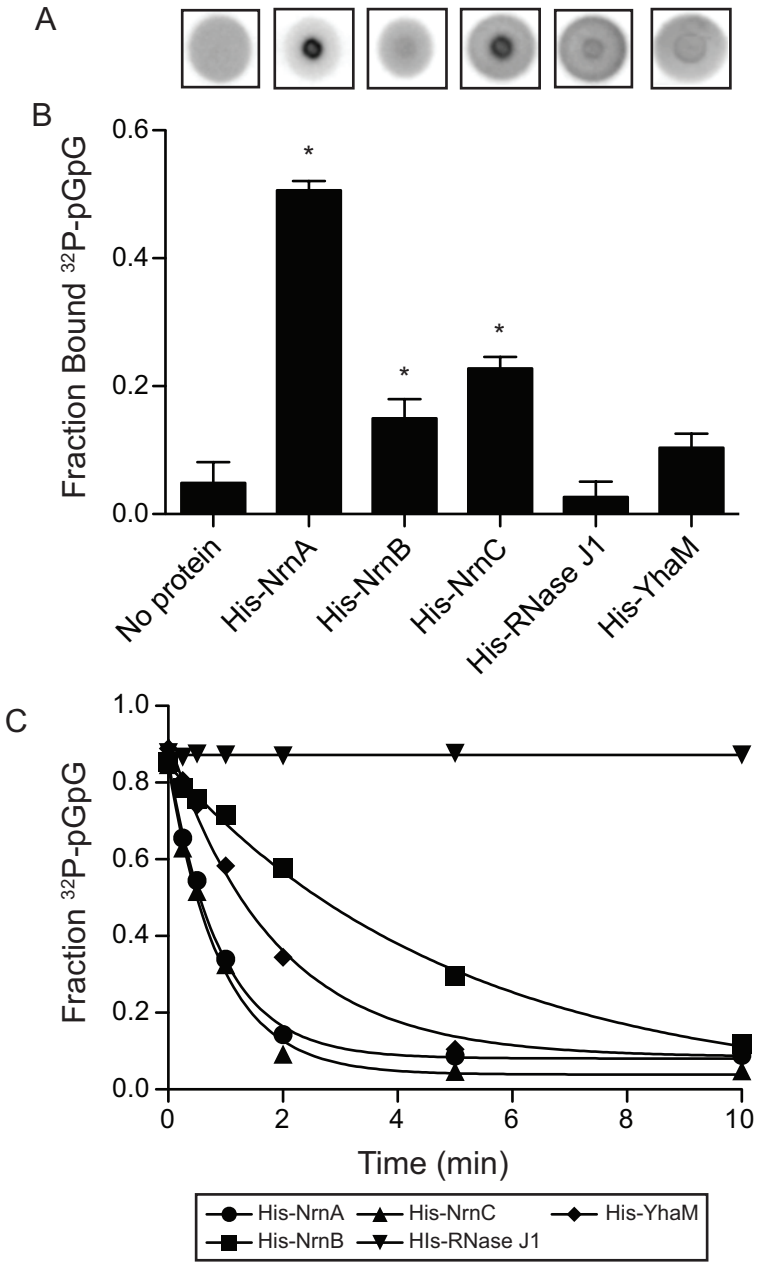

Figure 13. Binding and hydrolysis of pGpG by purified RNases. Image (A) and fraction bound quantification (B) of a DRaCALA to probe binding of 5 μM NrnA, NrnB, NrnC, RNase J1, and YhaM to ^{32}P-pGpG. Values shown are the average and SD of three independent experiments. * indicates $p < 0.05$ by Students' unpaired two-tailed *t*-test assuming equal variance. (C) The rate of 32P-pGpG hydrolysis by of purified NrnA (0.1 μM), NrnB (0.1 μM), NrnC (0.1 μM), RNase J1 (10 μM), and YhaM (10 μM) to 0.1 mM pGpG with ^{32}P-pGpG tracer.

strain, grown to mid-log, resuspended in activity buffer and normalized to the same OD_{600}, lysed and the lysates assayed for the ability to degrade ^{32}P-labled pGpG (Fig. 14). Empty vector lysates could not turn over pGpG, while all pGpG was degraded by the *orn* complementation strain by 20 minutes with a half life of ~10 min. As expected based on the in vitro data, neither expression of *rnjA* nor *yhaM* could restore the ability of lysates to degrade pGpG. However, complementation of *nrnA*, *nrnB*, and *nrnC* all allowed hydrolysis of pGpG. The *nrnB* lysates degraded pGpG more rapidly than lysates from cells expressing *orn*, with no pGpG remaining by 10 min (half life of 2.4 minutes), while the *nrnA* and *nrnC* complementation lysates had a slower pGpG turnover rate. However, factors such as expression levels and protein stability make it difficult to draw conclusions on the true relative activities of these enzymes in vivo. A Western blot detecting the levels of enzyme expressed in each strain would allow determination of protein levels after induction. Nevertheless, these results demonstrate that the nanoRNases NrnA, NrnB, and NrnC are likely able to also act as PDE-Bs and cleave pGpG.

3.5 NanoRNases can suppress increased biofilm and aggregation in PA14 Δ*orn*

The ability of NrnA, NrnB, and NrnCs to restore pGpG hydolysis in the PA14 Δ*orn* lysates indicates that these nanoRNases could restore the other c-di-GMP-dependent phenotypes seen in the PA14 Δ*orn* mutant strain to wild type levels. Previously, we showed that the Δ*orn* strain had elevated c-di-GMP via pGpG inhibition of the enzymes responsible for cleaving c-di-GMP, resulting in elevated aggregation and biofilm (119). Therefore, if any of these RNases can cleave pGpG,

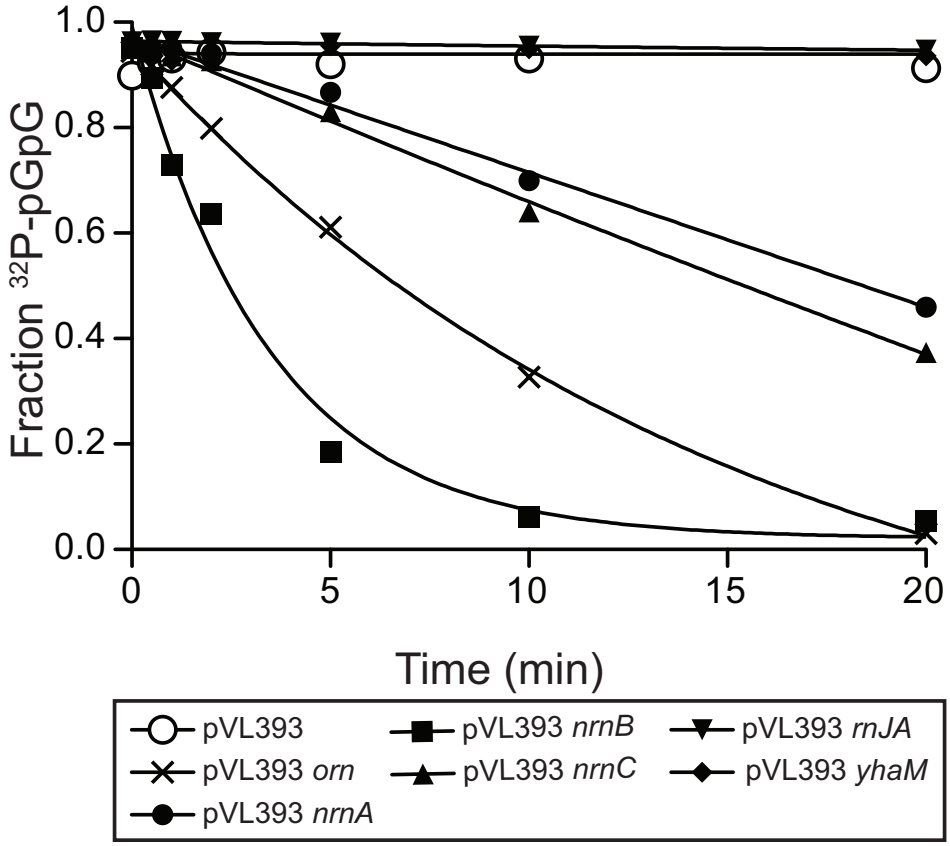

Figure 14. RNases can rescue PA14 Δ*orn* pGpG hydrolysis defect. The rate of pGpG cleavage by whole cell lysates of *P. aeruginosa* PA14 Δ*orn* complemented with the indicated RNase on pVL393, a single-copy IPTG inducible plasmid.

we expect them to return aggregation and pellicle biofilm formation to wild type levels. The aggregation assay shows the ability of the bacteria to adhere to each other and form large clumps that can settle out of the culture at the bottom of the culture tube. PA14 Δ*orn* containing an empty vector formed large aggregates, which settled to the bottom of the tube (Fig. 15A). Complementation of the PA14 Δ*orn* with plasmid-encoded *orn*, *nrnA*, *nrnB*, and *nrnC* fully prevented aggregate formation, reverting this phenotype to wild type (Fig. 15A). PA14 Δ*orn* strains complemented with *rnjA* and *yhaM* still formed aggregates, although both are slightly reduced in aggregate formation compared to the levels formed by the strain containing an empty vector. We previously showed that deletion of *orn* caused a ~ 2x increase in pellicle biofilm compare to wild type (Fig. 10C). As expected, the PA14 Δ*orn* with empty vector showed increased pellicle biofilm formation, with $A_{595} = 0.47 \pm 0.04$ (Fig. 15B) in crystal violet assays in microtiter wells. Complementation with *orn*, *nrnA*, *nrnB*, and *nrnC* reduced biofilm by ~ 3-fold, with $A_{595} = \sim 0.14 \pm 0.2$, 0.15 ± 0.2, 0.14 ± 0.2, and 0.15 ± 0.2 ($p < 0.001$), respectively (Fig. 15B). Complementation with both *rnjA* and *yhaM* could also partially reverted the increased biofilm phenotype by ~ 1.5-fold, reducing the crystal violet to $A_{595} = 0.31 \pm 0.2$ ($p < 0.01$) and 0.36 ± 0.04 ($p < 0.05$), respectively (Fig. 15B). Although *rnjA* and *yhaM* complemented PA14 Δ*orn* lysates fail to degrade pGpG, these two strains can at least partially reduce c-di-GMP mediated phenotypes in the PA14 Δ*orn* strain, suggesting some pGpG hydrolysis ability that was not detected in the lysate ex vivo experiments.These results indicate that the nanoRNases NrnA, NrnB and NrnC can functionally substitite for Orn in cleaving pGpG in vitro and are likely to be PDE-Bs.

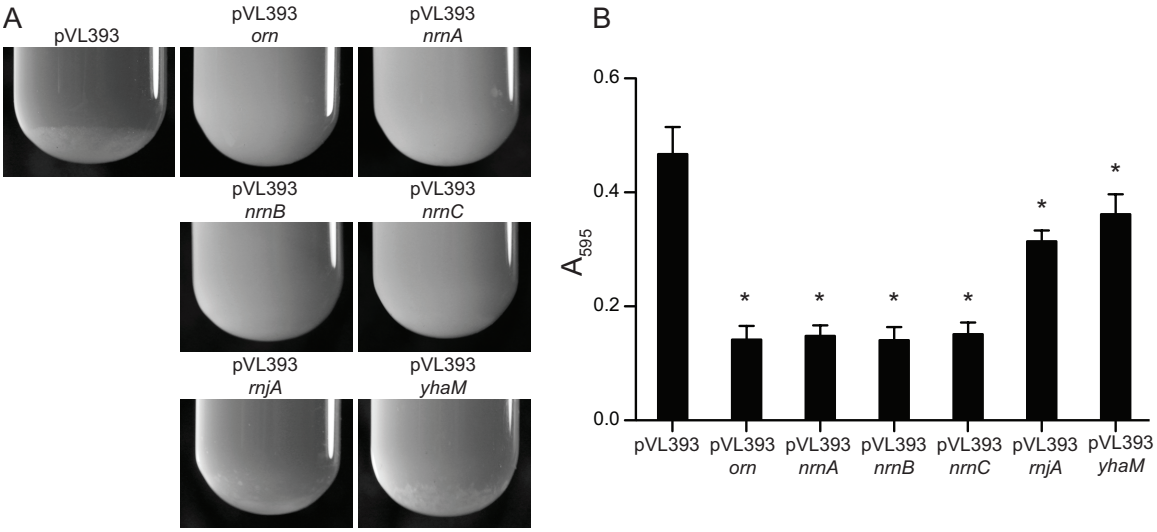

Figure 15. Complementation with RNases can reduce the elevated aggregation and biofilm in PA14 Δ*orn*. (A) Photograph of overnight cultures of PA14 Δ*orn* with either empty vector or complementation vectors showing auto-aggregate sedimenting at time 30 min after beginning of auto-aggregation assay. (B) The quantification of the biofilm formed by the PA14 Δ*orn* with either empty vector or complementation vector strains after 24 h of static culture. Biofilm cells were stained by crystal violet and quantified by reading the absorbance at A_{595}. Values are shown average and SD three independent experiments. * indicates $p < 0.05$ Students' unpaired two-tailed *t*-test assuming equal variance.

3.6 NanoRNases can rescue the growth defect in PA14 Δ*orn*

In addition to the c-di-GMP linked elevated aggregation and biofilm phenotypes, PA14 Δ*orn* forms smaller colonies and has slower growth than wild type in liquid culture (Fig. 18A, 18B). The ability of NrnA, NrnB, and NrnC to restore pGpG hydolysis indicates that they could potentially also rescue the growth defects seen in the PA14 Δ*orn* mutant strain. Complementation with a plasmid-born copy of the *P. aerugionsa orn* restored colony size (Fig. 16A) and growth in liquid media (Fig. 16B). As expected based on pGpG turnover by cell lysates, the empty vector and vectors with *rnjA* and *yhaM* could not restore either colony size or growth curve. Complementation with *nrnA*, *nrnB*, and *nrnC* all seemed to improve growth when compared to complementation with *orn*, resulting in cultures reaching a higher stationary phase OD_{600} compared to the *orn* rescueation strain. Taken together, these results indicate that NrnA, NrnB, and NrnC are PDE-Bs capable of rescuing growth at the same level as Orn, wheras RNase J1 and YhaM are not. This could be because RNaseJ1 and YhaM are not capable of in vivo turnover of pGpG, or because elevated intracellular pGpG levels and growth defect are not coupled.

3.7 Discussion

3.7.1 NanoRNases have PDE-B activity

The bacterial signaling nucleotide c-di-GMP is linearized to pGpG by PDE-As, which is hydrolyzed to two GMPs through the activity of an enzyme dubbed "PDE-B". We previously identified the major PDE-B enzyme in *P. aeruginosa* as Orn (119), which already had a known function in the turnover of nanoRNAs. Orn is

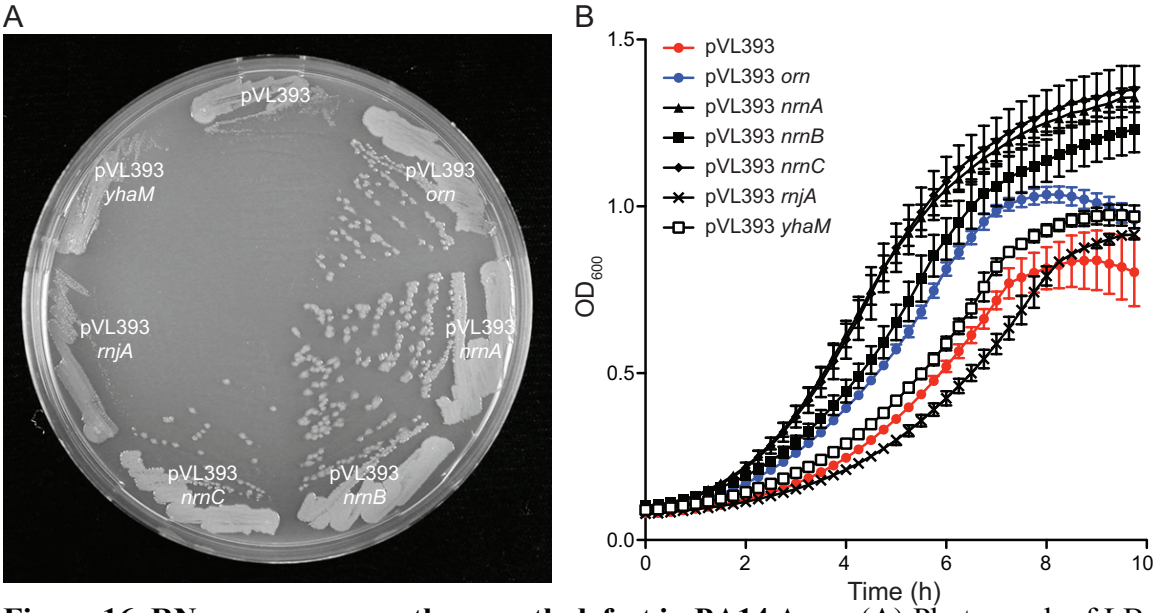

Figure 16. RNases can rescue the growth defect in PA14 Δ*orn*. (A) Photograph of LB-agar plate with IPTG induction showing difference in colony size of PA14 Δ*orn* with either empty vector or complementation vectors (B). The OD_{600} curve of the strains grown in LB with IPTG induction over a period of 10 hrs. Shown are the average and SD of three independent experiments.

believed to be the "finishing" enzyme, degrading the short oligoribonucleotides that accumulate to mononucleotides, which can then be recycled by the cell. This role can be filled by one or more of several RNases, depending on bacterial species (54, 58, 59).

Experiments here demonstrate that these RNases, dubbed "nanoRNAs" (54), are also capable of pGpG degradation and are the most likely candidate for PDE-B activity, meaning that conversion of c-di-GMP and RNA to mononucleotides converges at the nanoRNases. First, NrnA, NrnB, and NrnC are able to rapidly hydrolyze pGpG in vitro. Furthermore, they can rescue the pGpG hydrolysis defect of PA14 Δ*orn* lysates. Expression of NrnA, NrnB, and NrnC can rescue the enhanced biofilm formation and the growth defect of PA14 Δ*orn*. It appears that the RNase J1 cannot cleave pGpG in vivo and YhaM is much less active than NrnA, NrnB, and NrnC. Furthermore, as neither RNase J1 nor YhaM can restore the *P. aeruginosa* PA14 Δ*orn* in pGpG hydrolysis, decrease biofilm and aggregate formation, or rescue growth defects, they are likely not major PDE-Bs. The 3′ to 5′ exonucleases from *E. coli* cannot cleave two-nucleotide long RNAs in vitro. RNase R was able to hydrolyze RNA down to two nucleotides (120, 121), RNase II down to four (122, 123), and PNPase down to six (123), indicating that they are unlikely to be able to degrade nanoRNAs in vivo. It is possible that other RNases could also have yet unreported ability to degrade nanoRNAs. If so, they represent potential PDE-Bs for pGpG hydrolysis.

Loss of function of nanoRNases would result in an accumulation of pGpG, which could then accumulate to prevent c-di-GMP turnover via inhibition of the

PDE-As. If PDE-As from species other than *P. aeruginosa* are also inhibited by pGpG, nanoRNase activity could be involved in maintenance of c-di-GMP homeostasis. Current studies are underway to determine the effect of a dual *nrnA nrnB* deletion on *B. subtilis* c-di-GMP signaling. We expect levels of c-di-GMP to be elevated as we observe in the PA14 Δ*orn* strain. If this is true, it leads to the intriguing possibility of c-di-GMP signaling and RNA turnover crosstalk, as reduced nanoRNase activity would also cause increased c-di-GMP signaling. Currently, the processes of nanoRNase expression are unknown, although a Western blot of overnight cultures of *E. coli* showed no difference in Orn concentration at stationary compared to exponential phase (40). Investigation into the regulation of nanoRNase expression or activity during periods of elevated c-di-GMP could shed insight on c-di-GMP turnover.

3.7.2 Do NanoRNases also act as PDE-Bs for pApA and pApG?

The current experiments have focused on the identification of the PDE-Bs responsible for cleaving pGpG. Since nanoRNases are hypothesized to cleave all short oligoribonucleotides regardless of sequence, we also expect them to have activity against the linearized form of the other two cyclic di-nucleotide signaling molecules (pApA from c-di-AMP and pApG from cAG). Therefore, we have designed experiments to determine whether nanoRNases can use pApA and pApG as substrates, and whether pApA or pApG can inhibit the enzymatic activity of the proteins responsible for linearizing c-di-AMP and cAG, respectively.

3.7.3 The essentiality of Orn and NanoRNases

Orn was determined to be essential in *E. coli* (52) as attempts to generate an insertional mutant were unsuccessful. Orn appears to be essential in *V. cholerae* as well, since a transposon mutant of *orn* could not be recovered (63). However, it does not appear to be essential in *P. aeruginosa* as a transposon mutant of *orn* could be generated in PA14 (64), and we were able to create a viable in-frame deletion. Although viable, both the transposon insertion mutant and the deletion mutant displayed growth defects. The PA14 Δ*orn* mutant formed small colonies on plates and had slower growth rate and lower stationary phase optical density in liquid cultures.

The growth defect has been reported in all species where loss of Orn function has been engineered. Although a mutation of *orn* could not be recovered directly in *E. coli*, an insertional mutant could be generated when *orn* was provided in trans on a temperature sensitive plasmid (52). When grown at permissive temperature (31 °C) the bacteria formed normal colonies and grew well in liquid culture, but formed microcolonies and ceased growth at 44 °C (52). Another conditional *orn* mutant in *E. coli* had a 1.9-fold longer doubling time and formed small colonies (58). Additionally, lithium poisoning caused reduced growth in *E. coli* via a mechanism linked to Orn inhibition (53). Lithium inhibits the pAp-phosphatase activity of CysQ, and Orn was shown be inhibited by high levels of pAp in vitro (53). Lithium poisoning caused *E. coli* to form small colonies (53), reminiscent of those observed for the *E. coli* temperature sensitive *orn* depletion strain and our PA14 Δ*orn* strain, presumably due to Orn inhibition. Additionally, in the plant-associated bacterium

Pseudomonas putida, *orn* is encoded both on the genome and on a plant-inducible plasmid pQBR103 (65). While inactivation of the plasmid copy had no effect on growth M9 or LB media, an insertional inactivation of the chromosomal copy resulted increased doubling time, lower OD_{600} at stationary phase, and small colonies (65).

The loss of nanoRNases can also result in a growth defect, although like Orn, the effect varies between species. A transposon disruption of the *nrnA* homolog (MSMEG_2630) of *Mycobacteria smegmatis* showed only a slight growth defect (124). In contrast, the *nrnA* homolog (Rv2837c) of *Mycobacteria tuberculosis* appears to be essential for growth (125, 126). Interestingly, *M. tuberculosis* encodes both NrnA and Orn (Rv2511), but inactivation of each individual gene by transposon insertion seemed to cause loss of viability (125), indicating that NrnA and Orn may not be redundant in this species. However, a triple mutant of *nrnA*, *nrnB* and *yhaM* in *B. subtilis* was viable and showed only a small difference in doubling time (58). Transposon insertion frequency analysis showed that the promoter of *nrnC* (CCNA_03717, mistakenly annotated RNase D) from *C. crescentus* is essential (127). Finally, knocking down *nrnC* in *B. henselae* resulted reduced growth rate compared to wild type (59).

This leads to the question of why are *orn* and nanoRNases essential in some species and not others? A simple answer is that they are not essential in some species if the genome encodes another RNase that serves a redundant function. Another possibility is that loss of these RNases is harmful to all organisms, but the difference in viability is due to the ability of some organisms to better cope with the damaging

effects than others. This could explain why even viable mutant strains show growth defects. Loss of *orn* or nanoRNases could affect viability by depleting mononucleotides or through a toxic effect of accumulated nanoRNAs. Loss of the RNases necessary to completely hydrolyze RNA to mononucleotides would reduce the rate of nucleotide recycling, thus diminishing the cellular supply of free mononucleotides. Different organisms may have better mechanisms to cope with this reduction, either through better scavenging and uptake systems or more robust de novo synthesis pathways. Accumulated nanoRNAs themselves could also be the culprit. Depletion of Orn in *P. aeruginosa* PAO1 resulted in global gene expression changes due to transcription priming by accumulated nanoRNAs (39). These changes in gene expression could differentially disregulate gene expression in different organisms to cause loss of viability in some and only reduced growth in others. Additionally, accumulated nanoRNAs could bind proteins to affect their function, or be a cellular distress signal leading to reduced growth or death. The cellular processes affected in *orn* or nanoRNases mutants to result in loss of viability or reduced growth is currently unknown and is the topic investigated in the following chapter.

3.8 Materials and Methods

3.8.1 Primers, plasmids, strains and culture conditions

The genes *nrnA*, *nrnB*, *rnjA*, *yhaM* were cloned from *B. subtilis* strain 168 and *nrnC* was cloned from *C. crescentus* CB15 using the primers shown in Table 4 and introduced into the plasmids pVL791 and pVL393 using restriction endonuclease cloning with the enzymes NdeI and BamHI (New England Biolabs). The *P. aeruginosa* PA14 Δ*orn* plasmid complementation strains were grown in LB

supplemented with 50 μg/mL carbenecillin. Gene expression was induced by 100 mM IPTG. All liquid cultures were grown in 37 °C with shaking. Bacteria were struck on 1.5% LB-Agar supplemented with 100 mM IPTG and 50 μg/mL carbenecillin. For growth curves, an overnight culture of each PA14 Δ*orn* complementation strain was adjusted to OD_{600} = 0.01 in LB supplemented with 5 μg/mL and 200 μL was added to a well of a sterile 96-well plate. The plate was incubated, with shaking, at 37 °C in a SpectraMax M5 spectrophotometer (Molecular Devices). OD_{600} readings were taken at every 15 mins for 14 hrs to generate the growth curve. The exponential phase growth curve was fitted using the exponential growth equation $y = y_0(e^{kt})$ on GraphPad Prism, where y is the OD_{600}, x is time (h), y_0 is the y value when x = zero, k is the rate constant (1/h). The doubling time was found using ln(2)/k.

3.8.2 Protein purification

Proteins were purified over a Ni-NTA column as described in s 2.10.3. Instead of dialysis, proteins were desalted using buffer exchange over a Sephadex G-25 column. Proteins were stored at -80 °C in 50 mM Tris, pH 8.0, 100 mM NaCl.

3.8.3 DRaCALA binding assay

The use of DRaCALA to probe protein-ligand interactions has been previously described (43). To assay binding, 5 μM of pure protein in binding buffer (10 mM Tris, pH 8.0, 100 mM NaCl, 5 mM $CaCl_2$) was mixed with radiolabeled ligand (4 pM ^{32}P-pGpG), applied to nitrocellulose sheets, dried, imaged, and the fraction of ligand bound quantified.

3.8.4 Cell lysate and protein activity assays

The activity of whole cell lysates and purified proteins against ^{32}P-labeled substrates was measured by as in 2.10.5. The reactions were carried out at room temperature (21 °C) in reaction buffer (50 mM Tris, pH 8, 100 mM NaCl, and 5 mM $MnCl_2$ for NrnA, NrnB, NrnC and YhaM and 50 mM Tris, pH 8, 100 mM NaCl, and 5 mM $MgCl_2$ for Orn and RNase J1). Activity was measured by adding 0.1 mM of pGpG spiked 4 pM ^{32}P-pGpG tracer and to 0.1 μM NrnA, 0.1 μM NrnB, 0.1 μM NrnC,10 μM YhaM, or 10 μM RNase J1 in reaction buffer. Lysates were generated as follows: PA14 Δ*orn* carrying complementation vectors were grown overnight and subcultured 1:100 into fresh LB supplemented with 5 μg/mL carbenecillin and 100 mM IPTG. Bacteria were grown to OD_{600} ~ 0.4 at 37 °C with shaking, resuspended in 1/10th volume of reaction buffer and adjusted to the same OD_{600} (see above), supplemented with 10 μg/mL DNase, 250 μg/mL of lysozyme, and 10 mM PMSF, and lysed by sonication.

3.8.5 Aggregation and microtiter late biofilm assays

See 2.10.6 for aggregation assay and 2.10.7 for microtiter plate biofilm assay protocol. All strains were grown in LB.

Chapter 4: Identification of Oligoribonuclease-mediated Regulation in PA14

RNA-Seq experiments in Tables 3 & 4 were performed by Dr. Stephanie Joy analyzed with assistance from Jonathan Goodson. Microscopy images in Figs. 17 & 18C were taken by Cordelia A. Weiss. Xiaoran Shang assisted in performing the transposon mutagenesis screen.

4.1 Introduction

Orn is essential in *E. coli* and *V. cholerae*, bit not in *P. aeruginosa.* Although viable, the PA14 Δ*orn* mutant has a marked growth defect. Compared to wild type PA14, the Δ*orn* strain had a higher frequency of lysis when grown under agar pads (Fig. 17), formed smaller colonies on agar plates, reduced growth rate in liquid culture, lower optical density at stationary phase, and had a change in cell morphology at stationary phase that is suggestive of a cell division defect (Fig. 18). As discussed in 3.7.4, reduced growth rates and small colonies have been reported for some *orn* and nanoRNase mutants in a variety of bacterial species (52, 54, 58, 59, 65, 128). In PA14, the elevated pellicle biofilm and aggregate formation of the Δ*orn* mutant were dependent on the *pel* operon, however the growth defect was not rescued by deletion of the *pel* operon in the Δ*orn* mutant background (Fig. 18). Thus it remains unclear what mechanism(s) underlie the reduced growth rate in the *orn* mutant. There are several possible explanations for how the loss of Orn could cause

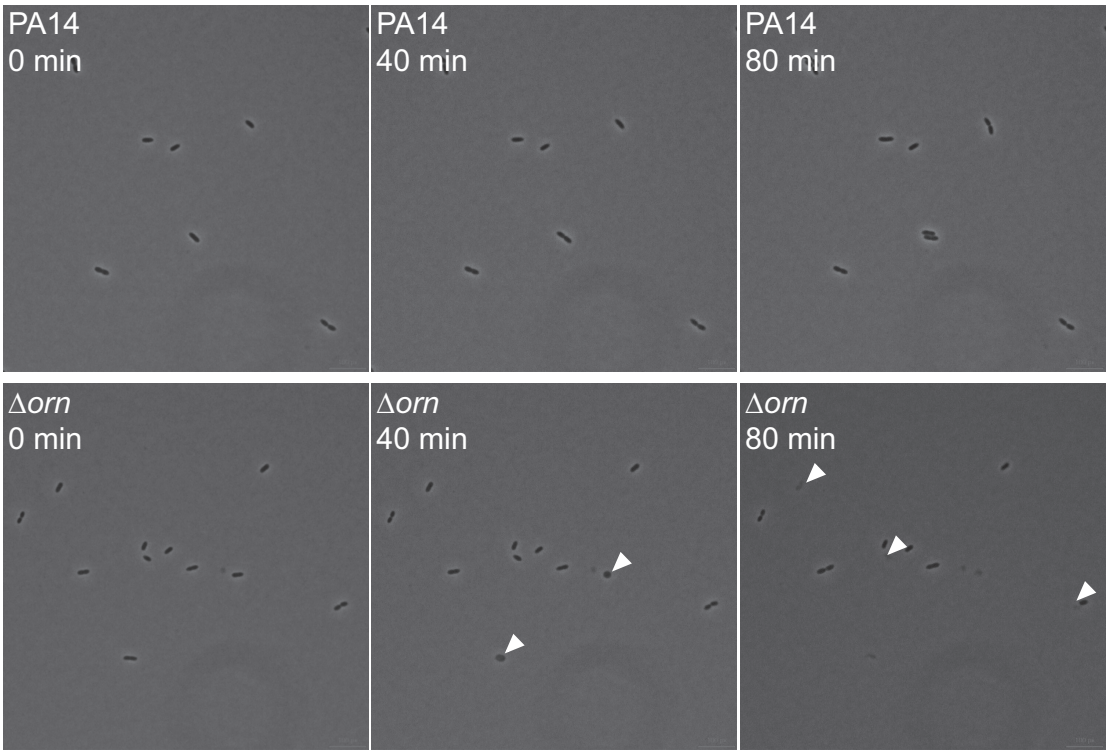

Figure 17. PA14 Δ*orn* has high rate of lysis compared to wild type PA14. PA14 wild type and Δ*orn* strains were grown to mid-log, then transferred to a sterile microscope slide and immobilized under an agarose pad for time-lapse microscopy imaging under phase contrast. Images were taken every 2 minutes. Shown are images taken at 0 min, 40 min, and 80 min. White arrowheads indicate the locations of bacteria that have rounded and lysed.

an inhibition of growth. Effects could be either direct, if Orn binds to and affects the activity of other proteins in addition to degrading short RNAs, or indirect because prevention of nanoRNA turnover is toxic.

In the first scenario, Orn would be expected to bind to a protein partner to affect its function. There is currently no solid evidence that Orn directly interacts with other proteins, although microscopy co-localization experiments of fluorescently tagged proteins suggest that Orn is a member of the RNA degradosome in *E. coli* (129). However, this observation was not confirmed by any co-immunopreciptation or pulldown assays. Interaction between some RNases of the degradosome can affect RNA turnover (see (130) for review). For example, in *E. coli*, the RNA helicase RhlB is not active unless bound to RNase E (131). If Orn does indeed participate in the degradosome, its loss could affect RNA turnover directly by altering the function of other RNases.

In the second scenario, the failure to hydrolyze nanoRNAs could be the cause of the growth phenotypes either through reduction of the accessible cellular nucleotide levels or through an effect of the nanoRNAs themselves. Until recently, the effects of nanoRNAs in bacteria had not been studied. However, in response to long-standing observations that in vitro transcription can be primed by short RNAs (132, 133), the Dove and Nickels labs recently conducted an intriguing study to investigate the possibility of in vivo transcriptional priming. To allow accumulation of nanoRNAs, they depleted *P. aeruginosa* PAO1 strain of Orn using a ClpXP protease system, resulting in global transcriptional changes (39). The authors hypothesized that these changes could have been due to alterations in mRNA stability

due to the presence of a 5´ monophosphate from priming by nanoRNAs rather than the 5´ triphosphate generated from transcription initiating from NTPs. In RNA turnover, the 5´ phosphorylation status affects transcript stability (see (134) for a review) because 5´ monophosphorylated transcripts are the preferred substrate for the major endonuclease RNase E (135). Therefore, priming by RNA fragments with a 5´ monophosphorylated end could reduce stability of transcripts. Alternatively, transcription priming was shown to alter the transcription start site, which could change the expression rate (39). Finally, it was suggested that since in vitro transcription by priming by nanoRNAs can increase transcription initiation efficiency (136), in vivo transcription could also be activated by accumulated nanoRNAs (39). Thus the growth and division phenotypes observed in PA14 Δ*orn* could be an effect on transcriptional priming by nanoRNAs.

It is also possible that nanoRNases could be affecting bacterial processes by other mechanisms. There could be protein receptors for nanoRNAs. Like pGpG, which was shown to inhibit the enzymatic action of the PDE-As responsible for cleaving c-di-GMP, RNA fragments could bind to and affect the function of other proteins. A potential receptor could be a stress response sensor that responds to accumulated oligoribonucleotides. Numerous other bacterial stress response pathways have been reported to respond to many different stressors, such as the heat shock response mediated by Hsps (see (137) for review), envelope stress response mediated by CpxA/CpxR in *E. coli* and other gram negatives (see (138) for review), and the stringent response mediated by the nucleotide second messenger (p)ppGpp (see (139) for a review). Thus, the concept of a stress response to improper RNA turnover is

attractive. A programmed cell death mechanism has been described for *P. aeruginosa* in which DNA damage results in cleavage of the AlpR transcription factor, causing depression of a positive regulator of a lysin cassette (140). The accumulated small RNAs in the Δ*orn* strain could also result in increased lysis via a regulated pathway.

To investigate the genetic causes of the altered growth phenotypes observed in our PA14 Δ*orn* strain and reveal a potential for Orn-mediated regulation, we took advantage of the small colony phenotype to conduct a suppressor screen using transposon mutagenesis. A suppressor mutation that restores wild type colony size could reveal the processes that have been disregulated in the *orn* mutant. This transposon mutagenesis colony size screen identified several transposon insertions in genes that restored colony size and may explain the growth phenotypes observe in the Δ*orn* strain, however full characterization of these mutants is still in process.

4.2 Colony size, growth defect and cell morphology are not *pel*-dependent

The PA14 Δ*orn* pellicle biofilm and aggregation phenotypes are *pel*-dependent, as deletion of the *pelA-G* operon (Δ*pel*) prevented pellicle biofilm and aggregate formation (Fig. 10 from Chapter 2). However, not all phenotypes in observed in the Δ*orn* strain were reversed by the introduction of the *pel* deletion. Compared to the parental PA14, the Δ*orn* strain had a smaller colony size, reduction in doubling time in liquid culture (1.6 h for Δ*orn* compared to 1.1 h for PA14), and a longer and often diplobacilloid cell morphology at stationary phase (Fig. 17). The small colony morphology in the Δ*orn*Δ*pel* double deletion strain was the same as that observed with the Δ*orn* strain, while the Δ*pel* operon mutant remained the same as wild type PA14 (Fig. 17A). The deletion of the *pel* operon also did not restore growth

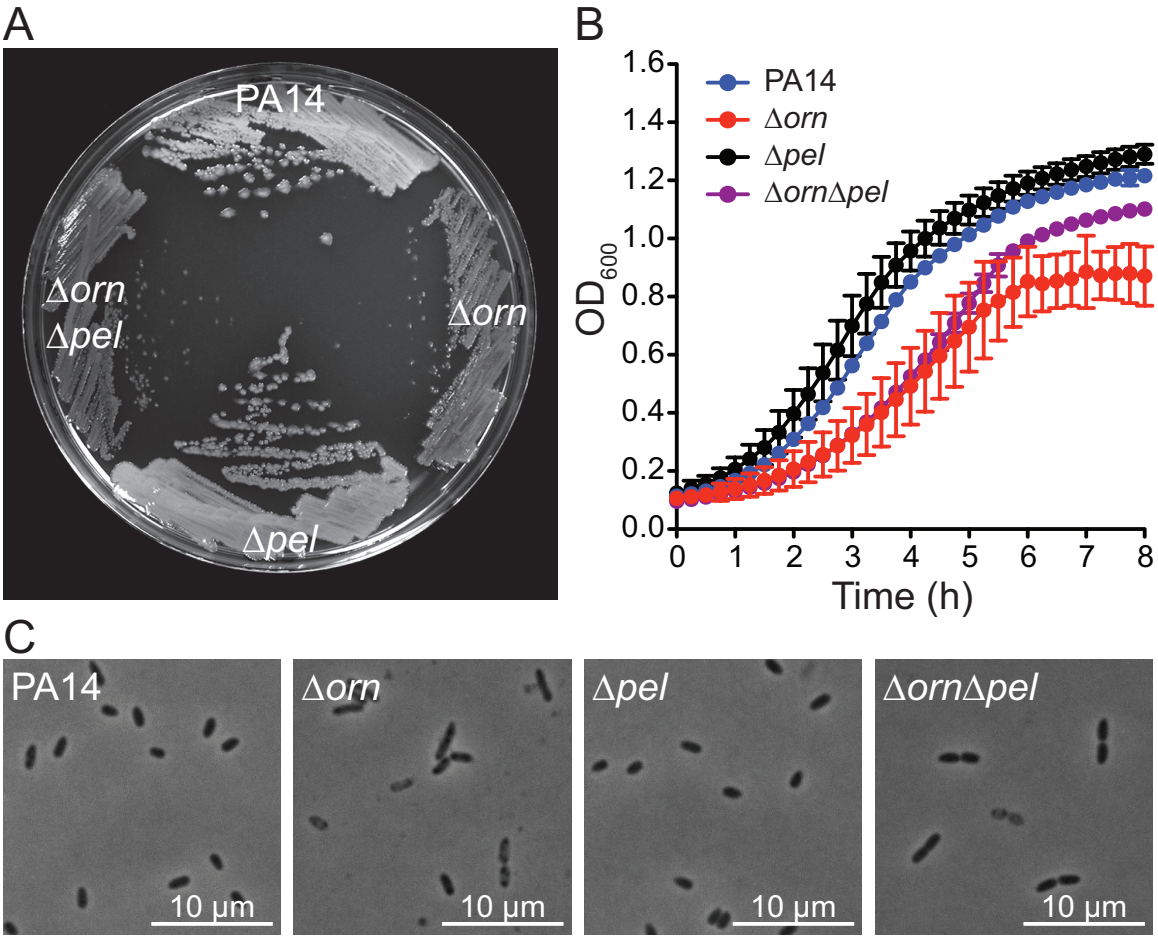

Figure 18. PA14 Δ*orn* has a growth defect that is *pel* independent. (A) An LB agar plate showing wild type PA14, Δ*pel*, Δ*orn* and Δ*orn*Δ*pel* colony sizes. (B) The growth curve in LB liquid culture comparing wild type PA14, Δ*orn, Δpel, and* Δ*orn*Δ*pel* over a period of 14 hrs. Values shown are the average and SD of three independent experiments. (C) Phase contrast microscopy image of overnight cultures of PA14 wild type, Δ*orn, Δpel,* Δ*orn*Δ*pel* at 1000x magnification.

in liquid culture to wild type levels, as shown by the OD_{600} over time (Fig. 17B). The doubling time for the Δ*pel* single mutant remained the same as for PA14 (1.1 h for both), while the Δ*orn*Δ*pel* double mutant was the same as that observed for the Δ*orn* strain (1.5 h and 1.6 h, respectively). Finally, introduction of the *pel* operon deletion and had no effect on cell morphology, with both Δ*orn* and Δ*orn*Δ*pel* showing longer cell bodies and more diplobacilli in stationary phase culture compared to wild type and Δ*pel* (Fig. 17C). Thus, unlike the biofilm phenotypes, these growth defects in the Δ*orn* strain are not dependent on production of the PEL exopolysaccharides and are instead dependent on one or more as yet unidentified processes.

4.3 A transposon mutagenesis screen for suppressor mutants of colony size

To identify other genes underlying the phenotypes observed in the Δ*orn* strain, a transposon mutagenesis screen (see Fig. 19 B for steps) was devised to identify second mutations that would restore Δ*orn* colony size to wild type. A pBT20 plasmid (Fig. 19 A) containing mini-mariner based transposon (108), was introduced into the *P. aeruginosa* PA14 Δ*orn*. This mini-mariner transposon inserts into TA sites. The *aacC1* gentamycin resistance gene allows for gentamycin-based selection of transposon mutants. The omega terminator permits interruption of transcription of adjacent genes, and an IPTG-inducible promoter allows activation of transcription of downstream genes.

Approximately 40,000 colonies were screened for mutants that fully or partially restored colony size to wild type on selective media. Twelve mutants were identified (named suppressors 1-12). Genomic DNA from the mutants was isolated, fragmented, cloned into the pVL-blunt cloning vector, transformed into bacteria and

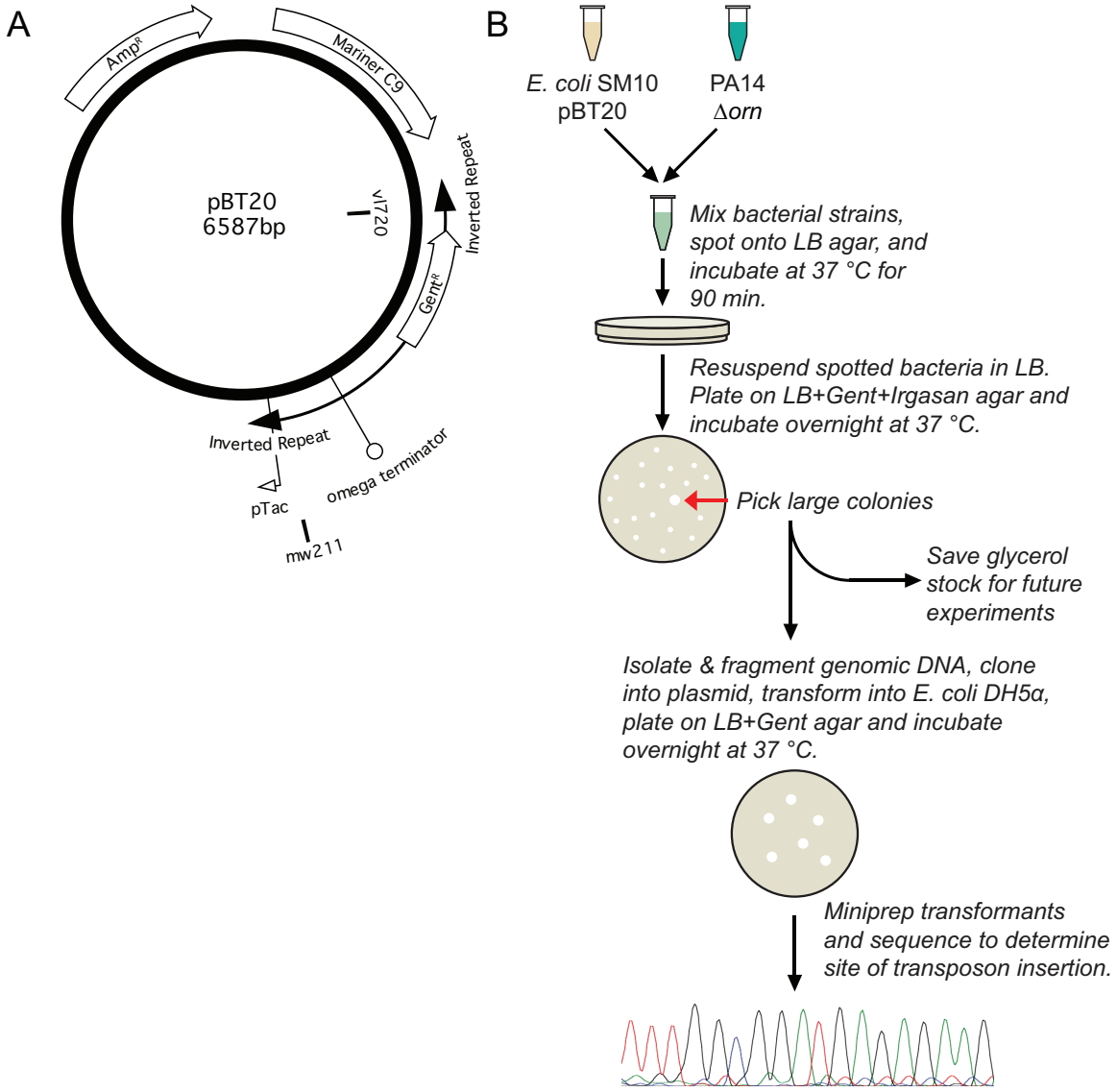

Figure 19. Diagram of pBT20 plasmid and transposon mutagenesis schematic. (A) Diagram of the plasmid pBT20 containing the mini-mariner transposon (double-arrowed line). The black arrowheads show locations of the inverted repeats on the transposon. Genes for ampicillin resistance (Amp^R) and the transposase (Mariner C9) are located on the plasmid, while the gene for gentamycin resistance ($Gent^R$) is located within the transposon. The transposon contains a *tac* promoter (pTac) and omega terminator, shown with white arrowhead and open circle, respectively. Black bars show the location of binding of sequencing primers mw211 and vl720. (B) Simplified schematic of the steps of the transposon mutagenesis screen for mutants that restore colony size in the PA14 Δ*orn* strain.

selected for gentamycin resistant strains, and the plasmids were miniprepped and sequenced to determine the site of transposon insertion. Four insertions were found in the same genomic region (Fig. 20A): suppressor 1 in PA14_22770, the first gene in operon just downstream of *yciBI*, suppressor 2 in *yciI*, and suppressors 3 and 4 upstream of *yciB*. Suppressor 5 had an insertion in *fleQ*, a c-di-GMP responsive transcription factor (27) (Fig. 20B). Suppressor 6 has an insertion in PA14_06940, a hypothetical protein of unknown function (Fig. 20C). Suppressors 7-9 had an insertion in the 16S-23S rRNA region, however it is not known which of the four possible rRNA operons in PA14 were hit due to sequencing limitations (Fig. 20D shows the possible locations of suppressors 8-10 in the four rRNA operons). Suppressor 10 had an insertion in *dnr*, a NO responsive transcriptional regulator (Fig. 20E). Suppressor 11 contained an insertion in *potB*, a member of a polyamine transporter operon with (Fig. 20F). Suppressor 12 had an insertion in PA14_27420, a HlyD family secretion protein (Fig. 20F). The initial screen selected for large colony size on LB agar plates supplemented with 75 µg/mL gentamycin and 25 µg/mL irgasan. Because it is possible that these larger colony sizes were due to a more rapid growth rate from increased ability to clear either antibiotic, the strains were also checked for colony size on LB agar plates without antibiotic (Fig. 21A). Suppressors 1-6, 11, and 12 were able to form colonies similar in size to the wild type PA14. However, suppressors 7-10 were not able to restore wild type colony size on these plates. They may have been able to form larger colonies in the initial screen due to an enhanced ability to grow in the presence of antibiotic selection and may not harbor mutations that can truly suppress the Δ*orn* strain growth defect.

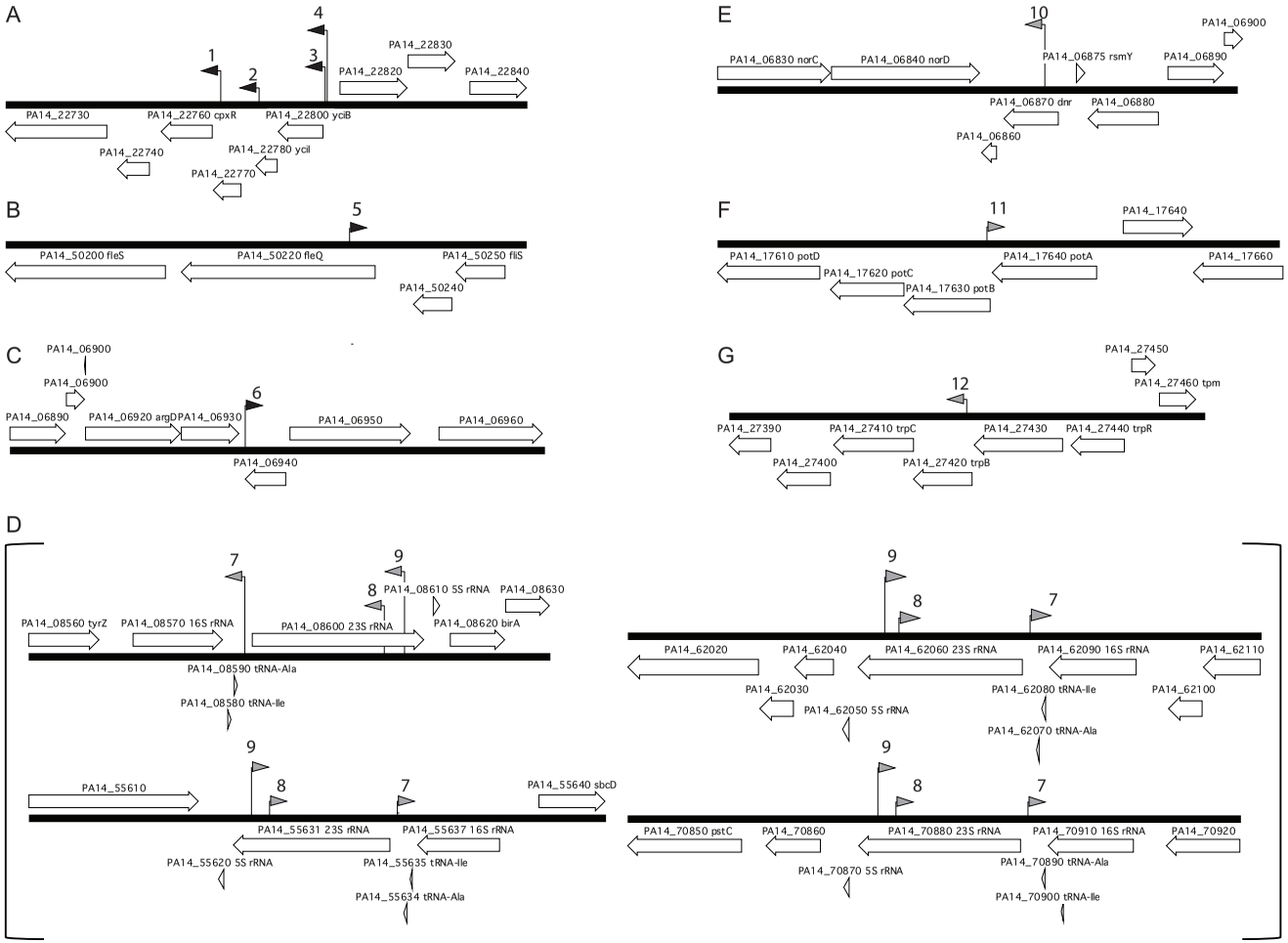

Figure 20. Location and direction of transposon insertions. The genomic region surrounding the transposon insertion sites for (A) suppressors 1-4, (B) suppressor 5, (C) suppressor 6, (D) all four rRNA operons where partial suppressors 7-9 may be, (E) suppressor 10 (F) partial suppressor 11, and (G) partial suppressor 12 are shown. Arrows indicate the transposon location and the direction of the *tac* promoter. Black arrows designate full suppressors and gray arrows designate partial suppressors.

4.4 The effect of suppressor mutations on growth in liquid culture

The growth curves in liquid cultures for all strains were generated and compared to the parental PA14 and Δ*orn* mutant (Fig. 21B). The doubling time in the Δ*orn* mutant was longer than the wild type (1.7 h compared to 1.2 h, respectively). The transposon mutants split into three populations: 1. those with doubling times similar to PA14 (suppressors 1, 5, 7, and 8, with doubling times of 1.2 h, 1.2 h, 1.1 h and 1.2 h respectively), 2. those similar to Δ*orn* (suppressors 4, 6, 9, and 12 with doubling times of 1.7 h, 1.5 h, 1.6 and 1.6 h respectively), and 3. those with intermediate doubling times (suppressors 2, 3, 10 and 11 with doubling times of 1.3 h, 1.3 h, 1.4 h and 1.3 h, respectively). Although able to rescue colony size on LB agar plates, suppressors 4, 6, and 12 could not rescue growth in liquid media. Conversely, although they were unable to rescue colony size in LB plates, suppressors 7 and 8 were able to fully rescue growth and 10 was able to partially rescue growth in liquid media. These data show that rescue of colony size on LB does not necessarily rescue the reduced doubling time of the Δ*orn* strain in liquid culture. This suggests that multiple pathways are involved in the small colony phenotype and growth defects. Thus we decided to assay whether the suppressors have differential effects on aggregation and pellicle biofilm.

4.5 The effect of suppressors on aggregation and biofilm formation

The Δ*orn* strain has increased aggregation and pellicle biofilm formation compared to the wild type PA14. These two phenotypes were *pel* operon dependent, as deletion of *pel* in the Δ*orn* background prevented pellicle biofilm and aggregation (see Fig. 10). We assayed if any of these colony size suppressor mutations could also

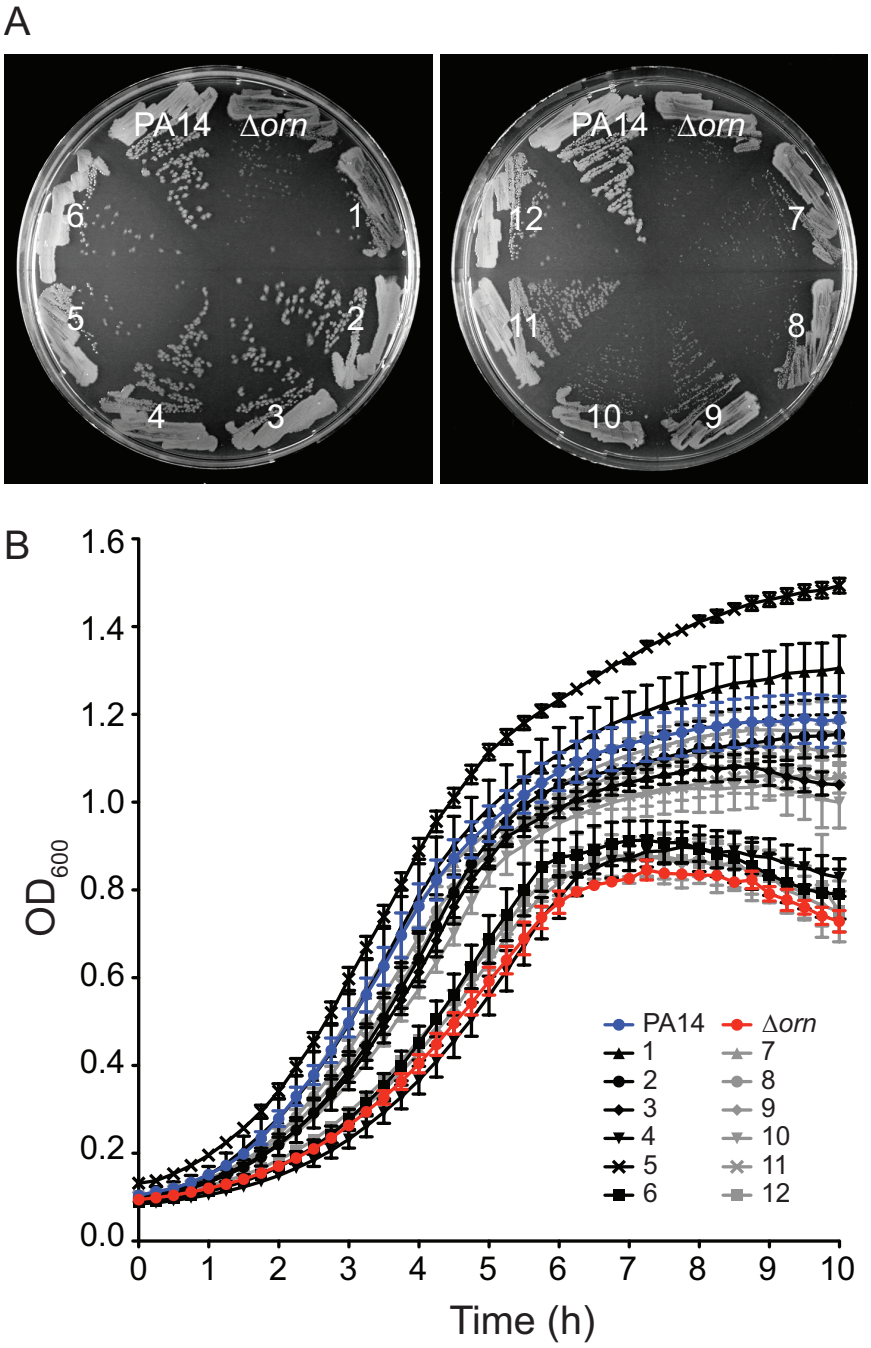

Figure 21. Growth phenotypes of the transposon suppressor mutants. (A) Photograph of LB-agar plates showing difference in colony size of suppressor strains 1-12 compared to wild type and Δ*orn* strains. (B) The OD_{600} curve of the parental PA14, Δ*orn*, and suppressor strains 1-12 grown in LB over a period of 10 hrs. Shown are the average and SD of three independent experiments.

suppress aggregation and pellicle biofilm formation. The auto-aggregation assay shows the ability of bacteria grown in liquid culture with agitation to adhere together to form large clumps that can settle out of suspension. As previously shown, the wild type PA14 remained in suspension, while the Δ*orn* strain formed large aggregates that settled out of suspension after 30 minutes (Fig. 22A). Suppressors 2-6 and 12 formed no aggregates and remained in suspension like PA14, suppressors 1 and 11 showed intermediate aggregate formation, while suppressors 7-10 aggregated at similar levels to the Δ*orn* strain. These were the mutants also unable to rescue colony size in LB media.

Bacteria grown in a stationary liquid culture can adhere to each other to form a pellicle biofilm at the air-media interface. As previously shown in the crystal violet microtiter plate assays for pellicle biofilm formation, the Δ*orn* strain formed ~ 2-fold more biofilm than wild type PA14 with A_{595} readings of 0.64 ± 0.01 and 0.30 ± 0.03 respectively, while deletion of the *pel* operon abolished biofilm formation (A_{595} of Δ*pel* = 0.027 ± 0.005 and A_{595} of Δ*orn*Δ*pel* = 0.044 ± 0.005) (Fig. 22B). The transposon mutants restored pellicle biofilm formation to wild type PA14 levels with the exception of suppressor 5, which showed nearly no crystal violet staining (Fig. 22B). Suppressor 5 had an insertion in *fleQ*, a transcription factor that promotes expression of the *pel* operon (27), which is necessary for in vitro biofilm formation (62). Thus, inactivation of the *fleQ* would be expected to reduce biofilm formation to Δ*pel* levels. Indeed, the A_{595} value for suppressor 5 was 0.035 ± 0.002, the same as Δ*pel* and Δ*orn*Δ*pel*. All together, these data indicate that while the transposon insertions were able to suppress the small colony growth phenotype, not all Δ*orn*

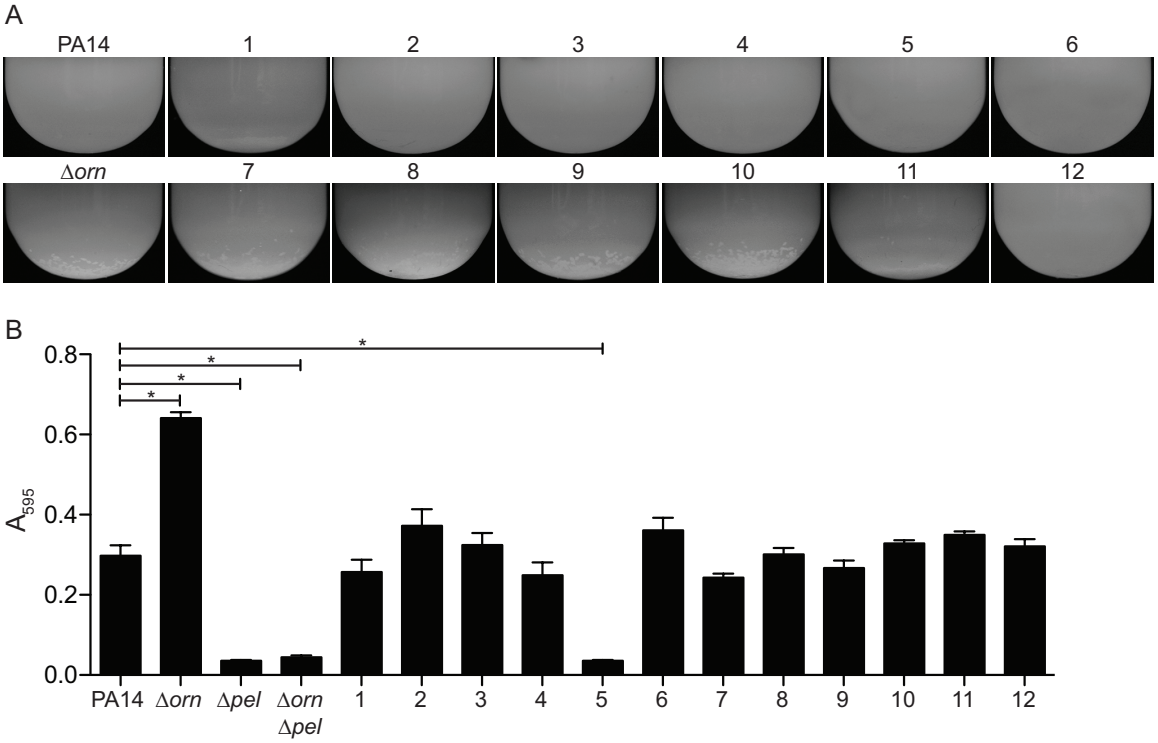

Figure 22. Biofilm phenotypes of the transposon suppressor mutants. (A) Photograph of overnight cultures of all suppressors and the *orn::tn* and *cat::tn* strains showing auto-aggregate sedimenting at time 30 min after beginning of auto-aggregation assay. (B) The quantification of the biofilm formed by the PA14 wild type, Δ*orn*, Δ*pel*, Δ*orn*Δ*pel*, and transposon suppressor strains after 24 h of static culture. Biofilm cells were stained by crystal violet and quantified by reading the absorbance at A_{595}. Values are shown average and standard deviation of three independent experiments. * indicates $p < 0.0001$ by Students' unpaired two-tailed *t*-test assuming equal variance.

phenotypes are suppressed by all of the suppressor mutants, indicating that the *orn* deletion is affecting multiple different regulatory pathways.

4.6 The effect of *orn* deletion on transcription

In parallel to the transposon suppressor screen, a preliminary RNA-Seq was performed to investigate the effect *orn* mutations have on transcription. PA14 wild type and Δ*orn* strains were grown to early- and mid-log (OD_{600} ~ 0.3 and ~ 0.5, respectively) and RNA isolated for analysis. Genes that showed up- or down-regulation of > 2 log2-fold change are shown in Tables 3 and 4, respectively (see Appendices).

Preliminary results show one change that may dovetail with the suppressor screen results. At OD_{600} = 0.5, the *potA* and *potB* transcripts increased 2.1 and 2.4 log2-fold change in the Δ*orn* strain compared to wild PA14. Partial suppressor 11 had an insertion in *potB*. (Fig. 20F). Because phenotypes such as increased aggregation and the cell morphology change associated with Δ*orn* do not emerge until stationary phase, the conclusions that can be drawn from the early growth phases may be limited. Furthermore, when the Dove and Nickels labs overexpressed Orn in *V. cholerae* and *E. coli*, transcriptional changes were only observed in stationary phase, indicating that the effects of Orn would not be seen during exponential growth (40). More RNA-Seq experiments to investigate transcriptional changes in later growth phases and in biofilm growth are planned. Although preliminary, these results taken together shed some light on the pathways affected in an *orn* mutant, giving interesting leads for further investigation on the reasons why the loss of *orn* causes loss of viability or growth inhibition.

4.7 Discussion

4.7.1 PA14 Δ*orn* phenotypes and c-di-GMP

Our earlier experiments indicated that elevated c-di-GMP mediated the aggregative and elevated c-di-GMP phenotypes observed in the Δ*orn* mutants via the c-di-GMP-regulated PEL exopolysaccharide (Fig. 10). However deletion of the *pel* operon had no effect on colony size, growth rate, or cell morphology in the Δ*orn* background (Fig. 17). We thus hypothesized that other, potentially non-c-di-GMP processes were involved in regulation of the growth rate and cell morphology changes observed in Δ*orn*. Nevertheless, suppressor 5 was an insertion in *fleQ*, a c-di-GMP responsive transcription factor responsible for the regulation of many genes, notably reducing transcription of motility genes and de-repressing transcription of biofilm exopolysaccharides genes when bound to c-di-GMP (27). An insertion in *fleQ* was able to fully suppress the Δ*orn* colony size defect and the liquid media growth defect and it also abolished aggregation and biofilm formation, suggesting that these phenotypes are all c-di-GMP-mediated. The aggregation and biofilm results were expected since they are dependent on the *pel* operon in PA14, and full expression of the *pel* genes requires FleQ binding to c-di-GMP to de-repress the *pel* operon (27). How *fleQ* inactivation can revert the growth and colony size phenotypes is less clear, but other process(es) regulated by *fleQ* besides PEL exopolysaccharide production must be in involved. One candidate is the *cdrAB* operon. This operon in PAO1 is also regulated by FleQ (141). Overexpression of *cdrAB* in PAO1 caused increased aggregation and formation of small, smooth colonies (141), similar to the what is observed in Δ*orn*. However, the authors' proposed mechanism for the CdrA-mediated

auto-aggregation and small colony formation required interaction with the PSL exopolysaccharide (141). The PA14 strain has a natural deletion in the *psl* operon resulting in no production of PSL (142). Therefore if *cdrAB* is the FleQ-regulated operon responsible for the Δ*orn* phenotypes, it must have another function. Alternatively, yet another member of the FleQ regulon could be responsible for suppression. If the *fleQ* mutant can be rescued, it points to additional players in the c-di-GMP regulon that are responsible for regulating *P. aeruginosa* growth rate. It would also be interesting to determine if pGpG could bind FleQ to affect its function. It was not identified in the binding screen because *V. cholerae* does have a FleQ homolog. If so, this could provide another layer by which FleQ activity could be regulated.

4.7.2 A role for Orn in cell division

Of the twelve suppressor mutants s of the small colony phenotype observed for the Δ*orn* strain, four independent transposon insertions were in the same region near the *yciBI* operon (Fig. 20A). The *yciBI* operon is a two-gene operon containing *yciB* annotated as intracellular septation protein A and *yciI* with an annotated YCII related domain. A mutant of the *yciB* homolog *ispA* in *S. flexneri* forms filaments in infections (143), indicating that it could play a role in septation. In *E. coli*, a *yciB* mutant showed 40% shorter cell length, while an overexpressing strain showed ~ 2-fold increased cell length (144). In a two-hybrid assay, YciB was shown to interact with both cell elongation and cell division proteins (145), and YciB was shown to interact with ZipA by a pull-down assay (144). Although not localized to the septum, YciB appears to be important for ZipA mid-cell localization, as ZipA is mislocalized

in a Δ*yciB* strain (144). These studies suggest a role for YciB in regulating bacterial cell cycle. Although it is not filamentous, at stationary phase Δ*orn* cells are longer than PA14 wild type and form more diplobacilli (Fig. 17C). It is possible that the Δ*orn* mutant has a longer cell size and division defect due to increased *yciB* expression or activity. Thus transposons in the *yciB* region could rescue cell division in Δ*orn*. A screen of the *E. coli* Keio collection of mutants for strains defective in biofilm formation identified *yciB* (146), supporting our observation that transposon insertions in this genomic region could reduce aggregation and pellicle formation. How a disruption of this gene causes reduced biofilm is uncertain.

Alternatively, the phenotypes observed in these mutants could be responsible for a polar effect. All four transposons inserted in the same direction and are all just upstream of an operon containing *cpxR*. The orientation of insertion would allow for *cpxR* expression from the *tac* promoter on the transposon. This gene encodes the transcription factor response regulator CpxR, activated by its cognate histidine kinase CpxA (147-149). This two-component system senses envelope stress and has also been implicated in adhesion, biofilm formation, and secretion (see (150, 151) for reviews). An *E. coli* mutant with constitutively phosphorylated CpxR showed randomized FtsZ ring localization and septation defects (152), indicating a role for CpxAR in cell division. In *P. aeruginosa* strain PAO1, depletion of the cell wall *amidase amiB*, which is responsible for separating daughter cells after division, causes growth inhibition and chaining morphology (153). A suppressor of this defect had an insertion in PA3206 (PA14_22730 in PA14), a CpxA-like protein (153).

Together, these studies suggest that *cpxR* expression could also be the true be the cause of the suppression observed with this set of transposon insertion mutants.

4.7.3 Other identified suppressor mutations and their potential functions

Suppressor 6 had a transposon insertion in PA14_06940. It is not in an operon and has no annotated domains. An insertion in this gene resulted in no change to the doubling time and restored aggregation and biofilm formation to wild type levels. It is adjacent to PA14_06950, a LuxR family transcriptional regulator, and the tac promoter is in the same direction as this transcription factor. It is therefore also possible that the effects of this insertion are due to a polar effect on this transcriptional regulator.

Suppressors 7-9 were insertions in the 16S-23S rRNA region. There are four of these rRNA regions in *P. aeruginosa* (154), however due to the sequencing technique utilized to identify the location of the transposon insertions, it is uncertain which of the four possible rRNA operons these transposons were located. The number of rRNA operons is correlated to doubling time in *E. coli* (155) and *B. subtilis* (156) and in general, more rRNA operons correlates with faster growth in many bacterial species (157, 158). However, why a transposon insertion in the 16S-23S rRNA region would affect colony size in Δ*orn* is unclear. It is possible that a polar effect of the transposons is responsible for the partial rescue. However, additional sequencing is needed to reveal the exact location of the insertions. Although identified as able to partially restore colony size in the initial colony size screen on LB agar plates with 75 μg/mL gentamycin and 25 μg/mL irgasan, there did not appear to be any colony size rescue when grown on LB agar with no antibiotics.

Therefore, it is not certain that suppressors 7-9 have mutations that are relevant to the growth defect seen in Δ*orn*.

Suppressor 10 suppressed the small colony phenotype on LB antibiotic plates. However, it had no effect on colony size in LB plates nor did it alter aggregation. It had an intermediate effect on rescuing growth in liquid culture but fully reduced biofilm formation to wild type levels. This suppressor had an insertion in *dnr*, a transcriptional regulator necessary for the expression of denitrification genes (159) upregulating the *nir*, *nor*, and *nos* operons (160) that are important for *P. aeruginosa* growth in anaerobic conditions. It has been shown that anaerobically growing *P. aeruginosa* PAO1 utilizing NO-based respiration formed longer cells and had elevated biofilm formation, which was reverted by a *nirS* mutation (161). The expression of *nir* is regulated by DNR (160), so an insertion in *dnr* may prevent *nirS*-mediated increases in biofilm formation. Furthermore, transcription of *dnr* was reduced 6.8 fold in a *P. aeruginosa* PAO1 *wspF* mutant which has elevated c-di-GMP (77), linking *dnr* transcription to c-di-GMP. Alternatively, *dnr* is adjacent to *rsmY*, which could be affected by the transposon insertion. RsmY is a small RNA whose expression is governed by the GacS/GacA two-component signaling system and acts to repress RsmA, which represses biofilm, pyocyanin, and quorum sensing (see (162) for review of Gac and Rsm signaling).

Suppressor 11 had an insertion in *potB,* a member of an operon responsible for polyamine transport (163). Why an insertion in the *pot* operon would partially revert growth rate, biofilm and aggregation is unknown, although promisingly the preliminary RNA-Seq data showed that at mid-log growth (OD_{600} ~ 0.5), the *potA*

and *potB* transcripts had a ~ 2 log2-fold change increase in Δ*orn* compared to wild type PA14. Thus it appears that the *pot* operon is upregulated in the absence of Orn. Transcription of *potA* and *potB* were also increased by ~ 2-fold in a *P. aeruginosa* PAO1 *wspF* mutant with elevated c-di-GMP (77). Together, these results suggest that polyamine transport could be c-di-GMP regulated.

Finally, suppressor 12 had an insertion in PA14_27420, a member of the HlyD family of secretion proteins. Proteins of this family make up the membrane fusion protein component of the Type I secretion system (see (164) for review of HlyD). It is uncertain why an insertion in this gene would result in a change in colony size and rescue of aggregation and biofilm, however efflux pump inhibitors have been shown to inhibit biofilm formation (165-168). Thus perhaps loss of full efflux pump function can prevent cell aggregates from forming.

4.7.4 Future directions

Because of the possibility of polar effects, complementation of the disrupted gene into the transposon mutants as well as clean in-frame deletions in the Δ*orn* background are currently being generated to determine the gene(s) responsible for the effects of the candidates identified. Additionally, due to the presence of an IPTG-inducible promoter in one portion of the transposon, it is possible to exploit this to further drive expression of adjacent genes. The tac promoter is leaky and may already be driving gene expression in the absence of IPTG. Growing these strains in the presence of IPTG inducer could further affect growth rate and could drive partial restoration of colony size to full restoration of coloy size. Alternatively, introduction

of the LacI repressor using a plasmid could revert colony size to small if gene expression driven by the transposon-encoded promoter is causing suppression.

Because these are mutantions that restore the phenotypes observed in an *orn* mutation to wild type, it would also be interesting to see if any of the implicated proteins bind pGpG or other nanoRNAs or if they interact with Orn. The Lee lab has a panel of NpN which can be 5′ labeled with ^{32}P to yield probes to assay binding by DRaCALA. If any proteins bind, they can be assayed for whether binding affects activity in or function in vitro. Currently, there are no demonstrated protein binding partners for Orn. Whether Orn can stably interact with another protein can be determined by pulldown with our His-tagged Orn protein to identify interacting partners from the cell.

Tn-Seq experiments are also planned in PA14 using a protocol previously established (169). (See (170) for first description of Tn-Seq by the Camilli lab and (171) for a review of the technique.) Transposon libraries of the wild type PA14 and the Δ*orn* strain are being generated for testing of fitness of growth in LB media. We expect to identify additional mutations able to suppress growth as well as synthetic lethal mutations that could not be detected in the colony size suppressor screen. Due to the nature of the colony size screen, which relied on visual identification of larger colony size as a readout of growth, it is likely that some mutations that are suppressors of growth defects were missed due to human error. Furthermore, this screen was limited by the number of colonies screened. The Tn-Seq will allow for sampling a larger population of mutants (the Tn-Seq library generated has ~200,000 mutant colonies compared to the ~40,000 screened in Chapter 4) to search for

mutations that can suppress growth defect. Furthermore, the colony size screen could not identify synthetic lethal mutants. These mutants, which would only be lethal in the Δ*orn* background, would not have grown in the transposon mutagenesis colony size screen. The identity of the secondary lethal mutants can shed light onto what genes or regulatory processes cause the deletion of *orn* to be lethal in *E. coli* but not in *P. aeruginosa* (52). It is possible that another RNase capable of degrading short oligoribonucleotides could be compensating in *P. aeruginosa*, and these might be identified in a screen to identify synthetic lethal mutations by in a PA14 Δ*orn* strain.

Finally, it would be intriguing to determine whether the effects seen in the Δ*orn* strain are due to changes in transcript levels, through protein-nanoRNA binding (either any nanoRNA or pGpG specifically) or through interaction of Orn with other proteins. On the transcriptional change front, the preliminary RNA-Seq data at early- and mid-log showed relatively few genes with greater than a 4 log2-fold change at these earlier growth phases. Of the results analyzed so far, the RNA-Seq and transposon mutagenesis have one point of overlap: transcription of *potB* is upregulated at mid-log in Δ*orn* compared to PA14 wild type and a transposon insertion in *potB* partially suppressed small colony phenotype in Δ*orn*. Intriguingly, the diguanylate cyclase SiaD is also upregulated at both early- and mid-log, suggesting that the elevated c-di-GMP observed in the Δ*orn* strain may derive not only from inhibited degradation but also from increased synthesis.. Additionally, RNA-Seq experiments will need to be conducted using samples grown to stationary phase and growing as biofilms. Transcriptome information from the PAO1 Orn depletion strain showed changes in genes linked to cell division (39). The microarray

revealed a ~ 2-fold decrease in *ftsZ* and ~ 2-fold increases in *ftsE*, *ftsX*, *minD* (39), which ties into our observation that insertions in a region of the genome encoding proteins that affect cell division suppress the Δ*orn* growth defects. To identify whether the transcriptome changes we see are due to just accumulated oligoribonucleotides rather than a specific effect of Orn itself, complementing with another active nanoRNase (see Chapter 3) should fully restore all transcriptional changes to wild type (39).

4.8 Materials and Methods

4.8.1 Strains and culture conditions

The *P. aeruginosa* PA14 Δ*orn*, Δ*pel*, and Δ*orn*Δ*pel* strains were generated as previously described (119) and in 2.9.2. Transposon mutants were maintained with gentamycin (15 µg/mL). All strains were grown in 37 °C with shaking in LB. For the growth curves, an overnight culture of each transposon mutant was adjusted to OD_{600} = 0.01 in LB and 200 µL was added to a well of a sterile 96-well plate. The plate was incubated, with shaking, at 37 °C in a SpectraMax M5 spectrophotometer (Molecular Devices). OD_{600} readings were taken at every 15 mins for 14 hrs to generate the growth curve. The exponential phase growth curve was fitted using the exponential growth equation $y = y_0(e^{kt})$ on GraphPad Prism, where y is the OD_{600}, x is time (h), y_0 is the y value when x = zero, k is the rate constant (1/h). The doubling time was found using ln(2)/k.

4.8.2 Transposon mutagenesis screen

The *P. aeruginosa* PA14 Δ*orn* was picked from single colonies, inoculated into LB at 37 °C with shaking overnight. Strains were subcultured into 10 mL of fresh LB and grown to OD_{600} = 0.4 at 37 °C with shaking, pelleted, and resuspended in x mL LB. pBTK20 in *E. coli* SMN10 was plated as a lawn onto LB agar plates containing 50 mg/mL carbenecillin and resuspended in 1 mL LB by swabbing with a sterile cotton swab. Five µL of PA14 Δ*orn* resuspension was mixed with 160 µL of *E. coli* SMN10 resuspension and 50 µL of mix was spotted onto a pre-dried and pre-warmed LB agar plate. The spots were allowed to fully absorb and dry for ~ 10 mins in a 37 °C incubator and incubated for 90 min. The spots were swabbed and resuspended in 1 mL LB each and 200 µL of each resuspension was plated onto an LB agar plate containing 75 µg/mL gentamycin and 25 µg/mL irgasan, yielding ~ 100-150 colonies per plate. A total of 250 plates were generated, yielding 40,000 colonies. Plates were incubated overnight at 37 °C and visually screened for larger colony size. Colonies of interest were picked, restruck for single colonies for validation of colony size changes, and saved for sequencing.

4.8.3 Sequencing of transposon mutants

Genomic DNA was isolated using ArchivePure DNA Cell/Tissue Kit (5 PRIME) according to manufacturer's instructions. Purified genomic DNA was digested using the blunt cutting restriction enzymes StuI and MscI according to manufacturer's instructions (New England Biolabs). The digested genomic DNA was cloned into StuI linearized pVL-blunt and plated on an LB agar plate containing 15 µg/mL gentamycin. Resulting colonies were isolated and miniprepped using Wizard

Plus SV Miniprep DNA Purification Kit (Promega) and sequenced using the transposon specific primers (see Table A1).

4.8.4 Aggregation and biofilm assays

See 2.10.6 for aggregation assay and 2.10.7 for microtiter plate biofilm assay. protocol All strains were grown in LB.

4.8.5 Microscopy

For agarose pad imaging of lysis, strains were grown in LB at 37 °C, spun down and resuspended in phosphate buffered saline (PBS), 3 µL was spotted onto agarose pads (1.5% agarose in PBS), transferred to sterile glass microscope slide, and placed in a glass bottom dish. For images of stationary phase bacteria, strains were grown to stationary phase in LB overnight at 37 °C with shaking and wet mounted on a glass slide with a coverslip. An Axio Observer.Z microscope (Zeiss) was used to image strains at 1000x magnification using phase contrast. Photographs were taken using ZEN 2012 imaging software (Zeiss).

4.8.6 RNA-Seq

PA14 wild type and Δ*orn* were grown in LB with 37 °C with shaking. Overnight cultures were subcultured into fresh LB and grown to OD_{600} ~ 0.3 and ~ 0.5 for RNA extraction using Qiagen RNeasy Mini Kit. Ribosomal RNA was removed from total RNA using Epicentre Ribo-Zero Magnetic Kit. Ribosomal free RNA was then fragmented and cDNA library was prepared using Epicentre ScriptSeq v2 RNA-Seq Library Preparation Kit. RNA-Seq libraries were sequenced using llumina HiSeq 1000 at the Institute for Bioscience & Biotechnology Research (IBBR)

at University of Maryland, College Park. Sequences were aligned to the PA14 reference genome using Bowtie2. Interactive Genome Viewer was used to visualize the data.

Chapter 5: Conclusions and Perspectives

5.1. Summary of dissertation research

Work presented in this dissertation demonstrates that Orn and other RNases with similar activity serve as the PDE-B responsible for the degradation of pGpG. When the Benziman lab first reported c-di-GMP in 1987 as an allosteric activator of cellulose synthase, they identified that an enzyme with DGC activity synthesized it from two GTPs, showed that it is linearized by PDE-As into pGpG, a two-nucleotide long RNA, which is finally further hydrolyzed to two GMPs by enzymes termed PDE-Bs (8). Despite years of research on c-di-GMP signaling, the identity of the PDE-B was not confirmed. In a screen of the *V. cholerae* ORFeome, one candidate binding protein was predicted to be an Orn homolog. Experiments demonstrate that Orn can cleave pGpG in vitro and is the major enzyme responsible for PDE-B activity in *P. aeruginosa* (119, 172). However, Orn is not encoded by all bacteria encoding c-di-GMP (94). Experiments here suggest that that NrnA (54), NrnB (58) and NrnC (59), RNases with functional but not structural homology to Orn, fill this role in other species. Data presented in this dissertation demonstrate that these RNases bind to and hydrolyze pGpG to GMP in vitro and can rescue the PA14 Δ*orn* phenotypic changes. Taken together, these results indicate that the RNases responsible for hydrolyzing two to five nucleotide long small RNAs are the PDE-Bs predicted by the Benziman lab. Thus, there appears to be a point of intersection between c-di-GMP and RNA degradation.

This dissertation also explores the possibility of pGpG having a regulatory role in bacteria. Although previously believed to be a non-functional degradation

product of c-di-GMP, we identified that pGpG can bind to and inhibit the EAL domain PDE RocR from *P. aeruginosa*, thus reducing the rate of c-di-GMP turnover in an in vitro dual DGC and PDE-A reaction. In support of this inhibition occurring in vivo, PA14 Δ*orn* mutants defective for pGpG cleavage had elevated c-di-GMP levels. Furthermore, in vitro inhibition of the EAL domain protein YfgF from *E. coli* has previously been reported (42) and a screen of the *V. cholerae* ORFeome screen for pGpG binding proteins identified eight EAL-domain binding proteins, suggesting that pGpG binding to and inhibition of EAL domains could be widespread. All together, this provides evidence that pGpG could have a function in maintaining c-di-GMP homeostasis in multiple bacterial species. Furthermore, the *V. cholerae* ORFeome screen identified other proteins that are potentially regulated by pGpG binding. Further experiments can determine whether these proteins are bona-fide pGpG-specific binding proteins and whether pGpG binding can alter their activities.

Finally, work here begins to unravel how loss of *orn* affects bacterial processes. Orn is essential in *E. coli* (52) and *V. cholerae* but not in *P. aeruginosa* (64) or *P. putida* (65). However, despite being viable, *orn* mutants in both *P. aeruginosa* and *P. putida* have impaired growth. Preliminary data from a transposon-mutagenesis screen for mutations that can restore small colony size in the Δ*orn* strain to wild type colony size as well as early RNA-Seq data reveal some processes that could be disrupted in *orn* mutants. All together, the results from this dissertation suggest that Orn could be involved in maintenance of c-di-GMP levels as well as regulation of other bacterial processes such as cell division. We propose that pGpG (or perhaps all nanoRNAs) could play a regulatory role in bacteria. The c-di-GMP

independent growh phenotypes observed in the PA14 Δ*orn* strain indicate that other mechanisms, including cell division and cell lysis, are being affected by accumulated nanoRNAs.

5.2 pGpG as a signaling molecule

One motivation for this dissertation research was to identify whether pGpG could function as a signaling molecule. Several lines of evidence suggest that pGpG could have an effect on bacterial physiology. First, work here indicates that pGpG is likely involved in c-di-GMP homeostasis. pGpG was shown to be able to bind to and inhibit the ability of the EAL-domain PDE-A RocR to cleave c-di-GMP in vitro, resulting in increased c-di-GMP half-life. Deletion of *orn* in *P. aeruginosa* resulted in elevated pGpG concentration as well as elevated c-di-GMP and increases in the c-di-GMP-regulated biofilm and aggregation phenotypes. Thus, the intracellular pGpG levels are likely important in regulation of c-di-GMP levels. In addition, the report that pGpG can inhibit c-di-GMP cleavage by an *E. coli* EAL domain protein (42), and the identification of eight EAL-domain containing that bound pGpG in the *V. cholerae* ORFeome screen all point to the likelihood that pGpG-mediated EAL-domain inhibition is a generalizable phenomena. In further support that pGpG could have signaling potential, the screen also identified other proteins that could be receptors: RNase G (VC0419), a DNA helicase (VC0371), a 5´-nucleotidase (VC2147), RecO (VC2459), guanylate kinase (VC2708) and a DHH/DHHA1 domain containing protein of unknown function (VCA0593). Because binding was detected via overexpression of the ORF in an *E. coli* cell lysate, it is not yet known whether all of these proteins are bona-fide pGpG-specific binding proteins or if they are false

positives. False positives in the ORFeome library could occur if these proteins activate the production of another pGpG binding protein in *E. coli*. This can be determined by purifying the protein of interest and assaying for binding. However, protein purification has proven challenging. Therefore, additional purification and expression optimization needs to be conducted in order to demonstrate binding of pGpG. Nevertheless, preliminary results suggest that purified RNase G and VCA0593 are able to bind pGpG (data not shown). VCA0593 contains a DHH/DHHA1 domain, making it a member of a large family of phosphoesterases (60) that include NrnA and NrnB (54, 58) as well as a PDE that linearizes c-di-AMP (92), making it an attractive candidate for another pGpG cleaving enzyme. Experiments are planned to assay VCA0593 hydrolysis activity against dinucleotides of different sequence.
RNase G could bind but not hydrolyze pGpG, so if pGpG can alter RNase G activity it could play a role in regulating RNA processing (see 3.7.2 for in-depth discussion).

5.3 Regulation of pGpG degradation

Signaling molecule levels must be tightly regulated in order to function effectively as a signal transduction system. Synthases must allow levels to rise rapidly and to a concentration in which binding occurs in response to stimulus and then be cleared once the stimulus is no longer present. The currently known bacterial signaling nucleotides all have specific and tightly regulated degradation enzymes that are responsible for removing them once signal termination is required: cAMP is hydrolyzed by CpdA to AMP (173), pppGpp is converted to ppGpp by GppA (174) and then hydrolyzed to GDP and pyrophosphate by SpoT (175, 176), c-di-AMP is linearized by HD domain and DHH/DHHA-1 domain enzymes (91, 92), c-di-GMP is

hydrolyzed by EAL (11) and HD-GYP domain enzymes (15), and cAMP-GMP is linearized by another class of HD-GYP proteins in *V. cholerae* (93). In contrast, Orn, NrnA, NrnB, and NrnC degrade all short oligoribonucleotides and are not pGpG specific. Although Orn and nanoRNases are not specific for pGpG, their activities could still be subject to regulation. Experimentally increasing intracellular nanoRNA concentration in *P. aeruginosa* PAO1 via depletion of Orn has been shown to cause transcriptional changes due to nanoRNA mediated transcription priming (39). In a follow up study in *E. coli*, it was reported that this priming was detected only in stationary phase in bacteria, suggesting growth-phase dependent regulation of nanoRNase activity (40). Whether and how Orn is regulated is currently unknown. It is possible that Orn transcription is controlled. Analysis of the upstream region of *P. aeruginosa* PA14 *orn* using the promoter prediction program BPROM (177) revealed a possible NarL promoter sequence in addition to the housekeeping promoter. The NarX-NarL two-component system is nitrate responsive transcriptional regulatory system responsible for transcription of genes necessary for nitrate/nitrite respiration (178), indicating that Orn expression could be altered during anaerobic growth conditions. Whether this is a true NarL binding site remains to be determined. There is another link between denitrification and Orn. Suppressor 10 of the *orn* growth defect had an insertion in *dnr*, a transcription factor involved in denitrification and NarL is an activator of *dnr* transcription (179). Thus regulation by NarL is an attractive possibility.

5.4 A potential role for pGpG in multi-tiered regulation by c-di-GMP

Synthesis of c-di-GMP initiates a cascade of events resulting in extensive changes in bacterial behavior. Recent studies show that there is now an emerging pattern in which c-di-GMP appears to regulate the same phenotype at multiple levels (Fig. 23). We have proposed to refer to this phenomenon as "sustained sensing" (45). Because the lifestyle changes regulated by c-di-GMP demand a high cost in cellular resources, as well as the opportunity cost of committing to the sessile lifestyle, it behooves the bacteria to repeatedly assess environmental conditions to ensure that conditions remain favorable to continue the lifestyle change. In this proposed sustained sensing mechanism, c-di-GMP first activates gene expression and, should environmental conditions persist after protein production, then binds to additional receptors to allosterically regulate protein function. Thus, c-di-GMP allows regulation at multiple steps within the same pathway. C-di-GMP sustained sensing relies on continued production of the same second messenger molecule over time. This property of sustained sensing provides two potential advantages: 1. it permits bacteria to rapidly re-sample the environment to re-activate already-synthesized proteins and 2. it bypasses the need for protein turnover to rapidly terminate the signaling nucleotide-triggered processes.

Two examples of c-di-GMP sustained sensing in activating a process include synthesis of the PEL polysaccharide in *P. aeruginosa* and the mannose-sensitive hemagglutinin (MSHA) pilus in *V. cholerae*. In the first example, c-di-GMP binds the FleQ transcription factor to permit transcription of the *pel* operon (27, 180). After transcription, c-di-GMP is also required to bind to PelD to allow PEL polysaccharide

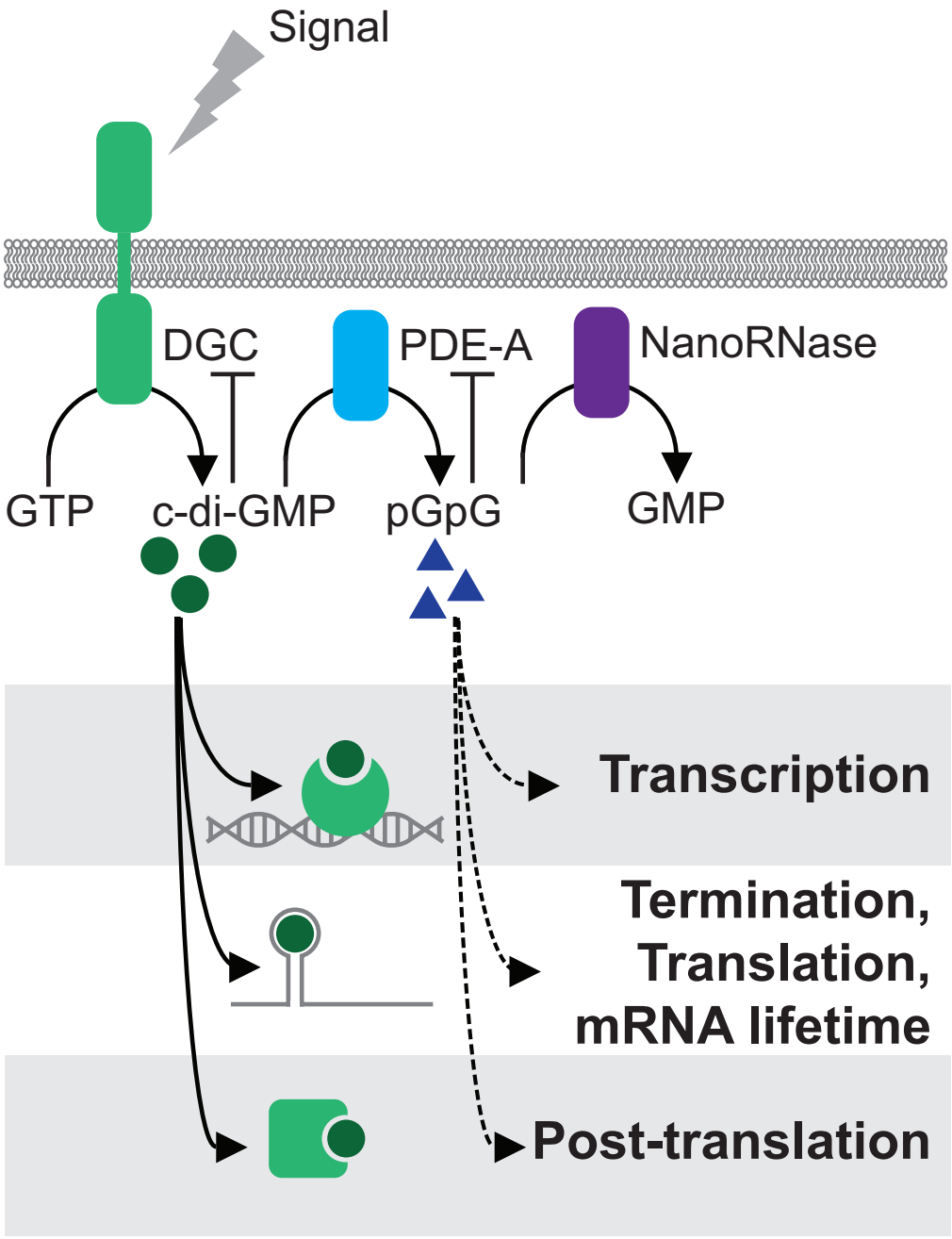

Figure 23. Multi-tiered regulation. Schematic of c-di-GMP turnover and processes regulated by c-di-GMP signaling. Signals can activate diguanylate cyclase to synthesize c-di-GMP, which then acts on transcription, transcript termination and/or translation, and post-translation protein activity. Signal termination occurs with the linearization of pGpG by PDE-As and then further by hydrolysis of pGpG to two GMPs by nanoRNases. The pGpG generated from c-di-GMP has the potential to also regulate transcription, mRNA stability, and post-translational protein activity.

synthesis (25). Similarly, elevated c-di-GMP levels allow transcription of the *msh* operon that synthesizes the MSHA pilus (47). However, c-di-GMP must still be present later to bind and activate the ATPase MshE in order to allow export of the MshA pilus to the cell surface (45, 181).

If the pGpG generated from c-di-GMP turnover proves to have signaling potential, it could contribute to the signaling cascade initiated by c-di-GMP synthesis to result in a continuation of sustained sensing. Loss of the Orn responsible for pGpG turnover has extensive effects on bacterial physiology, affecting biofilm formation, growth rate, and cell division. Whether pGpG directly regulates any of these effects still remains unknown. However, it is possible that pGpG could affect transcription by priming transcription, affecting protein translation by altering mRNA stability through interacting with RNases such as RNase G, and binding proteins to affect protein function as seen in EAL domain PDE-As. Further experiments demonstrating pGpG-specific regulation are necessary to confirm these theories.

5.5 Regulation by nanoRNAs

Deletion of *orn* in *P. aeruginosa* resulted in the formation of small colonies, longer doubling time, and altered cell morphology in stationary phase compared to wild type. There are several possibilities for the cause of these changes (discussed in more depth 3.7.4 and 4.1). They could be either indirect, in which loss of *orn* causes an accumulation in nanoRNAs or direct, because Orn binds to and affects the activity of other proteins. The latter scenario appears unlikely. Complementation with the structurally dissimilar NrnA, NrnB, and NrnC managed to restore the growth and cell division phenotype. Because they are not structurally homologous to Orn, it is

unlikely that complementation restored a protein-protein interaction. Additionally, complementation with catalytically inactive Orn alleles did not restore growth (data not shown). Nevertheless, identification of Orn-interacting protein partners could be valuable. It is currently unknown if Orn interacts with any proteins and binding partners could be regulators of Orn activity.

Experiments undertaken here have attempted to identify processes affected in the *orn* mutant. Transposon suppressors of the small colony phenotype observed in the *P. aeruginosa* PA14 Δ*orn* mutant and RNA-Seq comparing transcript levels between wild type and the Δ*orn* mutant have revealed several processes that could be regulated by Orn. The most promising based on preliminary data appear to be cell division, denitrification, and c-di-GMP signaling.

5.5.1 Cell division

The transposon suppressor screen identified four independent mutants with insertions in the same area in the genome near a gene implicated in cell division, *yciB*. Two were upstream of the *yciBI* operon, one was in *yciI*, and one was in PA14_22770, the first gene downstream of *yciI*. All four were able to suppress the elevated aggregation, biofilm formation, and growth defects of the Δ*orn* strain, although the insertion furthest from *yciB* (suppressor 1 in PA14_22770) appeared to be only partially able to suppress colony size and aggregation. A deletion of the *yciB* homolog in *S.* flexneri *S. flexneri* is filamentous during infection (143) and an *E. coli* *yciB* mutant had reduced cell length while an overexpressing strain had increased cell length (144). YciB was shown to interact with proteins involved in septation and elongation (145). Furthermore, a *yciB* mutant was also shown to have reduced biofilm

formation (146). The transposons could also be driving *cpxR* expression from the transposon-encoded *tac* promoter. CpxR is a two-component response regulated activated by CpxA (147-149) implicated in adhesion, biofilm formation, secretion, and division (see (150, 151) for reviews). An *E. coli* mutant that could not dephosphorylate CpxR had misplaced FtsZ ring (152). These are similar to the changes in cell morphology we observed. While the PA14 parental strain formed short bacilli in stationary cultures, the PA14 Δ*orn* strain was longer and also appeared to form more chained and diplobacilliod cells. Thus it is likely that the Δ*orn* mutant had growth issues due to disregulation of the cell division machinery.

How this disregulation is occurring is unknown. The Δ*orn* strain has elevated c-di-GMP and pGpG, either of which could be binding to previously unknown receptors to affect cell division. Alternatively, it is possible that accumulated short RNAs could be acting to prime transcription, resulting in wide-scale transcriptional changes, as was reported in *P. aeruginosa* depleted of Orn (39). In the microarray data comparing wild type to the depletion strain from that paper, six genes related to cell division were affected: the transcripts of *ftsE*, *ftsX* and *minD* were increased while *ftsZ* was decreased (39). Our RNA-Seq experiment did not indicate any changes in genes predicted to regulate cell division. However, RNA-Seq was not performed on cells grown to stationary phase, which is when we observed the cell division defects and altered cell morphology. Fluorescently tagged cell division proteins (FtsZ, MinC, MinD, ZapA, ZipA,) as well as the cytoskeletal protein MreB are being generated to introduce to the Δ*orn* strain to visualize the cell division process to determine where the process is occurring. Interestingly, overexpression of

RNase G in *E. coli* showed cell division defects (182), and we identified RNase G as a pGpG binding protein in the *V. cholerae* ORFeome screen. If pGpG binds the *P. aeruginosa* homolog of RNase G (PA14_58100) to alter its function, this could be one mechanism by which elevated pGpG affects cell division. Based on this hit, it would be interesting to determine whether any cell division machinery proteins can bind pGpG or other nanoRNAs.

5.5.2 Denitrification

P. aeruginosa is capable of denitrification, a process by which nitrogen oxides are utilized as terminal electron acceptors in the absence of oxygen. Genes involved in regulating denitrification could be involved in regulation of *orn* and may also be downstream targets of *orn*. NarL is a nitrate responsive transcriptional regulatory system responsible for transcription of genes necessary for nitrate and nitrite respiration (183). A predicted NarL binding site was located in the promoter region of *orn* in *P. aeruginosa* PA14, indicating that *orn* expression could be affected by NarL activation. Another gene upregulated by activated NarL is *dnr* (179). A transposon insertion in *dnr* in the Δ*orn* strain was able to suppress the Δ*orn* growth phenotypes. DNR activates transcription of the *nos* and *nor* genes (Tables 3 and 4) responsible for nitrous-oxide and nitric oxide reductase activity, respectively, during denitrification (159, 184). In our RNA-Seq of early- and mid-log cultures, *nos* and *nor* operon genes were ~ 2-fold decreased in the Δ*orn* strain compared to wild type PA14 in mid-log growth. Microarray of the *P. aeruginosa* Orn depletion strain also demonstrated a 2.7-fold decrease in *nosZ*, 4.5-fold decrease in *norB*, 3.2-fold decrease in *norC*, and a 9.5 fold increase of *dnr* transcript levels(39). Taken together, these preliminary data

indicate that Orn could be regulated during anaerobic growth to affect transcription of genes involved in denitrification. Interestingly, a *P. aeruginosa* mutant with elevated c-di-GMP signaling showed a decrease in *dnr* transcription (77), linking *dnr* to c-di-GMP signaling. Taken together, these results indicate that Orn could be regulated during anaerobic respiration and Orn and c-di-GMP could play a role in affecting expression of genes involved in denitrification. Confirmation of the NarL binding site and NarL regulation of Orn transcription, as well as confirmation of *dnr* involvement in suppressing the Δ*orn* growth defect are needed to demonstrate this relationship.

5.5.3 c-di-GMP signaling in PA14 Δ*orn*

Loss of *orn* in *P. aeruginosa* leads to elevated c-di-GMP levels. In vitro inhibition experiments indicate that one mechanism by which c-di-GMP can be elevated is via elevated pGpG binding to and preventing EAL domain PDE-A activity. Indeed in the Δ*orn* strain, levels of pGpG detected by LC-MS/MS were above K_d determined for the EAL domain PDE-A RocR, indicating that pGpG-mediated inhibition of PDE-As is possible. Additionally, our preliminary RNA-Seq results also showed an increase in transcription of a DGC, *siaD*, which would also elevate c-di-GMP. It is not certain how loss of *orn* would cause upregulation of *siaD*. Nevertheless, as a consequence, PA14 Δ*orn* showed increased biofilm and aggregation, which was dependent on the c-di-GMP regulated *pel* operon. However, we also observed that the Δ*orn* strain displayed growth defects that were independent of the *pel* operon, leading us to hypothesize that there were c-di-GMP independent processes regulated by Orn. Surprisingly, one transposon mutant suppressor that could restore growth to wild type had an insertion in *fleQ*. Like the Δ*orn*Δ*pel* double

mutant, the Δ*orn fleQ*::tn strain could not form aggregates or produce biofilm. Thus, it appears that there is another FleQ-regulated, and therefore c-di-GMP-regulated, process that is responsible for the growth defect.

Another observation suggests c-di-GMP involvement in the growth defect. The Δ*orn* strain also shares some characteristics with the "small colony variant" (SVC) isolated chronically infected patients, so called because they form smaller colonies on agar plates. SCVs have been isolated from cystic fibrosis patient lungs chronically infected with *P. aeruginosa* (185-187), other chronic *P. aeruginosa* infections (188) and from *P. aeruginosa* grown in biofilms in laboratory conditions (189), suggesting that the range of phenotypic changes observed for SCVs may be involved in better adaptation to specific environments. These SCVs arise due to multiple disparate mutations that ultimately result in higher c-di-GMP levels (for reviews, see (190, 191)). In general, SCVs form small and wrinkly colonies, have increased biofilm formation, increased auto-aggregation, increased adherence, reduced motility, and reduced growth rate. Like the SCVs, the Δ*orn* strain is hyper-aggregative, has elevated biofilm formation and reduced growth rate; unlike the SCVs, the Δ*orn* strain forms smooth colonies and are still motile (data not shown). Taken together, this suggests that increasing c-di-GMP in the cell could affect growth rate and colony size. Because there has been no report of a c-di-GMP sensing cell division regulator, it is tempting to think that pGpG, which would be generated at high levels during rapid c-di-GMP turnover and is elevated in the Δ*orn* strain, could be responsible for the reduced growth rate.

5.6. A role for c-di-GMP and pGpG in RNase activity

The data shown here demonstrate that c-di-GMP turnover and RNA turnover intersect at the nanoRNases. It is also possible that c-di-GMP and pGpG could play a role in regulating RNase activity. C-di-GMP has been implicated in RNA processing via regulation of PNPase activity from *E. coli* (192). PNPase is a member of the RNA degradosome in *E. coli* (130) and is a bifunctional enzyme that can act as a 3′ to 5′ exoribonuclease (193) and also as a 3′ polyribonucleotide polymerase that adds heteropolymeric tails to the 3′ end of mRNAs (194). PNPase was shown to bind c-di-GMP with a K_d of 2.9 μM, and the presence of c-di-GMP was shown to enhance PNPase polymerase activity in vitro (192). In this regulatory pathway, two O_2-sensing enzymes DosC and DosP act as DGC and PDE-A to synthesize and linearize c-di-GMP, respectively (192). DosC and DosP were shown to be in a complex with PNPase, and the authors proposed that synthesis of c-di-GMP by DosC allowed binding of c-di-GMP to PNPase to cause a activation of polymerase activity, while hydrolysis to pGpG by DosP would cause deactivation of polymerase activity (192). A *pnp* mutant in *E. coli* lost the ability to form biofilm (195), further implicating PNPase-mediated RNA processing in c-di-GMP-mediated bacterial behavior. Although a report of *Xanthamonas campestris* PNPase crystalized in the presence of c-di-GMP has been published (196), the full structure is not available and the location of the c-di-GMP binding pocket has not been shown. Unfortunately, the expression of PNPase (VC0647) was not detectable by SDS-PAGE in *V. cholerae* ORFeome, so we were not able to assay for pGpG binding to this protein. A PNPase homolog (PA14_62710) is encoded in *P. aeruginosa* PA14, indicating that c-di-GMP and

pGpG-mediated regulation of RNA turnover could be present in this species as well. If pGpG can also bind to PNPase to affect its activity or prevent c-di-GMP binding, it complicates the c-di-GMP-mediated PNPase regulation.

In our *V. cholerae* pGpG binding screen for pGpG binding proteins, we also hit another RNase, RNase G (VC2030), which did not bind c-di-GMP (45). RNase G did not cleave pGpG (data not shown), but we hypothesized that it could interact with pGpG at the 5´ sensor pocket. RNase G requires a 5´ monophosphate for cleavage (100) and the crystal structure showed the presence of a 5´ monophosphate binding site separate from the active site responsible for cleavage of RNA (104). The binding of a 5′ monophosphate was hypothesized to cause an allosteric change that permits cleavage of the RNA (104). RNase G overexpression in *E. coli* caused defects in cell division (182), with the formation of chaining cells and minicells. The PA14 Δ*orn* mutant seems to have a cell division defect as well (Fig. 18C), suggesting RNase G activity could be affected by pGpG via the 5´ monophosphate binding pocket. Furthermore, RNase E also requires a 5´ monophosphate on the substrate (135) and possesses a similar 5´ sensor pocket (104) However, RNase E was not identified in our screen, possibly due to poor expression as detected by SDS-PAGE. It is possible that binding of pGpG to this pocket could affect RNase G or RNase E function. A previous study demonstrated that an artificial guide sRNA with a 5´ monophosphate can activate cleavage of a target RNA by allosteric activation of RNase E through binding to the 5´ sensor; their study also showed this mechanism may be involved in MicC sRNA-mediated degradation of *ompD* mRNA (197). If pGpG can affect RNase G and RNase E activity by binding the 5´ sensor pocket, this would provide another

point of RNase regulation initiated by c-di-GMP synthesis. In this way, accumulated pGpG (or other nanoRNAs with a 5´ monphosphate) could act to slow general RNA degradation.

5.7. Structural basis for the ability of a subset of RNases to degrade nanoRNAs

A question raised during this research project was how 3´ to 5´exoribonucleases can distinguish between sizes of RNA substrate. Processive 3´ to 5´ exoribonucleases bind RNA and cleave monomers from the 3' end. In vitro, it appears that not all 3´ to 5´exoribonucleases can fully degrade oligoribonucleotides completely to monomers. Experiments with 5´ end-labeled oligoribonucleotides indicate that many of these enzymes appear to act processively, but wind up releasing a very short end product that is resistant to cleavage. These RNases givee final products that are monomers and an n-mer that was the terminal 5´ end of the original oligoribonucleotide (where n is 2-6, depending on RNase). For example, incubation of 5´ ^{32}P-labeled poly(A) substrates (either 6, 8, 10 or 17 nucleotides long) with RNase R or RNase II from *E. coli* resulted in accumulation of cleavage-resistant 2mers or 4mers, respectively (120). Similar results were obtained when incubating a 5´ ^{32}P-labeled 35mer poly(A) with RNase R from *S. typhimurium*, and *S. pneumonia*, and RNase II from *S. typhimurium* (198). Incubation of RNase T from *E coli* with a 5´ ^{32}P-labeled 17mer poly(A) or poly(U) resulted in an accumulation of 2mers resistant to cleavage, and RNase T had very poor affinity for pApA (K_m ~ 1000) almost no activity against pApA (k_{cat}/K_m ~ 0.04) (199). Thus, it appears that for these exoribonucleases, cleavage is processive until the substrate is reduced to a final oligo too short to be cleaved.

However, some 3´ to 5´exoribonucleases (the "nanoRNases" Orn, NrnA, NrnB, and NrnC) can bind to and cleave these very short RNAs down to monomers. They also appear to have a preference for shorter substrates. Loss of Orn in an *E. coli* conditional mutant accumulated 5mer and smaller RNAs compared to wild type (52), suggesting that Orn specifically degrades these short RNA substrates. In vitro, NrnA, NrnB and NrnC had minimal activity against 24mers. NrnA degraded a 24mer at 0.01 pmol/min/µg compared to 1.5 and 0.14 for 3mers and 5mers, respectively (54). NrnB has slight activity against 24mers with 2 pmol/min/µg vs 1 nmol/min/µg for 5mer of C (58). NrnC has more activity against 24mers than NrnA or NrnB, but still 1000x lower than than 5mers (8.3 pmol/min/µg protein vs 8 nmol/min/µg protein) (59). Although crystal structure information is not available for all of these RNases, there appears to be some structural basis for the length of oligoribonucleotides left by degradation by processive 3´ to 5´exoribonucleases. Comparison of the structures of the DEDD exoribonucleases can give an illustrative example.

RNase T and Orn both belong to the DEDDh sub-family of nucleases. They both crystalize as homodimers with the same orientation, causing the active site from one monomer to be opposite to RNA binding site provided by the other monomer (86, 200). However, they have different substrate preferences and Orn is able to hydrolyze 2mer oligoribonucleotides in vitro while RNase T cannot. This difference could be explained by the size of the RNA binding site and the DEDD active site in these proteins. RNase T has a large basic patch in the RNA binding site compared to a smaller basic patch in Orn, suggesting that RNase T can bind longer RNA substrates compared to Orn (86, 200). Orn also has a comparatively longer DEDD active site,

which is modeled to be able to fully accommodate a U 5mer, which is not true for other DEDD type DNases and RNases the authors modeled (86). RNase T can therefore interact with longer RNA species, but cannot cleave very short oligoribonucleotides as the enzyme has much lower affinity for these short substrates compared to longer substrates (199), likely due to differences in the RNA binding site. These observations indicate that while RNase T and Orn both belong to the same sub-family and have the same dimer orientation, differences in substrate binding and active site size can explain their differences in final product size.

RNase D is a DEDDy type RNase that appears to be specific for tRNA 3' end processing. Unlike RNase T and Orn, RNase D does not form a dimer. Instead, it is a monomer that forms a ring shape with 3 domains: 2 C-terminal domains (HRDC1 and HRDC2) and one domain containing the DEDDy site (201). In reporting the crystal structure of RNase D, the authors speculate that while short 2mer RNAs can be modeled into the DEDDy active site, its DEDD domain is highly negatively charged and may not be a good binding site (201). Thus, another part of the protein is required to bind RNAs for cleavage by the active site, which they proposed to be the two HDRC domains. They proposed, based on modeling of a dsRNA into the crystal structure of RNase D, that the cyclical funnel shape made by the three domains in RNase D might prefer binding RNA with secondary dsRNA structure. This could orient a 3' ssRNA overhang into the DEDDy catalytic site and explains its substrate preference for tRNAs (201).

NrnC is a recently reported DEDDy RNase that can cleave short single stranded oligoribonucleotides down to monomers (59). NrnC was often mis-annotated

RNase D despite being much shorter and lacking the two HDRC C-terminal domains and the RNase D motif in the DEDDy domain (59, 201). A protein from species of *Synechocystis* (UniProt: Q55641), was cited as an example of an incorrectly annotated RNase D based on its shorter length and missing motif prior to the report of NrnC (201). NrnC, identified from *B. birtlesii* (59) has 45% homology to this *Synechocystis* protein and 45% homology to a protein annotated RNase D in *C. crescentus* (CC_3603), which was proposed to be a NrnC homolog (59). Currently, the crystal structure of NrnC is not known, so the structural basis underlying its different substrate affinity and final product length is not certain. It is likely that the NrnC will also have a longer DEDD active site and a shorter RNA-binding basic patch observed in Orn.

The crystal structures of NrnA from *B. fragilis* and *M. smegmatis* have been solved (124, 202). It is a member of the DHH/DHHA1 domain family, which includes RecJ which binds and acts on single stranded DNA. Comparison of the solved structure of *M. smegmatis* NrnA to RecJ showed that it had a very similar structure in the DHH and the DHHA1 domains (124, 203). However, NrnA was crystalized as a homodimer and RecJ family exonucleases are monomers. The authors speculate that the linker between the DHH and DHHA1 domains forms the substrate binding cavity. An oligonucleotide/oligosaccharide-binding fold between the DHH and DHHA1 domain in RecJ is not present in NrnA was proposed to explain how RecJ can bind longer oligonucleotide substrates.

The structures of two members of the RNR family RNases can give insight into a mechanism that determines the length of the final end product of RNase

cleavage. The cystral structure of a RNR family RNase, RNase II from *E. coli*, has been solved (204). RNase II cleaves processively but leaves a final 4mer that is resistant to cleavage. RNase II has four domains: two cold shock domains (CSD1 and CSD2), one RNB catalytic domain, and an S1 RNA binding domain. It is proposed to cleave ssRNA by threading ssRNA via a channel made of the S1 domain and CSD1 and CSD2 domains (termed the "anchor region" or "clamp") into the buried active site in RNB, which appears to accommodate a 5mer RNA (205). The clamp binds the RNA strand and translocates the RNA into the catalytic site, causes packing of the five 3' bases in the catalytic site, which allows for cleavage. The monomer cleaved is released and the RNA strand is translocated by the clamping region again into the catalytic site (205). Once the oligoribonucleotide is < 5mer long, it is predicted to be fully within the active site and too short to interact with the clamping region. Thus, after a single cleavage, translocation and packing cannot occur and no additional cleavage or translocation happens, resulting in release of a 4mer (204, 205). A Y residue (Y253) in the clamping region was believed to be responsible for determining the end-product size in RNase II, as a Y253A mutant release a final product size of 10 nt instead of 4 (206). RNase R is structurally similar and thought to behave the same way as RNase II. RNase R leaves a 2mer end product in vivo (120). A mutant changing the equivalent Y residue (Y324) in RNase R to alanine also increased the final product size release from a 2mer to a 5mer (207), supporting the hypothesis that this residue is important in setting the length of the final end product.

Together, these structural studies indicate that there is a structural basis for the differential ability of 3´ to 5´exoribonucleases to degrade very short

oligoribonucleotides. As further crystal structure information is gathered, additional insights into the mechanism by which some RNases can preferentially degrade these very short RNA substrates may come to light. In the context of this thesis, it appears that any RNases capable of degrading nanoRNAs are able to serve as the PDE-B enzyme responsible for cleaving pGpG.

Appendices

Table 3. Genes > 2 log2-fold up or downregulated in PA14 compared to Δ*orn* at early-log (OD_{600} = 0.3).

Gene	*Name*	Function	log2 Change
PA14_00230		Rossmann fold nucleotide-binding protein	2.4
PA14_02010		hypothetical protein	-2.1
PA14_02110	*siaD*	diguanylate cyclase	2.4
PA14_02500	*exbB1*	transport protein ExbB	2.1
PA14_02510	*exbD1*	transport protein ExbD	-2.4
PA14_02610		phosphoribosyl-dephospho-CoA transferase	2.1
PA14_03420		hypothetical protein	-2.7
PA14_03830	*aguB*	N-carbamoylputrescine amidohydrolase	-2.1
PA14_06800		hypothetical protein	-2.1
PA14_06810	*norC*	nitric-oxide reductase subunit C	-2.1
PA14_06840		denitrification protein NorD	-2.4
PA14_06900		hypothetical protein	2.5
PA14_07330		hypothetical protein	-2.6
PA14_07890		ABC transporter permease	-2.2
PA14_07970		hypothetical protein	2.5
PA14_07980		hypothetical protein	2.2
PA14_08000		hypothetical protein	3.0
PA14_08010		hypothetical protein	2.3
PA14_08020		bacteriophage protein	2.7
PA14_08030		phage baseplate assembly protein	3.0
PA14_08040		phage tail protein	2.8
PA14_08050		tail fiber protein	2.3
PA14_08060		tail fiber assembly protein	2.3
PA14_08070		phage tail sheath protein	2.2
PA14_08090		phage tail tube protein	2.9
PA14_08100		hypothetical protein	3.0
PA14_08110		hypothetical protein	3.0
PA14_08120		tail length determinator protein	3.2
PA14_08130		hypothetical protein	2.8
PA14_08140		hypothetical protein	2.5
PA14_08150		phage late control gene D protein	2.4
PA14_08160		lytic enzyme	2.7
PA14_08180		hypothetical protein	4.4
PA14_08200		hypothetical protein	2.4
PA14_08210		hypothetical protein	3.0
PA14_08220		hypothetical protein	3.0
PA14_08230		hypothetical protein	3.5
PA14_08240		hypothetical protein	3.0
PA14_08250		hypothetical protein	2.1
PA14_08260		minor tail protein L	2.9
PA14_08270		hypothetical protein	2.4
PA14_08280		bacteriophage protein	2.5
PA14_08300		phage-related protein, tail component	2.7
PA14_08990	*rpsH*	30S ribosomal protein S8	-2.3
PA14_09070	*rpmJ*	50S ribosomal protein L36	-2.5
PA14_09220	*pchB*	isochorismate-pyruvate lyase	-2.6
PA14_09230	*pchC*	pyochelin biosynthetic protein PchC	-3.0
PA14_09300		ABC transporter ATP-binding protein	-2.8
PA14_09320		ABC transporter ATP-binding protein	-3.0
PA14_09340	*fptA*	Fe(III)-pyochelin outer membrane receptor	-2.4

PA14_09350		hypothetical protein	-2.3
PA14_09480	*phzA1*	phenazine biosynthesis protein	2.0
PA14_09500	*opmD*	outer membrane protein	2.4
PA14_10070		zinc-dependent oxidoreductase	2.2
PA14_10380		hypothetical protein	-2.2
PA14_10890		short-chain dehydrogenase	3.0
PA14_10900		alcohol dehydrogenase	2.7
PA14_11320		hypothetical protein	-2.6
PA14_13050		hypothetical protein	-4.1
PA14_13690		methyltransferase	2.1
PA14_13970		hypothetical protein	-2.5
PA14_15110		hypothetical protein	-2.5
PA14_16300		hypothetical protein	2.0
PA14_19500		hypothetical protein	6.2
PA14_19910		pyruvate dehydrogenase E1 component, beta chain	2.1
PA14_20150	*nosL*	NosL protein	-3.0
PA14_20170	*nosY*	NosY protein	-3.5
PA14_20180	*nosF*	NosF protein	-2.4
PA14_20200	*nosZ*	nitrous-oxide reductase	-2.3
PA14_20400	*phnK*	phosphonate C-P lyase system protein PhnK	2.1
PA14_20900		MFS transporter	-2.6
PA14_20950	*fabH2*	3-oxoacyl-ACP synthase	-2.5
PA14_20960		isomerase	-2.3
PA14_20980		short chain dehydrogenas	-2.3
PA14_21840		hypothetical protein	-2.3
PA14_22210		hypothetical protein	2.6
PA14_22220		hypothetical protein	3.0
PA14_22230		hypothetical protein	2.2
PA14_22240		hypothetical protein	3.0
PA14_22250		hypothetical protein	3.5
PA14_22260		hypothetical protein	3.3
PA14_22320		hypothetical protein	2.3
PA14_22980		sugar ABC transporter substrate-binding protein	-4.3
PA14_22990		ABC sugar transporter permease	-3.1
PA14_23000		ABC sugar transporter permease	-4.2
PA14_23010	*gltK*	ABC transporter ATP-binding protein	-2.9
PA14_23610		hydrolase	2.1
PA14_24650	*rmf*	ribosome modulation factor	-2.7
PA14_25630	*rpmF*	50S ribosomal protein L32	2.7
PA14_26300		hypothetical protein	-3.4
PA14_26460	*cobK*	cobalt-precorrin-6x reductase	2.9
PA14_27690		RNA polymerase sigma factor	2.3
PA14_28660	*infC*	translation initiation factor IF-3	-2.2
PA14_28980		Fe2+-dicitrate sensor	3.6
PA14_29530		type II secretion system protein	2.3
PA14_29980	*nuoE*	NADH dehydrogenase subunit E	2.0
PA14_30900		conjugal transfer protein TrbJ	2.1
PA14_30930		TrbC-like protein	2.5
PA14_30950		hypothetical protein	2.7
PA14_31080		conjugal transfer protein	-2.3
PA14_31160		hypothetical protein	3.5
PA14_31170		hypothetical protein	4.1
PA14_31450		hypothetical protein	-2.3
PA14_31500		AMP-binding protein	-2.2
PA14_32650		glutathione S-transferase	2.0
PA14_33060		hypothetical protein	3.2

PA14_33500	*pvdH*	diaminobutyrate--2-oxoglutarate aminotransferase	3.0
PA14_33520		thioesterase	2.2
PA14_34270		ABC transporter ATP-binding protein	2.0
PA14_34700		beta lactamase	6.0
PA14_34710		major facilitator transporter	5.7
PA14_35710		hypothetical protein	-2.5
PA14_35950		dehydrogenase	2.8
PA14_36480		hypothetical protein	2.2
PA14_36670		hypothetical protein	2.0
PA14_36680		hypothetical protein	2.9
PA14_36930		hypothetical protein	3.4
PA14_37370		esterase	2.3
PA14_37470		flavin-dependent oxidoreductase	2.8
PA14_37670		hypothetical protein	-3.3
PA14_39630		hypothetical protein	-3.4
PA14_39810		transmembrane sensor	2.5
PA14_42030		hypothetical protein	-2.2
PA14_42510		hypothetical protein	2.2
PA14_43370	*kdpC*	potassium-transporting ATPase subunit C	2.9
PA14_43380	*kdpB*	potassium-transporting ATPase subunit B	2.8
PA14_43400	*kdpA*	potassium-transporting ATPase subunit A	3.0
PA14_43830	*panB*	3-methyl-2-oxobutanoate hydroxymethyltransferase	-2.1
PA14_44230		hypothetical protein	-2.0
PA14_47070		hypothetical protein	-2.6
PA14_47390		transmembrane sensor	2.2
PA14_47860		oxidoreductase	2.3
PA14_47870		hypothetical protein	2.3
PA14_51390	*pqsD*	3-oxoacyl-ACP synthase	2.0
PA14_51420	*pqsB*	PqsB	2.2
PA14_52110		hypothetical protein	-2.3
PA14_52460	*mgtE*	Mg transporter MgtE	-2.5
PA14_52510		hypothetical protein	2.3
PA14_52570	*rsmA*	carbon storage regulator	-2.2
PA14_53070	*hpd*	4-hydroxyphenylpyruvate dioxygenase	-2.3
PA14_55110		hypothetical protein	-2.2
PA14_55290		hypothetical protein	2.4
PA14_55480	*hxcX*	HxcX type II secretion system protein	2.4
PA14_56480		hydrolase	2.8
PA14_56570		acyltransferase	-3.2
PA14_56780	*sodB*	superoxide dismutase	-2.1
PA14_57020	*groES*	co-chaperonin GroES	-2.2
PA14_57030	*fxsA*	FxsA protein	-2.6
PA14_59280	*pilP2*	type IV B pilus protein	2.1
PA14_59370		hypothetical protein	-2.2
PA14_59470		hypothetical protein	2.6
PA14_59490		hypothetical protein	2.8
PA14_59500		hypothetical protein	2.9
PA14_59510		hypothetical protein	3.8
PA14_59520		hypothetical protein	3.2
PA14_59670		hypothetical protein	2.1
PA14_59960	*dsbA2*	DsbA2 protein-disulfide isomerase	-2.1
PA14_60730		outer membrane protein	-2.1
PA14_60750	*pra*	protein activator	-2.2
PA14_63620	*lipC*	lipase LipC	2.9
PA14_63710		glycosyl transferase family protein	3.4
PA14_64260		hypothetical protein	2.2

PA14_64680	*ureJ*	hypothetical protein	-2.2
PA14_64700		RNA polymerase sigma factor	2.3
PA14_65410	*orn*	oligoribonuclease	-3.8
PA14_66875	*phaF*	polyhydroxyalkanoate synthesis protein PhaF	-2.0
PA14_67140		hypothetical protein	-2.1
PA14_67350	*hutU*	urocanate hydratase	2.2
PA14_67440		N-formimino-L-glutamate deiminase	2.2
PA14_68460		hypothetical protein	-2.3
PA14_68860	*gcvH1*	glycine cleavage system protein H	-2.2
PA14_70180	*rpmG*	50S ribosomal protein L33	2.2
PA14_71350		hypothetical protein	-2.5
PA14_72370		hypothetical protein	-2.1

Table 4. Genes > 2 log2-fold up or downregulated in PA14 compared to Δ*orn* at mid-log (OD_{600} = 0.5).

Gene	Name	Function	log2 Change
PA14_00230		Rossmann fold nucleotide-binding protein	2.47
PA14_02110	*siaD*	diguanylate cyclase	2.59
PA14_02130		hypothetical protein	2.66
PA14_02140		hypothetical protein	2.45
PA14_02150	*siaA*	hypothetical protein	3.36
PA14_02610		phosphoribosyl-dephospho-CoA transferase	2.49
PA14_04780		oxidoreductase	-2.11
PA14_06180	*fiuI*	RNA polymerase sigma factor	2.16
PA14_06790		cytochrome c oxidase subunit	-2.18
PA14_06800		hypothetical protein	-2.96
PA14_06810	*norC*	nitric-oxide reductase subunit C	-2.59
PA14_06830	*norB*	nitric-oxide reductase subunit B	-2.08
PA14_06840	*norD*	denitrification protein NorD	-2.76
PA14_07970	*ptrB*	hypothetical protein	3.02
PA14_07980		hypothetical protein	2.98
PA14_07990		hypothetical protein	2.69
PA14_08000		hypothetical protein	2.88
PA14_08010		hypothetical protein	2.83
PA14_08020		bacteriophage protein	3.36
PA14_08030		phage baseplate assembly protein	3.46
PA14_08040		phage tail protein	3.18
PA14_08050		tail fiber protein	2.81
PA14_08060		tail fiber assembly protein	2.92
PA14_08070		phage tail sheath protein	2.99
PA14_08090		phage tail tube protein	3.00
PA14_08100		hypothetical protein	3.20
PA14_08110		hypothetical protein	3.56
PA14_08120		tail length determinator protein	3.40
PA14_08130		hypothetical protein	3.25
PA14_08140		hypothetical protein	3.29
PA14_08150		phage late control gene D protein	2.98
PA14_08160		lytic enzyme	2.98
PA14_08180		hypothetical protein	4.11
PA14_08190		hypothetical protein	2.51
PA14_08200		hypothetical protein	2.80
PA14_08210		hypothetical protein	3.18
PA14_08220		hypothetical protein	3.92
PA14_08230		hypothetical protein	3.28
PA14_08240		hypothetical protein	3.47
PA14_08250		hypothetical protein	2.58
PA14_08260		minor tail protein L	3.32
PA14_08270		hypothetical protein	3.13
PA14_08280		bacteriophage protein	3.11
PA14_08300		phage-related protein, tail component	3.28
PA14_08310		hypothetical protein	2.22
PA14_09500	*opmD*	outer membrane protein	2.35
PA14_09530	*mexH*	RND efflux membrane fusion protein	2.15
PA14_09850		porin	2.00
PA14_10360		hypothetical protein	-2.23
PA14_10890		short-chain dehydrogenase	2.80
PA14_10900		alcohol dehydrogenase	2.67
PA14_13050		hypothetical protein	-4.18
PA14_13960		hypothetical protein	-2.14

PA14_14540		hypothetical protein	2.20
PA14_14550		hypothetical protein	2.42
PA14_17630	*potB*	polyamine transport protein PotB	2.40
PA14_17640	*potA*	polyamine transport protein PotA	2.11
PA14_19500		hypothetical protein	6.20
PA14_20140	*fpr*	ferredoxin--NADP+ reductase	-2.12
PA14_20150	*nosL*	NosL protein	-3.27
PA14_20170	*nosY*	NosY protein	-3.69
PA14_20180	*nosF*	NosF protein	-2.75
PA14_20200	*nosZ*	nitrous-oxide reductase	-2.97
PA14_20900		MFS transporter	-2.97
PA14_20920		hypothetical protein	-2.42
PA14_20940		acyl carrier protein	-3.24
PA14_20950	*fabH2*	3-oxoacyl-ACP synthase	-3.79
PA14_20960		isomerase	-3.32
PA14_20970	*cyp23*	cytochrome P450	-2.86
PA14_20980		short chain dehydrogenas	-3.12
PA14_21000		hypothetical protein	-2.80
PA14_21010		FAD-dependent monooxygenase	-2.90
PA14_21020		non-ribosomal peptide synthetase	-3.10
PA14_22210		hypothetical protein	2.26
PA14_22220		hypothetical protein	2.87
PA14_22230		hypothetical protein	2.40
PA14_22240		hypothetical protein	3.16
PA14_22250		hypothetical protein	4.47
PA14_22260		hypothetical protein	3.70
PA14_22320		hypothetical protein	3.16
PA14_22980		sugar ABC transporter substrate-binding protein	-5.21
PA14_22990		ABC sugar transporter permease	-4.31
PA14_23000		ABC sugar transporter permease	-4.77
PA14_23010	*gltK*	ABC transporter ATP-binding protein	-4.23
PA14_23090		keto-hydroxyglutarate-aldolase/keto-deoxy-phosphogluconate aldolase	-2.04
PA14_23590		transcriptional regulator	2.29
PA14_25630	*rpmF*	50S ribosomal protein L32	2.24
PA14_26300		hypothetical protein	-3.26
PA14_26460	*cobK*	cobalt-precorrin-6x reductase	2.71
PA14_27690		RNA polymerase sigma factor	2.24
PA14_28980		Fe2+-dicitrate sensor	3.49
PA14_29240		hydrolase	-2.06
PA14_29530		type II secretion system protein	2.33
PA14_30930		TrbC-like protein	2.47
PA14_30950		hypothetical protein	2.58
PA14_31080		conjugal transfer protein	-2.35
PA14_31100		plasmid partitioning protein	2.02
PA14_31160		hypothetical protein	3.88
PA14_31170		hypothetical protein	3.83
PA14_31500		AMP-binding protein	-2.54
PA14_31510		short-chain dehydrogenase	-2.05
PA14_33060		hypothetical protein	3.08
PA14_33500	*pvdH*	diaminobutyrate--2-oxoglutarate aminotransferase	2.66
PA14_33520		thioesterase	2.64
PA14_33710	*pvdO*	protein PvdO	2.03
PA14_33720	*pvdN*	protein PvdN	2.15
PA14_34700		beta lactamase	5.94
PA14_34710		major facilitator transporter	5.64

PA14_35160		hypothetical protein	2.48
PA14_35950		dehydrogenase	3.11
PA14_36480		hypothetical protein	2.39
PA14_36670		hypothetical protein	2.22
PA14_36680		hypothetical protein	2.79
PA14_36930		hypothetical protein	3.28
PA14_37370		esterase	2.39
PA14_37470		flavin-dependent oxidoreductase	2.52
PA14_37670		hypothetical protein	-2.59
PA14_38460	*gnyB*	acyl-CoA carboxyltransferase subunit beta	-2.17
PA14_38510	*hmgA*	homogentisate 1,2-dioxygenase	-2.06
PA14_39630		hypothetical protein	-3.27
PA14_39810		transmembrane sensor	2.22
PA14_42030		hypothetical protein	-2.02
PA14_42510		hypothetical protein	2.47
PA14_42580	*pscO*	translocation protein in type III secretion	2.04
PA14_42960		hypothetical protein	-2.13
PA14_43370	*kdpC*	potassium-transporting ATPase subunit C	3.00
PA14_43380	*kdpB*	potassium-transporting ATPase subunit B	2.87
PA14_43400	*kdpA*	potassium-transporting ATPase subunit A	2.56
PA14_43405	*kdbF*	potassium-transporting ATPase subunit F	2.24
PA14_46250		hypothetical protein	2.25
PA14_47070		hypothetical protein	-2.54
PA14_47390		transmembrane sensor	2.11
PA14_47870		hypothetical protein	2.57
PA14_48060	*aprA*	alkaline metalloproteinase	-2.93
PA14_48090	*aprF*	alkaline protease secretion outer membrane protein AprF precursor	-2.16
PA14_48100	*aprE*	alkaline protease secretion protein AprE	-2.32
PA14_52440		hypothetical protein	2.03
PA14_52480		hypothetical protein	2.15
PA14_52490		hypothetical protein	2.26
PA14_52500		hypothetical protein	2.41
PA14_52510		hypothetical protein	2.62
PA14_53070	*hpd*	4-hydroxyphenylpyruvate dioxygenase	-2.27
PA14_55100		hypothetical protein	-2.39
PA14_55110		hypothetical protein	-2.22
PA14_55480	*hxcX*	HxcX type II secretion system protein	2.23
PA14_56570		acyltransferase	-3.13
PA14_57030	*fxsA*	FxsA protein	-2.35
PA14_58410		porin	-2.09
PA14_59010		hypothetical protein	2.01
PA14_59220		pyocin S5	2.47
PA14_59470		hypothetical protein	2.92
PA14_59480		hypothetical protein	2.07
PA14_59490		hypothetical protein	2.66
PA14_59500		hypothetical protein	2.84
PA14_59510		hypothetical protein	3.51
PA14_59520		hypothetical protein	3.58
PA14_59530		hypothetical protein	2.57
PA14_60850	*mexC*	multidrug efflux RND membrane fusion protein	2.35
PA14_63040		hypothetical protein	2.15
PA14_63620	*lipC*	lipase LipC	2.78
PA14_63710		glycosyl transferase family protein	3.01
PA14_64260		hypothetical protein	2.44
PA14_64660	*ureF*	urease accessory protein UreF	-2.12

PA14_64700		RNA polymerase sigma factor	2.51
PA14_65410	*orn*	oligoribonuclease	-3.20
PA14_65990	*qacH*	SMR multidrug efflux transporter	2.07
PA14_67350	*hutU*	urocanate hydratase	2.26
PA14_70180	*rpmG*	50S ribosomal protein L33	2.07
PA14_71720		pyruvate carboxylase subunit B	-2.02

Table 5. Primers used in these studies.

Primer	Purpose	Sequence*
mw118	PA14 *orn* 5′	AACATATGCAGAACCCGCAGAACCTTAT
mw119	PA14 *orn* 3′ (no stop codon)	AAGGATCCGAGCTTGATGAAGTGGTCGCG
mw124	PA14 Δ*orn* upstream 5′	GAATTCTGGTTCGCGGTCGTGCTT
mw125	PA14 Δ*orn* upstream 3′	CATATGGTTCTGCATGGGGAGTCGCT
mw126	PA14 Δ*orn* downstream 5′	CATATGAAGCTCTGATCCGTCCGGG
mw127	PA14 Δ*orn* downstream 3′	AAGCTTGGGTTCCAGCAGGTCGGTAT
mw172	*orn* D11A	AGAACCCGCAGAACCTTATCTGGAT**AGCGCT**GGAGATGACCGGCCTCGAT
mw173	*orn* D11A	ATCGAGGCCGGTCATCTCC**AGCGCT**ATCCAGATAAGGTTCTGCGGGTTCT
mw174	*orn* E13A	CAGAACCTTATCTGGATCGACC**TGGCCA**TGACCGGCCTCGATCCGG
mw175	*orn* E13A	CCGGATCGAGGCCGGTCA**TGGCCA**GGTCGATCCAGATAAGGTTCTG
mw176	*orn* D111A	CGGCAACAGCATCTGCCAG**GCGCGC**CGCTTCCTCTATAGGCACAT
mw177	*orn* D111A	ATGTGCCTATAGAGGAAGCG**GCGCGC**CTGGCAGATGCTGTTGCCG
mw178	*orn* H157A	CGCGAGAGCTTCAAGAAGGGTAACAC**AGCGCT**GGCGCTGGACGATATCCG
mw179	*orn* H157A	CGGATATCGTCCAGCGCC**AGCGCT**GTGTTACCCTTCTTGAAGCTCTCGCG
mw180	*orn* D162A	CCCACCTGGCGCTGGACGCCATCCGCGAGTCGATCGCCG
mw181	*orn* D162A	CGGCGATCGACTCGCGGATGGCGTCCAGCGCCAGGTGGG
mw182	B.s. 168 *nrnA* 5′	AACATATGAAAACAGAATTGATCAG
mw184	B.s. 168 *nrnA* 3′(no stop codon)	AAGGATCCCTCGTGTTCTTTACATAATGT
mw185	B.s. 168 *nrnB* 5′	AACATATGTATCATTTATATTCACATAAC
mw187	B.s. 168 *nrnB* 3′(no stop codon)	AAGGATCCCTTGCGATGTTGATTTGC
mw205	B.s. 168 *rnjA* 5′	AACATATGAAATTTGTAAAAAATGATCAG
mw206	B.s. 168 *rnjA* 3′(no stop codon)	AAGGATCCAACCTCCATAATGATCGGC
mw207	B.s. 168 *yhaM* 5′	AACATATGGCTAAAGGGATTATGCTAC
mw208	B.s. 168 *yhaM* 3′(no stop codon)	AAGGATCCTTTATGAAATGTCGGTTTATAAAAG
mw209	CB15 *nrnC* 5′	AACATATGGCCAATTTCGTTCACGAG
mw210	CB15 *nrnC* 3′(no stop codon)	AAGGATCCGCTGTGGGCGAAGATGTCC
mw211	Transposon sequencing primer 1	GCCGACATCATAACGGTTCTGG
vl720	Transposon sequencing primer 2	CTTCATCCGGGGTCAGCACCA

Table 6. Plasmids used in these studies.

Plasmid	Description	Reference
pVL791	pET19 with N-terminal 10x His-tag	(25)
pVL847	pET19 with *malE* for N-terminal histidine-MBP tag	(25)
pVL791 Cb GW	pET19 with Gateway destination cassette	This study
pVL847 Gn GW	pVL847 with Gateway destination cassette and Gn^R	This study
pSMN10-Δ*orn*	pEX-based deletion vector for Δ *orn*	This study
pVL847 RocR	pVL847 with PA14 *rocR*	This study
pVL847 Gn GW VC0341	pVL847 Gn GW with *V. cholerae* VC0341 (*orn*)	This study
pVL847 PA14 *orn*	pVL847 with PA14 *orn*	This study
pVL847 D11A	pVL847 with PA14 *orn* D11A mutation	This study
pVL847 E13A	pVL847 with PA14 *orn* E13A mutation	This study
pVL847 D111A	pVL847 with PA14 *orn* D111A mutation	This study
pVL847 H157A	pVL847 with PA14 *orn* H157A mutation	This study
pVL847 D162A	pVL847 with PA14 *orn* D162A mutation	This study
pMMB	broad host range low copy vector, tac promoter, Gn^R	(208)
pMMB *orn*	pMMB with PA14 *orn*	This study
pMMB D11A	pMMB with PA14 *orn* D11A mutation	This study
pMMB E13A	pMMB with PA14 *orn* E13A mutation	This study
pMMB D111A	pMMB with PA14 *orn* D111A mutation	This study
pMMB H157A	pMMB with PA14 *orn* H157A mutation	This study
pMMB D162A	pMMB with PA14 *orn* D162A mutation	This study
pVL1112	pCTX with *pel* operon promoter fused to *lacZ*	(25)
pVL393	broad host range low copy vector, tac promoter, Amp^R	This study
pVL393 *orn*	pVL393 with PA14 *orn*	This study
pVL393 *nrnA*	pVL393 with B.s. 168 *nrnA*	This study
pVL393 *nrnB*	pVL393 with B.s. *nrnB*	This study
pVL393 *nrnC*	pVL393 with CB15 *nrnC*	This study
pVL393 *rnjA*	pVL393 with B.s. 168 *rnjA*	This study
pVL393 *yhaM*	pVL393 with B.s. 168 *yhaM*	This study
pVL791 *nrnA*	pVL791 with B.s. 168 *nrnA*	This study
pVL791 *nrnA*	pVL791 with B.s. 168 *nrnA*	This study
pVL791 *nrnB*	pVL791 with B.s. 168 *nrnB*	This study
pVL791 *nrnC*	pVL791 with CB15 *nrnC*	This study
pVL791 *rnjA*	pVL791 with B.s. 168 *rnjA*	This study
pVL791 *yhaM*	pVL791 with B.s. 168 *yhaM*	This study
pBT20	Transposon-containing plasmid	(108)
pVL-blunt	pCR-blunt based cloning vector	This study

Table 7. Strains used in these studies.

Plasmid	Description	Reference
E. coli BL21(DE3) pVL847 RocR	Purification of His-MBP-tagged PA14 RocR	This study
E. coli T7Iq pVL847 Gn GW VC0341	Purification of His-MBP-tagged *V. cholerae El Tor* N16961 Orn	This study
E. coli BL21(DE3) pVL847 PA14 *orn*	Purification of His-MBP-tagged PA14 Orn	This study
E. coli BL21(DE3) pVL847 D11A	Purification of His-MBP-tagged PA14 Orn D11A	This study
E. coli BL21(DE3) pVL847 E13A	Purification of His-MBP-tagged PA14 Orn E13A	This study
E. coli BL21(DE3) pVL847 D111A	Purification of His-MBP-tagged PA14 Orn D111A	This study
E. coli BL21(DE3) pVL847 H157A	Purification of His-MBP-tagged PA14 Orn H157A	This study
E. coli BL21(DE3) pVL847 D162A	Purification of His-MBP-tagged PA14 Orn D162A	This study
PA14	Wild type	(209)
PA14 Δ*orn*	In-frame deletion of *orn*, oligoribonuclease	This study
PA14 Δ*pel*	In-frame deletion of the *pel* operon (*pelA-G*)	(116)
PA14 Δ*orn*Δ*pel*	In-frame deletion of *orn* and the *pel* operon	This study
PA14 *cat*::tn	MrT7 transposon insertion in *cat*, chloramphenicol acetyltransferase	(64)
PA14 *orn*::tn	MrT7 transposon insertion in *orn*, oligoribonuclease	(64)
PA14 PA4108::tn	MrT7 transposon insertion in PA4108, HD-GYP domain	(64)
PA14 PA4781::tn	MrT7 transposon insertion in PA4781, HD-GYP domain	(64)
PA14 pMMB	Wild type with empty vector	This study
PA14 Δ*orn* pMMB	In-frame deletion of *orn* with empty vector	This study
PA14 Δ*orn* pMMB *orn*	Complementation with wild type *orn*	This study
PA14 Δ*orn* pMMB D11A	Complementation with D11A allele *orn*	This study
PA14 Δ*orn* pMMB E13A	Complementation with E13A allele *orn*	This study
PA14 Δ*orn* pMMB D111A	Complementation with D111A allele *orn*	This study
PA14 Δ*orn* pMMB H157A	Complementation with H157A allele *orn*	This study
PA14 Δ*orn* pMMB D162A	Complementation with D162A allele *orn*	This study
E. coli T7Iq pVL791 *nrnA*	Purification of 10x His-B.s. 168 NrnA	This study
E. coli T7Iq pVL791 *nrnB*	Purification of 10x His-B.s. 168 NrnB	This study
E. coli T7Iq pVL791 *nrnC*	Purification of 10x His-CB15 NrnC	This study
E. coli T7Iq pVL791 *rnjA*	Purification of 10x His-B.s. 168 RNase J1	This study
E. coli T7Iq pVL791 *yhaM*	Purification of 10x His-B.s. 168 YhaM	This study
PA14 Δ*orn* pVL393	In-frame deletion of *orn* with empty vector	This study
PA14 Δ*orn* pVL393 *orn*	Complementation with B.s. 168 NrnA	This study
PA14 Δ*orn* pVL393 *nrnA*	Complementation with B.s. 168 NrnB	This study
PA14 Δ*orn* pVL393 *nrnB*	Complementation with CB15 NrnC	This study
PA14 Δ*orn* pVL393 *nrnC*	Complementation with B.s. 168 RNase J1	This study
PA14 Δ*orn* pVL393 *rnjA*	Complementation with B.s. 168 YhaM	This study
PA14 Δ*orn* pVL393 *yhaM*	Complementation with B.s. 168 NrnB	This study
E. coli SM10-λ*pir* pBT20	Transposon mutagenesis	(210)

Table 8. Fraction bound of pGpG to *V. cholerae* ORFs from His and His-MBP libraries.

Shown are the adjusted* fraction bounds and averages of pGpG to ORFs from the His- and His-MBP libraries. ORFs were assayed for binding in at least duplicate. Empty cells indicate that no fraction bound was obtained. The average fraction bound, standard deviation, and average fraction bound plus 3x standard deviations are indicated below the table.

	His library				His-MBP library			
VC Number	Rep. 1	Rep. 2	Rep. 3	Average	Rep. 1	Rep. 2	Rep. 3	Average
VC0001					0.21	0.18	0.18	0.19
VC0002	0.25	0.25		0.25	0.12	0.14		0.13
VC0003	0.22	0.24	0.19	0.22	0.20	0.19		0.19
VC0004	0.29	0.29		0.29	0.20	0.19		0.19
VC0005	0.21	0.19		0.20	0.13	0.11	0.13	0.12
VC0006	0.24	0.25		0.25	0.18	0.20		0.19
VC0007	0.31	0.24		0.27	0.18	0.18		0.18
VC0008	0.25	0.25	0.26	0.25	0.15	0.13		0.14
VC0009	0.28	0.25		0.26	0.27	0.27		0.27
VC0010	0.22	0.23		0.23	0.20	0.19		0.19
VC0011	0.23	0.25	0.23	0.24	0.16	0.15		0.16
VC0012	0.22	0.26	0.24	0.24	0.20	0.20		0.20
VC0013	0.27	0.27	0.27	0.27	0.19	0.21		0.20
VC0014	0.22	0.21		0.22	0.17	0.16		0.16
VC0015	0.26	0.28		0.27	0.12	0.17	0.17	0.15
VC0016	0.26	0.25		0.26	0.15	0.16		0.16
VC0017	0.22	0.22	0.23	0.22	0.13	0.12		0.13
VC0018	0.25	0.23		0.24	0.15	0.10		0.13
VC0019	0.24	0.24		0.24	0.19	0.23		0.21
VC0020	0.23	0.21		0.22	0.17	0.15		0.16
VC0021	0.24	0.26		0.25	0.20	0.20		0.20
VC0022	0.26	0.27		0.26	0.24	0.23		0.23
VC0023	0.23	0.25	0.23	0.24	0.17	0.14		0.15
VC0024	0.23	0.21		0.22	0.15	0.14		0.15
VC0025	0.22	0.22	0.23	0.22	0.19	0.19		0.19
VC0026	0.24	0.23		0.23	0.16	0.16		0.16
VC0027	0.20	0.22		0.21	0.18	0.18		0.18
VC0028	0.22	0.23		0.22	0.15	0.11		0.13
VC0029	0.20	0.19		0.20	0.17	0.16		0.16
VC0030	0.18	0.19		0.19	0.12	0.13		0.13
VC0031	0.20	0.21		0.21	0.15	0.15		0.15
VC0032	0.21	0.20		0.20	0.16	0.13		0.15
VC0033	0.22	0.26		0.24	0.14	0.21		0.17
VC0034	0.28	0.31		0.30	0.18	0.17		0.17
VC0035	0.24	0.20		0.22	0.16	0.13		0.15
VC0036	0.27	0.27		0.27	0.20	0.19		0.19

VC0037	0.22	0.26		0.24	0.13	0.14		0.14
VC0038	0.24	0.24		0.24	0.14	0.15		0.15
VC0039	0.24	0.29		0.27	0.18	0.17		0.17
VC0040	0.28	0.24		0.26	0.17	0.17		0.17
VC0041	0.28	0.30		0.29	0.19	0.22		0.21
VC0042	0.29	0.31		0.30	0.17	0.21		0.19
VC0043	0.22	0.22		0.22	0.16	0.17		0.16
VC0044	0.22	0.20		0.21	0.12	0.14		0.13
VC0045	0.20	0.20	0.18	0.20	0.12	0.10		0.11
VC0046	0.27	0.24	0.27	0.26	0.16	0.15		0.15
VC0047	0.27	0.27		0.27	0.26	0.20	0.23	0.23
VC0048	0.22	0.26		0.24	0.18	0.19		0.18
VC0049	0.21	0.22		0.21	0.12	0.15		0.14
VC0050	0.23	0.26		0.24	0.20	0.18		0.19
VC0051	0.24	0.26		0.25	0.15	0.17		0.16
VC0052	0.23	0.24		0.24	0.15	0.21		0.18
VC0053	0.23	0.23		0.23	0.15	0.20		0.18
VC0054	0.24	0.23		0.23	0.15	0.19		0.17
VC0055	0.26	0.23		0.24	0.15	0.17		0.16
VC0056	0.22	0.22		0.22	0.13	0.17		0.15
VC0057	0.24	0.24		0.24	0.11	0.13		0.12
VC0058	0.22	0.23		0.22	0.16	0.16		0.16
VC0060	0.25	0.25		0.25	0.21	0.19		0.20
VC0061	0.24	0.23		0.24	0.15	0.13		0.14
VC0062	0.25	0.22		0.23	0.14	0.17		0.15
VC0063	0.26	0.29		0.28	0.18	0.16		0.17
VC0064	0.21	0.25		0.23	0.14	0.15		0.15
VC0065	0.22	0.22		0.22	0.18	0.16		0.17
VC0066	0.20	0.23		0.22	0.12	0.14		0.13
VC0067	0.21	0.21		0.21	0.17	0.18		0.18
VC0068	0.25	0.22		0.23	0.16	0.16		0.16
VC0069	0.28	0.24		0.26	0.19	0.19		0.19
VC0070	0.27	0.27	0.26	0.27	0.16	0.16		0.16
VC0071	0.21	0.25		0.23	0.11	0.10		0.10
VC0072	0.26	0.27		0.26	0.20	0.15	0.18	0.18
VC0073	0.30	0.30		0.30	0.22	0.21		0.22
VC0074	0.27	0.27	0.25	0.26	0.17	0.16		0.16
VC0075	0.32	0.29		0.30	0.22	0.23		0.23
VC0076	0.26	0.26		0.26	0.17	0.17		0.17
VC0077	0.24	0.23	0.23	0.23	0.17	0.17		0.17
VC0078	0.20	0.23		0.21	0.14	0.14		0.14
VC0079	0.27	0.32	0.26	0.28	0.20	0.19		0.20
VC0080	0.19	0.22		0.21	0.16	0.12		0.14

VC0081	0.31	0.33		0.32	0.25	0.23		0.24
VC0082	0.27	0.25		0.26	0.14	0.15		0.14
VC0083	0.24	0.24		0.24	0.17	0.19		0.18
VC0084	0.17	0.24		0.21	0.15	0.11		0.13
VC0085	0.22	0.21		0.21	0.13	0.13		0.13
VC0086	0.28	0.23	0.27	0.26	0.19	0.19		0.19
VC0087	0.23	0.25		0.24	0.18	0.18		0.18
VC0088	0.25	0.29		0.27	0.15	0.13		0.14
VC0089	0.22	0.23		0.22	0.15	0.16		0.16
VC0090	0.25	0.27		0.26	0.17	0.17		0.17
VC0091	0.18	0.20		0.19	0.16	0.17		0.17
VC0092	0.23	0.25	0.23	0.24	0.16	0.17		0.16
VC0093	0.22	0.25		0.23	0.17	0.16		0.17
VC0094	0.27	0.31		0.29	0.22	0.25		0.24
VC0095	0.22	0.23		0.22	0.15	0.16		0.16
VC0096	0.22	0.21		0.22	0.20	0.19		0.20
VC0097	0.20	0.22		0.21	0.14	0.19		0.16
VC0098	0.27	0.26		0.27	0.12	0.13		0.12
VC0099	0.30	0.34		0.32	0.19	0.23		0.21
VC0100	0.22	0.23		0.23				
VC0101	0.17	0.16		0.16	0.10	0.10	0.10	0.10
VC0102	0.22	0.25		0.24	0.12	0.13		0.12
VC0103	0.29	0.30		0.29	0.18	0.17	0.16	0.17
VC0104	0.22	0.23		0.22	0.14	0.16		0.15
VC0105	0.23	0.22		0.22	0.13	0.15	0.14	0.14
VC0106	0.23	0.24		0.23	0.16	0.15	0.14	0.15
VC0107	0.21	0.20		0.21	0.11	0.10		0.11
VC0108	0.23	0.26		0.25	0.19	0.19	0.16	0.18
VC0109	0.27	0.24		0.26	0.23	0.17		0.20
VC0110	0.15	0.18		0.16	0.16	0.15		0.16
VC0111	0.27	0.25		0.26	0.18	0.18	0.17	0.18
VC0112	0.27	0.27		0.27	0.20	0.17	0.18	0.18
VC0113	0.25	0.27		0.26	0.18	0.16	0.15	0.16
VC0114	0.13	0.15		0.14	0.11	0.10	0.12	0.11
VC0115	0.25	0.22		0.23	0.17	0.14	0.16	0.16
VC0116	0.22	0.25		0.24	0.23	0.19		0.21
VC0117	0.26	0.25		0.26	0.16	0.15	0.13	0.15
VC0118	0.26	0.26		0.26	0.19	0.20		0.19
VC0119	0.25	0.23		0.24	0.19	0.17	0.17	0.18
VC0120	0.25	0.26		0.25	0.18	0.15	0.17	0.17
VC0121	0.21	0.21		0.21	0.20	0.17	0.18	0.19
VC0123	0.22	0.22		0.22	0.17	0.16		0.17
VC0124	0.29	0.30		0.29	0.16	0.16	0.13	0.15

VC0125	0.24	0.25		0.25	0.17	0.16	0.23	0.18
VC0126	0.22	0.22		0.22	0.17	0.16		0.16
VC0127	0.22	0.22		0.22				
VC0128	0.29	0.31		0.30	0.18	0.18	0.14	0.17
VC0129	0.27	0.26		0.26	0.18	0.18	0.20	0.19
VC0130	0.20	0.20		0.20	0.18	0.16		0.17
VC0131	0.24	0.25		0.24	0.17	0.17	0.16	0.16
VC0132	0.15	0.15		0.15	0.13	0.14	0.12	0.13
VC0133	0.24	0.24		0.24	0.14	0.13		0.14
VC0134	0.27	0.28		0.27	0.20	0.20	0.21	0.20
VC0135	0.25	0.24		0.25	0.19	0.16	0.19	0.18
VC0136	0.28	0.29		0.28	0.20	0.21	0.18	0.20
VC0137	0.24	0.26		0.25	0.11	0.13	0.13	0.12
VC0138	0.22	0.20		0.21	0.15	0.15		0.15
VC0139	0.30	0.25		0.27	0.16	0.16	0.14	0.15
VC0140	0.21	0.23		0.22	0.21	0.21	0.21	0.21
VC0141	0.26	0.24		0.25	0.25	0.20		0.22
VC0142	0.29	0.30		0.30	0.19	0.19	0.21	0.20
VC0143	0.28	0.28	0.25	0.27	0.21	0.16		0.18
VC0144	0.20	0.22		0.21	0.21	0.19		0.20
VC0145	0.30	0.28		0.29	0.17	0.17		0.17
VC0146	0.28	0.27	0.26	0.27	0.14	0.14		0.14
VC0147	0.22	0.24	0.29	0.25	0.18	0.18		0.18
VC0148	0.27	0.24	0.28	0.26	0.15	0.17		0.16
VC0149	0.26	0.27	0.27	0.27	0.09	0.12		0.11
VC0150	0.27	0.27		0.27	0.21	0.20	0.21	0.21
VC0151	0.26	0.27	0.26	0.27	0.18	0.17		0.17
VC0152	0.27	0.24	0.24	0.25	0.19	0.19		0.19
VC0153	0.27	0.26	0.28	0.27	0.19	0.18		0.18
VC0154	0.24	0.22	0.22	0.23	0.17	0.14		0.16
VC0156	0.34	0.34	0.35	0.34	0.17	0.18		0.18
VC0157	0.31	0.27	0.30	0.29	0.17	0.20		0.18
VC0158	0.26	0.26	0.31	0.28	0.14	0.13		0.14
VC0159	0.28	0.33	0.27	0.29	0.21	0.22		0.22
VC0160	0.22	0.23		0.22	0.18	0.17		0.17
VC0161	0.25	0.24		0.25	0.17	0.17		0.17
VC0162	0.24	0.24	0.21	0.23	0.23	0.22		0.22
VC0163	0.17	0.21		0.19	0.18	0.15		0.17
VC0164	0.23	0.23		0.23	0.15	0.15		0.15
VC0165	0.28	0.29	0.27	0.28	0.18	0.16		0.17
VC0166	0.28	0.24	0.27	0.26	0.19	0.17		0.18
VC0167	0.26	0.27		0.27	0.11	0.13	0.12	0.12
VC0168	0.26	0.28		0.27	0.22	0.22		0.22

VC0169	0.25	0.25		0.25	0.25	0.22		0.24
VC0170	0.23	0.24		0.23	0.13	0.12		0.13
VC0171	0.21	0.22	0.23	0.22	0.16	0.18		0.17
VC0172	0.26	0.23		0.24	0.19	0.17	0.19	0.18
VC0173	0.30	0.34		0.32	0.26	0.22		0.24
VC0174	0.23	0.24	0.21	0.23	0.18	0.12		0.15
VC0175	0.24	0.24		0.24	0.26	0.20		0.23
VC0176	0.25	0.24		0.25	0.19	0.17	0.18	0.18
VC0177	0.21	0.23	0.21	0.22	0.18	0.15		0.17
VC0178	0.26	0.28	0.26	0.26	0.18	0.18		0.18
VC0179	0.21	0.20	0.20	0.20	0.22	0.22		0.22
VC0180	0.23	0.24	0.25	0.24	0.16	0.16		0.16
VC0181	0.26	0.25	0.23	0.24	0.18	0.19		0.19
VC0182	0.27	0.23	0.26	0.26	0.13	0.11		0.12
VC0183	0.18	0.24		0.21	0.13	0.12	0.09	0.11
VC0184	0.17	0.19	0.22	0.19	0.13	0.12		0.13
VC0185	0.25	0.23	0.26	0.25	0.18	0.18		0.18
VC0186	0.18	0.18	0.19	0.19	0.14	0.13		0.14
VC0187	0.26	0.25	0.22	0.24	0.15	0.12		0.14
VC0188	0.19	0.21		0.20	0.14	0.13		0.13
VC0189	0.26	0.32		0.29	0.22	0.22		0.22
VC0190	0.28	0.30		0.29	0.18	0.18		0.18
VC0191	0.32	0.32	0.29	0.31	0.24	0.27		0.25
VC0192	0.28	0.29	0.28	0.28	0.17	0.16		0.17
VC0193	0.21	0.23		0.22	0.18	0.14		0.16
VC0194	0.24	0.26		0.25	0.13	0.16		0.14
VC0195	0.29	0.26	0.27	0.27	0.21	0.21		0.21
VC0196	0.21	0.19	0.22	0.20	0.16	0.16		0.16
VC0197	0.27	0.27	0.28	0.27	0.18	0.17		0.18
VC0198	0.28	0.28	0.26	0.27	0.19	0.19		0.19
VC0199	0.10	0.21	0.23	0.18	0.20	0.22		0.21
VC0200	0.27	0.28		0.28	0.17	0.19		0.18
VC0201	0.28	0.30		0.29	0.18	0.17		0.18
VC0202	0.21	0.22		0.22	0.16	0.16		0.16
VC0203	0.23	0.21	0.21	0.22	0.22	0.20		0.21
VC0204	0.30	0.29	0.31	0.30	0.13	0.18		0.16
VC0205	0.23	0.24		0.23	0.17	0.16		0.17
VC0206	0.21	0.22	0.21	0.21	0.18	0.19		0.18
VC0207	0.35	0.37		0.36	0.21	0.21		0.21
VC0208	0.32	0.32		0.32	0.20	0.23		0.21
VC0209					0.13	0.11	0.12	0.12
VC0210	0.28	0.27	0.27	0.27	0.32	0.34		0.33
VC0211					0.13	0.17	0.14	0.15

VC0212	0.24	0.27	0.31	0.27	0.13	0.17		0.15
VC0213	0.17	0.18	0.22	0.19	0.11	0.17		0.14
VC0214					0.18	0.19	0.18	0.18
VC0215	0.23	0.22	0.24	0.23	0.15	0.23		0.19
VC0216	0.23	0.22		0.22	0.18	0.13		0.16
VC0217					0.19	0.19	0.20	0.19
VC0218					0.15	0.17	0.13	0.15
VC0219	0.17	0.18		0.17	0.13	0.14	0.17	0.15
VC0220	0.32	0.28		0.30	0.21	0.22		0.21
VC0221	0.27	0.28	0.28	0.28	0.17	0.19		0.18
VC0222	0.26	0.27		0.27	0.25	0.21		0.23
VC0223	0.23	0.24	0.25	0.24	0.20	0.20		0.20
VC0224	0.26	0.26	0.25	0.26	0.20	0.19		0.19
VC0225	0.25	0.22		0.24	0.13	0.16		0.14
VC0226					0.15	0.17	0.15	0.16
VC0227	0.28	0.23		0.25	0.20	0.17		0.18
VC0228	0.24	0.24		0.24	0.16	0.16		0.16
VC0229	0.23	0.23	0.22	0.23	0.18	0.20		0.19
VC0230	0.26	0.28		0.27	0.16	0.13		0.15
VC0231	0.23	0.20		0.22	0.15	0.13		0.14
VC0232					0.17	0.19	0.16	0.17
VC0233	0.34	0.33		0.34	0.18	0.15		0.17
VC0234	0.26	0.27		0.27	0.11	0.14		0.13
VC0235	0.22	0.24		0.23	0.13	0.16		0.15
VC0236	0.28	0.28	0.27	0.28	0.19	0.21		0.20
VC0237	0.30	0.27	0.26	0.28	0.23	0.22		0.22
VC0238	0.29	0.29	0.30	0.29	0.15	0.19		0.17
VC0239	0.21	0.21		0.21	0.12	0.13		0.12
VC0240	0.25	0.28		0.26	0.23	0.17	0.17	0.19
VC0241	0.18	0.21	0.20	0.20	0.15	0.19		0.17
VC0242	0.19	0.21	0.21	0.20	0.13	0.17		0.15
VC0243	0.23	0.24		0.23	0.19	0.19		0.19
VC0244	0.23	0.26	0.25	0.25	0.12	0.15		0.13
VC0245	0.30	0.28		0.29	0.15	0.18		0.16
VC0246	0.35	0.29		0.32	0.28	0.27		0.27
VC0247	0.27	0.28	0.30	0.28	0.16	0.16		0.16
VC0248					0.16	0.17	0.18	0.17
VC0249	0.29	0.28	0.27	0.28	0.16	0.16		0.16
VC0250	0.22	0.22		0.22	0.19	0.14		0.17
VC0251	0.24	0.20		0.22	0.21	0.23		0.22
VC0252	0.24	0.26	0.26	0.25	0.16	0.18		0.17
VC0253					0.15	0.17	0.22	0.18
VC0254	0.24	0.22		0.23	0.14	0.17	0.14	0.15

VC0255					0.15	0.16	0.15	0.15
VC0256	0.29	0.28	0.31	0.29	0.14	0.18		0.16
VC0257	0.23	0.21	0.24	0.22	0.19	0.17		0.18
VC0258	0.24	0.27		0.25	0.28	0.15		0.21
VC0259	0.27	0.27		0.27	0.25	0.20		0.22
VC0260	0.24	0.26		0.25	0.16	0.18		0.17
VC0261	0.21	0.21		0.21	0.10	0.09	0.10	0.10
VC0262	0.20	0.20		0.20	0.10	0.13		0.12
VC0263	0.13	0.15		0.14	0.17	0.19		0.18
VC0264	0.23	0.24		0.24	0.09	0.11		0.10
VC0265	0.28	0.24	0.26	0.26	0.21	0.21		0.21
VC0266	0.27	0.25		0.26	0.14	0.14		0.14
VC0267	0.18	0.17	0.18	0.18	0.17	0.16		0.16
VC0268	0.25	0.22		0.23	0.09	0.10		0.10
VC0269	0.25	0.22	0.22	0.23	0.13	0.13		0.13
VC0270	0.31	0.25		0.28	0.16	0.14		0.15
VC0271	0.17	0.18	0.17	0.18	0.17	0.16		0.16
VC0272					0.15	0.10	0.13	0.13
VC0273	0.20	0.21		0.20	0.11	0.14		0.13
VC0274	0.21	0.24		0.23	0.15	0.16		0.16
VC0275	0.24	0.24	0.21	0.23	0.13	0.10		0.11
VC0276	0.20	0.22		0.21	0.13	0.15		0.14
VC0277	0.19	0.20		0.20	0.19	0.18		0.19
VC0278	0.32	0.30		0.31	0.20	0.20		0.20
VC0279	0.25	0.23		0.24	0.16	0.17		0.16
VC0280	0.26	0.08	0.27	0.20	0.24	0.24		0.24
VC0281	0.29	0.27		0.28	0.19	0.20	0.15	0.18
VC0282	0.33	0.34		0.33	0.21	0.17		0.19
VC0283	0.26	0.25		0.25	0.16	0.18		0.17
VC0284	0.31	0.27		0.29	0.20	0.20		0.20
VC0285	0.25	0.23		0.24	0.15	0.17		0.16
VC0286	0.29	0.26		0.27	0.22	0.24	0.23	0.23
VC0287	0.23	0.21		0.22	0.20	0.21	0.21	0.21
VC0288	0.26	0.20		0.23	0.13	0.15		0.14
VC0289	0.27	0.08	0.28	0.21	0.14	0.15		0.14
VC0290	0.11	0.12		0.12	0.11	0.12		0.12
VC0291	0.25	0.24	0.25	0.25	0.20	0.18		0.19
VC0292					0.16	0.20	0.15	0.17
VC0293	0.24	0.23		0.23	0.08	0.14		0.11
VC0294					0.18	0.15	0.15	0.16
VC0295	0.19	0.20		0.19	0.19	0.17		0.18
VC0297	0.24	0.24		0.24	0.16	0.16		0.16
VC0298	0.18	0.18		0.18	0.12	0.12		0.12

VC0299	0.24	0.22		0.23	0.12	0.12		0.12
VC0300	0.21	0.20		0.20	0.17	0.19		0.18
VC0301	0.22	0.23		0.23	0.16	0.17		0.17
VC0302	0.28	0.27		0.28	0.19	0.21	0.16	0.18
VC0303	0.26	0.27		0.26	0.21	0.20		0.20
VC0304	0.23	0.26		0.25	0.13	0.15		0.14
VC0305	0.25	0.21		0.23	0.14	0.15		0.14
VC0306	0.20	0.23		0.22	0.18	0.11		0.15
VC0307	0.22	0.24		0.23	0.19	0.19		0.19
VC0308	0.24	0.25		0.25	0.20	0.21		0.21
VC0309	0.23	0.17		0.20	0.21	0.18		0.20
VC0311	0.28	0.23		0.26	0.15	0.18		0.16
VC0312	0.19	0.23		0.21	0.12	0.12		0.12
VC0313	0.23	0.26		0.24	0.19	0.18		0.19
VC0314	0.21	0.18		0.20	0.19	0.21	0.09	0.17
VC0316	0.28	0.25		0.26	0.18	0.18	0.17	0.18
VC0317	0.23	0.18		0.20	0.17	0.20		0.18
VC0318	0.22	0.27	0.21	0.23	0.17	0.16		0.17
VC0319	0.25	0.22		0.23	0.13	0.13		0.13
VC0320	0.26	0.28		0.27	0.24	0.19		0.21
VC0321	0.21	0.24	0.24	0.23	0.16	0.15		0.16
VC0322	0.24	0.25	0.25	0.25	0.18	0.19		0.18
VC0323	0.25	0.28		0.26	0.21	0.21	0.21	0.21
VC0324	0.22	0.21	0.22	0.22	0.13	0.15		0.14
VC0326	0.21	0.21	0.21	0.21	0.17	0.19		0.18
VC0327	0.21	0.22		0.22	0.15	0.19		0.17
VC0328	0.24	0.25		0.24	0.25	0.23		0.24
VC0329	0.23	0.25		0.24	0.21	0.21		0.21
VC0330	0.24	0.28	0.26	0.26	0.18	0.17		0.18
VC0331	0.25	0.24	0.23	0.24	0.15	0.13		0.14
VC0332	0.24	0.23	0.27	0.25	0.16	0.16		0.16
VC0333	0.29	0.29		0.29	0.15	0.18		0.16
VC0334					0.15	0.20	0.20	0.19
VC0335	0.23	0.23	0.24	0.24	0.19	0.19		0.19
VC0336	0.21	0.20		0.21	0.19	0.20	0.18	0.19
VC0337					0.27	0.29	0.31	0.29
VC0338	0.25	0.38		0.32	0.21	0.24	0.22	0.22
VC0339	0.27	0.27	0.27	0.27	0.17	0.16		0.16
VC0341	0.44	0.41		0.43	0.31	0.28	0.26	0.29
VC0342	0.24	0.25		0.24	0.11	0.13	0.15	0.13
VC0343					0.16	0.17	0.24	0.19
VC0344	0.28	0.30		0.29	0.28	0.32	0.30	0.30
VC0345	0.27	0.28	0.27	0.27	0.13	0.12		0.12

VC0346	0.21	0.22	0.23	0.22	0.15	0.15		0.15
VC0347	0.29	0.30	0.30	0.30	0.12	0.13		0.13
VC0348	0.24	0.25	0.25	0.25	0.13	0.13		0.13
VC0349	0.28	0.30	0.32	0.30	0.16	0.18		0.17
VC0350	0.38	0.39		0.38	0.21	0.21	0.21	0.21
VC0351	0.26	0.29	0.25	0.27	0.18	0.17		0.18
VC0352					0.14	0.14	0.16	0.15
VC0353	0.30	0.30		0.30	0.15	0.19	0.18	0.17
VC0354	0.27	0.26	0.26	0.26	0.23	0.22		0.23
VC0355	0.19	0.20	0.19	0.20	0.12	0.10		0.11
VC0356	0.24	0.24		0.24	0.21	0.17		0.19
VC0357	0.18	0.15	0.16	0.16	0.17	0.17		0.17
VC0358	0.26	0.27	0.31	0.28	0.15	0.16		0.16
VC0359	0.26	0.24		0.25	0.16	0.15	0.16	0.16
VC0360	0.24	0.28	0.27	0.26	0.13	0.14		0.13
VC0361	0.22	0.22	0.22	0.22	0.17	0.17		0.17
VC0362	0.23	0.23	0.23	0.23	0.18	0.17		0.17
VC0363	0.23	0.27	0.24	0.24	0.09	0.10		0.10
VC0364	0.25	0.25	0.24	0.24	0.11	0.11		0.11
VC0365	0.17	0.17		0.17	0.14	0.15		0.15
VC0366	0.28	0.30	0.25	0.27	0.12	0.12		0.12
VC0367	0.25	0.30		0.28	0.14	0.15		0.14
VC0368	0.25	0.25		0.25	0.13	0.17	0.17	0.16
VC0369	0.21	0.22		0.22	0.20	0.22		0.21
VC0370	0.25	0.21		0.23	0.18	0.21		0.20
VC0371	0.23	0.27	0.23	0.24	0.28	0.28		0.28
VC0372	0.23	0.23		0.23	0.19	0.19		0.19
VC0373	0.26	0.25	0.25	0.25	0.13	0.13		0.13
VC0374	0.24	0.22		0.23	0.20	0.16		0.18
VC0375	0.26	0.23		0.24	0.14	0.14		0.14
VC0376	0.25	0.22		0.23	0.19	0.18		0.18
VC0377	0.29	0.26		0.27	0.17	0.19		0.18
VC0378	0.21	0.20		0.21	0.14	0.13		0.13
VC0379	0.23	0.26		0.24	0.13	0.13		0.13
VC0380	0.22	0.23	0.22	0.22	0.15	0.18		0.16
VC0381	0.27	0.28		0.28	0.18	0.17		0.17
VC0382	0.22	0.24		0.23	0.10	0.14		0.12
VC0383	0.24	0.23		0.24	0.20	0.17		0.18
VC0384	0.23	0.23		0.23	0.21	0.19		0.20
VC0385	0.23	0.20		0.22	0.11	0.17		0.14
VC0386	0.20	0.23		0.22	0.16	0.17		0.16
VC0387	0.27	0.25		0.26	0.15	0.17		0.16
VC0388	0.16	0.15		0.15	0.15	0.13		0.14

VC0389	0.32	0.33		0.32	0.18	0.20		0.19
VC0390	0.31	0.24		0.28	0.11	0.13	0.12	0.12
VC0391	0.26	0.23		0.24	0.16	0.16		0.16
VC0392	0.29	0.32		0.30	0.12	0.12		0.12
VC0393	0.25	0.28		0.26	0.19	0.19		0.19
VC0394	0.29	0.31		0.30	0.16	0.18		0.17
VC0395	0.22	0.21		0.22	0.14	0.09		0.11
VC0396	0.23	0.22		0.22	0.12	0.18		0.15
VC0397	0.27	0.27		0.27	0.17	0.16		0.17
VC0399	0.23	0.22		0.22	0.13	0.13		0.13
VC0400	0.27	0.24		0.26	0.19	0.18		0.18
VC0401	0.23	0.23		0.23	0.14	0.14		0.14
VC0402	0.26	0.24		0.25	0.18	0.20		0.19
VC0403	0.29	0.30		0.29	0.17	0.20		0.19
VC0404	0.30	0.28		0.29	0.15	0.18		0.17
VC0405	0.22	0.20		0.21	0.13	0.15		0.14
VC0406	0.25	0.23		0.24	0.14	0.14		0.14
VC0407	0.25	0.25		0.25	0.13	0.14		0.13
VC0408	0.29	0.23		0.26	0.15	0.17		0.16
VC0409	0.30	0.30	0.28	0.29	0.14	0.15		0.14
VC0410	0.31	0.30		0.30	0.20	0.20		0.20
VC0411	0.24	0.22		0.23	0.14	0.13		0.14
VC0412	0.26	0.32		0.29	0.17	0.18		0.18
VC0413	0.25	0.24		0.25	0.12	0.16		0.14
VC0414	0.29	0.28		0.29	0.16	0.17		0.16
VC0415	0.22	0.21	0.21	0.21	0.20	0.19		0.20
VC0416	0.26	0.27		0.27	0.22	0.23		0.23
VC0417	0.27	0.27	0.26	0.27	0.16	0.16		0.16
VC0418	0.25	0.23		0.24	0.13	0.13		0.13
VC0419	0.42	0.42		0.42	0.18	0.17		0.17
VC0420	0.26	0.27		0.26	0.17	0.18	0.16	0.17
VC0421	0.26	0.27		0.26	0.20	0.17		0.19
VC0422	0.20	0.18		0.19	0.15	0.16		0.16
VC0423	0.20	0.30		0.25	0.15	0.17		0.16
VC0424	0.20	0.23		0.22	0.12	0.10		0.11
VC0425	0.25	0.27		0.26	0.12	0.15		0.13
VC0426	0.26	0.30		0.28	0.26	0.21	0.23	0.23
VC0427	0.29	0.30	0.28	0.29	0.13	0.13		0.13
VC0428	0.22	0.20		0.21	0.09	0.06	0.13	0.09
VC0429	0.25	0.24		0.25	0.20	0.18		0.19
VC0430	0.24	0.21		0.23	0.17	0.17		0.17
VC0431	0.25	0.27		0.26	0.13	0.15		0.14
VC0432	0.21	0.24		0.23	0.14	0.17		0.15

VC0433	0.22	0.23		0.23	0.20	0.23		0.22
VC0435	0.25	0.26	0.23	0.25	0.28	0.24		0.26
VC0436	0.23	0.25	0.24	0.24	0.11	0.11		0.11
VC0437	0.25	0.23		0.24	0.18	0.20		0.19
VC0439	0.27	0.26		0.26	0.22	0.18		0.20
VC0440	0.26	0.25	0.28	0.26	0.21	0.18		0.20
VC0441	0.19	0.21	0.23	0.21	0.13	0.14		0.13
VC0442					0.12		0.18	0.15
VC0443	0.15	0.17	0.19	0.17	0.23	0.23		0.23
VC0444	0.23	0.24		0.23	0.13	0.17		0.15
VC0445	0.15	0.23	0.25	0.21	0.16	0.14		0.15
VC0446	0.30	0.29		0.29	0.18	0.17		0.17
VC0447	0.23	0.25	0.26	0.25	0.16	0.19		0.17
VC0448	0.26	0.25		0.26	0.15	0.19		0.17
VC0449	0.32	0.31		0.32	0.21	0.18		0.19
VC0450	0.21	0.21		0.21	0.17	0.20		0.18
VC0451					0.15		0.19	0.17
VC0452	0.20	0.23	0.25	0.22	0.17	0.18		0.17
VC0453	0.26	0.25	0.25	0.26	0.14	0.13		0.14
VC0454	0.19	0.21	0.19	0.20	0.12	0.16		0.14
VC0455	0.22	0.21		0.21	0.14	0.14		0.14
VC0456	0.20	0.19	0.23	0.21	0.12	0.10		0.11
VC0457	0.21	0.19	0.23	0.21	0.15	0.13		0.14
VC0458	0.27	0.26		0.26	0.17	0.16	0.18	0.17
VC0459	0.25	0.28	0.29	0.27	0.20	0.19		0.19
VC0460	0.23	0.25	0.26	0.25	0.16	0.21		0.18
VC0461	0.23	0.22		0.22	0.14	0.15		0.15
VC0462	0.20	0.21	0.28	0.23	0.15	0.15		0.15
VC0463	0.21	0.21		0.21	0.18	0.20		0.19
VC0464	0.21	0.20		0.21	0.14	0.10	0.11	0.12
VC0465	0.24	0.26	0.25	0.25	0.14	0.17		0.16
VC0466	0.20	0.20		0.20	0.13	0.13	0.15	0.14
VC0467	0.20	0.20		0.20	0.20	0.19		0.19
VC0468	0.21	0.21		0.21	0.19	0.19		0.19
VC0469	0.20	0.20		0.20	0.13	0.13	0.16	0.14
VC0470	0.11	0.09		0.10	0.03	0.06	0.04	0.04
VC0471	0.27	0.25		0.26	0.16	0.12		0.14
VC0472	0.21	0.22	0.23	0.22	0.14	0.15		0.15
VC0473	0.30	0.29	0.28	0.29	0.14	0.16		0.15
VC0474	0.28	0.25		0.26	0.16	0.15		0.15
VC0475	0.21	0.22		0.22	0.16	0.15		0.15
VC0476	0.19	0.21		0.20	0.15	0.12		0.14
VC0477	0.28	0.26		0.27	0.15	0.19	0.20	0.18

VC0478	0.26	0.20		0.23	0.16	0.16		0.16
VC0479	0.25	0.25	0.24	0.25	0.17	0.22		0.19
VC0480	0.24	0.26		0.25	0.17	0.14		0.16
VC0481	0.26	0.25	0.27	0.26	0.24	0.26		0.25
VC0482	0.27	0.29		0.28	0.15	0.14	0.14	0.14
VC0483	0.27	0.24		0.26	0.23	0.15		0.19
VC0484	0.26	0.25		0.26	0.16	0.17		0.16
VC0485	0.22	0.25		0.24	0.20	0.16		0.18
VC0486	0.22	0.24	0.24	0.24	0.18	0.17		0.18
VC0487	0.25	0.25		0.25	0.13	0.15	0.16	0.15
VC0488	0.22	0.24		0.23	0.15	0.17	0.17	0.17
VC0489	0.21	0.21		0.21	0.17	0.13	0.15	0.15
VC0490	0.26	0.26		0.26	0.16	0.15		0.16
VC0491	0.26	0.25	0.26	0.25	0.15	0.19		0.17
VC0492	0.25	0.24		0.25	0.14	0.16	0.23	0.18
VC0493	0.30	0.26		0.28	0.20	0.18		0.19
VC0494	0.23	0.23	0.24	0.23	0.25	0.21		0.23
VC0495	0.28	0.29	0.28	0.28	0.18	0.16		0.17
VC0496	0.20	0.22	0.22	0.21	0.14	0.16		0.15
VC0497	0.31	0.29		0.30	0.13	0.17	0.15	0.15
VC0498	0.19	0.23		0.21	0.07	0.12	0.09	0.10
VC0499	0.20	0.24	0.21	0.22	0.16	0.16		0.16
VC0500	0.27	0.28		0.27	0.18	0.17		0.17
VC0501	0.31	0.32	0.29	0.30	0.18	0.13		0.15
VC0502	0.23	0.23	0.24	0.23	0.18	0.19		0.18
VC0503	0.30	0.29		0.29	0.19	0.19		0.19
VC0504	0.27	0.28		0.27	0.18	0.18		0.18
VC0505	0.30	0.28	0.26	0.28	0.16	0.17		0.16
VC0506	0.26	0.28		0.27	0.16	0.14		0.15
VC0507	0.35	0.32		0.34	0.18	0.20		0.19
VC0508	0.22	0.22	0.20	0.21	0.12	0.13		0.12
VC0509	0.24	0.23	0.25	0.24	0.16	0.17		0.16
VC0510	0.25	0.26	0.26	0.26	0.17	0.17		0.17
VC0511	0.25	0.27		0.26	0.22	0.23		0.23
VC0512	0.18	0.20	0.18	0.19	0.20	0.19		0.19
VC0513	0.17	0.21	0.19	0.19	0.11	0.13		0.12
VC0514	0.24	0.22		0.23	0.19	0.19		0.19
VC0515	0.22	0.23		0.23	0.15	0.18		0.17
VC0516	0.27	0.26	0.21	0.25	0.18	0.18		0.18
VC0517	0.18	0.20		0.19	0.10	0.10		0.10
VC0518	0.29	0.27		0.28	0.19	0.12	0.17	0.16
VC0519	0.21	0.22	0.23	0.22	0.12	0.16		0.14
VC0520	0.27	0.24		0.26	0.17	0.19		0.18

VC0521	0.24	0.23		0.23	0.12	0.17		0.14
VC0522	0.24	0.25	0.25	0.24	0.17	0.21		0.19
VC0523	0.26	0.25	0.27	0.26	0.25	0.17		0.21
VC0524	0.23	0.26	0.23	0.24	0.11	0.12		0.11
VC0525	0.22	0.21	0.17	0.20	0.18	0.07		0.12
VC0526	0.32	0.31		0.32	0.22	0.22		0.22
VC0527	0.30	0.33		0.32	0.33	0.29	0.30	0.31
VC0528	0.19	0.23	0.21	0.21	0.17	0.17		0.17
VC0529	0.19	0.21	0.20	0.20	0.12	0.14		0.13
VC0530	0.26	0.27		0.27	0.14	0.12		0.13
VC0531	0.27	0.30	0.28	0.28	0.23	0.24		0.23
VC0532	0.21	0.22	0.23	0.22	0.09	0.12		0.11
VC0533	0.30	0.29		0.29	0.21	0.24		0.22
VC0534	0.23	0.21	0.21	0.22	0.17	0.19		0.18
VC0535	0.24	0.23		0.24	0.20	0.17		0.18
VC0536	0.29	0.30		0.29	0.19	0.19		0.19
VC0537	0.24	0.26	0.27	0.26	0.14	0.15		0.14
VC0538	0.22	0.29	0.25	0.26	0.18	0.19		0.19
VC0539	0.30	0.32	0.28	0.30	0.22	0.23		0.22
VC0540	0.25	0.27	0.26	0.26	0.20	0.18		0.19
VC0541	0.24	0.26	0.27	0.26	0.22	0.20		0.21
VC0542	0.24	0.22		0.23	0.14	0.13		0.14
VC0543	0.24	0.22		0.23	0.13	0.16		0.14
VC0544	0.19	0.20		0.19	0.11	0.09		0.10
VC0545	0.20	0.23	0.21	0.21	0.17	0.18		0.17
VC0546					0.18	0.18	0.16	0.17
VC0547	0.20	0.18		0.19	0.20	0.18		0.19
VC0548					0.17	0.15	0.14	0.15
VC0549					0.19	0.17	0.18	0.18
VC0550	0.22	0.22		0.22	0.12	0.13		0.13
VC0551	0.23	0.23		0.23	0.19	0.21		0.20
VC0552	0.23	0.22		0.22	0.19	0.18		0.18
VC0553	0.30	0.28		0.29	0.24	0.23		0.23
VC0554	0.22	0.21		0.22	0.15	0.15		0.15
VC0555					0.20	0.17	0.19	0.19
VC0556	0.23	0.23		0.23	0.13	0.13		0.13
VC0557	0.23	0.28		0.26	0.15	0.15		0.15
VC0558	0.27	0.27		0.27	0.17	0.21		0.19
VC0559	0.28	0.28		0.28	0.24	0.23		0.23
VC0560	0.22	0.25		0.23	0.15	0.16		0.15
VC0561	0.23	0.23	0.24	0.24	0.16	0.17		0.16
VC0562	0.22	0.24		0.23	0.12	0.13		0.13
VC0563	0.24	0.25		0.25	0.15	0.16		0.15

VC0564	0.23	0.23		0.23	0.15	0.16		0.15
VC0565	0.30	0.31		0.30	0.17	0.18		0.17
VC0567	0.32	0.28		0.30	0.17	0.18		0.18
VC0568	0.26	0.23		0.25	0.18	0.16		0.17
VC0569					0.15	0.17	0.14	0.15
VC0570					0.15	0.14	0.14	0.14
VC0571	0.29	0.29		0.29	0.17	0.17		0.17
VC0572	0.24	0.23		0.23	0.26	0.21		0.24
VC0573	0.25	0.24		0.25	0.17	0.16		0.17
VC0574	0.25	0.22		0.24	0.18	0.17		0.17
VC0575	0.32	0.28		0.30	0.21	0.18		0.20
VC0576	0.22	0.27		0.25	0.15	0.16		0.15
VC0577	0.23	0.23		0.23	0.16	0.16		0.16
VC0578	0.27	0.31		0.29	0.17	0.15		0.16
VC0579	0.26	0.19		0.23	0.16	0.23	0.18	0.19
VC0580	0.23	0.23		0.23	0.16	0.18		0.17
VC0581	0.26	0.24		0.25	0.16	0.17		0.17
VC0582	0.22	0.26		0.24	0.17	0.17		0.17
VC0583	0.22	0.22		0.22	0.14	0.15		0.15
VC0584	0.24	0.23		0.23	0.15	0.16		0.15
VC0585	0.24	0.23		0.24	0.16	0.20		0.18
VC0586	0.25	0.25		0.25	0.17	0.17		0.17
VC0587	0.37	0.33		0.35	0.27	0.28	0.25	0.27
VC0588	0.31	0.29		0.30	0.15	0.19		0.17
VC0589	0.20	0.13		0.17	0.17	0.18		0.17
VC0590	0.36	0.34		0.35	0.16	0.24	0.18	0.19
VC0591	0.25	0.22		0.23	0.16	0.17		0.17
VC0592	0.24	0.30		0.27	0.19	0.14		0.17
VC0593	0.21	0.20	0.19	0.20	0.16	0.15		0.15
VC0596	0.18	0.18		0.18	0.16	0.15	0.15	0.16
VC0597	0.22	0.24		0.23	0.16	0.18		0.17
VC0598	0.22	0.21		0.21	0.17	0.17		0.17
VC0599	0.25	0.26		0.26	0.21	0.18		0.19
VC0600	0.30	0.32		0.31	0.30	0.21	0.22	0.25
VC0601	0.19	0.22		0.20	0.19	0.21		0.20
VC0602	0.29	0.28		0.29	0.22	0.23		0.23
VC0603	0.26	0.27		0.27	0.19	0.21		0.20
VC0604	0.23	0.23		0.23	0.15	0.19		0.17
VC0605	0.20	0.21		0.21	0.15	0.13		0.14
VC0606	0.25	0.24		0.24	0.16	0.15		0.15
VC0607	0.26	0.24		0.25	0.20	0.23	0.21	0.21
VC0609	0.32	0.27		0.29	0.18	0.18	0.21	0.19
VC0610	0.24	0.24		0.24	0.16	0.18	0.15	0.17

VC0611	0.24	0.24		0.24	0.17	0.22	0.21	0.20
VC0612	0.26	0.25		0.25	0.17	0.16		0.16
VC0613	0.22	0.21		0.22	0.18	0.15		0.16
VC0614	0.17	0.16		0.16	0.12	0.11	0.13	0.12
VC0615	0.23	0.22		0.23	0.16	0.13	0.17	0.16
VC0616	0.24	0.23		0.24	0.14	0.13	0.14	0.14
VC0617	0.21	0.25		0.23	0.10	0.11	0.15	0.12
VC0619	0.26	0.25		0.25	0.20	0.16	0.17	0.18
VC0620	0.26	0.26		0.26	0.18	0.21	0.22	0.20
VC0621	0.29	0.30		0.30	0.25	0.27		0.26
VC0622	0.26	0.28		0.27	0.25	0.23		0.24
VC0623	0.18	0.21		0.20	0.15	0.09	0.09	0.11
VC0624	0.27	0.26	0.25	0.26	0.17	0.15		0.16
VC0625	0.27	0.26	0.26	0.26	0.20	0.19		0.20
VC0626	0.23	0.23	0.27	0.25	0.18	0.14		0.16
VC0627	0.22	0.26		0.24				
VC0628	0.32	0.29	0.28	0.29	0.27	0.23		0.25
VC0629	0.28	0.29		0.28	0.18	0.19		0.19
VC0630	0.31	0.34		0.33	0.19	0.15		0.17
VC0631	0.26	0.25	0.26	0.26	0.14	0.15		0.15
VC0632	0.31	0.28		0.29	0.18	0.16		0.17
VC0633	0.24	0.25	0.27	0.25	0.20	0.20		0.20
VC0634	0.28	0.30		0.29	0.18	0.16		0.17
VC0635	0.22	0.22	0.23	0.22	0.12	0.13		0.13
VC0636	0.26	0.26		0.26	0.15	0.14		0.14
VC0637	0.28	0.26		0.27	0.20	0.19		0.19
VC0638	0.28	0.31		0.29	0.19	0.19		0.19
VC0639	0.24	0.26		0.25	0.16	0.16		0.16
VC0640	0.31	0.19	0.18	0.23	0.19	0.19		0.19
VC0641	0.27	0.24		0.26	0.14	0.17		0.16
VC0642	0.25	0.24	0.21	0.23	0.16	0.19		0.18
VC0643	0.25	0.23		0.24	0.17	0.21		0.19
VC0644	0.28	0.25	0.27	0.27	0.19	0.21		0.20
VC0645	0.23	0.26	0.26	0.25	0.13	0.10		0.12
VC0646	0.25	0.27		0.26	0.20	0.19	0.22	0.20
VC0647	0.26	0.28	0.25	0.26	0.18	0.19		0.19
VC0648	0.26	0.24	0.26	0.25	0.13	0.12		0.12
VC0649	0.22	0.24	0.24	0.23	0.13	0.11		0.12
VC0650	0.29	0.28		0.29	0.20	0.16		0.18
VC0651	0.22	0.23	0.23	0.23	0.16	0.15		0.16
VC0652	0.26	0.25	0.24	0.25	0.16	0.13		0.14
VC0653	0.66	0.71		0.69	0.52	0.46		0.49
VC0654	0.14	0.18		0.16	0.16	0.16		0.16

VC0655	0.24	0.26		0.25	0.20	0.18	0.17	0.18
VC0656	0.11	0.23		0.17	0.14	0.12		0.13
VC0657	0.29	0.30		0.30	0.21	0.19		0.20
VC0658	0.56	0.57		0.56	0.51	0.57		0.54
VC0659	0.22	0.22		0.22	0.16	0.15	0.15	0.15
VC0660	0.22	0.28		0.25	0.17	0.19	0.16	0.17
VC0661	0.28	0.26		0.27	0.15	0.19		0.17
VC0662	0.28	0.28		0.28	0.22	0.23	0.23	0.22
VC0663	0.16	0.16		0.16	0.13	0.14		0.13
VC0664	0.20	0.22		0.21	0.14	0.13		0.14
VC0665	0.27	0.31		0.29	0.17	0.13		0.15
VC0666	0.24	0.25		0.24	0.16	0.17		0.17
VC0667	0.18	0.17		0.18	0.13	0.12		0.12
VC0668	0.26	0.23		0.25	0.14	0.14		0.14
VC0669	0.22	0.24		0.23	0.13	0.18	0.18	0.16
VC0670	0.21	0.21		0.21	0.15	0.14	0.14	0.14
VC0671	0.28	0.27		0.27	0.14	0.17		0.15
VC0672	0.24	0.26		0.25	0.16	0.17		0.16
VC0673	0.29	0.28		0.28	0.23	0.20		0.22
VC0674	0.23	0.22		0.23	0.18	0.18		0.18
VC0675	0.27	0.24	0.26	0.26	0.16	0.17		0.16
VC0676	0.21	0.20		0.21				
VC0677	0.24	0.22		0.23	0.12	0.14		0.13
VC0678	0.27	0.25		0.26	0.15	0.14		0.14
VC0679	0.30	0.26		0.28	0.18	0.17		0.18
VC0680	0.26	0.22		0.24	0.20	0.23		0.22
VC0681	0.28	0.24	0.27	0.26	0.18	0.19		0.19
VC0682	0.27	0.27		0.27	0.13	0.16		0.15
VC0683	0.27	0.26		0.27	0.18	0.17		0.17
VC0684	0.23	0.23		0.23	0.14	0.17		0.15
VC0685	0.24	0.23		0.23	0.13	0.12		0.12
VC0686	0.27	0.21		0.24	0.11	0.12	0.15	0.13
VC0687	0.37	0.36		0.37	0.22	0.22		0.22
VC0688	0.29	0.29		0.29	0.20	0.16		0.18
VC0689	0.24	0.27	0.25	0.25	0.13	0.13		0.13
VC0690	0.19	0.16		0.17	0.21	0.22		0.22
VC0691	0.22	0.21		0.21	0.15	0.15		0.15
VC0692	0.19	0.21		0.20	0.14	0.14		0.14
VC0693	0.10	0.22	0.24	0.19	0.13	0.13		0.13
VC0694	0.24	0.26		0.25				
VC0695	0.24	0.24		0.24	0.15	0.14		0.14
VC0696	0.23	0.21		0.22	0.14	0.14		0.14
VC0697	0.24	0.23		0.23				

VC0698	0.27	0.29		0.28	0.15	0.20		0.17
VC0699	0.19	0.21		0.20	0.15	0.21		0.18
VC0700	0.27	0.28		0.27	0.16	0.13		0.15
VC0701	0.26	0.27		0.27	0.19	0.18		0.18
VC0702	0.23	0.23	0.23	0.23	0.17	0.19		0.18
VC0703	0.30	0.26		0.28	0.19	0.20	0.22	0.20
VC0704	0.25	0.23		0.24	0.19	0.19		0.19
VC0705	0.20	0.19		0.20	0.19	0.14		0.16
VC0706	0.28	0.29	0.27	0.28	0.17	0.19		0.18
VC0707	0.23	0.25		0.24	0.17	0.17		0.17
VC0708	0.18	0.20		0.19	0.19	0.19		0.19
VC0709	0.24	0.24		0.24	0.16	0.17	0.19	0.18
VC0710	0.26	0.23		0.24	0.18	0.18		0.18
VC0711	0.20	0.21		0.21	0.13	0.13		0.13
VC0712	0.14	0.16		0.15	0.21	0.18		0.19
VC0713	0.23	0.22		0.22	0.11	0.12		0.11
VC0714	0.22	0.22	0.22	0.22	0.18	0.18		0.18
VC0715	0.23	0.23		0.23	0.11	0.11		0.11
VC0716	0.25	0.24	0.26	0.25	0.21	0.17		0.19
VC0717	0.26	0.26	0.26	0.26	0.18	0.15		0.17
VC0718	0.22	0.26		0.24	0.15	0.16		0.16
VC0719	0.22	0.20	0.21	0.21	0.18	0.18		0.18
VC0720	0.30	0.28	0.28	0.29	0.23	0.21		0.22
VC0721	0.28	0.32		0.30	0.22	0.20		0.21
VC0722	0.22	0.21	0.21	0.22	0.15	0.13		0.14
VC0723	0.23	0.23		0.23	0.20	0.19		0.19
VC0724	0.29	0.28		0.29	0.16	0.18		0.17
VC0725	0.27	0.28		0.28	0.16	0.16		0.16
VC0726	0.22	0.22		0.22	0.14	0.13	0.14	0.13
VC0727	0.21	0.21		0.21	0.15	0.13	0.17	0.15
VC0728	0.22	0.22		0.22	0.14	0.16		0.15
VC0729	0.22	0.22		0.22	0.16	0.19		0.18
VC0730	0.19	0.18		0.18	0.12	0.12	0.12	0.12
VC0731	0.23	0.24		0.24	0.13	0.15		0.14
VC0732	0.25	0.24		0.24	0.19	0.19	0.18	0.19
VC0733	0.27	0.28		0.27	0.25	0.23		0.24
VC0734	0.33	0.29		0.31	0.17	0.16		0.17
VC0735	0.24	0.26		0.25	0.20	0.18		0.19
VC0736	0.26	0.29		0.27	0.14	0.15		0.15
VC0737	0.23	0.22		0.23	0.23	0.20	0.16	0.20
VC0738	0.25	0.25		0.25	0.22	0.15		0.19
VC0739	0.24	0.22		0.23	0.20	0.16		0.18
VC0740	0.18	0.19		0.19	0.15	0.14	0.16	0.15

VC0741	0.25	0.25		0.25	0.19	0.18		0.19
VC0742	0.18	0.22		0.20	0.15	0.16	0.18	0.16
VC0743	0.33	0.30	0.29	0.31	0.20	0.20		0.20
VC0744	0.28	0.27	0.25	0.26	0.23	0.22		0.22
VC0745	0.22	0.22		0.22	0.21	0.21		0.21
VC0746	0.26	0.26		0.26	0.21	0.18		0.19
VC0747	0.27	0.26		0.26	0.14	0.13		0.14
VC0748	0.22	0.21		0.22	0.15	0.17		0.16
VC0749	0.27	0.26		0.26	0.20	0.21		0.20
VC0750	0.25	0.25		0.25	0.17	0.18		0.18
VC0751	0.25	0.24		0.24	0.17	0.20	0.17	0.18
VC0752	0.19	0.20	0.21	0.20	0.15	0.15		0.15
VC0753	0.28	0.30		0.29	0.10	0.09		0.10
VC0754	0.25	0.27		0.26	0.20	0.16	0.18	0.18
VC0755	0.24	0.25		0.25	0.19	0.17		0.18
VC0756	0.22	0.23	0.23	0.23	0.16	0.17		0.16
VC0757	0.26	0.26		0.26	0.14	0.13		0.13
VC0758	0.21	0.21		0.21	0.15	0.17	0.17	0.16
VC0759	0.25	0.27		0.26	0.15	0.21		0.18
VC0760	0.26	0.28	0.29	0.28	0.13	0.14		0.14
VC0761	0.25	0.23		0.24	0.24	0.23		0.23
VC0762	0.30	0.27		0.29	0.22	0.22	0.25	0.23
VC0763	0.25	0.22	0.24	0.23	0.19	0.20		0.19
VC0764	0.22	0.22		0.22	0.16	0.16		0.16
VC0765	0.24	0.26		0.25	0.13	0.15		0.14
VC0766	0.32	0.29		0.30	0.27	0.20		0.24
VC0767	0.32	0.30		0.31	0.25	0.22		0.24
VC0768	0.26	0.26		0.26	0.20	0.17		0.18
VC0769	0.23	0.21		0.22	0.13	0.14	0.14	0.14
VC0770	0.22	0.24		0.23	0.19	0.20		0.20
VC0771	0.27	0.29		0.28	0.14	0.15		0.15
VC0772	0.16	0.17		0.17	0.20	0.19	0.20	0.20
VC0773	0.23	0.22		0.22	0.13	0.14	0.14	0.14
VC0774	0.22	0.22	0.22	0.22	0.16	0.17		0.16
VC0775	0.23	0.25		0.24	0.14	0.17		0.15
VC0776	0.26	0.26		0.26	0.15	0.15		0.15
VC0777	0.28	0.28		0.28	0.19	0.19		0.19
VC0778	0.23	0.21		0.22	0.19	0.16		0.18
VC0779	0.28	0.28		0.28	0.20	0.19		0.19
VC0780	0.25	0.29		0.27	0.20	0.20		0.20
VC0781	0.25	0.27		0.26	0.14	0.14		0.14
VC0782	0.24	0.23		0.23	0.15	0.12		0.14
VC0783	0.24	0.23		0.23	0.12	0.18	0.18	0.16

VC0784	0.29	0.27		0.28	0.14	0.16		0.15
VC0785	0.29	0.27		0.28	0.11	0.12	0.15	0.13
VC0786	0.20	0.23		0.21	0.13	0.14		0.14
VC0787	0.27	0.28		0.27	0.18	0.21		0.20
VC0788	0.21	0.20		0.20	0.20	0.22	0.17	0.20
VC0789	0.23	0.22		0.23	0.16	0.18		0.17
VC0790	0.32	0.26		0.29	0.17	0.17		0.17
VC0791	0.26	0.24		0.25	0.09	0.13		0.11
VC0792	0.27	0.25		0.26	0.21	0.20		0.21
VC0793	0.19	0.24		0.21	0.20	0.15	0.19	0.18
VC0793	0.21	0.24		0.22	0.15	0.16		0.16
VC0794	0.27	0.22		0.25	0.21	0.17	0.15	0.18
VC0795	0.33	0.34		0.33	0.18	0.24		0.21
VC0796	0.29	0.30		0.29	0.14	0.19		0.17
VC0797	0.24	0.24		0.24	0.20	0.17		0.19
VC0798	0.21	0.20		0.20	0.12	0.13		0.12
VC0799	0.23	0.26		0.24	0.14	0.17		0.16
VC0800	0.22	0.20		0.21	0.15	0.22		0.18
VC0801	0.27	0.26		0.27	0.19	0.18		0.18
VC0802	0.31	0.26		0.29	0.16	0.20		0.18
VC0803	0.26	0.24		0.25	0.18	0.19		0.19
VC0805	0.26	0.27		0.26	0.14	0.20		0.17
VC0806	0.26	0.26	0.29	0.27	0.10	0.09		0.09
VC0807	0.29	0.28	0.30	0.29	0.24	0.22		0.23
VC0808	0.20	0.21		0.20	0.10	0.12	0.11	0.11
VC0809	0.27	0.26	0.29	0.28	0.25	0.19		0.22
VC0810	0.33	0.35	0.33	0.34	0.31	0.27		0.29
VC0811	0.25	0.29		0.27	0.18	0.20		0.19
VC0812	0.25	0.25		0.25	0.13	0.13		0.13
VC0813	0.26	0.20	0.21	0.22	0.16	0.15		0.15
VC0814	0.25	0.24	0.25	0.25	0.15	0.13		0.14
VC0815	0.23	0.23	0.25	0.24	0.26	0.18		0.22
VC0816					0.19	0.13	0.13	0.15
VC0817	0.26	0.24		0.25	0.11	0.16		0.14
VC0818	0.24	0.26		0.25	0.17	0.17		0.17
VC0819	0.19	0.20	0.17	0.19	0.25	0.19		0.22
VC0820	0.21	0.25		0.23	0.14	0.11	0.11	0.12
VC0821	0.28	0.24	0.25	0.26	0.16	0.17		0.16
VC0822	0.21	0.25		0.23	0.17	0.15	0.12	0.15
VC0823	0.27	0.22		0.25	0.22	0.26		0.24
VC0824	0.28	0.30		0.29	0.25	0.24	0.21	0.23
VC0825	0.25	0.27		0.26	0.14	0.13		0.13
VC0826	0.25	0.24		0.24	0.20	0.17		0.18

VC0827	0.20	0.23		0.21	0.19	0.20	0.19	0.19
VC0828	0.32	0.23		0.27	0.24	0.30		0.27
VC0829	0.24	0.25		0.24	0.13	0.13		0.13
VC0830	0.22	0.22	0.26	0.23	0.16	0.17		0.16
VC0831	0.28	0.27		0.28	0.18	0.17		0.18
VC0832	0.23	0.26		0.25	0.15	0.15		0.15
VC0833	0.37	0.35		0.36	0.21	0.19	0.18	0.19
VC0834	0.30	0.32		0.31	0.19	0.14		0.16
VC0835	0.21	0.20		0.21	0.15	0.15	0.14	0.15
VC0836	0.24	0.24		0.24	0.16	0.19		0.18
VC0837	0.26	0.23		0.24	0.16	0.17	0.15	0.16
VC0838	0.24	0.24	0.24	0.24	0.17	0.14		0.15
VC0839	0.25	0.26	0.23	0.24	0.19	0.19		0.19
VC0840	0.24	0.26		0.25	0.27	0.20	0.18	0.21
VC0841	0.28	0.25	0.26	0.26	0.15	0.14		0.15
VC0842	0.29	0.24		0.26	0.20	0.20		0.20
VC0843	0.31	0.33		0.32	0.29	0.23	0.21	0.25
VC0846	0.27	0.24		0.25	0.16	0.12		0.14
VC0847	0.27	0.28		0.27	0.14	0.15		0.15
VC0848	0.18	0.21		0.20	0.10	0.10		0.10
VC0849	0.24	0.21		0.22	0.16	0.17		0.17
VC0850	0.24	0.24	0.28	0.25	0.14	0.13		0.13
VC0851	0.24	0.26		0.25	0.16	0.18		0.17
VC0852	0.24	0.20		0.22	0.14	0.14	0.13	0.13
VC0853	0.23	0.22		0.23	0.16	0.15	0.14	0.15
VC0854	0.21	0.22		0.21	0.16	0.18		0.17
VC0855	0.24	0.26		0.25	0.17	0.20		0.19
VC0856	0.27	0.28		0.28	0.16	0.16		0.16
VC0857	0.27	0.27		0.27	0.21	0.22		0.21
VC0858	0.34	0.35		0.34	0.29	0.28		0.29
VC0859	0.32	0.33		0.32	0.22	0.19		0.21
VC0860	0.28	0.26		0.27	0.23	0.23		0.23
VC0861	0.24	0.28		0.26	0.19	0.20		0.19
VC0862	0.31	0.29		0.30	0.24	0.23		0.24
VC0863	0.27	0.28		0.27	0.26	0.19		0.22
VC0864	0.25	0.24		0.25	0.15	0.16		0.16
VC0865	0.22	0.24	0.23	0.23	0.18	0.15		0.16
VC0866	0.26	0.24		0.25	0.16	0.17		0.17
VC0867	0.24	0.23	0.25	0.24	0.17	0.23		0.20
VC0868	0.28	0.26		0.27	0.15	0.15		0.15
VC0869	0.22	0.21		0.22	0.17	0.16		0.17
VC0870	0.25	0.20		0.23	0.15	0.16		0.16
VC0871	0.23	0.22	0.24	0.23	0.18	0.19		0.18

VC0872	0.24	0.24	0.25	0.24	0.16	0.15		0.15
VC0873	0.25	0.31		0.28	0.16	0.17		0.16
VC0874	0.27	0.23		0.25	0.15	0.18		0.16
VC0875	0.27	0.26		0.27	0.16	0.15		0.15
VC0876	0.25	0.27		0.26	0.17	0.17		0.17
VC0877	0.23	0.23	0.27	0.24	0.15	0.14		0.14
VC0878	0.26	0.25	0.25	0.25	0.14	0.16		0.15
VC0879	0.23	0.25	0.23	0.23	0.17	0.14		0.15
VC0880	0.28	0.27		0.27	0.31	0.27		0.29
VC0881	0.25	0.23		0.24	0.14	0.12		0.13
VC0882	0.24	0.24	0.23	0.24	0.16	0.16		0.16
VC0883	0.20	0.20		0.20	0.18	0.20		0.19
VC0884	0.25	0.20		0.22	0.17	0.13		0.15
VC0885	0.24	0.26	0.25	0.25	0.23	0.19		0.21
VC0886	0.23	0.26		0.25	0.17	0.19		0.18
VC0887	0.19	0.18		0.18	0.12	0.13		0.13
VC0888	0.28	0.26		0.27	0.18	0.15		0.16
VC0889	0.29	0.26		0.27	0.19	0.16		0.18
VC0890	0.23	0.24	0.23	0.23	0.15	0.17		0.16
VC0891	0.25	0.26	0.24	0.25	0.22	0.24		0.23
VC0892	0.25	0.25		0.25	0.24	0.17		0.20
VC0893	0.28	0.27		0.27	0.24	0.20		0.22
VC0894	0.26	0.22	0.20	0.23	0.15	0.14		0.15
VC0895	0.26	0.28		0.27	0.15	0.18		0.17
VC0897	0.25	0.23	0.26	0.25	0.25	0.26		0.26
VC0898	0.21	0.20		0.20	0.18	0.10		0.14
VC0899	0.22	0.22	0.24	0.23	0.15	0.13		0.14
VC0900	0.27	0.28		0.28	0.18	0.15		0.17
VC0901	0.21	0.21		0.21	0.17	0.17		0.17
VC0902	0.17	0.17	0.17	0.17	0.11	0.16		0.14
VC0903					0.15	0.18	0.18	0.17
VC0904	0.21	0.21	0.20	0.21	0.19	0.17		0.18
VC0905	0.17	0.20	0.17	0.18	0.17	0.17		0.17
VC0906	0.29	0.31	0.32	0.31	0.16	0.18		0.17
VC0907					0.13		0.14	0.14
VC0908					0.16	0.16	0.18	0.17
VC0909	0.30	0.24		0.27	0.15	0.15		0.15
VC0910	0.30	0.30	0.30	0.30	0.15	0.18		0.16
VC0911	0.26	0.27		0.27	0.11	0.12		0.12
VC0912	0.24	0.24		0.24	0.14	0.16		0.15
VC0914	0.25	0.22		0.24	0.19	0.16		0.17
VC0915	0.27	0.25		0.26	0.12	0.10		0.11
VC0916	0.21	0.21		0.21	0.16	0.16		0.16

VC0917	0.21	0.22	0.27	0.23	0.16	0.14		0.15
VC0918	0.22	0.23	0.27	0.24	0.12	0.13		0.13
VC0919					0.15	0.13	0.15	0.14
VC0920	0.18	0.18	0.19	0.18	0.14	0.14		0.14
VC0921	0.28	0.28	0.29	0.28	0.19	0.18		0.19
VC0922	0.33	0.28		0.30	0.22	0.23		0.23
VC0923	0.22	0.23	0.23	0.23	0.18	0.17		0.17
VC0924	0.29	0.28		0.29	0.17	0.19		0.18
VC0925	0.23	0.22		0.22	0.16	0.15		0.15
VC0926	0.26	0.29		0.28	0.14	0.14		0.14
VC0927	0.28	0.23		0.25	0.19	0.21		0.20
VC0928	0.28	0.27		0.28				
VC0929	0.32	0.28		0.30	0.22	0.21		0.22
VC0930	0.26	0.27		0.26	0.16	0.17		0.16
VC0931	0.33	0.31		0.32	0.20	0.20	0.20	0.20
VC0932	0.25	0.24		0.25	0.14	0.16	0.17	0.16
VC0934	0.22	0.22		0.22	0.21	0.20		0.20
VC0935	0.24	0.25		0.24	0.15	0.18		0.17
VC0936	0.30	0.28		0.29	0.15	0.16	0.16	0.15
VC0937	0.31	0.29		0.30	0.17	0.20		0.19
VC0938	0.28	0.30		0.29	0.21	0.23		0.22
VC0939	0.22	0.23	0.24	0.23	0.16	0.17		0.17
VC0940	0.24	0.26	0.26	0.25	0.22	0.21		0.22
VC0941	0.18	0.19	0.21	0.19	0.11	0.10		0.10
VC0943	0.23	0.25	0.23	0.24	0.19	0.20		0.19
VC0944	0.21	0.19		0.20	0.12	0.13		0.12
VC0945	0.27	0.30		0.29	0.13	0.17	0.18	0.16
VC0946	0.24	0.20		0.22	0.13	0.19	0.17	0.16
VC0947	0.29	0.30	0.31	0.30	0.19	0.20		0.20
VC0948	0.31	0.34	0.30	0.32	0.14	0.12		0.13
VC0949	0.27	0.30		0.28	0.22	0.21		0.21
VC0950	0.25	0.24		0.25	0.17	0.17	0.17	0.17
VC0951	0.25	0.25	0.27	0.26	0.15	0.12		0.14
VC0952	0.23	0.25	0.23	0.24	0.16	0.19		0.18
VC0953	0.23	0.22	0.24	0.23	0.21	0.22		0.22
VC0954	0.24	0.24		0.24	0.22	0.20		0.21
VC0955	0.27	0.26		0.27	0.20	0.21		0.20
VC0957	0.23	0.23		0.23	0.10	0.10	0.10	0.10
VC0958	0.25	0.26		0.25	0.22	0.16	0.15	0.18
VC0959	0.24	0.21	0.18	0.21	0.12	0.11		0.11
VC0960	0.25	0.26		0.25	0.13	0.14		0.14
VC0961	0.24	0.22		0.23	0.13	0.16		0.15
VC0962	0.26	0.22	0.24	0.24	0.12	0.14		0.13

VC0963	0.29	0.26		0.27	0.17	0.19		0.18
VC0964	0.25	0.33	0.28	0.28	0.14	0.15		0.14
VC0965	0.25	0.23		0.24	0.11	0.12		0.11
VC0966	0.19	0.21		0.20	0.17	0.16		0.16
VC0967	0.29	0.27	0.28	0.28	0.20	0.19		0.19
VC0968	0.23	0.22	0.22	0.22	0.16	0.18		0.17
VC0969	0.26	0.25	0.27	0.26	0.26	0.18		0.22
VC0970	0.18	0.23	0.19	0.20	0.17	0.18		0.17
VC0972	0.21	0.22	0.25	0.23	0.15	0.15		0.15
VC0973	0.27	0.27	0.26	0.27	0.16	0.19		0.18
VC0974	0.20	0.28	0.21	0.23	0.16	0.18		0.17
VC0975	0.23	0.22		0.23	0.27	0.29		0.28
VC0976	0.27	0.27	0.30	0.28	0.27	0.23		0.25
VC0977	0.27	0.25	0.24	0.26	0.13	0.16		0.14
VC0978	0.21	0.21		0.21	0.16	0.19		0.18
VC0979	0.29	0.29	0.32	0.30	0.22	0.21		0.22
VC0980	0.18	0.19	0.18	0.18	0.09	0.08		0.08
VC0981	0.25	0.23	0.22	0.23	0.12	0.14		0.13
VC0982	0.23	0.27		0.25	0.18	0.17		0.17
VC0983	0.29	0.32	0.25	0.29	0.18	0.16		0.17
VC0984	0.27	0.29	0.27	0.27	0.23	0.25		0.24
VC0985	0.17	0.20	0.19	0.18	0.20	0.16		0.18
VC0986	0.25	0.26		0.25	0.14	0.19		0.17
VC0987	0.26	0.26	0.23	0.25	0.16	0.16		0.16
VC0988	0.27	0.23	0.21	0.24	0.16	0.16		0.16
VC0989	0.31	0.31		0.31	0.15	0.15		0.15
VC0990	0.23	0.22	0.22	0.23	0.14	0.16		0.15
VC0991	0.25	0.20	0.22	0.22	0.15	0.15		0.15
VC0992	0.31	0.29	0.28	0.29	0.22	0.17		0.20
VC0993	0.26	0.27	0.26	0.26	0.11	0.13		0.12
VC0994	0.23	0.23	0.24	0.23	0.14	0.14		0.14
VC0995	0.26	0.26		0.26	0.18	0.22		0.20
VC0996					0.16	0.17	0.19	0.17
VC0997	0.29	0.27		0.28	0.13	0.18		0.16
VC0998	0.24	0.24		0.24	0.15	0.15	0.17	0.16
VC0999	0.27	0.26		0.26	0.23	0.20		0.21
VC1000	0.28	0.25		0.26	0.13	0.12		0.13
VC1001	0.28	0.29	0.26	0.28	0.12	0.14		0.13
VC1002	0.26	0.33		0.29	0.16	0.18		0.17
VC1003	0.28	0.30		0.29	0.19	0.20		0.20
VC1004	0.23	0.25		0.24	0.17	0.18		0.17
VC1005	0.27	0.29		0.28	0.19	0.20		0.19
VC1006	0.21	0.21		0.21	0.15	0.17		0.16

VC1007	0.26	0.26		0.26	0.18	0.19		0.18
VC1008	0.26	0.27		0.27	0.23	0.19		0.21
VC1009	0.23	0.22		0.22	0.15	0.15		0.15
VC1010	0.21	0.24		0.22	0.16	0.15		0.15
VC1011	0.25	0.26		0.25	0.14	0.12		0.13
VC1012	0.29	0.29		0.29	0.21	0.18		0.19
VC1013	0.26	0.24		0.25	0.18	0.17		0.17
VC1014	0.24	0.25	0.26	0.25	0.15	0.15		0.15
VC1015	0.26	0.26		0.26	0.14	0.11		0.12
VC1016	0.26	0.26		0.26	0.20	0.20		0.20
VC1017	0.26	0.27		0.27	0.26	0.20		0.23
VC1018	0.25	0.24		0.25	0.13	0.08	0.09	0.10
VC1020	0.25	0.24		0.25	0.21	0.14		0.18
VC1021	0.22	0.19		0.20	0.13	0.13		0.13
VC1022					0.16	0.15	0.17	0.16
VC1023	0.30	0.29		0.29	0.14	0.10		0.12
VC1024	0.25	0.23		0.24	0.14	0.14		0.14
VC1025	0.20	0.15		0.17	0.19	0.17		0.18
VC1026	0.27	0.26		0.26	0.14	0.16		0.15
VC1027	0.25	0.25		0.25	0.13	0.15		0.14
VC1028	0.25	0.24		0.25	0.14	0.15		0.14
VC1029	0.20	0.24		0.22	0.15	0.13	0.14	0.14
VC1030	0.23	0.23		0.23	0.13	0.15		0.14
VC1031	0.19	0.15		0.17	0.20	0.18		0.19
VC1032	0.31	0.29		0.30	0.21	0.23		0.22
VC1033	0.23	0.21		0.22	0.19	0.20		0.19
VC1034	0.23	0.27		0.25	0.13	0.12		0.13
VC1035	0.37	0.30		0.33	0.25	0.28	0.25	0.26
VC1036	0.16	0.18		0.17	0.04	0.09		0.07
VC1037	0.23	0.22		0.23	0.17	0.18	0.16	0.17
VC1038	0.25	0.24		0.24	0.14	0.14		0.14
VC1039	0.22	0.23		0.23	0.15	0.12		0.14
VC1040	0.24	0.22		0.23	0.15	0.17		0.16
VC1041	0.25	0.29		0.27	0.17	0.17		0.17
VC1043	0.30	0.28		0.29	0.16	0.18	0.15	0.17
VC1044	0.27	0.29		0.28	0.14	0.13		0.14
VC1045	0.31	0.29		0.30	0.17	0.20		0.18
VC1046	0.25	0.24		0.24	0.16	0.12		0.14
VC1047	0.22	0.24		0.23	0.18	0.17		0.18
VC1048	0.21	0.20		0.21	0.10	0.06	0.08	0.08
VC1049	0.22	0.23		0.22	0.16	0.12	0.14	0.14
VC1050	0.19	0.20		0.19	0.18	0.21		0.20
VC1051	0.24	0.25		0.24	0.22	0.19		0.20

VC1052	0.43	0.43		0.43	0.17	0.21	0.19	0.19
VC1053	0.25	0.25		0.25	0.15	0.21		0.18
VC1054	0.23	0.21		0.22	0.18	0.18		0.18
VC1055	0.25	0.24		0.24	0.11	0.12	0.13	0.12
VC1056	0.31	0.32		0.32	0.12	0.14	0.14	0.13
VC1057	0.27	0.25		0.26	0.15	0.13		0.14
VC1058	0.26	0.22		0.24	0.13	0.15	0.14	0.14
VC1059	0.23	0.26		0.24	0.13	0.16	0.17	0.15
VC1060	0.25	0.25		0.25	0.20	0.15	0.18	0.18
VC1061	0.25	0.20		0.23	0.15	0.13		0.14
VC1062	0.27	0.32		0.29	0.20	0.21		0.20
VC1063	0.27	0.26		0.26	0.16	0.17	0.17	0.17
VC1064	0.39	0.34		0.36	0.22	0.20		0.21
VC1065	0.19	0.21		0.20	0.17	0.16		0.17
VC1066	0.27	0.26		0.27	0.11	0.12		0.12
VC1067	0.21	0.24		0.22	0.14	0.15	0.14	0.14
VC1068	0.25	0.27		0.26	0.14	0.15		0.14
VC1069	0.18	0.22		0.20	0.19	0.15	0.15	0.16
VC1070	0.22	0.23		0.23	0.19	0.17		0.18
VC1071	0.35	0.31		0.33	0.18	0.19		0.18
VC1072	0.27	0.27		0.27	0.15	0.15		0.15
VC1074	0.30	0.30		0.30	0.18	0.17		0.18
VC1075	0.21	0.22		0.22	0.11	0.10		0.10
VC1077	0.25	0.24		0.24	0.19	0.22		0.21
VC1078	0.25	0.27		0.26	0.18	0.15		0.16
VC1079	0.24	0.24		0.24	0.17	0.16	0.18	0.17
VC1080	0.22	0.22		0.22	0.17	0.19		0.18
VC1081	0.23	0.24		0.24	0.12	0.12		0.12
VC1082	0.21	0.22		0.22	0.11	0.13		0.12
VC1083	0.26	0.26		0.26	0.18	0.14		0.16
VC1084	0.22	0.25		0.24	0.20	0.18		0.19
VC1085	0.21	0.28		0.24	0.15	0.15		0.15
VC1086	0.31	0.32		0.32	0.22	0.21		0.21
VC1087	0.21	0.22		0.22	0.17	0.16		0.17
VC1088	0.29	0.33		0.31	0.22	0.21		0.22
VC1089	0.23	0.22		0.23	0.16	0.17		0.17
VC1090	0.24	0.24		0.24	0.23	0.22	0.19	0.22
VC1091	0.25	0.28		0.27	0.16	0.16		0.16
VC1092	0.26	0.24	0.26	0.25	0.17	0.16		0.16
VC1093	0.23	0.23		0.23	0.18	0.17		0.17
VC1094	0.27	0.27	0.25	0.26	0.16	0.17		0.16
VC1095	0.21	0.23	0.22	0.22	0.17	0.19		0.18
VC1096	0.20	0.19	0.18	0.19	0.14	0.14		0.14

VC1097	0.28	0.27		0.28	0.16	0.18		0.17
VC1098	0.27	0.30		0.28	0.24	0.19		0.21
VC1099	0.25	0.29	0.28	0.27	0.18	0.16		0.17
VC1100	0.18	0.18	0.16	0.17	0.14	0.13		0.14
VC1101	0.24	0.22	0.25	0.24	0.14	0.14		0.14
VC1102	0.31	0.33		0.32	0.21	0.22		0.22
VC1103	0.24	0.24		0.24	0.15	0.13		0.14
VC1104	0.28	0.27		0.28	0.22	0.20		0.21
VC1105	0.26	0.25		0.26	0.11	0.11		0.11
VC1106	0.21	0.25		0.23	0.17	0.12		0.14
VC1107	0.32	0.34		0.33	0.21	0.20		0.20
VC1108	0.36	0.35		0.36	0.20	0.16		0.18
VC1109	0.19	0.23		0.21	0.10	0.18	0.17	0.15
VC1110	0.26	0.26		0.26	0.22	0.22		0.22
VC1111	0.24	0.27		0.26	0.18	0.13		0.15
VC1112	0.27	0.26	0.25	0.26	0.18	0.15		0.16
VC1113	0.20	0.20		0.20	0.12	0.12		0.12
VC1114	0.25	0.26		0.26	0.20	0.18		0.19
VC1115	0.24	0.26		0.25	0.13	0.15		0.14
VC1116	0.30	0.24		0.27	0.24	0.23	0.25	0.24
VC1117	0.28	0.25		0.26	0.12	0.14		0.13
VC1118	0.26	0.25		0.25	0.13	0.13		0.13
VC1119	0.28	0.29		0.28	0.16	0.18		0.17
VC1120	0.27	0.27		0.27	0.17	0.18		0.18
VC1121	0.31	0.28		0.29	0.20	0.22		0.21
VC1122	0.26	0.25		0.26	0.17	0.20		0.18
VC1123	0.29	0.31		0.30	0.13	0.16		0.14
VC1124	0.25	0.25		0.25	0.17	0.16	0.17	0.17
VC1125	0.20	0.21		0.20	0.19	0.21		0.20
VC1126	0.30	0.23	0.25	0.26	0.15	0.15		0.15
VC1127	0.29	0.31		0.30	0.17	0.17		0.17
VC1128	0.27	0.26	0.26	0.26	0.21	0.19		0.20
VC1129	0.35	0.39		0.37	0.21	0.21	0.20	0.21
VC1130	0.24	0.26		0.25	0.15	0.15	0.14	0.15
VC1131	0.21	0.23		0.22	0.15	0.17	0.18	0.17
VC1132	0.27	0.27		0.27	0.22	0.15	0.15	0.17
VC1133	0.25	0.24		0.24	0.18	0.18		0.18
VC1134	0.27	0.26		0.27	0.15	0.17	0.15	0.15
VC1135	0.28	0.25		0.26	0.15	0.15		0.15
VC1136	0.28	0.25		0.26	0.19	0.17		0.18
VC1137	0.23	0.24		0.24	0.17	0.18		0.17
VC1138	0.22	0.22		0.22	0.14	0.18		0.16
VC1139	0.25	0.25		0.25	0.20	0.19		0.20

VC1140	0.20	0.21		0.20	0.12	0.14		0.13
VC1141	0.26	0.26		0.26	0.17	0.15		0.16
VC1142	0.24	0.25		0.25	0.17	0.15		0.16
VC1143	0.25	0.25		0.25	0.17	0.16		0.17
VC1144	0.27	0.27		0.27	0.17	0.20		0.19
VC1145	0.33	0.29		0.31	0.23	0.22		0.23
VC1146	0.25	0.24		0.24	0.18	0.16		0.17
VC1147	0.22	0.22		0.22	0.19	0.13		0.16
VC1148	0.23	0.27	0.28	0.26	0.20	0.18		0.19
VC1149	0.29	0.25		0.27	0.19	0.21		0.20
VC1150	0.23	0.23		0.23	0.13	0.13		0.13
VC1151	0.31	0.26		0.28	0.21	0.21		0.21
VC1152	0.22	0.22		0.22	0.18	0.24		0.21
VC1153	0.18	0.19		0.18	0.15	0.14		0.14
VC1154	0.29	0.27		0.28	0.19	0.17		0.18
VC1155	0.22	0.23		0.22	0.13	0.14		0.13
VC1156	0.26	0.22		0.24	0.14	0.15	0.18	0.16
VC1158	0.18	0.18		0.18	0.18	0.15		0.17
VC1159	0.26	0.25		0.25	0.16	0.16		0.16
VC1160	0.18	0.22		0.20	0.18	0.16		0.17
VC1161	0.26	0.23		0.25	0.15	0.13		0.14
VC1162	0.28	0.23		0.25	0.10	0.17		0.13
VC1163	0.23	0.24		0.24	0.14	0.15		0.15
VC1164	0.23	0.23		0.23	0.10	0.11		0.11
VC1165	0.28	0.26		0.27	0.17	0.18		0.17
VC1166	0.18	0.25		0.22	0.14	0.14	0.11	0.13
VC1167	0.24	0.24		0.24	0.23	0.16	0.16	0.18
VC1169	0.28	0.26	0.25	0.26	0.19	0.16		0.17
VC1170	0.23	0.26		0.25	0.13	0.16		0.15
VC1171	0.25	0.23	0.22	0.23	0.19	0.19		0.19
VC1172	0.22	0.22	0.21	0.22	0.17	0.14		0.15
VC1173	0.26	0.27	0.28	0.27	0.15	0.16		0.16
VC1174	0.20	0.23		0.22	0.08	0.10		0.09
VC1175	0.23	0.22		0.23	0.22	0.18		0.20
VC1176	0.25	0.26		0.25	0.20	0.16		0.18
VC1177	0.23	0.21		0.22	0.20	0.17		0.18
VC1178	0.28	0.27	0.26	0.27	0.20	0.20		0.20
VC1179	0.26	0.27		0.26	0.19	0.18		0.18
VC1180	0.30	0.32	0.33	0.32	0.20	0.21		0.21
VC1181	0.25	0.28	0.28	0.27	0.22	0.21		0.22
VC1182	0.26	0.29	0.27	0.27	0.17	0.14		0.16
VC1183	0.15	0.17		0.16	0.14	0.14		0.14
VC1184	0.23	0.27		0.25	0.10	0.12		0.11

VC1185	0.25	0.27		0.26	0.13	0.17		0.15
VC1186	0.23	0.20		0.21	0.17	0.16		0.16
VC1187	0.26	0.31		0.29	0.22	0.20	0.22	0.21
VC1188	0.24	0.23		0.23	0.18	0.15		0.16
VC1189	0.24	0.26		0.25	0.18	0.21	0.20	0.20
VC1190	0.24	0.23		0.23	0.12	0.14		0.13
VC1191	0.26	0.26		0.26				
VC1192	0.23	0.28		0.26	0.13	0.14		0.14
VC1193	0.24	0.22		0.23	0.17	0.16		0.16
VC1194	0.18	0.19		0.19				
VC1195	0.32	0.29		0.30	0.13	0.14		0.13
VC1196	0.23	0.20		0.22	0.24	0.18	0.18	0.20
VC1197	0.26	0.26		0.26	0.19	0.19	0.20	0.19
VC1198	0.24	0.21		0.22	0.16	0.20		0.18
VC1199	0.26	0.29		0.28	0.20	0.19		0.20
VC1200	0.25	0.23		0.24	0.21	0.17		0.19
VC1201	0.26	0.29		0.27	0.25	0.19	0.18	0.21
VC1202	0.22	0.22	0.21	0.22	0.20	0.20		0.20
VC1203	0.19	0.18	0.19	0.18	0.11	0.13		0.12
VC1204	0.26	0.25		0.25	0.13	0.17	0.11	0.14
VC1205	0.27	0.26		0.27	0.21	0.19		0.20
VC1206	0.22	0.23	0.24	0.23	0.15	0.14		0.15
VC1207	0.24	0.25		0.24	0.19	0.17		0.18
VC1208	0.21	0.19		0.20	0.15	0.13		0.14
VC1209	0.25	0.25		0.25	0.18	0.18		0.18
VC1210	0.25	0.27	0.27	0.26	0.14	0.14		0.14
VC1211	0.30	0.28		0.29	0.22	0.24		0.23
VC1212	0.21	0.21		0.21	0.20	0.16		0.18
VC1213	0.26	0.25		0.26	0.19	0.17		0.18
VC1214	0.25	0.26		0.25	0.14	0.15		0.14
VC1215	0.26	0.27		0.27	0.16	0.16	0.14	0.15
VC1216	0.16	0.17		0.16	0.10	0.09		0.09
VC1217	0.29	0.28		0.28	0.14	0.14		0.14
VC1218	0.26	0.25		0.25	0.21	0.19	0.21	0.20
VC1219	0.23	0.21		0.22	0.14	0.16		0.15
VC1220	0.19	0.20	0.22	0.20	0.17	0.15		0.16
VC1221	0.28	0.22		0.25				
VC1222	0.26	0.24		0.25	0.13	0.14		0.13
VC1223	0.27	0.27		0.27	0.27	0.27	0.23	0.25
VC1224	0.30	0.32		0.31	0.24	0.25		0.24
VC1225	0.25	0.25		0.25	0.18	0.18	0.22	0.19
VC1226	0.18	0.19		0.19				
VC1227	0.22	0.20		0.21	0.15	0.16	0.14	0.15

VC1228	0.24	0.25		0.24	0.18	0.19	0.15	0.17
VC1229	0.27	0.26		0.26	0.25	0.23	0.25	0.24
VC1230	0.28	0.26		0.27	0.24	0.23		0.23
VC1231	0.22	0.22		0.22	0.15	0.13	0.14	0.14
VC1232	0.29	0.26		0.28	0.23	0.20		0.21
VC1233	0.26	0.30		0.28	0.21	0.20		0.20
VC1234	0.21	0.16		0.19	0.15	0.13		0.14
VC1235	0.31	0.33		0.32	0.21	0.20		0.20
VC1236	0.20	0.24		0.22	0.13	0.13		0.13
VC1237	0.24	0.26		0.25	0.12	0.14		0.13
VC1238	0.23	0.24		0.24	0.17	0.21		0.19
VC1239	0.28	0.26		0.27	0.14	0.19		0.17
VC1240	0.20	0.19		0.19				
VC1241	0.26	0.27		0.26	0.24	0.25		0.24
VC1242	0.25	0.23		0.24	0.17	0.18		0.17
VC1243	0.25	0.22		0.24	0.18	0.17		0.18
VC1244	0.34	0.36		0.35	0.20	0.18		0.19
VC1245	0.21	0.21		0.21	0.13	0.13	0.12	0.13
VC1246	0.27	0.26		0.26	0.19	0.14		0.17
VC1247	0.16	0.16		0.16	0.16	0.14		0.15
VC1248	0.33	0.37		0.35	0.18	0.18		0.18
VC1249	0.25	0.22		0.24	0.10	0.12		0.11
VC1250	0.25	0.22		0.24	0.14	0.16		0.15
VC1251	0.32	0.28		0.30	0.14	0.15	0.19	0.16
VC1252	0.26	0.26		0.26	0.15	0.14		0.14
VC1253	0.28	0.25		0.26				
VC1254	0.19	0.19		0.19	0.12	0.10	0.11	0.11
VC1255	0.24	0.23	0.25	0.24	0.19	0.13		0.16
VC1256	0.27	0.24		0.26	0.15	0.19		0.17
VC1257	0.15	0.18		0.16	0.16	0.17		0.17
VC1258	0.21	0.20		0.21	0.15	0.18		0.17
VC1259	0.38	0.28		0.33	0.20	0.18		0.19
VC1260	0.25	0.23		0.24	0.13	0.13		0.13
VC1261	0.32	0.31		0.31	0.17	0.15		0.16
VC1262	0.30	0.28		0.29	0.23	0.15		0.19
VC1263	0.27	0.31	0.30	0.29	0.16	0.17		0.17
VC1265	0.25	0.23		0.24	0.17	0.17		0.17
VC1266	0.21	0.24	0.19	0.21	0.12	0.17		0.15
VC1267	0.24	0.24	0.26	0.25	0.15	0.13		0.14
VC1268	0.23	0.24	0.25	0.24	0.17	0.13		0.15
VC1269	0.27	0.27	0.28	0.27	0.21	0.18		0.20
VC1270	0.23	0.23		0.23	0.18	0.19		0.18
VC1271	0.23	0.24	0.27	0.25	0.17	0.17		0.17

VC1272	0.24	0.24		0.24	0.15	0.15		0.15
VC1273	0.27	0.26		0.27	0.12	0.15		0.14
VC1274	0.25	0.28	0.24	0.25	0.25	0.16		0.21
VC1275	0.29	0.26	0.29	0.28	0.19	0.17		0.18
VC1276	0.25	0.27		0.26	0.21	0.20		0.21
VC1277	0.27	0.31	0.26	0.28	0.26	0.16		0.21
VC1278	0.30	0.28	0.27	0.28	0.24	0.17		0.20
VC1279	0.28	0.24	0.26	0.26	0.18	0.18		0.18
VC1280	0.28	0.27	0.28	0.28	0.21	0.12		0.16
VC1281					0.17	0.11	0.14	0.14
VC1282	0.23	0.29	0.29	0.27	0.19	0.19		0.19
VC1283					0.19	0.19	0.13	0.17
VC1284	0.23	0.27	0.21	0.24	0.20	0.19		0.19
VC1285	0.26	0.25	0.27	0.26	0.14	0.12		0.13
VC1286	0.27	0.29	0.28	0.28	0.18	0.17		0.17
VC1287	0.23	0.25		0.24	0.19	0.13	0.14	0.16
VC1288	0.25	0.24		0.24	0.24	0.21		0.22
VC1289	0.23	0.21	0.22	0.22	0.18	0.16		0.17
VC1290	0.17	0.20	0.23	0.20	0.17	0.19		0.18
VC1291	0.20	0.21	0.25	0.22	0.13	0.14		0.13
VC1292					0.18	0.16	0.17	0.17
VC1293	0.20	0.20		0.20	0.10	0.11		0.10
VC1294	0.25	0.25		0.25	0.17	0.19		0.18
VC1295	0.29	0.32		0.31	0.16	0.24		0.20
VC1296	0.26	0.27		0.27	0.14	0.12		0.13
VC1297	0.27	0.24	0.26	0.26	0.16	0.15		0.16
VC1298	0.26	0.24		0.25	0.20	0.22		0.21
VC1299	0.27	0.29		0.28	0.13	0.12		0.13
VC1300	0.20	0.19		0.20	0.12	0.10		0.11
VC1301	0.30	0.33		0.32	0.17	0.21		0.19
VC1302	0.24	0.28		0.26	0.19	0.14		0.16
VC1303	0.16	0.21		0.19	0.17	0.15		0.16
VC1304	0.22	0.23		0.23	0.12	0.15		0.13
VC1305	0.29	0.29		0.29	0.17	0.20		0.18
VC1306	0.23	0.27		0.25	0.20	0.20		0.20
VC1307	0.23	0.25		0.24	0.25	0.24	0.23	0.24
VC1308	0.25	0.27		0.26	0.15	0.16		0.15
VC1309	0.23	0.23		0.23	0.17	0.17		0.17
VC1310	0.26	0.25		0.26	0.15	0.11		0.13
VC1311	0.28	0.28		0.28	0.22	0.18		0.20
VC1312	0.17	0.15		0.16	0.18	0.16		0.17
VC1313	0.21	0.20		0.20	0.16	0.16		0.16
VC1314	0.29	0.28		0.28	0.13	0.17		0.15

VC1315	0.25	0.26		0.26	0.14	0.18		0.16
VC1316	0.24	0.29		0.27	0.10	0.13		0.11
VC1317	0.24	0.24		0.24	0.18	0.14		0.16
VC1319	0.27	0.25		0.26	0.15	0.20		0.18
VC1320	0.25	0.28	0.25	0.26	0.14	0.12		0.13
VC1321	0.34	0.32		0.33	0.23	0.21		0.22
VC1322	0.27	0.27		0.27	0.27	0.23	0.20	0.24
VC1323	0.22	0.23	0.25	0.23	0.17	0.16		0.16
VC1324	0.27	0.27		0.27	0.24	0.21	0.23	0.23
VC1325	0.19	0.18		0.19	0.13	0.10		0.11
VC1326	0.26	0.21		0.23	0.15	0.16		0.16
VC1327	0.25	0.26		0.26	0.13	0.14		0.13
VC1329	0.25	0.25		0.25	0.19	0.19		0.19
VC1330	0.28	0.27	0.24	0.26	0.26	0.26		0.26
VC1331	0.24	0.28		0.26	0.21	0.19		0.20
VC1332	0.31	0.31		0.31	0.25	0.27	0.27	0.26
VC1333	0.23	0.23		0.23	0.18	0.17		0.18
VC1334	0.26	0.30		0.28	0.14	0.14		0.14
VC1335	0.26	0.30	0.27	0.28	0.14	0.15		0.15
VC1336	0.23	0.24	0.23	0.23	0.19	0.17		0.18
VC1337	0.26	0.26	0.27	0.27	0.20	0.20		0.20
VC1338	0.22	0.24		0.23	0.15	0.21		0.18
VC1339	0.20	0.21	0.21	0.21	0.13	0.13		0.13
VC1340	0.28	0.34		0.31	0.17	0.16		0.16
VC1341	0.22	0.20		0.21	0.14	0.18		0.16
VC1342	0.27	0.29		0.28	0.14	0.14		0.14
VC1343	0.23	0.22		0.22	0.16	0.12		0.14
VC1344	0.23	0.24		0.23	0.15	0.16		0.15
VC1345	0.27	0.25		0.26	0.09	0.11		0.10
VC1346	0.25	0.26		0.26	0.19	0.18		0.19
VC1348	0.18	0.17		0.18	0.10	0.11		0.10
VC1349	0.23	0.24		0.23	0.18	0.22	0.22	0.21
VC1350	0.21	0.22		0.21	0.16	0.15		0.15
VC1351	0.34	0.29		0.31	0.21	0.24		0.22
VC1352	0.23	0.22		0.22	0.16	0.13		0.14
VC1353	0.22	0.21		0.22	0.17	0.19		0.18
VC1354	0.24	0.19		0.21	0.16	0.19		0.18
VC1355					0.15	0.17	0.18	0.17
VC1356	0.27	0.29	0.24	0.27	0.13	0.18		0.16
VC1357					0.17	0.14	0.15	0.15
VC1358					0.19	0.14	0.17	0.17
VC1359	0.29	0.30		0.30	0.14	0.13		0.13
VC1360	0.19	0.20		0.20	0.22	0.18		0.20

VC1361	0.30	0.32		0.31	0.23	0.21		0.22
VC1362	0.20	0.24		0.22	0.17	0.17		0.17
VC1363	0.23	0.21	0.23	0.22	0.15	0.14		0.15
VC1364	0.30	0.23	0.29	0.27	0.20	0.19		0.20
VC1365	0.27	0.23	0.26	0.25	0.19	0.15		0.17
VC1366	0.20	0.20		0.20	0.21	0.20		0.21
VC1367	0.29	0.26		0.27	0.16	0.19		0.17
VC1368	0.22	0.19	0.19	0.20	0.19	0.19		0.19
VC1369	0.27	0.25	0.24	0.26	0.19	0.19		0.19
VC1370	0.28	0.26	0.28	0.28	0.20	0.20		0.20
VC1371	0.22	0.19		0.21	0.19	0.16		0.17
VC1372	0.28	0.26	0.28	0.27	0.21	0.22		0.22
VC1373	0.23	0.23		0.23	0.18	0.21		0.19
VC1374	0.24	0.25		0.25	0.18	0.20		0.19
VC1375	0.26	0.28	0.26	0.27	0.22	0.22		0.22
VC1377	0.26	0.29		0.28	0.16	0.15		0.15
VC1378	0.19	0.20		0.19	0.15	0.15		0.15
VC1379	0.24	0.23	0.26	0.24	0.16	0.17		0.17
VC1380	0.18	0.19		0.18	0.15	0.18		0.16
VC1381	0.21	0.22		0.21	0.16	0.13		0.15
VC1382	0.27	0.23		0.25	0.18	0.14	0.17	0.16
VC1383	0.30	0.27		0.28	0.16	0.19		0.18
VC1384	0.30	0.31		0.31	0.22	0.21		0.22
VC1385	0.22	0.18		0.20	0.31	0.29	0.19	0.26
VC1386	0.24	0.26		0.25	0.15	0.14		0.14
VC1387	0.16	0.22		0.19	0.25	0.17	0.21	0.21
VC1388	0.23	0.25		0.24	0.14	0.10		0.12
VC1389	0.22	0.21		0.21	0.14	0.17		0.16
VC1390	0.20	0.19		0.20	0.16	0.16		0.16
VC1391	0.15	0.20		0.17	0.18	0.17		0.17
VC1392	0.25	0.26		0.26	0.18	0.18		0.18
VC1393	0.33	0.28		0.31	0.17	0.18		0.18
VC1394	0.28	0.29	0.29	0.28	0.12	0.10		0.11
VC1395	0.24	0.25		0.25	0.17	0.15		0.16
VC1396	0.24	0.24		0.24	0.19	0.19		0.19
VC1397	0.23	0.21		0.22	0.16	0.14		0.15
VC1398	0.24	0.23	0.24	0.23	0.12	0.16		0.14
VC1399	0.22	0.24		0.23	0.19	0.19		0.19
VC1400	0.22	0.23	0.21	0.22	0.16	0.14		0.15
VC1401	0.20	0.21		0.20	0.18	0.19		0.19
VC1402	0.19	0.20		0.20	0.15	0.16		0.15
VC1403	0.20	0.25		0.23	0.14	0.16		0.15
VC1404	0.31	0.26		0.29	0.17	0.17		0.17

VC1405	0.32	0.27		0.29	0.25	0.29		0.27
VC1406	0.25	0.25		0.25	0.12	0.14		0.13
VC1407	0.22	0.19		0.20	0.16	0.16		0.16
VC1408	0.25	0.18		0.22	0.19	0.25		0.22
VC1409	0.29	0.31		0.30	0.23	0.23		0.23
VC1410	0.24	0.26		0.25	0.18	0.17		0.17
VC1411	0.19	0.23		0.21	0.16	0.16		0.16
VC1412	0.23	0.23		0.23	0.21	0.21		0.21
VC1413	0.25	0.25		0.25	0.22	0.19		0.20
VC1414	0.27	0.22		0.25	0.15	0.17		0.16
VC1415	0.22	0.22	0.24	0.23	0.18	0.17		0.17
VC1416	0.19	0.20		0.20	0.16	0.14		0.15
VC1417	0.26	0.26		0.26	0.19	0.18		0.19
VC1418	0.24	0.21		0.23	0.11	0.09		0.10
VC1419	0.19	0.20		0.19	0.16	0.17		0.16
VC1420	0.30	0.29	0.32	0.30	0.19	0.18		0.18
VC1421	0.31	0.34		0.32	0.18	0.17		0.18
VC1422	0.29	0.32		0.30	0.12	0.14		0.13
VC1423	0.27	0.25		0.26	0.17	0.17		0.17
VC1424	0.22	0.20		0.21	0.17	0.18		0.17
VC1425	0.21	0.20		0.20	0.17	0.18	0.15	0.17
VC1426	0.26	0.24		0.25	0.23	0.22		0.23
VC1427	0.30	0.25	0.27	0.27	0.23	0.18		0.21
VC1428	0.23	0.23		0.23	0.21	0.19		0.20
VC1429	0.24	0.27	0.24	0.25	0.19	0.23		0.21
VC1430	0.20	0.20	0.17	0.19	0.09	0.09		0.09
VC1431	0.24	0.24		0.24	0.12	0.14		0.13
VC1432	0.22	0.27	0.27	0.25	0.17	0.16		0.16
VC1433	0.21	0.23		0.22	0.14	0.13		0.14
VC1434	0.20	0.19		0.19	0.20	0.10	0.12	0.14
VC1435	0.33	0.30		0.31	0.22	0.25		0.23
VC1436	0.29	0.24		0.27	0.18	0.17		0.17
VC1437	0.23	0.25		0.24	0.19	0.15		0.17
VC1438	0.28	0.28		0.28	0.19	0.20		0.20
VC1439	0.29	0.29		0.29	0.20	0.20		0.20
VC1440	0.29	0.27		0.28	0.14	0.17		0.15
VC1441	0.31	0.28		0.29	0.14	0.19		0.16
VC1442	0.28	0.24		0.26	0.19	0.18		0.19
VC1443	0.25	0.25		0.25	0.18	0.19		0.19
VC1444	0.23	0.23		0.23	0.15	0.15		0.15
VC1445	0.25	0.24		0.24	0.14	0.18		0.16
VC1446	0.23	0.19		0.21	0.20	0.17		0.19
VC1447	0.27	0.27		0.27	0.19	0.18		0.19

VC1448	0.32	0.26		0.29	0.23	0.21	0.22
VC1449	0.28	0.23		0.25	0.15	0.15	0.15
VC1450	0.23	0.22		0.22	0.15	0.16	0.15
VC1452	0.23	0.23		0.23	0.08	0.12	0.10
VC1453	0.18	0.16		0.17	0.18	0.17	0.18
VC1454	0.29	0.26		0.28	0.17	0.17	0.17
VC1455	0.25	0.28		0.26	0.15	0.18	0.16
VC1456	0.30	0.28		0.29	0.18	0.19	0.18
VC1457	0.23	0.23		0.23	0.19	0.18	0.19
VC1458	0.35	0.31		0.33	0.22	0.26	0.24
VC1459	0.22	0.23		0.23	0.18	0.25	0.22
VC1460	0.35	0.30		0.32	0.19	0.18	0.19
VC1461	0.29	0.36		0.33	0.23	0.27	0.25
VC1462	0.26	0.25		0.26	0.15	0.16	0.16
VC1463	0.22	0.25		0.24	0.16	0.20	0.18
VC1464	0.23	0.31		0.27	0.14	0.15	0.14
VC1465	0.18	0.20		0.19	0.13	0.13	0.13
VC1466	0.22	0.23		0.23	0.16	0.13	0.15
VC1467	0.28	0.24	0.26	0.26	0.29	0.20	0.25
VC1468	0.24	0.24	0.23	0.24	0.15	0.15	0.15
VC1469	0.30	0.26		0.28	0.17	0.14	0.16
VC1470	0.23	0.21		0.22	0.07	0.09	0.08
VC1471	0.27	0.32	0.26	0.28	0.15	0.15	0.15
VC1472	0.28	0.28		0.28	0.18	0.15	0.17
VC1473	0.26	0.26		0.26	0.18	0.19	0.19
VC1474	0.24	0.24	0.24	0.24	0.19	0.15	0.17
VC1475	0.26	0.24		0.25	0.14	0.13	0.13
VC1476	0.22	0.22		0.22	0.19	0.19	0.19
VC1477	0.23	0.28		0.26	0.14	0.16	0.15
VC1478	0.20	0.26		0.23	0.12	0.16	0.14
VC1479	0.27	0.28		0.27	0.19	0.16	0.17
VC1480	0.35	0.36	0.30	0.34	0.20	0.19	0.19
VC1481	0.22	0.27		0.24	0.14	0.19	0.17
VC1482	0.21	0.20		0.21	0.11	0.13	0.12
VC1483	0.21	0.22		0.21	0.14	0.16	0.15
VC1484	0.25	0.27		0.26	0.18	0.17	0.17
VC1485	0.27	0.29		0.28	0.19	0.19	0.19
VC1486	0.25	0.26		0.26	0.15	0.15	0.15
VC1487	0.26	0.27		0.26	0.17	0.14	0.15
VC1488	0.21	0.18		0.19	0.13	0.13	0.13
VC1489	0.29	0.26	0.25	0.27	0.11	0.12	0.12
VC1490	0.24	0.24		0.24	0.25	0.23	0.24
VC1491	0.20	0.21		0.20	0.20	0.18	0.19

VC1492	0.23	0.24		0.23	0.17	0.17	0.17	0.17
VC1493	0.28	0.27		0.27	0.18	0.20	0.18	0.19
VC1494	0.25	0.26		0.26	0.15	0.15		0.15
VC1495	0.24	0.24	0.25	0.24	0.22	0.23		0.22
VC1496	0.23	0.21		0.22	0.17	0.16		0.17
VC1497	0.30	0.27		0.29	0.17	0.14		0.16
VC1498	0.21	0.23		0.22	0.17	0.14	0.15	0.15
VC1499	0.33	0.39		0.36	0.23	0.14		0.18
VC1500	0.28	0.31		0.29	0.23	0.19		0.21
VC1501	0.28	0.29		0.28	0.17	0.14		0.16
VC1502	0.28	0.28		0.28	0.13	0.17		0.15
VC1503	0.24	0.25	0.26	0.25	0.15	0.15		0.15
VC1505	0.26	0.26	0.28	0.27	0.18	0.19		0.18
VC1506	0.25	0.20	0.25	0.24	0.14	0.15		0.15
VC1507	0.26	0.26	0.31	0.28	0.16	0.19		0.17
VC1508	0.22	0.21		0.21	0.19	0.20		0.19
VC1509	0.21	0.27	0.21	0.23	0.16	0.18		0.17
VC1510	0.26	0.32	0.27	0.28	0.21	0.17		0.19
VC1511	0.31	0.28	0.29	0.29	0.22	0.23		0.22
VC1512	0.27	0.23	0.26	0.26	0.14	0.16		0.15
VC1513	0.21	0.19		0.20	0.16	0.17		0.16
VC1514	0.21	0.22		0.21	0.16	0.15	0.14	0.15
VC1515	0.25	0.25		0.25	0.17	0.17		0.17
VC1516	0.25	0.26		0.25	0.21	0.19		0.20
VC1517	0.26	0.28		0.27	0.21	0.21		0.21
VC1518	0.22	0.21	0.23	0.22	0.17	0.17		0.17
VC1519	0.27	0.25	0.29	0.27	0.16	0.17		0.17
VC1520	0.20	0.24		0.22	0.16	0.10		0.13
VC1521	0.29	0.26		0.28	0.20	0.14		0.17
VC1523	0.24	0.23		0.23	0.13	0.15		0.14
VC1524	0.21	0.22	0.21	0.21	0.24	0.25		0.24
VC1525	0.27	0.25		0.26	0.20	0.18		0.19
VC1526	0.21	0.18	0.16	0.18	0.17	0.19		0.18
VC1527	0.23	0.21		0.22	0.12	0.15		0.13
VC1528	0.18	0.19	0.18	0.18	0.15	0.13		0.14
VC1529	0.26	0.23	0.23	0.24	0.17	0.17		0.17
VC1530	0.20	0.22	0.19	0.21	0.17	0.21		0.19
VC1531	0.17	0.17	0.18	0.17	0.12	0.13		0.12
VC1532	0.21	0.22		0.22	0.16	0.16		0.16
VC1533	0.24	0.23	0.22	0.23	0.12	0.14		0.13
VC1534	0.22	0.21	0.22	0.22	0.15	0.16		0.15
VC1535	0.26	0.25	0.27	0.26	0.20	0.23		0.21
VC1537	0.29	0.29	0.30	0.29	0.18	0.18		0.18

VC1538	0.23	0.21	0.21	0.22	0.15	0.17		0.16
VC1539	0.22	0.21	0.23	0.22	0.10	0.12		0.11
VC1540	0.27	0.25		0.26	0.20	0.20	0.18	0.20
VC1541	0.25	0.26	0.24	0.25	0.20	0.20		0.20
VC1542	0.23	0.25	0.26	0.24	0.16	0.18		0.17
VC1543	0.30	0.28		0.29	0.16	0.15		0.16
VC1544	0.25	0.27	0.28	0.27	0.18	0.16		0.17
VC1545	0.27	0.28		0.28	0.22	0.17		0.19
VC1546	0.31	0.29	0.31	0.30	0.19	0.21		0.20
VC1547	0.25	0.25	0.25	0.25	0.17	0.16		0.17
VC1548	0.21	0.23	0.22	0.22	0.17	0.24		0.20
VC1549	0.26	0.24		0.25	0.16	0.14		0.15
VC1550	0.28	0.28	0.31	0.29	0.16	0.15		0.16
VC1551	0.23	0.27		0.25	0.15	0.17		0.16
VC1552	0.21	0.20		0.21	0.13	0.13		0.13
VC1553	0.27	0.26		0.26	0.15	0.15		0.15
VC1554	0.30	0.33		0.31	0.14	0.13		0.14
VC1555	0.22	0.20		0.21	0.16	0.14		0.15
VC1556	0.22	0.23	0.23	0.23	0.09	0.12		0.10
VC1557	0.22	0.19	0.20	0.20	0.12	0.14		0.13
VC1558	0.24	0.21	0.23	0.23	0.14	0.14		0.14
VC1559	0.18	0.21		0.20	0.16	0.14		0.15
VC1560	0.24	0.20		0.22	0.14	0.17		0.16
VC1561	0.24	0.25		0.25	0.17	0.13		0.15
VC1562	0.24	0.23	0.24	0.24	0.21	0.14		0.18
VC1563	0.24	0.26		0.25	0.20	0.17		0.19
VC1565	0.23	0.23		0.23	0.20	0.19		0.19
VC1566	0.25	0.22		0.24	0.15	0.12		0.13
VC1567	0.18	0.22		0.20	0.19	0.19		0.19
VC1568	0.23	0.25		0.24	0.16	0.15		0.16
VC1569	0.23	0.24		0.23	0.15	0.17		0.16
VC1570	0.18	0.19		0.19	0.18	0.21		0.19
VC1571	0.28	0.28		0.28	0.27	0.26		0.27
VC1572	0.20	0.23		0.21	0.16	0.15	0.16	0.16
VC1573	0.32	0.28	0.28	0.29	0.14	0.13		0.14
VC1574	0.25	0.21		0.23	0.18	0.16		0.17
VC1575	0.21	0.20		0.20	0.15	0.13		0.14
VC1576	0.23	0.22		0.23	0.16	0.18		0.17
VC1577	0.21	0.20		0.20	0.13	0.14		0.13
VC1578	0.28	0.27		0.28	0.17	0.19		0.18
VC1579	0.20	0.20		0.20	0.15	0.20	0.17	0.17
VC1580	0.26	0.24		0.25	0.09	0.14		0.11
VC1581	0.26	0.26	0.27	0.26	0.17	0.20		0.18

VC1582	0.25	0.22		0.23	0.18	0.15		0.16
VC1583	0.13	0.19		0.16	0.11	0.12		0.12
VC1584	0.31	0.29		0.30	0.25	0.22		0.23
VC1585	0.32	0.28		0.30	0.25	0.20		0.23
VC1586	0.27	0.28		0.28	0.12	0.14	0.14	0.13
VC1587	0.20	0.24		0.22	0.19	0.18		0.18
VC1588	0.30	0.26		0.28	0.29	0.20		0.24
VC1589	0.30	0.21		0.26	0.15	0.14		0.14
VC1590	0.21	0.22	0.23	0.22	0.15	0.14		0.15
VC1591	0.23	0.23		0.23	0.15	0.16		0.15
VC1592	0.44	0.38		0.41	0.43	0.49		0.46
VC1593	0.28	0.30	0.33	0.30	0.20	0.19		0.19
VC1595	0.18	0.21		0.20	0.10	0.10		0.10
VC1596	0.19	0.23		0.21	0.17	0.19		0.18
VC1597	0.28	0.27		0.27	0.23	0.17		0.20
VC1598	0.24	0.26		0.25	0.16	0.16		0.16
VC1599	0.21	0.21		0.21	0.16	0.18		0.17
VC1600	0.22	0.23		0.23	0.23	0.22		0.22
VC1601	0.31	0.27		0.29	0.20	0.18		0.19
VC1602	0.21	0.25		0.23	0.13	0.16		0.14
VC1603	0.21	0.25		0.23	0.14	0.12		0.13
VC1604	0.30	0.30	0.33	0.31	0.21	0.20		0.20
VC1605	0.25	0.23	0.25	0.25	0.18	0.16		0.17
VC1606	0.19	0.21		0.20	0.12	0.09		0.11
VC1607	0.25	0.24		0.25	0.15	0.14	0.14	0.14
VC1608	0.27	0.27	0.28	0.27	0.23	0.30		0.26
VC1609	0.31	0.33	0.28	0.31	0.22	0.22		0.22
VC1610	0.23	0.21		0.22	0.18	0.19		0.19
VC1611	0.25	0.26	0.24	0.25	0.22	0.30		0.26
VC1612	0.28	0.29	0.30	0.29	0.16	0.17		0.17
VC1613					0.24	0.26	0.23	0.24
VC1614	0.31	0.30	0.29	0.30	0.16	0.14		0.15
VC1615	0.18	0.18	0.20	0.19	0.14	0.13		0.13
VC1616	0.25	0.27		0.26	0.16	0.14		0.15
VC1617	0.24	0.21	0.20	0.22	0.14	0.15		0.15
VC1618	0.31	0.29		0.30	0.18	0.19		0.19
VC1619	0.24	0.23	0.26	0.24	0.19	0.18		0.18
VC1621	0.22	0.22		0.22	0.14	0.15		0.14
VC1622	0.22	0.21		0.22	0.11	0.14		0.13
VC1623	0.25	0.23		0.24	0.15	0.15		0.15
VC1624	0.27	0.27		0.27	0.14	0.15		0.15
VC1625	0.25	0.20		0.22	0.18	0.15	0.14	0.16
VC1627	0.26	0.29		0.27	0.20	0.21		0.20

VC1628	0.20	0.19		0.20	0.19	0.17		0.18
VC1629	0.31	0.29		0.30	0.27	0.30		0.28
VC1630	0.26	0.25		0.26	0.15	0.13		0.14
VC1631	0.24	0.25		0.24	0.21	0.19		0.20
VC1632	0.24	0.23		0.23	0.12	0.13		0.13
VC1633	0.19	0.16		0.18	0.13	0.14		0.14
VC1634	0.28	0.28		0.28	0.17	0.19		0.18
VC1635	0.23	0.23		0.23	0.11	0.13		0.12
VC1636	0.25	0.24		0.24	0.13	0.20		0.16
VC1637	0.21	0.19		0.20	0.14	0.11		0.13
VC1638	0.29	0.26		0.28	0.13	0.15		0.14
VC1639	0.25	0.26		0.25	0.17	0.18		0.17
VC1640	0.24	0.30		0.27	0.20	0.21		0.21
VC1641	0.49	0.47		0.48	0.52	0.59		0.55
VC1642	0.28	0.30		0.29	0.12	0.14		0.13
VC1643	0.35	0.33		0.34	0.19	0.19		0.19
VC1644	0.27	0.24		0.25	0.18	0.20		0.19
VC1646	0.23	0.23		0.23	0.22	0.21	0.22	0.22
VC1647	0.20	0.22		0.21	0.14	0.14		0.14
VC1648	0.26	0.26		0.26	0.20	0.25		0.22
VC1649	0.28	0.22		0.25	0.19	0.26		0.22
VC1651	0.27	0.26		0.27	0.22	0.17		0.19
VC1652	0.55	0.60		0.58	0.24	0.25	0.23	0.24
VC1653	0.23	0.24		0.23	0.17	0.16		0.16
VC1654	0.21	0.25		0.23	0.14	0.13		0.13
VC1656	0.27	0.25		0.26	0.18	0.18		0.18
VC1657	0.21	0.22	0.26	0.23	0.17	0.18		0.17
VC1658	0.25	0.24		0.24	0.22	0.20		0.21
VC1659	0.28	0.27		0.28	0.18	0.22		0.20
VC1660	0.22	0.23		0.23	0.16	0.16		0.16
VC1661	0.23	0.22		0.22	0.12	0.12		0.12
VC1662	0.23	0.29		0.26	0.23	0.23		0.23
VC1663	0.23	0.18		0.21	0.16	0.14		0.15
VC1664	0.20	0.18		0.19	0.12	0.11		0.11
VC1665	0.27	0.29		0.28	0.24	0.20		0.22
VC1666	0.21	0.19		0.20	0.16	0.16		0.16
VC1667	0.24	0.25		0.25	0.19	0.21		0.20
VC1668	0.24	0.23		0.24	0.14	0.15		0.15
VC1669	0.30	0.33		0.32	0.20	0.18		0.19
VC1670	0.31	0.31		0.31	0.21	0.24		0.23
VC1671	0.24	0.23	0.24	0.23	0.16	0.17		0.17
VC1672	0.14	0.16	0.16	0.16	0.16	0.16		0.16
VC1673	0.26	0.24		0.25	0.16	0.15		0.16

VC1674	0.26	0.28	0.28	0.28	0.12	0.13		0.12
VC1675	0.29	0.29	0.29	0.29	0.15	0.19		0.17
VC1676	0.25	0.26	0.29	0.27	0.25	0.23		0.24
VC1677	0.29	0.30		0.29	0.22	0.17		0.19
VC1678	0.24	0.25	0.24	0.24	0.15	0.12		0.14
VC1679	0.27	0.29	0.28	0.28	0.19	0.20		0.20
VC1680	0.19	0.22		0.21	0.18	0.16		0.17
VC1681	0.24	0.22	0.24	0.23	0.17	0.15		0.16
VC1682	0.29	0.28	0.30	0.29	0.18	0.17		0.17
VC1683	0.28	0.25		0.27	0.16	0.18		0.17
VC1684	0.31	0.29	0.29	0.29	0.14	0.17		0.15
VC1685	0.24	0.25	0.26	0.25	0.12	0.16		0.14
VC1686	0.25	0.27	0.23	0.25	0.15	0.19		0.17
VC1687	0.15	0.16	0.16	0.16	0.12	0.13		0.12
VC1688	0.23	0.26		0.25	0.22	0.21		0.22
VC1689	0.25	0.26	0.25	0.25	0.17	0.21		0.19
VC1690	0.22	0.23		0.22	0.12	0.18		0.15
VC1691	0.19	0.18		0.19	0.15	0.16	0.18	0.16
VC1692	0.21	0.24		0.22	0.15	0.16		0.16
VC1693	0.20	0.24		0.22	0.17	0.13		0.15
VC1695	0.30	0.32	0.30	0.31	0.19	0.21		0.20
VC1696	0.27	0.25	0.26	0.26	0.13	0.14		0.13
VC1697	0.20	0.23	0.21	0.22	0.12	0.13		0.13
VC1698	0.22	0.23	0.24	0.23	0.13	0.13		0.13
VC1699	0.26	0.27		0.26	0.15	0.15		0.15
VC1700	0.22	0.24	0.24	0.23	0.18	0.17		0.18
VC1701	0.25	0.24	0.25	0.24	0.19	0.23		0.21
VC1702	0.23	0.23	0.25	0.23	0.19	0.21		0.20
VC1703	0.26	0.24	0.25	0.25	0.19	0.24		0.22
VC1704	0.20	0.19		0.20	0.15	0.15		0.15
VC1705	0.24	0.24		0.24	0.14	0.15		0.15
VC1706	0.21	0.25	0.23	0.23	0.13	0.14		0.13
VC1707	0.26	0.26	0.28	0.27	0.17	0.14		0.16
VC1708	0.29	0.30	0.31	0.30	0.24	0.26		0.25
VC1709	0.28	0.23		0.26	0.17	0.24		0.20
VC1710	0.62	0.69		0.65	0.61	0.55		0.58
VC1711	0.24	0.24		0.24	0.15	0.17		0.16
VC1712	0.21	0.20		0.21	0.19	0.21	0.18	0.19
VC1713	0.27	0.30		0.28	0.17	0.18	0.18	0.18
VC1714	0.19	0.22		0.20	0.15	0.16	0.10	0.14
VC1715	0.26	0.26		0.26	0.18	0.17	0.18	0.18
VC1716	0.25	0.26		0.25	0.15	0.20	0.21	0.19
VC1717	0.19	0.19		0.19	0.15	0.14		0.15

VC1718	0.23	0.24		0.24	0.18	0.17	0.18	0.18
VC1719	0.24	0.25		0.25	0.12	0.13	0.16	0.13
VC1720	0.21	0.21		0.21	0.12	0.13	0.17	0.14
VC1721	0.27	0.25		0.26	0.10	0.13	0.16	0.13
VC1722	0.23	0.24		0.23	0.14	0.16	0.17	0.15
VC1724	0.26	0.24		0.25	0.19	0.24		0.21
VC1725	0.28	0.29		0.29	0.23	0.22		0.23
VC1726	0.21	0.21		0.21	0.14	0.16	0.17	0.15
VC1727	0.21	0.20		0.20	0.15	0.17		0.16
VC1728	0.14	0.17		0.15	0.13	0.12		0.12
VC1729	0.21	0.24		0.23	0.20	0.16		0.18
VC1730	0.27	0.25		0.26	0.19	0.22	0.18	0.20
VC1731	0.32	0.27		0.29	0.21	0.19		0.20
VC1732	0.30	0.24		0.27	0.13	0.13		0.13
VC1733	0.22	0.21		0.21	0.13	0.16		0.15
VC1734	0.28	0.24		0.26	0.23	0.21		0.22
VC1735	0.21	0.18		0.19	0.15	0.16		0.16
VC1736	0.25	0.21		0.23	0.16	0.15		0.16
VC1737	0.23	0.24		0.23	0.19	0.17		0.18
VC1738	0.22	0.21		0.22	0.15	0.15		0.15
VC1740	0.28	0.27		0.27	0.22	0.21		0.21
VC1741	0.24	0.36		0.30	0.16	0.16		0.16
VC1742	0.25	0.25		0.25	0.18	0.18		0.18
VC1743	0.15	0.14		0.14	0.12	0.14		0.13
VC1744	0.23	0.27		0.25	0.16	0.16		0.16
VC1745	0.25	0.27		0.26	0.10	0.11		0.10
VC1746	0.21	0.19		0.20	0.08	0.10		0.09
VC1747	0.26	0.24		0.25	0.16	0.18		0.17
VC1748	0.28	0.27		0.27	0.21	0.20		0.21
VC1749	0.29	0.26		0.27	0.17	0.15		0.16
VC1750	0.25	0.25	0.24	0.25	0.20	0.21		0.20
VC1751	0.24	0.22		0.23	0.19	0.16		0.17
VC1752	0.28	0.28		0.28	0.24	0.20		0.22
VC1753	0.29	0.25		0.27	0.13	0.13		0.13
VC1754	0.31	0.29	0.28	0.29	0.16	0.15		0.16
VC1755	0.29	0.30		0.29	0.19	0.20		0.19
VC1756	0.20	0.22		0.21	0.16	0.15		0.15
VC1757	0.26	0.30		0.28	0.16	0.17		0.16
VC1758	0.23	0.23		0.23	0.14	0.15		0.15
VC1759	0.22	0.22		0.22	0.12	0.12		0.12
VC1760	0.21	0.22		0.22	0.16	0.16		0.16
VC1761	0.19	0.17		0.18	0.13	0.14		0.14
VC1762	0.27	0.24	0.25	0.25	0.18	0.19		0.18

VC1763	0.24	0.30		0.27	0.23	0.20		0.21
VC1764	0.28	0.28		0.28	0.21	0.22		0.21
VC1765	0.15	0.19		0.17	0.12	0.07	0.07	0.09
VC1766	0.30	0.26		0.28	0.12	0.13		0.13
VC1767	0.26	0.28		0.27	0.21	0.18		0.20
VC1768	0.27	0.24		0.25	0.14	0.14		0.14
VC1769	0.23	0.26		0.25	0.12	0.15		0.13
VC1770	0.23	0.23		0.23	0.20	0.17		0.18
VC1771	0.26	0.25		0.26	0.18	0.14	0.15	0.16
VC1772	0.36	0.36		0.36	0.18	0.20		0.19
VC1773	0.22	0.22		0.22	0.16	0.16		0.16
VC1774	0.27	0.23		0.25	0.18	0.17		0.18
VC1775	0.31	0.33	0.27	0.30	0.20	0.21		0.20
VC1776	0.17	0.16		0.17	0.14	0.12		0.13
VC1777	0.21	0.18		0.19	0.22	0.19		0.20
VC1778	0.23	0.27		0.25	0.16	0.15		0.16
VC1779	0.30	0.25		0.28	0.15	0.15		0.15
VC1780	0.18	0.20		0.19	0.21	0.20		0.20
VC1781	0.27	0.28		0.28	0.16	0.16		0.16
VC1782	0.21	0.27		0.24	0.15	0.16		0.16
VC1783	0.18	0.25		0.22	0.13	0.12		0.12
VC1784	0.22	0.23		0.22	0.11	0.19		0.15
VC1785	0.24	0.30		0.27	0.14	0.13		0.14
VC1786	0.23	0.23		0.23	0.12	0.16		0.14
VC1787	0.28	0.25		0.27	0.11	0.11		0.11
VC1788	0.23	0.24		0.23	0.20	0.18		0.19
VC1789	0.23	0.20		0.21	0.15	0.13		0.14
VC1790	0.26	0.25		0.26	0.19	0.18		0.18
VC1791	0.24	0.23		0.24	0.18	0.17		0.17
VC1792	0.22	0.23		0.22	0.12	0.13		0.12
VC1793	0.23	0.24		0.23	0.17	0.17		0.17
VC1794	0.24	0.23		0.23	0.13	0.13		0.13
VC1795	0.23	0.24		0.24	0.23	0.16		0.19
VC1796	0.30	0.26		0.28	0.11	0.13		0.12
VC1797	0.21	0.21		0.21	0.10	0.13		0.11
VC1798	0.24	0.22	0.22	0.23	0.13	0.16		0.14
VC1799	0.28	0.27		0.27	0.13	0.14		0.13
VC1800	0.29	0.29		0.29	0.18	0.21		0.20
VC1801	0.27	0.28		0.28	0.16	0.19		0.17
VC1802	0.27	0.26		0.26	0.17	0.18		0.17
VC1803	0.24	0.23		0.24	0.15	0.16		0.16
VC1804	0.21	0.22		0.22	0.14	0.13		0.13
VC1805	0.26	0.26		0.26	0.16	0.14		0.15

VC1806	0.14	0.16		0.15	0.11	0.10	0.09	0.10
VC1807	0.32	0.27		0.30	0.14	0.18	0.18	0.16
VC1808	0.24	0.23		0.24	0.13	0.13		0.13
VC1809	0.25	0.26		0.26	0.16	0.16		0.16
VC1810	0.23	0.24		0.24	0.20	0.17		0.18
VC1811	0.24	0.24		0.24	0.18	0.15		0.17
VC1812	0.24	0.24		0.24				
VC1813	0.22	0.25		0.23	0.14	0.15		0.14
VC1814	0.18	0.19		0.19	0.18	0.17		0.17
VC1815	0.27	0.27		0.27				
VC1816	0.21	0.18		0.19	0.11	0.12		0.12
VC1817	0.26	0.24		0.25	0.18	0.22		0.20
VC1818	0.27	0.28		0.28	0.13	0.14		0.14
VC1819	0.23	0.26		0.24	0.17	0.18		0.17
VC1820	0.21	0.25		0.23	0.21	0.16		0.18
VC1821	0.27	0.25		0.26	0.21	0.19		0.20
VC1822	0.23	0.23		0.23	0.21	0.18		0.20
VC1823	0.21	0.26		0.24	0.17	0.19	0.15	0.17
VC1824	0.23	0.25		0.24	0.18	0.18	0.14	0.17
VC1825	0.20	0.24		0.22	0.13	0.14	0.13	0.13
VC1826	0.29	0.29		0.29	0.14	0.15	0.17	0.15
VC1827	0.15	0.22		0.19	0.18	0.21		0.20
VC1828	0.22	0.23		0.22	0.21	0.18		0.20
VC1829	0.25	0.26		0.26	0.11	0.13		0.12
VC1830	0.27	0.30		0.28	0.21	0.16	0.13	0.17
VC1831	0.26	0.29		0.28	0.20	0.17	0.16	0.17
VC1832	0.24	0.23		0.23	0.13	0.09		0.11
VC1833	0.22	0.20		0.21	0.08	0.08		0.08
VC1834	0.30	0.26		0.28	0.10	0.12		0.11
VC1835	0.29	0.29		0.29	0.21	0.16		0.18
VC1836	0.27	0.29		0.28	0.17	0.16		0.16
VC1837	0.30	0.39		0.35	0.20	0.18	0.17	0.18
VC1838	0.25	0.27		0.26	0.20	0.14		0.17
VC1839	0.27	0.30		0.28	0.17	0.17		0.17
VC1840	0.25	0.26		0.25	0.18	0.15		0.17
VC1841	0.13	0.17		0.15	0.11	0.09	0.13	0.11
VC1842	0.27	0.28		0.28	0.13	0.19	0.16	0.16
VC1843	0.22	0.22	0.22	0.22	0.11	0.13		0.12
VC1844	0.23	0.24		0.24	0.25	0.27		0.26
VC1845	0.28	0.28		0.28	0.17	0.17	0.19	0.18
VC1846	0.20	0.21		0.20	0.12	0.19		0.15
VC1847	0.18	0.22		0.20				
VC1848	0.27	0.24		0.25	0.21	0.22		0.21

VC1849	0.15	0.17		0.16	0.17	0.13		0.15
VC1851	0.25	0.28		0.26	0.19	0.22		0.21
VC1852	0.23	0.22		0.23	0.13	0.15		0.14
VC1853	0.24	0.26		0.25	0.13	0.18		0.16
VC1854	0.17	0.19		0.18	0.22	0.22		0.22
VC1855	0.25	0.23		0.24	0.17	0.18		0.18
VC1856	0.29	0.29		0.29				
VC1857	0.29	0.29		0.29	0.17	0.13		0.15
VC1858	0.29	0.28		0.28	0.09	0.09	0.13	0.10
VC1859	0.27	0.30		0.28	0.15	0.17		0.16
VC1860	0.23	0.25		0.24	0.17	0.20	0.22	0.20
VC1861	0.26	0.27		0.27	0.12	0.13		0.12
VC1862	0.23	0.24		0.24	0.23	0.23	0.23	0.23
VC1863	0.22	0.25		0.23	0.19	0.18	0.21	0.19
VC1864	0.25	0.23		0.24				
VC1865	0.29	0.25		0.27				
VC1866	0.22	0.24		0.23	0.16	0.15		0.15
VC1868	0.20	0.22		0.21	0.19	0.15		0.17
VC1869	0.28	0.27		0.27				
VC1870	0.30	0.25		0.27	0.19	0.19	0.20	0.20
VC1871	0.21	0.23		0.22	0.13	0.16	0.15	0.15
VC1872	0.28	0.28		0.28	0.13	0.14		0.14
VC1873	0.16	0.16		0.16	0.12	0.13	0.15	0.13
VC1874	0.29	0.28		0.28	0.18	0.18	0.17	0.18
VC1875	0.22	0.21		0.21	0.14	0.15	0.12	0.14
VC1876	0.25	0.29		0.27	0.15	0.19		0.17
VC1877	0.22	0.23	0.25	0.24	0.21	0.18		0.19
VC1878	0.35	0.32		0.34	0.17	0.14		0.15
VC1879	0.31	0.28		0.30	0.21	0.17	0.21	0.19
VC1880	0.24	0.22		0.23	0.24	0.22	0.20	0.22
VC1881	0.14	0.17		0.15	0.14	0.13	0.15	0.14
VC1882	0.23	0.23	0.22	0.23	0.16	0.19		0.17
VC1883	0.24	0.27		0.25	0.16	0.18	0.17	0.17
VC1884	0.28	0.31		0.29	0.19	0.21	0.22	0.21
VC1885	0.21	0.22		0.21	0.17	0.18	0.16	0.17
VC1886	0.27	0.26		0.27	0.23	0.19		0.21
VC1887	0.26	0.25		0.25	0.18	0.16	0.20	0.18
VC1888	0.22	0.24		0.23	0.14	0.17		0.16
VC1889	0.25	0.24		0.25	0.16	0.16	0.15	0.16
VC1890	0.23	0.26		0.25	0.18	0.18	0.15	0.17
VC1891	0.26	0.24		0.25	0.15	0.18		0.17
VC1892	0.28	0.26		0.27	0.16	0.17		0.16
VC1893	0.22	0.24		0.23				

VC1894	0.29	0.27		0.28	0.17	0.13		0.15
VC1895	0.27	0.28		0.27	0.23	0.23		0.23
VC1896	0.22	0.21		0.22	0.18	0.21	0.19	0.20
VC1897	0.25	0.24		0.24	0.19	0.22		0.20
VC1898	0.24	0.25		0.24	0.17	0.19		0.18
VC1899	0.25	0.25		0.25	0.21	0.22		0.21
VC1900	0.31	0.31		0.31	0.16	0.16		0.16
VC1901	0.33	0.31	0.26	0.30	0.21	0.25		0.23
VC1902	0.31	0.28		0.29	0.21	0.22		0.22
VC1903	0.29	0.29		0.29	0.26	0.20		0.23
VC1904	0.22	0.22		0.22				
VC1905	0.22	0.23		0.23	0.14	0.14		0.14
VC1906	0.24	0.25		0.25	0.21	0.19		0.20
VC1907	0.26	0.26	0.26	0.26	0.16	0.13		0.14
VC1908	0.20	0.23		0.22	0.18	0.14		0.16
VC1909	0.30	0.27		0.29	0.15	0.18		0.16
VC1910	0.22	0.25		0.23	0.12	0.15	0.14	0.14
VC1911	0.25	0.27		0.26	0.18	0.13	0.14	0.15
VC1912	0.28	0.32	0.34	0.31	0.21	0.20		0.20
VC1913	0.38	0.30		0.34	0.18	0.15	0.17	0.17
VC1914					0.15	0.18	0.20	0.18
VC1915	0.30	0.27	0.27	0.28	0.20	0.17		0.18
VC1916	0.31	0.29	0.30	0.30	0.18	0.19		0.18
VC1917	0.32	0.34		0.33	0.20	0.20	0.17	0.19
VC1918	0.27	0.27	0.27	0.27	0.17	0.17		0.17
VC1919	0.25	0.27	0.26	0.26	0.13	0.15		0.14
VC1920	0.22	0.22		0.22	0.17	0.14		0.16
VC1921	0.23	0.28	0.23	0.25	0.16	0.14		0.15
VC1922	0.17	0.21		0.19	0.21	0.15	0.14	0.17
VC1923	0.22	0.28		0.25	0.13	0.22	0.20	0.18
VC1924					0.19	0.20	0.23	0.20
VC1925	0.28	0.31		0.29	0.27	0.24	0.23	0.25
VC1926	0.24	0.27	0.27	0.26	0.14	0.13		0.14
VC1927	0.39	0.34	0.34	0.35	0.20	0.21		0.20
VC1928	0.21	0.16	0.15	0.17	0.17	0.15		0.16
VC1929	0.22	0.21		0.22	0.21	0.19		0.20
VC1930	0.28	0.27		0.27	0.22	0.18		0.20
VC1931	0.19	0.17		0.18	0.11	0.08		0.09
VC1932	0.33	0.28		0.31	0.19	0.15		0.17
VC1933	0.29	0.31	0.28	0.29	0.16	0.16		0.16
VC1934	0.25	0.23		0.24	0.20	0.17		0.19
VC1935	0.29	0.37		0.33	0.17	0.17		0.17
VC1936	0.23	0.21	0.21	0.21	0.23	0.21		0.22

VC1937	0.28	0.27	0.30	0.28	0.16	0.16		0.16
VC1938	0.23	0.24		0.24	0.19	0.20	0.20	0.20
VC1939	0.26	0.28		0.27	0.17	0.19		0.18
VC1940	0.26	0.24	0.25	0.25	0.14	0.14		0.14
VC1941	0.27	0.28	0.30	0.28	0.22	0.21		0.21
VC1942	0.22	0.23	0.22	0.22	0.16	0.18		0.17
VC1943	0.22	0.21		0.22	0.18	0.20		0.19
VC1944	0.25	0.27	0.26	0.26	0.14	0.15		0.15
VC1945	0.21	0.25		0.23	0.14	0.13		0.14
VC1946	0.25	0.26		0.25	0.18	0.21		0.20
VC1947	0.25	0.26	0.26	0.26	0.21	0.19		0.20
VC1948	0.22	0.24		0.23	0.12	0.13		0.13
VC1949	0.24	0.24		0.24	0.17	0.17		0.17
VC1950	0.26	0.25		0.26	0.22	0.22		0.22
VC1951	0.28	0.29		0.28	0.19	0.18		0.18
VC1952	0.21	0.26		0.24				
VC1953	0.29	0.30		0.30	0.21	0.24		0.22
VC1954	0.26	0.25		0.26	0.19	0.21		0.20
VC1955	0.39	0.32		0.35	0.19	0.17		0.18
VC1956	0.28	0.28		0.28	0.22	0.27		0.24
VC1957	0.25	0.27		0.26	0.18	0.18		0.18
VC1958					0.14	0.09	0.11	0.11
VC1959	0.25	0.25		0.25	0.18	0.16		0.17
VC1960	0.19	0.21		0.20				
VC1961	0.28	0.26		0.27	0.17	0.19		0.18
VC1962	0.26	0.25	0.27	0.26	0.18	0.19		0.19
VC1963	0.26	0.22	0.26	0.24	0.16	0.16		0.16
VC1964	0.29	0.29	0.28	0.29	0.20	0.18		0.19
VC1965	0.23	0.21	0.22	0.22	0.14	0.15		0.14
VC1966	0.30	0.28		0.29	0.20	0.17		0.19
VC1967	0.24	0.23		0.24	0.21	0.18		0.20
VC1968	0.26	0.25	0.25	0.26	0.17	0.15		0.16
VC1969	0.18	0.20		0.19	0.16	0.13	0.12	0.14
VC1970	0.26	0.27		0.27	0.19	0.22		0.20
VC1971	0.21	0.22		0.22	0.11	0.12		0.12
VC1972	0.19	0.20		0.19	0.15	0.19		0.17
VC1973	0.24	0.23	0.22	0.23	0.14	0.12		0.13
VC1974	0.23	0.19	0.25	0.22	0.15	0.15		0.15
VC1975	0.21	0.21	0.20	0.21	0.13	0.15		0.14
VC1976	0.24	0.23		0.23	0.18	0.18		0.18
VC1977	0.21	0.27	0.24	0.24	0.15	0.16		0.16
VC1978	0.29	0.28	0.24	0.27	0.26	0.24		0.25
VC1979	0.27	0.27	0.27	0.27	0.18	0.17		0.17

VC1980	0.23	0.24	0.25	0.24	0.17	0.17		0.17
VC1981	0.29	0.29	0.33	0.30	0.25	0.25		0.25
VC1982					0.15	0.17	0.16	0.16
VC1983	0.20	0.21	0.20	0.20	0.12	0.11		0.11
VC1984					0.19	0.22	0.22	0.21
VC1985	0.31	0.28	0.24	0.28	0.16	0.18		0.17
VC1986	0.19	0.17	0.17	0.17	0.16	0.13		0.15
VC1987	0.27	0.26	0.26	0.27	0.23	0.22		0.22
VC1988					0.13	0.22	0.12	0.16
VC1989	0.23	0.21	0.19	0.21	0.12	0.12		0.12
VC1990	0.23	0.25		0.24	0.19	0.15		0.17
VC1991	0.22	0.22	0.22	0.22	0.19	0.20		0.19
VC1992	0.25	0.26	0.24	0.25	0.16	0.16		0.16
VC1993	0.24	0.23		0.23	0.14	0.16		0.15
VC1994	0.27	0.30		0.29	0.27	0.22		0.24
VC1995	0.20	0.22	0.22	0.21	0.15	0.14		0.15
VC1996					0.21	0.23	0.29	0.24
VC1997	0.24	0.23		0.24	0.21	0.24		0.22
VC1998	0.25	0.19	0.23	0.22	0.12	0.13		0.12
VC1999	0.25	0.23	0.25	0.24	0.13	0.11		0.12
VC2000	0.24	0.25		0.24	0.13	0.12		0.13
VC2001	0.27	0.26		0.26	0.15	0.15		0.15
VC2002	0.21	0.22		0.22	0.14	0.17		0.16
VC2003	0.25	0.24	0.24	0.25	0.12	0.11		0.12
VC2004	0.25	0.23		0.24	0.19	0.23		0.21
VC2005	0.24	0.26	0.23	0.24	0.15	0.18		0.16
VC2006	0.24	0.22		0.23	0.14	0.22		0.18
VC2007	0.24	0.21		0.22	0.12	0.13		0.12
VC2008	0.21	0.23		0.22	0.18	0.18		0.18
VC2009	0.20	0.23		0.21	0.14	0.16		0.15
VC2010	0.28	0.28		0.28	0.19	0.21		0.20
VC2011	0.33	0.32		0.32	0.17	0.21		0.19
VC2012	0.28	0.30		0.29	0.16	0.16		0.16
VC2013	0.28	0.25		0.27	0.22	0.22		0.22
VC2014	0.28	0.29	0.24	0.27	0.12	0.11		0.11
VC2015	0.26	0.24		0.25	0.14	0.14		0.14
VC2016	0.24	0.23	0.24	0.24	0.14	0.18		0.16
VC2017	0.22	0.21	0.22	0.22	0.17	0.20		0.18
VC2018	0.25	0.27		0.26	0.12	0.08		0.10
VC2019	0.23	0.25		0.24	0.20	0.18		0.19
VC2021	0.22	0.22		0.22	0.13	0.14		0.13
VC2022	0.21	0.17		0.19	0.09	0.15		0.12
VC2023	0.21	0.18		0.19	0.13	0.13		0.13

VC2024	0.27	0.27		0.27	0.17	0.14		0.16
VC2025	0.27	0.25		0.26	0.17	0.15		0.16
VC2026	0.23	0.24		0.24	0.17	0.15		0.16
VC2027	0.27	0.25		0.26	0.16	0.13		0.15
VC2028	0.21	0.23		0.22	0.16	0.17		0.17
VC2029	0.21	0.23		0.22	0.20	0.18		0.19
VC2030	0.27	0.25		0.26	0.14	0.11	0.12	0.12
VC2031	0.24	0.27		0.25	0.20	0.20		0.20
VC2032	0.34	0.31		0.32	0.21	0.25		0.23
VC2033	0.27	0.28		0.27	0.16	0.17		0.17
VC2034	0.18	0.17		0.18	0.23	0.25	0.15	0.21
VC2035	0.35	0.32		0.34	0.18	0.20		0.19
VC2036	0.24	0.24		0.24	0.23	0.24		0.23
VC2037	0.26	0.25		0.26	0.22	0.21		0.21
VC2039	0.21	0.24		0.22	0.21	0.18		0.19
VC2040	0.23	0.23		0.23	0.19	0.16		0.18
VC2041	0.23	0.25		0.24	0.18	0.16		0.17
VC2042	0.23	0.22		0.23	0.20	0.23		0.22
VC2043	0.26	0.28		0.27	0.21	0.17		0.19
VC2044	0.24	0.24		0.24	0.18	0.16		0.17
VC2045	0.20	0.23		0.21	0.10	0.14		0.12
VC2046	0.27	0.24		0.25	0.16	0.12		0.14
VC2047	0.24	0.23		0.24	0.15	0.16		0.16
VC2048	0.26	0.30		0.28	0.22	0.24		0.23
VC2049	0.27	0.31		0.29	0.25	0.21		0.23
VC2051	0.27	0.27		0.27	0.17	0.17		0.17
VC2052	0.35	0.29		0.32	0.26	0.18		0.22
VC2053	0.26	0.28		0.27	0.21	0.21		0.21
VC2054	0.24	0.25		0.25	0.16	0.16		0.16
VC2055	0.28	0.29		0.28	0.16	0.15		0.16
VC2056	0.26	0.25		0.26	0.18	0.20		0.19
VC2057	0.20	0.20		0.20	0.13	0.12		0.12
VC2058	0.23	0.27		0.25	0.18	0.23		0.21
VC2059	0.23	0.22		0.22	0.14	0.14		0.14
VC2060	0.26	0.27		0.27	0.16	0.18		0.17
VC2061	0.27	0.28		0.28	0.13	0.16		0.15
VC2062	0.24	0.20		0.22	0.16	0.20		0.18
VC2063	0.22	0.21		0.22	0.16	0.15		0.15
VC2064	0.21	0.22		0.21	0.14	0.16		0.15
VC2065	0.22	0.24	0.22	0.22	0.17	0.11		0.14
VC2066	0.17	0.20		0.19	0.10	0.13		0.12
VC2067	0.20	0.18		0.19	0.19	0.22		0.20
VC2068	0.19	0.17		0.18	0.12	0.13		0.13

VC2069	0.23	0.26		0.25	0.20	0.15		0.18
VC2070	0.20	0.18		0.19	0.10	0.14		0.12
VC2071	0.23	0.24	0.24	0.24	0.13	0.15		0.14
VC2072	0.21	0.22		0.21	0.15	0.14		0.15
VC2073	0.24	0.22		0.23	0.20	0.13		0.17
VC2074	0.22	0.24		0.23	0.14	0.13		0.14
VC2075	0.25	0.26	0.25	0.25	0.13	0.14		0.14
VC2076					0.10	0.09	0.13	0.11
VC2077	0.24	0.28		0.26	0.19	0.18		0.19
VC2078	0.24	0.27		0.25				
VC2079	0.21	0.21		0.21	0.18	0.18		0.18
VC2080	0.21	0.21		0.21	0.17	0.14		0.16
VC2081					0.14	0.15	0.15	0.15
VC2082					0.13	0.17	0.18	0.16
VC2083	0.33	0.29	0.26	0.29	0.22	0.20		0.21
VC2084	0.20	0.23	0.23	0.22	0.13	0.14		0.14
VC2085	0.26	0.23	0.26	0.25	0.22	0.22		0.22
VC2086	0.25	0.24	0.25	0.25	0.14	0.19		0.16
VC2087	0.24	0.21		0.22	0.11	0.12	0.15	0.13
VC2088	0.17	0.16	0.18	0.17	0.19	0.15		0.17
VC2089	0.22	0.23	0.22	0.23	0.20	0.20		0.20
VC2090	0.21	0.24		0.22	0.15	0.12	0.11	0.13
VC2091	0.33	0.28		0.30	0.20	0.16		0.18
VC2092	0.23	0.22	0.24	0.23	0.21	0.22		0.21
VC2093					0.15	0.15	0.17	0.16
VC2094	0.26	0.21	0.19	0.22	0.21	0.21		0.21
VC2095	0.20	0.23	0.23	0.22	0.15	0.15		0.15
VC2096	0.28	0.29	0.34	0.30	0.19	0.21		0.20
VC2097	0.21	0.26	0.25	0.24	0.17	0.12		0.15
VC2098	0.24	0.26	0.24	0.25	0.13	0.11		0.12
VC2099	0.23	0.25	0.25	0.24	0.12	0.16		0.14
VC2100	0.34	0.32	0.30	0.32	0.19	0.18		0.19
VC2101	0.22	0.23	0.26	0.24	0.18	0.19		0.18
VC2102	0.23	0.22	0.23	0.22	0.16	0.15		0.15
VC2103	0.24	0.25		0.25	0.14	0.13		0.13
VC2105	0.27	0.27	0.26	0.27	0.13	0.19		0.16
VC2106	0.24	0.24	0.23	0.23	0.19	0.19		0.19
VC2107	0.20	0.20		0.20	0.16	0.14		0.15
VC2108	0.25	0.24		0.24	0.10	0.12		0.11
VC2109	0.25	0.29		0.27	0.18	0.19	0.16	0.18
VC2110	0.24	0.21		0.23	0.17	0.15		0.16
VC2111	0.25	0.27	0.27	0.26	0.12	0.13		0.12
VC2112	0.27	0.26		0.27	0.17	0.18	0.18	0.18

VC2113	0.23	0.22	0.22	0.23	0.12	0.15		0.14
VC2114	0.26	0.24	0.24	0.25	0.18	0.22		0.20
VC2115	0.20	0.20		0.20	0.19	0.17	0.19	0.19
VC2116	0.24	0.23		0.23	0.15	0.17		0.16
VC2117	0.27	0.25		0.26	0.21	0.19		0.20
VC2118	0.26	0.26		0.26	0.12	0.16		0.14
VC2119	0.23	0.22		0.22	0.16	0.17	0.17	0.17
VC2120	0.28	0.30		0.29	0.13	0.16	0.15	0.15
VC2121	0.27	0.25		0.26	0.16	0.19	0.20	0.18
VC2122	0.23	0.22	0.27	0.24	0.25	0.25		0.25
VC2123	0.27	0.24		0.26	0.22	0.19		0.20
VC2124	0.24	0.28		0.26	0.29	0.24	0.22	0.25
VC2125	0.22	0.21	0.27	0.23	0.14	0.12		0.13
VC2126	0.30	0.29		0.29	0.15	0.16		0.16
VC2127	0.26	0.25	0.23	0.25	0.20	0.16		0.18
VC2128	0.26	0.26		0.26	0.19	0.18		0.18
VC2129	0.23	0.21		0.22	0.13	0.10	0.12	0.12
VC2130	0.21	0.23		0.22	0.20	0.17	0.14	0.17
VC2131	0.23	0.23		0.23	0.16	0.20	0.17	0.18
VC2132	0.21	0.22		0.22	0.08	0.12	0.10	0.10
VC2133	0.32	0.33		0.33	0.20	0.22		0.21
VC2134	0.33	0.31		0.32	0.14	0.12	0.22	0.16
VC2135	0.31	0.27	0.23	0.27	0.16	0.18		0.17
VC2136	0.25	0.24	0.24	0.24	0.15	0.13		0.14
VC2137	0.27	0.26		0.27	0.14	0.28	0.24	0.22
VC2138	0.25	0.26		0.26	0.17	0.18		0.17
VC2139	0.18	0.24		0.21	0.14	0.11	0.13	0.13
VC2140	0.25	0.22		0.23	0.16	0.19	0.18	0.18
VC2141	0.20	0.18		0.19	0.13	0.11	0.10	0.11
VC2142	0.22	0.24		0.23	0.16	0.17		0.17
VC2143	0.26	0.28	0.25	0.26	0.16	0.16		0.16
VC2144	0.25	0.27	0.26	0.26	0.14	0.14		0.14
VC2145	0.21	0.23	0.19	0.21	0.10	0.09		0.10
VC2146	0.25	0.26		0.26	0.14	0.16	0.17	0.16
VC2147	0.30	0.27	0.26	0.28	0.21	0.21		0.21
VC2148	0.21	0.20		0.21	0.18	0.19	0.20	0.19
VC2149	0.29	0.22	0.23	0.25	0.22	0.21		0.21
VC2150	0.25	0.26	0.25	0.25	0.16	0.16		0.16
VC2151	0.22	0.23		0.23	0.16	0.20	0.18	0.18
VC2152	0.19	0.18	0.22	0.20	0.12	0.11		0.12
VC2153	0.18	0.21		0.20	0.12	0.13		0.13
VC2154	0.25	0.23		0.24	0.16	0.18	0.19	0.17
VC2155	0.27	0.27		0.27	0.13	0.14		0.14

VC2156	0.23	0.23		0.23	0.09	0.12	0.12	0.11
VC2157	0.21	0.22		0.22	0.14	0.14		0.14
VC2158	0.28	0.27		0.27	0.16	0.18		0.17
VC2159	0.26	0.22	0.25	0.24	0.14	0.14		0.14
VC2160	0.24	0.26	0.25	0.25	0.13	0.15		0.14
VC2161	0.26	0.25	0.26	0.26	0.17	0.17		0.17
VC2162	0.30	0.25	0.29	0.28	0.20	0.19		0.20
VC2163	0.25	0.22		0.24	0.12	0.12		0.12
VC2164	0.24	0.25		0.25	0.15	0.19		0.17
VC2165	0.27	0.20	0.20	0.22	0.11	0.12		0.11
VC2166	0.31	0.25	0.25	0.27	0.18	0.18		0.18
VC2167	0.17	0.18	0.19	0.18	0.14	0.14		0.14
VC2168	0.24	0.23		0.23	0.13	0.10		0.12
VC2169	0.29	0.28		0.29	0.17	0.22		0.20
VC2170	0.29	0.27		0.28	0.16	0.16		0.16
VC2171	0.17	0.22	0.18	0.19	0.17	0.17		0.17
VC2172	0.27	0.21	0.20	0.23	0.14	0.15		0.14
VC2174	0.54	0.60		0.57	0.36	0.37		0.36
VC2175	0.20	0.24	0.21	0.21	0.16	0.15		0.15
VC2176	0.18	0.18	0.18	0.18	0.20	0.17		0.19
VC2177	0.29	0.27	0.27	0.28	0.16	0.18		0.17
VC2178					0.19	0.20	0.21	0.20
VC2179	0.19	0.20	0.20	0.20	0.16	0.12		0.14
VC2180	0.31	0.30		0.31	0.15	0.14		0.14
VC2181	0.25	0.24		0.25	0.13	0.15		0.14
VC2182	0.23	0.24		0.24	0.17	0.16		0.16
VC2183	0.24	0.21	0.25	0.23	0.14	0.15		0.15
VC2184	0.25	0.25		0.25	0.19	0.20		0.20
VC2185	0.21	0.21		0.21	0.18	0.21		0.20
VC2186					0.14	0.14	0.13	0.14
VC2187	0.22	0.24		0.23	0.20	0.15		0.17
VC2188	0.24	0.23		0.24	0.14	0.18		0.16
VC2189	0.25	0.28		0.26	0.17	0.17		0.17
VC2190	0.22	0.16		0.19	0.14	0.14		0.14
VC2191	0.24	0.22		0.23	0.16	0.16		0.16
VC2192	0.23	0.22		0.23	0.19	0.17		0.18
VC2193	0.23	0.24		0.23	0.19	0.17		0.18
VC2194	0.26	0.26		0.26	0.19	0.23		0.21
VC2195	0.27	0.25		0.26	0.15	0.19		0.17
VC2196	0.22	0.24		0.23	0.16	0.14		0.15
VC2197	0.23	0.22		0.23	0.14	0.13		0.13
VC2198	0.23	0.22		0.22	0.19	0.17		0.18
VC2199	0.22	0.20		0.21	0.15	0.17		0.16

VC2200	0.24	0.25		0.24	0.19	0.17		0.18
VC2201	0.22	0.20		0.21	0.14	0.18		0.16
VC2202	0.21	0.24		0.23	0.14	0.14		0.14
VC2203	0.25	0.27		0.26	0.25	0.19		0.22
VC2204					0.17	0.15	0.13	0.15
VC2205	0.23	0.24		0.23	0.15	0.16		0.15
VC2206	0.26	0.25		0.25	0.13	0.13		0.13
VC2207	0.20	0.26		0.23	0.27	0.20		0.23
VC2208	0.26	0.23		0.25	0.17	0.17		0.17
VC2209	0.21	0.19		0.20	0.13	0.16	0.12	0.14
VC2210	0.19	0.21		0.20	0.12	0.13		0.13
VC2211	0.26	0.25		0.25	0.15	0.18		0.17
VC2212	0.23	0.27		0.25	0.18	0.13		0.15
VC2213	0.24	0.23		0.23	0.15	0.14		0.14
VC2214	0.24	0.24	0.24	0.24	0.14	0.13		0.14
VC2215	0.23	0.22		0.23	0.19	0.19		0.19
VC2216	0.25	0.24		0.24	0.15	0.19		0.17
VC2217	0.21	0.22		0.21	0.22	0.20		0.21
VC2218	0.21	0.22		0.22	0.10	0.14		0.12
VC2219	0.23	0.23		0.23	0.20	0.15		0.18
VC2220	0.26	0.19		0.23	0.18	0.19		0.18
VC2221	0.30	0.29		0.30	0.18	0.18		0.18
VC2222	0.21	0.24		0.22	0.16	0.18	0.18	0.17
VC2223	0.26	0.28		0.27	0.18	0.12	0.18	0.16
VC2224	0.28	0.22		0.25	0.20	0.23		0.21
VC2225	0.23	0.22		0.23	0.13	0.14		0.14
VC2226	0.23	0.23		0.23	0.15	0.15		0.15
VC2227	0.22	0.25		0.24	0.22	0.26	0.20	0.23
VC2228	0.25	0.25		0.25	0.19	0.22		0.21
VC2229	0.26	0.23		0.25	0.13	0.14		0.14
VC2230	0.23	0.21		0.22	0.17	0.14	0.16	0.16
VC2231	0.36	0.37		0.36	0.15	0.15		0.15
VC2232	0.27	0.26		0.27	0.23	0.21	0.22	0.22
VC2233	0.24	0.24	0.25	0.24	0.12	0.16		0.14
VC2234	0.24	0.24		0.24	0.11	0.12	0.13	0.12
VC2235	0.24	0.23		0.24	0.13	0.15	0.16	0.14
VC2236	0.28	0.30		0.29	0.13	0.17		0.15
VC2237	0.24	0.31		0.27	0.16	0.15		0.15
VC2238	0.28	0.29		0.29	0.19	0.19	0.18	0.19
VC2239	0.25	0.24		0.25	0.10	0.15	0.15	0.13
VC2240	0.18	0.19		0.19	0.15	0.15	0.16	0.15
VC2241	0.23	0.28		0.26	0.21	0.20		0.21
VC2242	0.19	0.21		0.20	0.18	0.19		0.18

VC2243	0.20	0.17		0.18	0.20	0.19		0.19
VC2244	0.26	0.24		0.25	0.11	0.15	0.17	0.14
VC2245	0.28	0.26		0.27	0.16	0.10		0.13
VC2246	0.08	0.13		0.11	0.12	0.11		0.12
VC2247	0.28	0.28		0.28	0.12	0.16		0.14
VC2248	0.27	0.27		0.27				
VC2249	0.24	0.23		0.24	0.13	0.14	0.15	0.14
VC2250	0.35	0.22		0.28	0.22	0.22		0.22
VC2252	0.29	0.27		0.28	0.24	0.17		0.20
VC2253	0.25	0.28		0.27	0.27	0.21	0.20	0.23
VC2254	0.22	0.22		0.22	0.21	0.17		0.19
VC2255	0.23	0.25	0.25	0.24	0.19	0.17		0.18
VC2256	0.27	0.28		0.28	0.16	0.18		0.17
VC2258	0.27	0.22		0.25	0.19	0.19	0.18	0.19
VC2259	0.21	0.23		0.22	0.13	0.13		0.13
VC2260	0.23	0.23	0.23	0.23	0.13	0.17		0.15
VC2261	0.22	0.25		0.24	0.14	0.15		0.14
VC2262	0.22	0.24		0.23	0.14	0.16		0.15
VC2263	0.26	0.28		0.27	0.14	0.19	0.17	0.16
VC2264	0.23	0.23	0.24	0.23	0.13	0.11		0.12
VC2265	0.24	0.28		0.26	0.20	0.20		0.20
VC2266	0.31	0.31		0.31	0.17	0.16		0.16
VC2267	0.28	0.24		0.26	0.13	0.17		0.15
VC2268	0.28	0.29		0.29	0.18	0.12		0.15
VC2269	0.25	0.24	0.25	0.25	0.18	0.17		0.18
VC2270	0.22	0.26		0.24	0.16	0.16		0.16
VC2271	0.22	0.23	0.24	0.23	0.20	0.19		0.19
VC2272	0.21	0.21		0.21	0.11	0.13		0.12
VC2273	0.21	0.19		0.20	0.16	0.16		0.16
VC2274	0.26	0.25	0.26	0.26	0.17	0.15		0.16
VC2275	0.27	0.27	0.24	0.26	0.13	0.16		0.14
VC2276	0.25	0.23		0.24	0.19	0.18		0.19
VC2277	0.29	0.30		0.30	0.24	0.28		0.26
VC2278	0.31	0.33		0.32	0.24	0.20		0.22
VC2279	0.24	0.25		0.24	0.23	0.20		0.21
VC2280	0.29	0.28	0.25	0.27	0.14	0.18		0.16
VC2281	0.29	0.25		0.27	0.15	0.14		0.15
VC2282	0.23	0.26		0.25	0.20	0.15	0.17	0.18
VC2283	0.27	0.29		0.28	0.21	0.17		0.19
VC2284	0.24	0.24		0.24	0.20	0.18		0.19
VC2285	0.24	0.17		0.21	0.20	0.16		0.18
VC2286	0.27	0.27		0.27	0.15	0.16		0.15
VC2287	0.27	0.28		0.27	0.17	0.15		0.16

VC2288	0.26	0.27	0.26	0.19	0.17	0.16	0.18
VC2289	0.22	0.28	0.25	0.30	0.29		0.29
VC2290	0.30	0.28	0.29	0.26	0.21		0.24
VC2291	0.22	0.23	0.23	0.24	0.27	0.26	0.26
VC2292	0.32	0.30	0.31				
VC2293	0.26	0.26	0.26	0.23	0.20		0.22
VC2294	0.25	0.28	0.27	0.19	0.21		0.20
VC2295	0.26	0.25	0.25	0.19	0.17		0.18
VC2296	0.25	0.23	0.24	0.14	0.16		0.15
VC2297	0.27	0.29	0.28				
VC2298	0.19	0.23	0.21	0.20	0.17		0.19
VC2299	0.21	0.21	0.21	0.20	0.14	0.16	0.16
VC2300	0.25	0.22	0.24	0.22	0.21		0.21
VC2301	0.24	0.23	0.23	0.16	0.15	0.13	0.15
VC2302	0.27	0.27	0.27	0.18	0.21		0.20
VC2303	0.24	0.22	0.23	0.11	0.21		0.16
VC2304	0.30	0.31	0.31	0.19	0.25		0.22
VC2305	0.26	0.25	0.26	0.21	0.22		0.22
VC2306	0.28	0.30	0.29	0.19	0.15	0.19	0.18
VC2307	0.24	0.25	0.24	0.11	0.14		0.12
VC2308	0.19	0.21	0.20	0.14	0.16		0.15
VC2309	0.24	0.23	0.24				
VC2310	0.31	0.32	0.31	0.18	0.20	0.19	0.19
VC2311	0.24	0.23	0.23	0.15	0.15		0.15
VC2312	0.18	0.18	0.18	0.15	0.14		0.15
VC2313	0.24	0.24	0.24	0.20	0.16		0.18
VC2314	0.26	0.25	0.26	0.15	0.19		0.17
VC2315	0.27	0.26	0.26	0.18	0.18	0.17	0.18
VC2316	0.28	0.27	0.27	0.17	0.18		0.18
VC2317	0.19	0.21	0.20	0.25	0.22	0.19	0.22
VC2318	0.24	0.25	0.25	0.21	0.19	0.21	0.20
VC2319	0.27	0.30	0.29	0.22	0.18		0.20
VC2320	0.27	0.25	0.26	0.17	0.17		0.17
VC2321	0.27	0.29	0.28	0.12	0.11	0.16	0.13
VC2322	0.23	0.23	0.23	0.16	0.13	0.17	0.16
VC2323	0.23	0.21	0.22	0.15	0.21		0.18
VC2324	0.28	0.24	0.26	0.16	0.15		0.15
VC2325	0.26	0.28	0.27	0.29	0.25		0.27
VC2326	0.23	0.23	0.23	0.16	0.13		0.14
VC2327	0.25	0.27	0.26	0.15	0.15	0.17	0.16
VC2328	0.19	0.21	0.20	0.17	0.17		0.17
VC2329	0.20	0.22	0.21	0.13	0.14		0.14
VC2330	0.26	0.28	0.27				

VC2331	0.26	0.24		0.25	0.22	0.23	0.19	0.21
VC2332	0.23	0.26		0.25	0.18	0.15		0.16
VC2333	0.26	0.27		0.26	0.17	0.20		0.18
VC2334	0.19	0.20		0.20	0.11	0.10		0.11
VC2335	0.22	0.21		0.21	0.14	0.13		0.13
VC2336	0.23	0.22		0.22	0.13	0.12		0.13
VC2337	0.29	0.30		0.29	0.18	0.16		0.17
VC2338	0.24	0.27		0.26	0.12	0.17	0.18	0.16
VC2339	0.22	0.23		0.23	0.24	0.21		0.23
VC2340	0.27	0.26		0.27	0.16	0.14		0.15
VC2341	0.29	0.30		0.30	0.15	0.13		0.14
VC2342	0.22	0.22		0.22	0.17	0.15		0.16
VC2343	0.26	0.27		0.26	0.17	0.17		0.17
VC2344	0.22	0.23		0.23	0.14	0.15		0.15
VC2345	0.25	0.28		0.27				
VC2346	0.24	0.24		0.24				
VC2347	0.20	0.19		0.20				
VC2348	0.19	0.17		0.18	0.19	0.17		0.18
VC2349	0.23	0.25		0.24	0.16	0.15		0.16
VC2350	0.29	0.27		0.28	0.17	0.19	0.19	0.19
VC2351	0.27	0.25		0.26	0.12	0.12		0.12
VC2352	0.22	0.22		0.22	0.15	0.13		0.14
VC2353	0.25	0.26		0.26	0.16	0.17	0.16	0.17
VC2354	0.25	0.28		0.26	0.18	0.19		0.18
VC2355	0.32	0.23		0.28	0.16	0.15	0.15	0.15
VC2356	0.33	0.27		0.30	0.23	0.30	0.28	0.27
VC2357	0.15	0.23		0.19	0.15	0.13		0.14
VC2358	0.29	0.30	0.26	0.29	0.18	0.17		0.18
VC2359	0.20	0.22		0.21	0.13	0.14		0.14
VC2360	0.23	0.22		0.22	0.19	0.18		0.18
VC2361	0.28	0.25		0.26	0.15	0.16	0.15	0.15
VC2362	0.27	0.25		0.26	0.17	0.16	0.17	0.17
VC2363	0.24	0.26		0.25	0.18	0.17	0.16	0.17
VC2364	0.25	0.24		0.25	0.18	0.16		0.17
VC2364.1	0.21	0.20		0.21	0.14	0.16		0.15
VC2365	0.21	0.21		0.21	0.18	0.18	0.17	0.18
VC2366	0.25	0.27		0.26	0.13	0.15		0.14
VC2367	0.27	0.23		0.25	0.14	0.14	0.14	0.14
VC2368	0.16	0.18		0.17	0.12	0.14	0.14	0.13
VC2369	0.28	0.26		0.27	0.18	0.17		0.18
VC2370	0.24	0.23		0.24	0.25	0.24	0.28	0.26
VC2371	0.25	0.24		0.24	0.18	0.17		0.18
VC2372	0.26	0.27		0.26	0.17	0.18		0.18

VC2373	0.26	0.25		0.26	0.19	0.22	0.19	0.20
VC2374	0.29	0.29		0.29	0.11	0.13		0.12
VC2376	0.26	0.26		0.26	0.18	0.19	0.17	0.18
VC2377	0.28	0.25		0.27	0.23	0.15	0.15	0.18
VC2378	0.27	0.24		0.26	0.16	0.16		0.16
VC2379	0.26	0.30		0.28	0.19	0.18		0.18
VC2380	0.35	0.28		0.31	0.22	0.23		0.22
VC2381	0.29	0.30		0.30	0.20	0.21		0.20
VC2382	0.33	0.30		0.31	0.22	0.24		0.23
VC2383	0.23	0.22		0.23	0.14	0.16		0.15
VC2384	0.24	0.22		0.23	0.22	0.21		0.21
VC2385	0.26	0.27		0.27	0.17	0.18		0.18
VC2386	0.23	0.22		0.23	0.16	0.16	0.18	0.17
VC2387	0.27	0.29		0.28	0.16	0.16		0.16
VC2388	0.31	0.27		0.29	0.21	0.19		0.20
VC2389	0.25	0.23		0.24	0.10	0.11	0.12	0.11
VC2390	0.28	0.31	0.27	0.29	0.18	0.19		0.18
VC2391	0.29	0.25		0.27	0.20	0.18		0.19
VC2392	0.17	0.17		0.17	0.20	0.17		0.19
VC2393	0.21	0.25		0.23				
VC2394	0.19	0.20		0.20	0.15	0.18		0.16
VC2395	0.25	0.25		0.25	0.17	0.17		0.17
VC2396	0.23	0.26		0.24				
VC2397	0.23	0.24	0.22	0.23	0.10	0.11		0.11
VC2398	0.25	0.27	0.28	0.27	0.19	0.19		0.19
VC2399	0.31	0.30		0.30	0.14	0.18		0.16
VC2400	0.26	0.09	0.26	0.20	0.19	0.20		0.20
VC2401	0.26	0.27		0.27	0.18	0.20		0.19
VC2402	0.26	0.26	0.26	0.26	0.20	0.21		0.21
VC2403	0.21	0.20		0.21				
VC2404	0.32	0.30		0.31	0.25	0.20	0.21	0.22
VC2405	0.22	0.24		0.23	0.18	0.20	0.17	0.18
VC2406	0.28	0.26		0.27	0.15	0.19		0.17
VC2408	0.23	0.25		0.24	0.20	0.17	0.22	0.20
VC2409	0.25	0.24		0.24	0.21	0.22		0.22
VC2410	0.26	0.24		0.25	0.13	0.18		0.16
VC2411	0.24	0.25		0.24	0.13	0.17		0.15
VC2412	0.26	0.28	0.28	0.28	0.15	0.14		0.15
VC2414	0.26	0.27		0.27	0.19	0.17		0.18
VC2415	0.26	0.26		0.26	0.17	0.18		0.17
VC2416	0.24	0.23		0.24	0.16	0.16	0.16	0.16
VC2417	0.19	0.21		0.20	0.12	0.15		0.13
VC2419	0.25	0.23		0.24	0.10	0.11		0.10

VC2420	0.25	0.26		0.26				
VC2421	0.17	0.22		0.19	0.15	0.15		0.15
VC2422	0.26	0.25		0.25				
VC2423	0.27	0.26		0.26	0.15	0.16		0.16
VC2424	0.20	0.18		0.19	0.17	0.16		0.17
VC2425	0.31	0.29		0.30	0.14	0.12	0.14	0.14
VC2426	0.30	0.33		0.32	0.29	0.22		0.26
VC2427	0.30	0.24		0.27	0.16	0.17		0.16
VC2428	0.24	0.27		0.25	0.14	0.13		0.14
VC2429	0.19	0.17		0.18	0.09	0.14	0.14	0.13
VC2430	0.28	0.27		0.28	0.13	0.16		0.14
VC2431	0.25	0.27		0.26	0.16	0.18		0.17
VC2432	0.22	0.25		0.24	0.14	0.14		0.14
VC2433	0.25	0.24		0.24	0.16	0.17		0.16
VC2434	0.35	0.31		0.33	0.20	0.19		0.20
VC2435	0.24	0.25		0.25	0.12	0.19		0.15
VC2436	0.32	0.27		0.29	0.18	0.17		0.17
VC2437	0.22	0.25		0.24	0.18	0.19	0.17	0.18
VC2438	0.24	0.21		0.23	0.19	0.18		0.19
VC2439	0.22	0.25		0.24	0.16	0.16		0.16
VC2440	0.22	0.25		0.23	0.26	0.27	0.24	0.26
VC2441	0.26	0.24		0.25	0.17	0.17		0.17
VC2442	0.25	0.24		0.25	0.18	0.17		0.18
VC2443	0.29	0.27		0.28	0.17	0.25		0.21
VC2444	0.25	0.27		0.26	0.26	0.24	0.27	0.26
VC2445	0.27	0.29		0.28	0.17	0.24	0.25	0.22
VC2446	0.16	0.16		0.16	0.10	0.13	0.16	0.13
VC2447	0.25	0.26		0.25	0.16	0.17		0.16
VC2448	0.19	0.20	0.20	0.20	0.17	0.14		0.16
VC2449	0.27	0.25		0.26	0.31	0.27	0.28	0.29
VC2450	0.25	0.27		0.26	0.15	0.19		0.17
VC2451	0.25	0.27		0.26	0.20	0.20		0.20
VC2452	0.24	0.27		0.25	0.19	0.20	0.19	0.19
VC2453	0.25	0.22		0.23	0.13	0.16		0.14
VC2454	0.27	0.26		0.27				
VC2455	0.27	0.27		0.27	0.21	0.21	0.21	0.21
VC2456	0.23	0.24		0.23	0.25	0.22		0.23
VC2457	0.28	0.25	0.27	0.27	0.11	0.12		0.12
VC2458	0.19	0.18		0.18	0.10	0.13		0.11
VC2459	0.36	0.34	0.38	0.36	0.15	0.14		0.14
VC2460	0.26	0.23		0.24	0.20	0.18	0.17	0.18
VC2461	0.22	0.22	0.19	0.21	0.24	0.23		0.23
VC2462	0.32	0.31	0.25	0.30	0.24	0.27		0.26

VC2463	0.21	0.22		0.22				
VC2464	0.23	0.27	0.24	0.25	0.19	0.17		0.18
VC2465	0.30	0.32	0.28	0.30	0.19	0.23		0.21
VC2466	0.26	0.32	0.26	0.28	0.23	0.19		0.21
VC2467	0.22	0.22		0.22	0.21	0.23		0.22
VC2468	0.23	0.23		0.23	0.12	0.15		0.13
VC2469	0.21	0.22		0.21	0.17	0.17		0.17
VC2470	0.29	0.28		0.28	0.24	0.21		0.23
VC2471					0.16	0.18	0.13	0.16
VC2472	0.23	0.22		0.22	0.15	0.15	0.18	0.16
VC2473					0.20	0.18	0.16	0.18
VC2474	0.22	0.22		0.22	0.11	0.14		0.13
VC2475	0.30	0.29		0.29	0.16	0.14		0.15
VC2476	0.25	0.24		0.25	0.11	0.11		0.11
VC2478	0.26	0.24		0.25	0.19	0.16		0.18
VC2479	0.22	0.22		0.22	0.17	0.19		0.18
VC2480	0.22	0.17		0.19	0.15	0.13		0.14
VC2481	0.28	0.27		0.28	0.15	0.15		0.15
VC2482	0.29	0.28		0.28	0.25	0.27		0.26
VC2483	0.21	0.22		0.22	0.19	0.19		0.19
VC2484	0.24	0.21		0.22	0.20	0.19		0.19
VC2485	0.26	0.26		0.26	0.12	0.14		0.13
VC2486	0.23	0.25		0.24	0.13	0.12		0.12
VC2487	0.31	0.29		0.30	0.14	0.16		0.15
VC2488	0.09	0.12		0.11	0.19	0.20		0.20
VC2489	0.29	0.28		0.29	0.13	0.15		0.14
VC2490	0.24	0.21		0.22	0.14	0.13		0.14
VC2491	0.26	0.25		0.25	0.20	0.17		0.19
VC2492	0.20	0.19		0.20	0.09	0.09		0.09
VC2493	0.21	0.25		0.23	0.13	0.16		0.15
VC2494	0.30	0.31		0.31	0.19	0.18		0.19
VC2495	0.27	0.25		0.26	0.13	0.13		0.13
VC2496	0.22	0.23		0.22	0.15	0.14		0.15
VC2497	0.23	0.21		0.22	0.14	0.16		0.15
VC2498	0.27	0.28		0.28	0.12	0.11		0.12
VC2499	0.26	0.24		0.25	0.12	0.14		0.13
VC2500	0.24	0.28	0.25	0.26	0.15	0.15		0.15
VC2501	0.28	0.26		0.27	0.16	0.15		0.16
VC2502	0.26	0.23		0.24	0.15	0.15		0.15
VC2503	0.27	0.27		0.27	0.20	0.17		0.18
VC2504	0.23	0.24	0.21	0.22	0.15	0.15		0.15
VC2505	0.26	0.28	0.26	0.27	0.19	0.16		0.18
VC2506	0.25	0.25		0.25	0.17	0.13		0.15

VC2507	0.24	0.26		0.25	0.15	0.14		0.15
VC2508	0.23	0.24	0.23	0.23	0.17	0.18		0.17
VC2509	0.30	0.27		0.28	0.21	0.21		0.21
VC2511	0.22	0.24	0.20	0.22	0.15	0.15		0.15
VC2512	0.21	0.22		0.22	0.14	0.13		0.14
VC2513	0.36	0.34		0.35	0.18	0.15		0.17
VC2514	0.17	0.16		0.16	0.14	0.18		0.16
VC2515	0.29	0.26		0.28	0.12	0.14		0.13
VC2516	0.21	0.22		0.22	0.12	0.12		0.12
VC2517	0.28	0.25		0.26	0.13	0.12		0.13
VC2518	0.22	0.21	0.22	0.22	0.16	0.16		0.16
VC2519	0.32	0.34		0.33	0.17	0.21		0.19
VC2520	0.20	0.20	0.21	0.20	0.15	0.15		0.15
VC2521	0.23	0.25		0.24	0.14	0.11		0.13
VC2522	0.30	0.31	0.29	0.30	0.22	0.21		0.21
VC2523	0.23	0.24	0.23	0.23	0.13	0.20		0.17
VC2524	0.29	0.25		0.27	0.14	0.14		0.14
VC2525	0.28	0.25		0.27	0.19	0.20		0.20
VC2527	0.20	0.22		0.21	0.21	0.24		0.22
VC2528					0.16	0.15	0.15	0.15
VC2529	0.21	0.23		0.22	0.12	0.15		0.14
VC2530					0.17	0.14	0.13	0.15
VC2531	0.22	0.25		0.24	0.19	0.15		0.17
VC2532	0.23	0.22		0.22	0.16	0.15		0.16
VC2534	0.25	0.26		0.26	0.24	0.21		0.23
VC2535	0.23	0.22		0.23	0.19	0.20		0.19
VC2536					0.14	0.17	0.13	0.15
VC2537	0.22	0.26		0.24	0.15	0.20		0.18
VC2538	0.36	0.36		0.36	0.23	0.25		0.24
VC2539	0.24	0.23		0.23	0.17	0.15		0.16
VC2540	0.22	0.23		0.22	0.15	0.20		0.17
VC2541	0.26	0.24		0.25	0.20	0.13		0.17
VC2542	0.23	0.24		0.24	0.22	0.19		0.20
VC2543	0.27	0.34		0.30	0.20	0.19		0.19
VC2544	0.26	0.29		0.27	0.20	0.15		0.18
VC2545	0.23	0.23		0.23	0.17	0.15		0.16
VC2546					0.11	0.14	0.16	0.14
VC2547	0.24	0.19		0.21	0.17	0.17	0.12	0.15
VC2548	0.26	0.27		0.26	0.16	0.15		0.16
VC2549	0.14	0.13		0.14	0.16	0.13		0.14
VC2551					0.21	0.22	0.21	0.21
VC2552	0.25	0.23		0.24	0.17	0.20		0.18
VC2553					0.14	0.10	0.13	0.12

VC2554	0.31	0.29		0.30	0.24	0.21		0.23
VC2555	0.26	0.26		0.26	0.22	0.22		0.22
VC2557	0.20	0.20		0.20	0.19	0.22		0.20
VC2558	0.25	0.24		0.24	0.19	0.20		0.19
VC2559	0.22	0.24		0.23	0.19	0.19		0.19
VC2560	0.22	0.23		0.22	0.15	0.14		0.14
VC2561	0.22	0.23	0.23	0.23	0.13	0.13		0.13
VC2562	0.24	0.25		0.25	0.15	0.11	0.11	0.12
VC2563	0.27	0.26		0.26	0.19	0.18		0.18
VC2564	0.19	0.21		0.20	0.16	0.14		0.15
VC2565	0.26	0.23		0.25	0.15	0.16		0.16
VC2566	0.29	0.30		0.29	0.17	0.17		0.17
VC2567	0.26	0.26		0.26	0.20	0.19		0.20
VC2568	0.25	0.21	0.23	0.23	0.13	0.12		0.12
VC2569	0.27	0.29	0.27	0.27	0.17	0.15		0.16
VC2570	0.24	0.23		0.24	0.14	0.15		0.15
VC2571	0.24	0.24		0.24	0.18	0.19	0.17	0.18
VC2572	0.21	0.28	0.23	0.24	0.11	0.12		0.11
VC2573	0.22	0.22	0.24	0.23	0.12	0.15		0.14
VC2574	0.23	0.23		0.23	0.16	0.16		0.16
VC2575	0.24	0.25		0.24	0.21	0.21	0.21	0.21
VC2576	0.24	0.25	0.27	0.25	0.15	0.16		0.15
VC2577	0.22	0.23		0.22	0.09	0.12		0.11
VC2578	0.24	0.26		0.25	0.18	0.17	0.25	0.20
VC2579	0.22	0.21		0.22	0.17	0.19		0.18
VC2580	0.22	0.27	0.22	0.24	0.14	0.15		0.14
VC2581	0.24	0.23		0.23	0.22	0.20		0.21
VC2582	0.23	0.23		0.23	0.15	0.15		0.15
VC2583	0.18	0.19	0.21	0.19	0.12	0.12		0.12
VC2584	0.23	0.21	0.25	0.23	0.16	0.22		0.19
VC2585	0.20	0.21	0.20	0.21	0.15	0.13		0.14
VC2586	0.18	0.19		0.19	0.19	0.16		0.18
VC2587	0.25	0.27		0.26	0.18	0.15	0.22	0.18
VC2588	0.23	0.22		0.22	0.20	0.18		0.19
VC2589	0.25	0.26	0.28	0.27	0.15	0.15		0.15
VC2590	0.22	0.23		0.23	0.19	0.20		0.19
VC2591	0.20	0.22		0.21	0.18	0.18		0.18
VC2592	0.23	0.22		0.23	0.15	0.15		0.15
VC2593	0.18	0.23		0.20	0.08	0.10		0.09
VC2594	0.22	0.22		0.22	0.15	0.15		0.15
VC2595	0.24	0.24	0.26	0.25	0.18	0.16		0.17
VC2596	0.21	0.22		0.22	0.16	0.18		0.17
VC2597	0.26	0.27	0.28	0.27	0.16	0.15		0.15

VC2598	0.23	0.24		0.23	0.18	0.14		0.16
VC2599	0.21	0.19		0.20	0.13	0.15		0.14
VC2600	0.27	0.29		0.28	0.18	0.21		0.19
VC2601	0.23	0.23	0.28	0.24	0.27	0.27		0.27
VC2602	0.20	0.21		0.21	0.21	0.19		0.20
VC2603	0.20	0.22		0.21	0.19	0.14		0.16
VC2604	0.23	0.24		0.23	0.17	0.13		0.15
VC2605	0.25	0.23		0.24	0.20	0.11		0.15
VC2606	0.23	0.26		0.25	0.15	0.16		0.15
VC2607	0.18	0.17	0.16	0.17	0.14	0.14		0.14
VC2608	0.19	0.20		0.19	0.19	0.20		0.20
VC2609	0.22	0.22		0.22	0.17	0.15		0.16
VC2610	0.26	0.25		0.25	0.15	0.19		0.17
VC2611	0.24	0.26		0.25	0.22	0.21	0.15	0.19
VC2612	0.20	0.22		0.21	0.14	0.13		0.14
VC2613	0.24	0.22	0.26	0.24	0.16	0.16		0.16
VC2614	0.18	0.19		0.19	0.19	0.20		0.20
VC2615	0.22	0.19	0.24	0.22	0.14	0.13		0.14
VC2616	0.19	0.21		0.20	0.19	0.18		0.19
VC2617	0.17	0.16	0.17	0.16	0.16	0.14		0.15
VC2618	0.24	0.23		0.24	0.12	0.11		0.11
VC2619	0.22	0.22	0.22	0.22	0.15	0.14		0.14
VC2620	0.27	0.28		0.27	0.18	0.20		0.19
VC2621	0.18	0.16		0.17	0.07	0.06		0.07
VC2622	0.26	0.29		0.28	0.15	0.16		0.15
VC2623	0.24	0.22		0.23	0.17	0.16		0.16
VC2624	0.31	0.28		0.29	0.17	0.17		0.17
VC2625	0.22	0.20		0.21	0.15	0.17		0.16
VC2626	0.22	0.21	0.25	0.23	0.17	0.19		0.18
VC2627	0.24	0.27		0.26	0.21	0.22		0.21
VC2628	0.25	0.21		0.23	0.17	0.14		0.16
VC2629	0.23	0.24		0.24	0.16	0.16		0.16
VC2631	0.22	0.21		0.21	0.14	0.13		0.13
VC2632	0.29	0.20		0.25	0.19	0.28		0.23
VC2633	0.28	0.28		0.28	0.25	0.23		0.24
VC2634	0.21	0.21		0.21	0.15	0.16		0.15
VC2635	0.24	0.28		0.26	0.15	0.15		0.15
VC2636	0.24	0.28		0.26	0.18	0.14		0.16
VC2637	0.17	0.19		0.18	0.19	0.17		0.18
VC2638	0.24	0.27		0.25	0.13	0.14		0.14
VC2639	0.26	0.23		0.25	0.21	0.19		0.20
VC2640	0.24	0.23		0.23	0.19	0.16		0.18
VC2641	0.16	0.14		0.15	0.20	0.16		0.18

VC2642	0.24	0.25		0.24	0.17	0.16		0.17
VC2643	0.24	0.19		0.22	0.17	0.20		0.18
VC2644	0.25	0.24	0.26	0.25	0.17	0.17		0.17
VC2645	0.23	0.22		0.22	0.14	0.15		0.14
VC2646	0.25	0.28		0.27	0.19	0.20		0.20
VC2647	0.27	0.23	0.24	0.24	0.13	0.18		0.16
VC2648	0.27	0.25		0.26	0.16	0.17		0.16
VC2649	0.26	0.24		0.25	0.18	0.23		0.20
VC2650	0.22	0.23	0.24	0.23	0.20	0.21		0.21
VC2651	0.23	0.22		0.23	0.24	0.17	0.14	0.18
VC2652	0.21	0.24		0.23	0.18	0.18		0.18
VC2653	0.21	0.20		0.20	0.17	0.21		0.19
VC2654	0.32	0.31	0.27	0.30	0.18	0.19		0.18
VC2655	0.19	0.21		0.20	0.18	0.16	0.15	0.16
VC2656	0.23	0.23		0.23	0.13	0.18		0.16
VC2657	0.23	0.23		0.23	0.16	0.17		0.17
VC2658	0.27	0.26		0.26	0.24	0.20		0.22
VC2659	0.32	0.35		0.33	0.22	0.20		0.21
VC2660	0.23	0.23		0.23	0.17	0.17		0.17
VC2661	0.24	0.21		0.23	0.15	0.16		0.16
VC2662	0.25	0.29		0.27	0.15	0.12		0.13
VC2663	0.25	0.26		0.25	0.23	0.21	0.28	0.24
VC2664	0.24	0.24		0.24	0.13	0.10		0.11
VC2665	0.30	0.26		0.28	0.18	0.16	0.15	0.16
VC2666	0.15	0.28		0.21	0.14	0.14		0.14
VC2667	0.24	0.20		0.22	0.09	0.09		0.09
VC2668	0.24	0.16		0.20	0.19	0.17		0.18
VC2669	0.18	0.22	0.18	0.19	0.20	0.15		0.18
VC2670	0.21	0.23	0.23	0.22	0.16	0.16		0.16
VC2671	0.29	0.29		0.29	0.19	0.20		0.19
VC2672	0.20	0.22		0.21	0.14	0.15		0.14
VC2673	0.26	0.28	0.26	0.27	0.21	0.19		0.20
VC2674	0.23	0.24		0.23	0.13	0.13		0.13
VC2675	0.23	0.21		0.22	0.13	0.15		0.14
VC2676	0.27	0.28		0.27	0.21	0.17		0.19
VC2677	0.19	0.22		0.20	0.16	0.15		0.15
VC2678	0.24	0.24		0.24	0.19	0.19		0.19
VC2679	0.24	0.24		0.24	0.16	0.14		0.15
VC2680	0.28	0.23		0.26	0.20	0.22		0.21
VC2681	0.25	0.25		0.25	0.18	0.20		0.19
VC2682	0.21	0.25		0.23	0.23	0.23		0.23
VC2683	0.22	0.22		0.22	0.15	0.14		0.14
VC2684	0.27	0.26		0.27	0.16	0.14		0.15

VC2685	0.17	0.19		0.18	0.16	0.14		0.15
VC2686	0.22	0.22		0.22	0.14	0.19		0.17
VC2687	0.21	0.27		0.24	0.21	0.18		0.19
VC2688	0.21	0.25		0.23	0.16	0.16		0.16
VC2689	0.25	0.25		0.25	0.19	0.20	0.18	0.19
VC2690	0.21	0.24		0.23	0.18	0.19		0.18
VC2691	0.30	0.30		0.30	0.18	0.18		0.18
VC2692	0.29	0.27		0.28	0.14	0.14		0.14
VC2693	0.27	0.28		0.28	0.20	0.18		0.19
VC2694	0.32	0.28		0.30	0.14	0.16		0.15
VC2695	0.30	0.30		0.30	0.14	0.15		0.14
VC2696	0.22	0.20		0.21	0.14	0.17		0.15
VC2697	0.25	0.27		0.26	0.14	0.15		0.15
VC2698	0.21	0.19		0.20	0.13	0.16		0.14
VC2699	0.24	0.20		0.22	0.18	0.22		0.20
VC2700	0.23	0.23		0.23	0.17	0.16		0.17
VC2701	0.32	0.31		0.31	0.18	0.19		0.19
VC2702	0.21	0.30		0.25	0.13	0.16		0.15
VC2703	0.27	0.27		0.27	0.18	0.19		0.19
VC2704	0.25	0.25	0.24	0.25	0.20	0.23		0.22
VC2705	0.27	0.25		0.26	0.19	0.23		0.21
VC2706	0.27	0.25		0.26	0.19	0.19		0.19
VC2708	0.46	0.47		0.46	0.29	0.29		0.29
VC2709	0.22	0.22	0.22	0.22	0.13	0.13		0.13
VC2710	0.25	0.24		0.25	0.18	0.22		0.20
VC2711	0.30	0.26		0.28	0.20	0.21		0.20
VC2712	0.27	0.30		0.28	0.23	0.17		0.20
VC2713	0.27	0.28		0.28	0.16	0.20		0.18
VC2714	0.27	0.28		0.27	0.18	0.18		0.18
VC2715	0.35	0.41		0.38	0.17	0.17		0.17
VC2716	0.20	0.20		0.20	0.17	0.16		0.17
VC2717	0.23	0.27		0.25	0.17	0.14		0.15
VC2718	0.23	0.26	0.23	0.24	0.19	0.20		0.20
VC2719	0.23	0.20		0.21	0.17	0.17		0.17
VC2720	0.25	0.25		0.25	0.19	0.15		0.17
VC2721	0.25	0.28		0.27	0.19	0.14		0.16
VC2722	0.16	0.15	0.17	0.16	0.15	0.15		0.15
VC2723	0.29	0.26		0.28	0.19	0.20	0.17	0.19
VC2724	0.26	0.25	0.26	0.26	0.20	0.23		0.21
VC2725	0.26	0.24		0.25	0.16	0.18		0.17
VC2726	0.26	0.26	0.26	0.26	0.15	0.17		0.16
VC2727	0.29	0.34	0.31	0.31	0.19	0.19		0.19
VC2728	0.26	0.24	0.24	0.25	0.16	0.16		0.16

VC2729	0.29	0.32		0.30	0.24	0.23		0.24
VC2730	0.23	0.25		0.24	0.22	0.20		0.21
VC2731	0.22	0.22		0.22	0.20	0.17		0.18
VC2732	0.26	0.28		0.27	0.13	0.13		0.13
VC2733	0.25	0.26		0.26	0.14	0.11	0.12	0.13
VC2734	0.34	0.31		0.32	0.20	0.18		0.19
VC2735	0.22	0.20	0.22	0.21	0.16	0.17		0.16
VC2736	0.20	0.27	0.24	0.24	0.12	0.12		0.12
VC2737	0.22	0.24		0.23	0.25	0.24	0.19	0.23
VC2738	0.27	0.24		0.26	0.19	0.13		0.16
VC2739	0.25	0.26		0.26	0.17	0.16		0.16
VC2740	0.25	0.25	0.22	0.24	0.22	0.23		0.22
VC2741	0.19	0.23		0.21	0.19	0.21	0.17	0.19
VC2742	0.30	0.27	0.27	0.28	0.15	0.17		0.16
VC2743	0.18	0.23	0.21	0.21	0.13	0.13		0.13
VC2744	0.27	0.24		0.26	0.17	0.13		0.15
VC2745	0.25	0.33	0.26	0.28	0.15	0.14		0.14
VC2746	0.27	0.25		0.26	0.18	0.14		0.16
VC2747	0.24	0.25		0.25	0.19	0.13	0.16	0.16
VC2748	0.30	0.29		0.29	0.16	0.15		0.16
VC2749	0.31	0.30		0.30	0.23	0.16		0.19
VC2750	0.41	0.41		0.41	0.44	0.39		0.42
VC2751	0.21	0.21		0.21	0.17	0.18		0.18
VC2752	0.22	0.25		0.24	0.18	0.16	0.17	0.17
VC2754	0.24	0.25		0.24	0.17	0.16		0.17
VC2755	0.29	0.24		0.27	0.17	0.20		0.19
VC2756	0.28	0.26		0.27	0.22	0.21		0.22
VC2757	0.21	0.22		0.22	0.14	0.14		0.14
VC2758	0.24	0.21		0.22	0.14	0.17		0.16
VC2759	0.22	0.20	0.19	0.20	0.12	0.15		0.14
VC2760	0.21	0.22	0.22	0.22	0.14	0.17		0.16
VC2761	0.27	0.24		0.26	0.17	0.17		0.17
VC2762	0.24	0.24		0.24	0.26	0.18	0.21	0.22
VC2763	0.23	0.23		0.23	0.13	0.15		0.14
VC2764	0.21	0.21	0.23	0.22	0.12	0.17		0.14
VC2765	0.22	0.23	0.25	0.23	0.17	0.24		0.20
VC2767	0.21	0.21		0.21	0.24	0.18		0.21
VC2768	0.23	0.24	0.24	0.24	0.18	0.18		0.18
VC2769	0.20	0.24	0.26	0.23	0.15	0.16		0.15
VC2770	0.22	0.21		0.21	0.27	0.17	0.16	0.20
VC2771	0.27	0.26	0.27	0.27	0.20	0.21		0.20
VC2772	0.22	0.21	0.22	0.22	0.10	0.13		0.12
VC2773	0.31	0.31		0.31	0.17	0.17		0.17

VC2774	0.24	0.25	0.24	0.24	0.16	0.16	0.16
VC2775	0.24	0.22	0.24	0.24	0.16	0.19	0.17
VCA0001	0.24	0.26		0.25	0.21	0.21	0.21
VCA0002	0.33	0.33	0.31	0.32	0.13	0.19	0.16
VCA0003	0.21	0.20	0.14	0.18	0.16	0.16	0.16
VCA0004	0.27	0.25		0.26	0.16	0.18	0.17
VCA0005	0.20	0.21	0.22	0.21	0.14	0.16	0.15
VCA0006	0.23	0.25	0.24	0.24	0.12	0.13	0.12
VCA0007	0.21	0.21	0.23	0.22	0.12	0.12	0.12
VCA0008	0.24	0.24		0.24	0.17	0.15	0.16
VCA0009	0.32	0.26		0.29	0.22	0.20	0.21
VCA0010	0.19	0.20	0.21	0.20	0.11	0.15	0.13
VCA0011	0.21	0.19		0.20	0.15	0.18	0.16
VCA0012	0.22	0.26		0.24	0.18	0.20	0.19
VCA0013	0.21	0.22		0.22	0.13	0.12	0.12
VCA0014	0.26	0.27		0.26	0.18	0.19	0.18
VCA0016	0.23	0.19		0.21	0.12	0.11	0.11
VCA0017	0.17	0.17		0.17	0.15	0.15	0.15
VCA0018	0.21	0.20		0.20	0.18	0.18	0.18
VCA0019	0.26	0.28		0.27	0.17	0.17	0.17
VCA0020	0.26	0.28		0.27	0.19	0.16	0.17
VCA0021	0.24	0.21		0.22	0.15	0.17	0.16
VCA0022	0.35	0.36		0.36	0.24	0.23	0.23
VCA0023	0.23	0.24		0.23	0.17	0.12	0.15
VCA0024	0.30	0.30		0.30	0.17	0.20	0.18
VCA0025	0.32	0.32		0.32	0.21	0.16	0.18
VCA0026	0.26	0.26		0.26	0.13	0.10	0.11
VCA0027	0.23	0.20		0.22	0.17	0.13	0.15
VCA0028	0.23	0.22		0.23	0.19	0.14	0.17
VCA0029	0.20	0.25		0.23	0.14	0.16	0.15
VCA0030	0.25	0.24		0.24	0.13	0.18	0.16
VCA0031	0.21	0.20	0.25	0.22	0.14	0.12	0.13
VCA0032	0.27	0.21		0.24	0.13	0.12	0.12
VCA0033	0.21	0.23	0.24	0.23	0.16	0.15	0.15
VCA0034	0.19	0.22		0.20	0.15	0.18	0.17
VCA0035	0.22	0.27		0.24	0.20	0.16	0.18
VCA0036	0.26	0.20		0.23	0.18	0.15	0.16
VCA0037	0.14	0.14		0.14	0.13	0.14	0.13
VCA0038	0.27	0.31		0.29	0.19	0.16	0.17
VCA0039	0.24	0.24		0.24	0.13	0.10	0.11
VCA0040	0.23	0.21		0.22	0.15	0.21	0.18
VCA0041	0.26	0.23		0.24	0.15	0.17	0.16
VCA0042	0.17	0.22		0.20	0.14	0.14	0.14

VCA0043	0.22	0.26		0.24	0.16	0.17		0.16
VCA0044	0.26	0.20		0.23	0.11	0.12	0.15	0.12
VCA0046	0.27	0.25		0.26	0.14	0.14		0.14
VCA0047	0.28	0.24		0.26	0.18	0.16		0.17
VCA0048	0.26	0.23		0.24	0.16	0.13		0.15
VCA0049	0.28	0.28		0.28	0.14	0.15		0.14
VCA0050	0.20	0.19	0.20	0.20	0.14	0.16		0.15
VCA0051	0.21	0.21		0.21	0.16	0.13	0.14	0.14
VCA0052	0.26	0.26		0.26	0.17	0.20		0.18
VCA0053	0.21	0.23		0.22	0.13	0.12		0.13
VCA0054	0.24	0.25		0.25	0.13	0.15		0.14
VCA0055	0.26	0.27		0.27	0.16	0.23		0.19
VCA0056	0.26	0.20		0.23	0.15	0.15		0.15
VCA0057	0.22	0.25	0.26	0.24	0.22	0.22		0.22
VCA0058	0.27	0.24		0.26	0.29	0.19		0.24
VCA0060	0.23	0.24	0.27	0.25	0.15	0.15		0.15
VCA0061	0.28	0.25		0.27	0.17	0.17		0.17
VCA0062	0.27	0.27		0.27	0.12	0.17	0.14	0.15
VCA0063	0.26	0.28	0.30	0.28	0.15	0.15		0.15
VCA0064	0.23	0.20		0.21	0.15	0.20		0.17
VCA0065	0.22	0.26		0.24	0.24	0.19		0.21
VCA0066	0.31	0.31		0.31	0.17	0.17		0.17
VCA0067	0.29	0.24		0.26	0.19	0.17		0.18
VCA0068	0.33	0.30		0.31	0.20	0.20		0.20
VCA0069	0.26	0.28		0.27	0.12	0.19	0.17	0.16
VCA0070	0.21	0.19	0.20	0.20	0.15	0.16		0.16
VCA0071	0.26	0.26	0.26	0.26	0.19	0.19		0.19
VCA0072	0.29	0.31	0.30	0.30	0.15	0.17		0.16
VCA0073	0.24	0.23	0.26	0.24	0.22	0.18		0.20
VCA0074	0.25	0.22	0.24	0.24	0.18	0.17		0.17
VCA0075	0.30	0.31		0.30	0.18	0.19		0.18
VCA0076	0.29	0.31		0.30	0.20	0.20		0.20
VCA0077	0.26	0.27		0.27	0.16	0.15		0.16
VCA0078	0.26	0.25		0.26	0.20	0.20		0.20
VCA0079	0.23	0.26	0.26	0.25	0.22	0.24		0.23
VCA0080	0.64	0.62		0.63	0.54	0.56		0.55
VCA0081	0.28	0.25		0.26	0.10	0.11	0.15	0.12
VCA0082	0.28	0.29	0.26	0.28	0.18	0.13		0.16
VCA0083	0.27	0.28	0.28	0.28	0.23	0.23		0.23
VCA0084	0.25	0.24	0.26	0.25	0.17	0.18		0.17
VCA0085	0.16	0.17	0.18	0.17	0.20	0.21		0.21
VCA0086	0.24	0.25	0.25	0.25	0.10	0.13		0.12
VCA0087	0.25	0.23		0.24	0.12	0.14	0.19	0.15

VCA0089	0.27	0.29		0.28	0.21	0.18		0.19
VCA0090	0.26	0.26		0.26	0.18	0.20		0.19
VCA0091	0.25	0.26	0.26	0.26	0.16	0.17		0.17
VCA0092	0.22	0.23	0.23	0.23	0.16	0.15		0.15
VCA0093	0.20	0.20		0.20	0.15	0.18		0.17
VCA0094	0.28	0.25	0.27	0.27	0.19	0.20		0.19
VCA0095	0.21	0.21	0.20	0.20	0.22	0.21		0.21
VCA0096	0.24	0.25	0.27	0.25	0.17	0.15		0.16
VCA0097	0.22	0.25		0.24	0.17	0.14		0.16
VCA0098	0.23	0.31	0.23	0.25	0.14	0.16		0.15
VCA0099	0.25	0.27	0.26	0.26	0.18	0.17		0.18
VCA0100	0.26	0.27	0.28	0.27	0.16	0.18		0.17
VCA0101	0.23	0.22		0.22	0.21	0.19		0.20
VCA0102	0.28	0.28	0.27	0.28	0.16	0.15		0.16
VCA0103	0.20	0.20		0.20	0.16	0.15		0.16
VCA0104	0.21	0.23	0.24	0.23	0.18	0.19		0.18
VCA0105	0.10	0.22	0.23	0.18	0.17	0.18		0.17
VCA0106	0.26	0.27		0.26	0.15	0.14	0.21	0.17
VCA0107	0.16	0.15	0.16	0.16	0.12	0.14		0.13
VCA0108	0.23	0.28		0.25	0.17	0.15	0.10	0.14
VCA0109	0.26	0.29	0.29	0.28	0.13	0.13		0.13
VCA0110	0.21	0.24		0.22	0.20	0.16		0.18
VCA0111	0.18	0.16	0.16	0.17	0.19	0.18		0.18
VCA0112	0.28	0.30		0.29	0.17	0.16		0.17
VCA0113	0.27	0.28	0.26	0.27	0.20	0.17		0.18
VCA0114	0.24	0.26	0.25	0.25	0.16	0.15		0.16
VCA0115	0.23	0.23		0.23	0.15	0.16		0.16
VCA0116	0.25	0.25		0.25	0.14	0.19		0.16
VCA0117	0.25	0.24		0.24	0.17	0.16		0.17
VCA0118	0.28	0.26	0.31	0.28	0.21	0.19		0.20
VCA0119	0.24	0.25		0.24	0.16	0.12		0.14
VCA0120	0.25	0.24		0.25	0.17	0.17		0.17
VCA0121	0.27	0.25	0.23	0.25	0.25	0.17		0.21
VCA0122	0.23	0.23	0.24	0.24	0.13	0.14		0.14
VCA0123	0.20	0.21		0.21	0.20	0.15		0.18
VCA0124	0.29	0.24	0.25	0.26	0.23	0.19		0.21
VCA0125	0.20	0.20	0.23	0.21	0.17	0.15		0.16
VCA0126	0.10	0.24	0.24	0.19	0.15	0.17		0.16
VCA0127	0.24	0.25	0.26	0.25	0.17	0.17		0.17
VCA0128	0.23	0.24		0.23	0.20	0.16		0.18
VCA0129	0.28	0.30		0.29	0.22	0.18	0.20	0.20
VCA0130	0.28	0.25		0.26	0.15	0.15	0.19	0.16
VCA0131	0.21	0.20		0.20	0.13	0.13		0.13

VCA0132	0.26	0.27		0.26	0.10	0.12	0.16	0.13
VCA0133	0.22	0.24		0.23	0.16	0.15	0.17	0.16
VCA0134	0.17	0.20		0.18	0.10	0.13	0.14	0.12
VCA0135	0.22	0.22		0.22	0.17	0.10		0.13
VCA0136	0.24	0.24		0.24	0.15	0.17	0.16	0.16
VCA0137	0.25	0.24		0.25	0.22	0.19		0.21
VCA0138	0.24	0.24		0.24	0.21	0.18	0.19	0.19
VCA0139	0.22	0.21		0.22	0.19	0.20		0.19
VCA0140	0.23	0.21		0.22	0.12	0.14		0.13
VCA0141	0.21	0.21		0.21	0.22	0.19		0.20
VCA0142	0.22	0.23	0.23	0.23	0.15	0.15		0.15
VCA0143	0.23	0.23		0.23	0.17	0.14		0.15
VCA0144	0.23	0.23		0.23	0.13	0.16		0.15
VCA0145	0.22	0.23		0.22	0.17	0.16		0.17
VCA0146	0.27	0.30		0.29	0.20	0.19		0.20
VCA0147	0.20	0.22		0.21	0.13	0.14		0.14
VCA0148	0.32	0.29		0.30	0.12	0.17		0.14
VCA0149	0.23	0.23		0.23	0.27	0.20		0.23
VCA0150	0.29	0.25		0.27	0.11	0.13		0.12
VCA0151	0.30	0.28	0.29	0.29	0.19	0.22		0.20
VCA0152	0.26	0.25		0.25	0.16	0.21		0.19
VCA0153	0.32	0.36		0.34	0.26	0.28		0.27
VCA0154	0.25	0.28		0.27	0.19	0.18		0.18
VCA0155	0.20	0.23		0.21	0.14	0.17		0.16
VCA0156	0.19	0.23		0.21	0.19	0.16		0.18
VCA0157	0.22	0.22		0.22	0.18	0.15		0.17
VCA0158	0.22	0.24		0.23	0.21	0.21		0.21
VCA0159	0.20	0.21		0.21	0.10	0.11		0.11
VCA0160	0.26	0.25		0.25	0.14	0.19		0.16
VCA0161	0.25	0.21		0.23	0.12	0.14		0.13
VCA0162	0.24	0.25		0.24	0.17	0.17		0.17
VCA0163	0.26	0.26		0.26	0.24	0.21	0.25	0.23
VCA0164	0.24	0.20		0.22	0.18	0.16		0.17
VCA0165	0.24	0.22		0.23	0.17	0.17		0.17
VCA0166	0.25	0.26		0.26	0.20	0.20	0.19	0.19
VCA0167	0.23	0.20		0.22	0.18	0.15		0.16
VCA0168	0.26	0.27		0.26	0.14	0.15		0.14
VCA0171	0.30	0.27	0.24	0.27	0.23	0.22		0.22
VCA0172	0.24	0.28		0.26	0.19	0.17		0.18
VCA0173	0.29	0.27		0.28	0.23	0.23		0.23
VCA0174	0.24	0.26		0.25	0.12	0.15		0.13
VCA0175	0.22	0.26		0.24	0.12	0.13		0.12
VCA0176	0.26	0.25	0.22	0.24	0.20	0.19		0.20

VCA0177	0.26	0.30		0.28	0.19	0.17		0.18
VCA0178	0.22	0.24		0.23	0.11	0.12		0.12
VCA0179	0.20	0.17		0.19	0.19	0.20		0.20
VCA0180	0.15	0.15		0.15	0.08	0.11		0.10
VCA0181	0.27	0.32		0.29	0.25	0.24		0.25
VCA0182	0.30	0.27		0.29	0.23	0.16		0.20
VCA0183	0.24	0.24		0.24	0.17	0.18		0.18
VCA0184	0.29	0.24		0.27	0.16	0.16		0.16
VCA0185	0.25	0.27		0.26	0.20	0.17		0.19
VCA0186	0.23	0.21		0.22	0.17	0.17		0.17
VCA0187	0.24	0.27		0.25	0.20	0.22		0.21
VCA0188	0.28	0.27		0.27	0.20	0.22		0.21
VCA0189	0.24	0.26		0.25	0.18	0.18		0.18
VCA0190	0.22	0.28		0.25	0.13	0.13		0.13
VCA0191	0.24	0.24		0.24	0.16	0.15		0.15
VCA0192	0.17	0.19		0.18	0.16	0.11		0.14
VCA0193	0.31	0.31		0.31	0.25	0.18		0.22
VCA0194	0.30	0.28		0.29	0.21	0.19		0.20
VCA0195	0.23	0.23	0.24	0.23	0.18	0.18		0.18
VCA0196	0.24	0.24	0.26	0.25	0.16	0.23		0.20
VCA0197	0.31	0.30		0.31	0.23	0.24		0.24
VCA0199	0.25	0.26		0.26	0.13	0.13	0.14	0.14
VCA0200	0.21	0.22		0.22	0.12	0.15		0.13
VCA0201	0.23	0.27		0.25	0.16	0.16		0.16
VCA0202	0.23	0.22		0.23	0.15	0.20	0.17	0.17
VCA0203	0.22	0.22	0.22	0.22	0.15	0.16		0.15
VCA0204	0.27	0.28		0.28	0.15	0.12	0.13	0.13
VCA0205	0.33	0.35		0.34	0.16	0.19	0.18	0.18
VCA0206	0.26	0.27		0.26	0.17	0.18		0.17
VCA0207	0.30	0.23	0.22	0.25	0.18	0.18		0.18
VCA0208	0.44	0.27	0.23	0.31	0.19	0.19		0.19
VCA0209	0.25	0.24	0.24	0.24	0.17	0.14		0.15
VCA0210	0.18	0.26	0.20	0.21	0.18	0.18		0.18
VCA0211	0.22	0.27		0.24	0.14	0.17		0.16
VCA0212	0.28	0.27	0.29	0.28	0.17	0.17		0.17
VCA0213	0.29	0.27	0.26	0.28	0.18	0.18		0.18
VCA0214	0.26	0.27		0.26	0.21	0.21	0.25	0.22
VCA0215	0.26	0.25		0.26	0.14	0.16		0.15
VCA0216	0.29	0.30		0.29	0.21	0.22	0.27	0.23
VCA0217	0.27	0.29	0.27	0.28	0.21	0.20		0.20
VCA0218	0.29	0.28	0.27	0.28	0.21	0.20		0.20
VCA0219	0.21	0.22		0.22	0.14	0.14		0.14
VCA0220	0.24	0.27	0.26	0.26	0.18	0.18		0.18

VCA0221	0.28	0.20	0.21	0.23	0.17	0.18		0.18
VCA0222	0.24	0.28	0.25	0.26	0.18	0.16		0.17
VCA0224	0.34	0.30		0.32	0.20	0.21		0.21
VCA0225	0.23	0.22		0.22	0.17	0.14	0.15	0.15
VCA0226	0.22	0.21		0.22	0.19	0.20		0.20
VCA0227	0.24	0.27		0.25	0.14	0.15		0.15
VCA0228	0.31	0.33	0.29	0.31	0.20	0.20		0.20
VCA0229	0.27	0.26		0.26	0.17	0.20		0.18
VCA0230	0.19	0.21		0.20	0.11	0.14	0.13	0.13
VCA0231	0.35	0.31	0.30	0.32	0.19	0.16		0.17
VCA0232	0.21	0.24		0.23	0.16	0.18	0.26	0.20
VCA0233	0.24	0.22		0.23	0.18	0.16	0.21	0.18
VCA0234	0.14	0.16		0.15	0.15	0.19	0.17	0.17
VCA0235	0.28	0.26		0.27	0.13	0.14	0.14	0.14
VCA0236	0.21	0.22	0.23	0.22	0.18	0.17		0.18
VCA0237	0.26	0.29	0.26	0.27	0.11	0.14		0.13
VCA0238	0.32	0.31	0.28	0.30	0.19	0.21		0.20
VCA0239	0.24	0.25		0.25	0.16	0.18	0.16	0.17
VCA0240	0.25	0.23	0.21	0.23	0.14	0.15		0.15
VCA0241	0.28	0.23	0.29	0.27	0.11	0.11		0.11
VCA0242	0.23	0.23		0.23	0.07	0.11		0.09
VCA0243	0.33	0.30	0.28	0.30	0.17	0.14		0.16
VCA0244	0.31	0.21	0.23	0.25	0.14	0.14		0.14
VCA0245	0.23	0.25		0.24	0.18	0.17		0.17
VCA0246	0.27	0.27		0.27	0.23	0.23		0.23
VCA0247	0.25	0.21	0.25	0.24	0.18	0.20		0.19
VCA0248	0.26	0.24	0.27	0.26	0.11	0.13		0.12
VCA0249	0.26	0.29	0.30	0.28	0.24	0.18		0.21
VCA0250	0.29	0.30		0.30	0.18	0.17		0.18
VCA0251	0.26	0.25		0.26	0.14	0.14		0.14
VCA0252	0.25	0.29		0.27	0.14	0.16		0.15
VCA0253	0.23	0.25		0.24	0.16	0.16		0.16
VCA0255	0.26	0.28	0.25	0.26	0.17	0.17		0.17
VCA0256	0.22	0.23		0.22	0.20	0.21		0.20
VCA0258	0.20	0.19		0.19	0.16	0.16		0.16
VCA0259					0.16	0.15	0.13	0.15
VCA0260	0.25	0.24		0.24	0.16	0.20		0.18
VCA0262	0.24	0.25		0.25	0.22	0.23		0.22
VCA0263	0.20	0.17		0.18	0.11	0.13		0.12
VCA0264	0.26	0.30		0.28	0.18	0.14		0.16
VCA0265	0.18	0.18		0.18	0.15	0.14		0.14
VCA0266	0.22	0.22		0.22	0.14	0.16		0.15
VCA0267	0.26	0.28		0.27	0.19	0.21		0.20

VCA0268	0.26	0.29	0.28	0.17	0.15		0.16
VCA0269	0.24	0.21	0.22	0.16	0.19		0.17
VCA0270	0.24	0.26	0.25	0.18	0.22		0.20
VCA0271	0.21	0.23	0.22	0.18	0.17		0.18
VCA0272				0.15	0.16	0.17	0.16
VCA0273				0.15	0.16	0.13	0.15
VCA0274	0.27	0.24	0.25	0.22	0.18		0.20
VCA0275				0.21	0.21	0.19	0.20
VCA0276	0.24	0.23	0.24	0.14	0.16		0.15
VCA0277	0.23	0.23	0.23	0.20	0.16		0.18
VCA0278	0.19	0.20	0.20	0.26	0.22		0.24
VCA0279	0.23	0.22	0.22	0.11	0.13		0.12
VCA0280	0.23	0.25	0.24	0.22	0.22	0.22	0.22
VCA0281	0.25	0.28	0.27	0.15	0.14		0.15
VCA0282	0.28	0.28	0.28	0.18	0.18		0.18
VCA0283	0.18	0.17	0.18	0.17	0.15	0.17	0.16
VCA0284	0.24	0.25	0.25	0.23	0.18		0.21
VCA0285	0.20	0.23	0.22	0.17	0.17		0.17
VCA0286	0.24	0.25	0.25	0.18	0.17		0.17
VCA0287	0.21	0.21	0.21	0.20	0.20		0.20
VCA0288	0.24	0.24	0.24	0.14	0.18		0.16
VCA0289	0.25	0.24	0.24	0.19	0.18		0.18
VCA0290	0.27	0.24	0.26	0.14	0.21		0.17
VCA0291	0.22	0.23	0.23	0.16	0.15		0.16
VCA0292	0.23	0.23	0.23	0.20	0.16		0.18
VCA0294	0.25	0.25	0.25	0.13	0.13		0.13
VCA0295	0.34	0.32	0.33	0.32	0.29		0.31
VCA0296	0.24	0.26	0.25	0.23	0.17		0.20
VCA0297	0.25	0.26	0.25	0.21	0.17		0.19
VCA0298	0.23	0.24	0.24	0.15	0.11		0.13
VCA0299	0.26	0.24	0.25	0.11	0.14		0.12
VCA0300	0.24	0.24	0.24	0.20	0.20		0.20
VCA0301	0.22	0.24	0.23	0.12	0.12		0.12
VCA0303	0.23	0.23	0.23	0.15	0.20		0.17
VCA0304	0.26	0.27	0.26	0.14	0.13		0.14
VCA0305	0.23	0.22	0.22	0.19	0.16		0.17
VCA0306	0.23	0.24	0.23	0.11	0.11		0.11
VCA0307	0.30	0.31	0.31	0.30	0.30	0.25	0.28
VCA0308	0.27	0.29	0.28	0.19	0.21	0.17	0.19
VCA0309	0.25	0.25	0.25	0.15	0.17		0.16
VCA0310	0.26	0.26	0.26	0.27	0.20		0.24
VCA0312	0.20	0.22	0.21	0.13	0.14		0.13
VCA0313	0.21	0.21	0.21	0.22	0.22		0.22

VCA0314	0.24	0.25		0.24	0.15	0.15		0.15
VCA0315	0.26	0.27		0.26	0.14	0.14		0.14
VCA0316	0.25	0.25		0.25	0.13	0.13		0.13
VCA0317	0.32	0.31		0.31	0.27	0.21		0.24
VCA0319	0.24	0.26		0.25	0.13	0.15		0.14
VCA0320	0.21	0.23		0.22	0.12	0.14		0.13
VCA0321	0.20	0.22		0.21	0.18	0.17		0.17
VCA0322	0.27	0.26		0.26	0.17	0.17		0.17
VCA0323	0.23	0.23	0.24	0.23	0.15	0.13		0.14
VCA0324	0.26	0.27		0.27	0.15	0.14	0.13	0.14
VCA0326	0.26	0.27		0.27	0.18	0.21		0.20
VCA0327	0.23	0.28		0.26	0.10	0.12	0.10	0.10
VCA0328	0.26	0.26	0.26	0.26	0.14	0.19		0.17
VCA0329					0.15	0.14	0.16	0.15
VCA0330	0.25	0.25	0.26	0.25	0.13	0.15		0.14
VCA0331	0.34	0.30		0.32	0.18	0.19		0.19
VCA0333					0.15	0.15	0.16	0.15
VCA0334	0.22	0.28	0.27	0.26	0.17	0.18		0.17
VCA0335					0.14	0.15	0.15	0.15
VCA0336	0.27	0.26		0.27	0.20	0.16		0.18
VCA0337	0.26	0.26	0.27	0.26	0.15	0.17		0.16
VCA0338	0.25	0.26		0.26	0.21	0.19	0.19	0.20
VCA0339	0.28	0.25		0.26	0.20	0.18		0.19
VCA0340	0.30	0.28	0.28	0.29	0.21	0.28		0.24
VCA0341	0.23	0.24		0.24	0.20	0.21	0.14	0.18
VCA0342	0.19	0.22	0.23	0.21	0.17	0.18		0.17
VCA0343					0.16	0.19	0.22	0.19
VCA0344					0.23	0.27	0.26	0.25
VCA0345	0.22	0.25	0.28	0.25	0.12	0.15		0.13
VCA0346	0.20	0.16	0.16	0.17	0.13	0.12		0.12
VCA0347	0.23	0.22		0.22	0.18	0.20		0.19
VCA0349	0.25	0.26		0.26	0.21	0.20	0.18	0.19
VCA0350					0.21	0.21	0.20	0.21
VCA0351	0.28	0.20	0.20	0.23	0.20	0.19		0.20
VCA0352	0.29	0.29		0.29	0.18	0.20		0.19
VCA0353	0.17	0.18		0.17	0.11	0.14		0.12
VCA0354	0.22	0.23		0.22	0.15	0.17		0.16
VCA0355	0.14	0.17		0.15	0.17	0.18		0.17
VCA0356	0.21	0.22		0.21	0.15	0.15		0.15
VCA0357					0.15	0.11	0.12	0.13
VCA0358	0.23	0.20	0.22	0.22	0.16	0.12		0.14
VCA0359	0.21	0.21		0.21	0.13	0.17		0.15
VCA0360	0.27	0.27		0.27	0.19	0.22		0.20

VCA0361	0.25	0.20		0.23	0.11	0.11		0.11
VCA0362	0.22	0.23		0.23	0.14	0.15		0.15
VCA0363	0.26	0.27		0.27	0.18	0.20		0.19
VCA0364					0.17	0.12	0.16	0.15
VCA0366	0.24	0.23	0.24	0.24	0.23	0.22		0.23
VCA0367	0.11	0.13		0.12	0.10	0.14		0.12
VCA0368	0.29	0.28		0.28	0.21	0.21		0.21
VCA0369	0.22	0.21		0.22	0.19	0.18		0.18
VCA0370	0.24	0.25		0.25	0.17	0.20		0.19
VCA0371	0.26	0.27	0.23	0.25	0.20	0.17		0.19
VCA0372	0.22	0.19		0.21	0.17	0.17		0.17
VCA0373					0.15	0.12	0.12	0.13
VCA0374	0.26	0.27	0.24	0.26	0.16	0.15		0.16
VCA0376					0.25	0.23	0.18	0.22
VCA0379	0.30	0.26		0.28	0.17	0.18		0.18
VCA0380	0.23	0.21		0.22	0.13	0.16		0.15
VCA0381	0.23	0.22		0.23	0.15	0.17		0.16
VCA0382	0.28	0.27	0.27	0.27	0.15	0.14		0.15
VCA0383	0.25	0.25		0.25	0.18	0.22		0.20
VCA0384					0.17	0.15	0.15	0.16
VCA0385	0.16	0.17		0.16	0.17	0.16		0.17
VCA0386	0.14	0.15		0.15	0.13	0.15		0.14
VCA0387	0.20	0.23		0.21	0.22	0.16		0.19
VCA0388	0.29	0.28		0.28	0.16	0.18		0.17
VCA0389	0.22	0.24		0.23	0.16	0.19		0.18
VCA0390					0.20	0.20	0.19	0.19
VCA0391	0.25	0.27	0.23	0.25	0.15	0.14		0.14
VCA0392	0.25	0.25	0.24	0.25	0.16	0.19		0.18
VCA0393	0.25	0.22		0.23	0.12	0.15		0.13
VCA0394					0.26	0.24	0.19	0.23
VCA0395	0.20	0.19		0.19	0.17	0.16		0.17
VCA0396	0.24	0.27		0.25	0.17	0.19		0.18
VCA0397	0.26	0.26		0.26	0.21	0.20		0.21
VCA0398	0.26	0.25		0.26	0.15	0.14		0.15
VCA0399	0.18	0.18		0.18	0.13	0.19		0.16
VCA0400	0.20	0.21	0.18	0.19	0.14	0.14		0.14
VCA0401	0.25	0.25		0.25	0.15	0.18	0.16	0.16
VCA0402	0.23	0.24		0.24	0.15	0.15		0.15
VCA0403	0.20	0.21		0.20	0.15	0.17	0.18	0.17
VCA0404					0.20	0.19	0.15	0.18
VCA0405	0.29	0.27		0.28	0.16	0.17		0.16
VCA0406	0.30	0.28		0.29	0.20	0.23		0.21
VCA0407					0.14	0.13	0.13	0.13

VCA0408	0.29	0.30	0.29	0.29	0.23	0.22		0.23
VCA0409	0.31	0.29		0.30	0.18	0.20		0.19
VCA0410	0.24	0.23		0.24	0.20	0.20		0.20
VCA0411					0.18	0.16	0.14	0.16
VCA0412	0.27	0.22		0.24	0.14	0.12		0.13
VCA0413	0.22	0.21		0.21	0.16	0.17		0.17
VCA0414	0.28	0.25		0.26	0.24	0.18		0.21
VCA0415	0.25	0.21	0.25	0.23	0.14	0.14		0.14
VCA0417	0.24	0.25	0.23	0.24	0.16	0.16		0.16
VCA0418	0.22	0.19		0.21	0.15	0.17		0.16
VCA0419	0.27	0.26		0.26	0.20	0.18		0.19
VCA0420	0.20	0.24		0.22	0.14	0.15		0.14
VCA0421	0.33	0.32		0.33	0.17	0.18		0.17
VCA0422	0.24	0.25		0.24	0.14	0.18		0.16
VCA0423	0.20	0.18	0.19	0.19	0.13	0.13		0.13
VCA0424	0.31	0.34		0.33	0.22	0.25		0.24
VCA0425	0.27	0.25		0.26	0.18	0.17		0.18
VCA0426	0.23	0.22	0.20	0.22	0.13	0.15		0.14
VCA0427	0.24	0.24		0.24	0.15	0.18		0.16
VCA0428	0.26	0.28	0.28	0.28	0.20	0.20		0.20
VCA0429	0.20	0.19		0.19	0.10	0.16	0.15	0.14
VCA0430	0.26	0.23		0.24	0.15	0.18		0.17
VCA0431	0.21	0.21	0.21	0.21	0.15	0.14		0.15
VCA0432	0.18	0.16	0.15	0.16	0.12	0.12		0.12
VCA0433					0.16	0.14	0.17	0.16
VCA0434	0.24	0.25		0.25	0.18	0.18		0.18
VCA0435	0.26	0.08	0.25	0.20	0.12	0.14		0.13
VCA0436	0.26	0.23	0.26	0.25	0.18	0.18		0.18
VCA0437	0.27	0.27		0.27	0.24	0.18	0.16	0.19
VCA0438					0.22	0.24	0.24	0.23
VCA0439	0.20	0.21		0.21	0.14	0.19	0.15	0.16
VCA0440					0.22	0.23	0.28	0.24
VCA0441	0.24	0.25	0.25	0.25	0.13	0.12		0.12
VCA0442	0.26	0.25	0.26	0.26	0.21	0.21		0.21
VCA0443	0.24	0.25	0.25	0.25	0.23	0.21		0.22
VCA0444					0.09	0.07	0.07	0.08
VCA0445					0.17	0.17	0.17	0.17
VCA0446					0.13	0.15	0.14	0.14
VCA0447	0.26	0.25		0.26	0.15	0.22		0.19
VCA0448	0.33	0.27	0.27	0.29	0.23	0.20		0.22
VCA0449	0.24	0.24		0.24	0.18	0.20		0.19
VCA0450	0.21	0.21		0.21	0.14	0.16		0.15
VCA0451	0.26	0.25		0.26	0.20	0.19		0.19

VCA0453	0.25	0.24		0.24	0.15	0.15		0.15
VCA0454	0.28	0.35		0.32	0.20	0.18		0.19
VCA0455	0.28	0.30		0.29	0.13	0.09		0.11
VCA0456	0.24	0.25	0.22	0.24	0.14	0.15		0.15
VCA0457	0.29	0.33		0.31	0.16	0.17		0.16
VCA0458	0.27	0.31		0.29	0.17	0.16		0.17
VCA0459	0.26	0.21		0.23	0.19	0.23		0.21
VCA0460	0.22	0.23		0.23	0.20	0.19		0.20
VCA0461	0.25	0.23		0.24	0.21	0.21		0.21
VCA0462	0.24	0.24		0.24	0.15	0.18		0.16
VCA0463	0.21	0.23		0.22	0.14	0.15		0.14
VCA0464	0.22	0.24		0.23	0.16	0.19		0.18
VCA0465	0.32	0.27		0.30	0.15	0.13		0.14
VCA0466	0.28	0.26		0.27	0.18	0.17		0.18
VCA0467	0.25	0.23		0.24	0.12	0.11		0.12
VCA0468	0.21	0.22		0.21	0.18	0.19		0.18
VCA0469	0.22	0.24	0.22	0.23	0.15	0.12		0.14
VCA0470	0.24	0.28		0.26	0.16	0.16		0.16
VCA0471	0.23	0.22		0.23	0.19	0.22		0.21
VCA0472	0.25	0.23		0.24	0.24	0.26		0.25
VCA0473	0.22	0.24		0.23	0.13	0.13		0.13
VCA0474	0.25	0.27		0.26	0.19	0.17		0.18
VCA0476	0.25	0.25		0.25	0.12	0.13		0.12
VCA0477	0.22	0.24		0.23	0.20	0.17		0.19
VCA0479	0.26	0.27		0.26	0.17	0.16		0.16
VCA0481	0.22	0.24		0.23	0.08	0.09	0.05	0.07
VCA0482	0.23	0.24		0.24	0.15	0.13		0.14
VCA0483	0.28	0.32		0.30	0.20	0.19		0.20
VCA0484	0.22	0.22		0.22	0.18	0.14		0.16
VCA0485	0.26	0.24		0.25	0.08	0.08		0.08
VCA0487	0.22	0.20		0.21	0.16	0.17		0.16
VCA0488	0.22	0.25		0.24	0.12	0.13		0.13
VCA0490	0.22	0.21		0.22	0.15	0.13		0.14
VCA0491	0.28	0.27		0.28	0.20	0.18		0.19
VCA0492	0.20	0.23		0.22	0.19	0.17		0.18
VCA0493	0.24	0.25		0.25	0.22	0.19		0.21
VCA0494	0.23	0.23		0.23	0.16	0.14		0.15
VCA0495	0.21	0.22		0.21	0.14	0.17		0.16
VCA0496	0.23	0.24		0.24	0.17	0.21		0.19
VCA0498	0.25	0.26		0.26	0.14	0.16		0.15
VCA0499	0.24	0.22		0.23	0.16	0.17	0.13	0.15
VCA0500	0.24	0.23		0.23	0.14	0.18		0.16
VCA0501	0.26	0.26		0.26	0.16	0.16		0.16

VCA0502	0.20	0.19		0.19	0.13	0.13		0.13
VCA0505	0.23	0.25		0.24	0.13	0.14		0.14
VCA0506	0.24	0.21		0.23	0.15	0.16		0.15
VCA0507	0.24	0.30		0.27	0.16	0.13		0.14
VCA0508	0.23	0.22		0.22	0.18	0.19		0.19
VCA0509	0.27	0.26		0.27	0.17	0.18		0.18
VCA0510	0.22	0.22		0.22	0.20	0.19		0.19
VCA0511	0.25	0.23		0.24	0.17	0.18		0.17
VCA0512	0.22	0.22		0.22	0.15	0.18		0.17
VCA0513	0.23	0.25		0.24	0.14	0.13		0.14
VCA0514	0.24	0.26	0.24	0.25	0.20	0.18		0.19
VCA0515	0.23	0.25	0.23	0.23	0.15	0.14		0.15
VCA0516	0.28	0.25		0.27	0.18	0.22		0.20
VCA0517	0.24	0.24		0.24	0.16	0.14		0.15
VCA0518	0.24	0.25		0.25	0.15	0.10		0.12
VCA0519	0.25	0.31		0.28	0.16	0.15		0.16
VCA0520	0.23	0.25		0.24	0.15	0.15		0.15
VCA0521	0.23	0.25		0.24	0.17	0.15		0.16
VCA0522	0.27	0.22		0.25	0.15	0.15		0.15
VCA0523	0.22	0.25		0.23	0.13	0.15		0.14
VCA0524					0.16	0.05	0.22	0.14
VCA0525	0.26	0.27	0.24	0.26	0.28	0.27		0.27
VCA0526	0.23	0.25		0.24	0.22	0.17	0.26	0.22
VCA0527	0.21	0.23	0.27	0.24	0.16	0.18		0.17
VCA0528	0.23	0.22		0.23	0.09	0.12		0.11
VCA0529	0.33	0.29	0.32	0.31	0.21	0.17		0.19
VCA0530	0.27	0.26		0.27	0.16	0.15		0.15
VCA0531	0.29	0.28		0.28	0.17	0.21		0.19
VCA0532					0.14	0.18	0.16	0.16
VCA0533	0.24	0.28		0.26	0.16	0.17		0.16
VCA0534	0.27	0.29		0.28	0.28	0.17	0.27	0.24
VCA0535	0.18	0.24	0.26	0.22	0.15	0.17		0.16
VCA0538	0.24	0.26	0.25	0.25	0.27	0.22		0.24
VCA0539	0.21	0.22	0.23	0.22	0.14	0.13		0.14
VCA0540	0.26	0.24	0.20	0.23	0.25	0.24		0.24
VCA0541	0.26	0.21	0.25	0.24	0.18	0.19		0.18
VCA0542	0.26	0.26		0.26	0.16	0.14		0.15
VCA0543	0.28	0.29	0.27	0.28	0.14	0.17		0.16
VCA0546	0.24	0.27	0.25	0.25	0.21	0.23		0.22
VCA0547	0.25	0.24	0.24	0.24	0.16	0.21		0.18
VCA0548	0.25	0.24	0.23	0.24	0.22	0.20		0.21
VCA0549	0.21	0.21	0.18	0.20	0.15	0.19		0.17
VCA0550	0.22	0.28	0.26	0.25	0.21	0.24		0.22

VCA0551	0.22	0.23		0.22	0.14	0.17		0.15
VCA0552	0.25	0.20		0.23	0.17	0.18		0.17
VCA0553	0.20	0.20		0.20	0.11	0.13		0.12
VCA0554	0.25	0.25		0.25	0.19	0.15		0.17
VCA0555	0.22	0.20	0.21	0.21	0.19	0.17		0.18
VCA0556	0.25	0.25		0.25	0.13	0.14		0.14
VCA0557	0.21	0.23		0.22	0.18	0.14		0.16
VCA0558	0.21	0.23		0.22	0.15	0.13	0.14	0.14
VCA0559	0.22	0.24		0.23	0.20	0.19		0.20
VCA0560	0.25	0.26		0.26	0.20	0.18		0.19
VCA0561	0.27	0.25	0.27	0.26	0.12	0.11		0.12
VCA0562	0.24	0.23	0.23	0.23	0.23	0.19		0.21
VCA0563	0.23	0.22		0.23	0.17	0.17	0.11	0.15
VCA0564	0.33	0.34		0.33	0.20	0.22		0.21
VCA0565	0.26	0.27		0.27	0.23	0.19	0.19	0.20
VCA0566	0.33	0.31		0.32	0.27	0.25		0.26
VCA0567	0.29	0.29		0.29	0.18	0.22	0.17	0.19
VCA0568	0.27	0.23		0.25	0.15	0.18	0.18	0.17
VCA0569	0.25	0.26		0.26	0.17	0.18		0.17
VCA0570	0.23	0.22		0.23	0.14	0.15		0.14
VCA0571	0.26	0.24		0.25	0.17	0.18		0.17
VCA0572	0.20	0.19		0.19	0.15	0.15	0.16	0.16
VCA0573	0.25	0.26		0.25	0.23	0.21		0.22
VCA0574	0.24	0.24		0.24	0.14	0.16		0.15
VCA0575	0.25	0.24		0.24	0.15	0.17		0.16
VCA0576	0.24	0.25		0.24	0.19	0.19		0.19
VCA0577	0.21	0.23		0.22	0.15	0.21		0.18
VCA0578	0.30	0.30		0.30	0.17	0.16	0.18	0.17
VCA0579	0.22	0.22		0.22	0.12	0.19		0.15
VCA0580	0.22	0.20		0.21	0.15	0.14		0.14
VCA0581	0.24	0.24		0.24	0.17	0.17		0.17
VCA0582	0.20	0.19		0.20	0.19	0.10	0.15	0.15
VCA0583	0.25	0.18		0.22	0.16	0.18		0.17
VCA0584	0.24	0.24		0.24	0.20	0.18		0.19
VCA0585	0.18	0.16		0.17	0.20	0.18		0.19
VCA0586	0.21	0.19		0.20	0.11	0.09	0.11	0.10
VCA0587	0.24	0.26		0.25	0.17	0.18		0.18
VCA0588	0.22	0.22		0.22	0.12	0.12	0.13	0.13
VCA0589	0.25	0.25	0.25	0.25	0.14	0.15		0.15
VCA0590	0.26	0.24		0.25	0.17	0.17	0.18	0.17
VCA0591	0.22	0.21		0.22	0.16	0.14		0.15
VCA0592	0.21	0.20		0.21	0.19	0.14	0.15	0.16
VCA0593	0.58	0.57		0.58	0.64	0.56	0.62	0.61

VCA0594	0.29	0.28		0.29	0.19	0.18		0.19
VCA0595	0.26	0.26		0.26	0.14	0.16	0.17	0.16
VCA0596	0.32	0.33		0.32	0.17	0.19		0.18
VCA0597	0.24	0.23	0.23	0.24	0.17	0.19		0.18
VCA0598	0.29	0.24		0.27	0.19	0.17		0.18
VCA0599	0.29	0.29		0.29	0.15	0.20	0.21	0.19
VCA0600	0.29	0.30		0.30	0.18	0.15		0.17
VCA0601	0.23	0.27		0.25	0.22	0.21		0.22
VCA0602	0.25	0.22		0.23	0.19	0.13	0.16	0.16
VCA0603	0.24	0.22		0.23	0.13	0.18	0.15	0.15
VCA0604	0.25	0.23		0.24	0.12	0.16	0.16	0.15
VCA0605	0.21	0.21		0.21	0.11	0.12		0.12
VCA0606	0.28	0.29		0.28	0.19	0.12		0.15
VCA0607	0.20	0.21		0.21	0.22	0.17	0.16	0.18
VCA0608	0.27	0.27		0.27	0.23	0.22	0.21	0.22
VCA0609	0.18	0.23		0.20	0.14	0.14		0.14
VCA0610	0.21	0.19		0.20	0.12	0.15	0.16	0.14
VCA0611	0.26	0.26		0.26	0.22	0.19		0.21
VCA0612	0.31	0.26		0.28	0.16	0.17	0.19	0.17
VCA0613	0.24	0.26		0.25	0.23	0.26		0.24
VCA0614	0.09	0.13		0.11	0.15	0.16		0.15
VCA0615	0.08	0.13		0.10	0.17	0.14		0.16
VCA0616	0.20	0.19		0.20	0.17	0.15	0.17	0.16
VCA0617	0.09	0.14		0.12	0.15	0.13		0.14
VCA0618	0.21	0.21		0.21	0.12	0.10		0.11
VCA0619	0.18	0.18		0.18	0.13	0.14		0.14
VCA0620	0.25	0.25		0.25	0.14	0.16		0.15
VCA0621	0.27	0.24		0.26	0.12	0.16	0.16	0.15
VCA0622	0.27	0.27		0.27	0.19	0.18		0.19
VCA0623	0.26	0.26		0.26	0.16	0.16	0.16	0.16
VCA0624	0.23	0.22		0.23	0.13	0.17		0.15
VCA0626	0.23	0.24		0.23	0.11	0.12		0.11
VCA0627	0.21	0.23		0.22	0.16	0.14	0.15	0.15
VCA0628	0.25	0.19		0.22	0.17	0.13	0.14	0.15
VCA0629	0.29	0.30		0.30	0.23	0.19	0.19	0.20
VCA0630	0.24	0.24	0.25	0.24	0.13	0.12		0.12
VCA0631	0.33	0.29		0.31	0.12	0.19		0.16
VCA0632	0.24	0.23		0.23	0.18	0.16	0.20	0.18
VCA0633	0.26	0.25	0.26	0.26	0.19	0.19		0.19
VCA0634	0.22	0.22		0.22	0.13	0.09		0.11
VCA0635	0.28	0.27	0.26	0.27	0.13	0.15		0.14
VCA0636	0.24	0.25	0.25	0.25	0.14	0.17		0.16
VCA0637	0.22	0.24		0.23	0.16	0.15		0.15

VCA0638	0.28	0.29		0.29	0.18	0.21		0.20
VCA0639	0.24	0.25	0.23	0.24	0.15	0.17		0.16
VCA0640	0.25	0.27		0.26	0.24	0.19		0.22
VCA0641	0.32	0.32	0.29	0.31	0.25	0.21		0.23
VCA0642	0.31	0.28	0.26	0.28	0.16	0.18		0.17
VCA0644	0.23	0.25		0.24	0.17	0.14		0.15
VCA0645	0.23	0.22	0.23	0.23	0.16	0.15		0.15
VCA0646	0.27	0.30		0.29	0.20	0.16		0.18
VCA0647	0.18	0.18	0.17	0.18	0.19	0.17		0.18
VCA0648	0.19	0.19		0.19	0.18	0.14		0.16
VCA0649	0.25	0.23		0.24	0.18	0.15		0.16
VCA0650	0.23	0.24		0.24	0.15	0.16	0.15	0.15
VCA0651	0.30	0.29		0.30	0.13	0.20	0.19	0.17
VCA0652	0.21	0.21		0.21				
VCA0653	0.29	0.29		0.29	0.11	0.14	0.15	0.13
VCA0654	0.27	0.24		0.26	0.14	0.17		0.15
VCA0655	0.24	0.26		0.25	0.13	0.15	0.14	0.14
VCA0656	0.23	0.22		0.23	0.11	0.14		0.13
VCA0657	0.17	0.17		0.17	0.08	0.10		0.09
VCA0658	0.23	0.23		0.23	0.16	0.16		0.16
VCA0659	0.29	0.31		0.30	0.19	0.18		0.18
VCA0660	0.24	0.24		0.24	0.12	0.10		0.11
VCA0661	0.28	0.27		0.28	0.13	0.13		0.13
VCA0662	0.24	0.27		0.25	0.18	0.18	0.17	0.18
VCA0663	0.28	0.29		0.28	0.16	0.18		0.17
VCA0664	0.30	0.28		0.29	0.18	0.24	0.22	0.21
VCA0665	0.31	0.33		0.32	0.19	0.22		0.21
VCA0666	0.23	0.22		0.23	0.17	0.16		0.16
VCA0667	0.25	0.24		0.25	0.20	0.19	0.19	0.19
VCA0668	0.28	0.27		0.28	0.15	0.11	0.10	0.12
VCA0669	0.27	0.28		0.28	0.18	0.16		0.17
VCA0670	0.25	0.24		0.24				
VCA0671	0.25	0.25		0.25	0.14	0.14		0.14
VCA0672	0.19	0.17		0.18	0.13	0.09	0.13	0.12
VCA0673	0.24	0.25		0.24	0.19	0.17		0.18
VCA0674	0.20	0.25		0.23	0.15	0.15		0.15
VCA0675	0.28	0.23		0.26	0.25	0.24		0.25
VCA0676	0.21	0.24		0.22	0.11	0.10		0.11
VCA0677	0.18	0.19		0.19	0.19	0.15		0.17
VCA0678	0.24	0.23		0.23	0.18	0.18	0.19	0.18
VCA0679	0.23	0.24		0.24	0.14	0.15		0.14
VCA0680	0.20	0.20		0.20	0.21	0.18		0.19
VCA0681	0.39	0.41		0.40	0.51	0.57		0.54

VCA0682	0.16	0.14		0.15	0.14	0.16	0.17	0.16
VCA0683	0.26	0.27		0.26	0.20	0.21		0.20
VCA0684	0.27	0.28		0.28	0.19	0.16		0.17
VCA0685	0.20	0.19		0.20	0.18	0.17		0.17
VCA0686	0.23	0.24		0.23	0.16	0.15		0.15
VCA0687	0.23	0.23		0.23	0.16	0.16		0.16
VCA0688	0.20	0.22	0.22	0.21	0.11	0.09		0.10
VCA0689	0.19	0.19		0.19	0.15	0.16		0.15
VCA0690	0.22	0.23		0.22				
VCA0691	0.20	0.20		0.20	0.15	0.16		0.15
VCA0692	0.27	0.24		0.26	0.22	0.26	0.23	0.24
VCA0693	0.26	0.26		0.26	0.17	0.21	0.21	0.20
VCA0694	0.28	0.27		0.27	0.13	0.16		0.15
VCA0695	0.23	0.23		0.23	0.18	0.19		0.18
VCA0696	0.27	0.29		0.28	0.23	0.26		0.25
VCA0697	0.31	0.35	0.31	0.32	0.17	0.16		0.17
VCA0698	0.24	0.25		0.24	0.20	0.19	0.26	0.22
VCA0699	0.23	0.23		0.23				
VCA0700	0.22	0.21		0.21	0.11	0.13		0.12
VCA0701	0.24	0.24		0.24	0.15	0.18	0.21	0.18
VCA0702	0.23	0.25		0.24	0.17	0.20		0.19
VCA0703	0.30	0.27		0.28	0.20	0.17		0.19
VCA0704	0.31	0.33		0.32	0.15	0.11		0.13
VCA0705	0.29	0.27		0.28	0.18	0.18		0.18
VCA0706	0.28	0.30		0.29	0.12	0.19		0.15
VCA0707	0.38	0.39		0.39	0.19	0.17	0.23	0.19
VCA0708	0.33	0.30		0.31	0.22	0.18		0.20
VCA0709	0.29	0.28		0.29	0.14	0.16		0.15
VCA0710	0.25	0.27		0.26	0.18	0.16	0.17	0.17
VCA0711	0.24	0.26		0.25	0.20	0.17		0.18
VCA0712	0.25	0.26		0.26	0.14	0.11		0.12
VCA0713	0.18	0.17		0.18	0.10	0.11	0.15	0.12
VCA0714	0.28	0.26		0.27	0.19	0.18	0.20	0.19
VCA0715	0.30	0.31		0.30	0.17	0.16	0.22	0.18
VCA0716	0.28	0.29		0.29	0.20	0.17		0.18
VCA0717	0.30	0.29		0.30	0.30	0.30		0.30
VCA0718	0.26	0.24		0.25	0.21	0.21		0.21
VCA0719	0.26	0.25		0.26	0.16	0.18	0.19	0.18
VCA0720	0.24	0.25		0.24	0.11	0.12		0.11
VCA0721	0.25	0.28		0.27	0.16	0.15	0.18	0.17
VCA0722	0.31	0.26		0.28	0.15	0.16	0.24	0.18
VCA0723	0.21	0.25		0.23	0.17	0.12		0.15
VCA0724	0.21	0.21		0.21	0.14	0.17	0.19	0.17

VCA0725	0.31	0.33		0.32	0.23	0.20		0.21
VCA0726	0.24	0.24		0.24	0.11	0.10		0.11
VCA0727	0.23	0.22		0.22	0.16	0.13		0.15
VCA0728	0.25	0.25		0.25	0.14	0.16		0.15
VCA0729	0.24	0.22		0.23	0.15	0.14		0.14
VCA0730	0.28	0.25		0.27	0.18	0.19	0.19	0.19
VCA0731	0.24	0.23		0.24	0.16	0.17		0.17
VCA0732	0.21	0.22		0.22	0.21	0.20		0.21
VCA0733	0.28	0.26		0.27				
VCA0734	0.22	0.24		0.23	0.17	0.18	0.17	0.17
VCA0735	0.19	0.21		0.20	0.12	0.15	0.13	0.13
VCA0736	0.27	0.27		0.27	0.20	0.16		0.18
VCA0737	0.26	0.29		0.28	0.12	0.15		0.14
VCA0738	0.23	0.22		0.23	0.17	0.15		0.16
VCA0739	0.25	0.26		0.26	0.10	0.14		0.12
VCA0740	0.31	0.31		0.31	0.18	0.20		0.19
VCA0741	0.28	0.27		0.28	0.15	0.19	0.15	0.16
VCA0742	0.24	0.24		0.24	0.20	0.18	0.19	0.19
VCA0743	0.25	0.27		0.26	0.16	0.13		0.14
VCA0744	0.24	0.26		0.25	0.17	0.16	0.20	0.17
VCA0745	0.26	0.23		0.24	0.16	0.10	0.15	0.14
VCA0746	0.28	0.28		0.28	0.19	0.19		0.19
VCA0747	0.22	0.24	0.21	0.22	0.14	0.14		0.14
VCA0748	0.26	0.27		0.26	0.13	0.15		0.14
VCA0749	0.25	0.24		0.24	0.20	0.18		0.19
VCA0750	0.25	0.24		0.24	0.11	0.13		0.12
VCA0751	0.24	0.26		0.25				
VCA0752	0.27	0.26		0.26	0.17	0.18		0.18
VCA0753	0.28	0.28		0.28	0.19	0.16	0.22	0.19
VCA0754	0.28	0.32		0.30	0.27	0.22		0.24
VCA0755	0.24	0.21		0.22	0.18	0.19		0.19
VCA0756	0.26	0.28		0.27	0.23	0.22		0.22
VCA0757	0.18	0.20		0.19	0.18	0.16		0.17
VCA0758	0.27	0.27		0.27	0.17	0.19		0.18
VCA0759	0.14	0.16		0.15	0.15	0.14		0.14
VCA0760	0.19	0.20		0.19	0.13	0.18		0.15
VCA0761	0.23	0.24		0.24				
VCA0762	0.26	0.22		0.24				
VCA0763	0.24	0.24		0.24	0.22	0.21	0.20	0.21
VCA0764	0.26	0.26		0.26	0.18	0.18	0.26	0.21
VCA0765	0.15	0.16		0.16	0.14	0.15		0.15
VCA0766	0.24	0.24		0.24	0.12	0.11		0.11
VCA0767	0.24	0.23		0.23	0.12	0.14		0.13

VCA0768	0.23	0.21		0.22	0.14	0.13		0.14
VCA0769	0.20	0.23		0.22	0.16	0.14		0.15
VCA0770	0.24	0.24		0.24	0.09	0.12		0.11
VCA0771	0.24	0.24		0.24	0.13	0.15		0.14
VCA0772	0.26	0.26		0.26	0.18	0.18		0.18
VCA0773	0.31	0.28	0.27	0.29	0.17	0.17		0.17
VCA0774	0.24	0.23		0.23	0.10	0.13		0.11
VCA0775	0.25	0.27		0.26	0.16	0.16	0.15	0.16
VCA0776	0.25	0.24		0.25	0.20	0.18	0.22	0.20
VCA0777	0.21	0.20		0.21	0.18	0.15	0.17	0.17
VCA0778	0.27	0.27		0.27	0.20	0.16		0.18
VCA0779	0.27	0.25		0.26	0.20	0.27	0.24	0.24
VCA0780	0.24	0.24		0.24	0.10	0.10		0.10
VCA0781	0.30	0.28		0.29	0.20	0.20		0.20
VCA0782	0.23	0.25		0.24	0.14	0.15		0.15
VCA0783	0.23	0.22		0.23	0.16	0.17	0.18	0.17
VCA0784	0.30	0.28		0.29	0.16	0.16		0.16
VCA0785	0.35	0.33		0.34	0.19	0.20	0.21	0.20
VCA0786	0.19	0.18		0.18	0.16	0.15		0.15
VCA0787	0.26	0.24		0.25	0.25	0.20	0.16	0.20
VCA0788	0.23	0.24		0.24				
VCA0789	0.26	0.30		0.28	0.17	0.15		0.16
VCA0790	0.20	0.21		0.20	0.14	0.14	0.15	0.15
VCA0791	0.25	0.28		0.27				
VCA0792	0.29	0.29		0.29	0.20	0.15		0.18
VCA0793	0.29	0.26		0.28	0.14	0.17		0.15
VCA0794	0.30	0.29		0.30	0.18	0.21		0.20
VCA0795	0.27	0.26		0.27	0.16	0.16		0.16
VCA0796	0.26	0.23		0.24	0.19	0.19	0.17	0.18
VCA0797	0.23	0.24		0.23	0.15	0.14		0.15
VCA0798	0.22	0.23		0.23	0.15	0.17		0.16
VCA0799	0.29	0.26		0.28	0.19	0.17		0.18
VCA0800	0.28	0.31		0.30	0.17	0.21		0.19
VCA0801	0.24	0.26		0.25	0.17	0.15	0.17	0.16
VCA0802	0.30	0.31		0.31	0.23	0.23	0.23	0.23
VCA0803	0.26	0.27		0.26	0.22	0.18	0.20	0.20
VCA0804	0.34	0.26		0.30	0.19	0.19		0.19
VCA0805	0.21	0.21		0.21	0.02	0.02		0.02
VCA0806	0.24	0.21		0.22				
VCA0807	0.24	0.24		0.24	0.18	0.18		0.18
VCA0808	0.18	0.20		0.19	0.27	0.23	0.26	0.25
VCA0809	0.25	0.23		0.24	0.19	0.21	0.20	0.20
VCA0810	0.22	0.21		0.21	0.13	0.13		0.13

VCA0811	0.28	0.25	0.26				
VCA0812	0.18	0.19	0.19	0.11	0.11	0.11	0.11
VCA0813	0.29	0.25	0.27	0.16	0.16	0.14	0.15
VCA0814	0.29	0.25	0.27	0.15	0.16	0.12	0.14
VCA0815	0.25	0.25	0.25	0.19	0.17	0.18	0.18
VCA0816	0.22	0.21	0.22	0.17	0.16		0.16
VCA0817	0.36	0.29	0.33	0.18	0.20	0.18	0.19
VCA0819	0.24	0.28	0.26	0.18	0.17	0.17	0.17
VCA0820	0.18	0.18	0.18	0.16	0.16		0.16
VCA0821	0.22	0.23	0.23	0.18	0.19		0.18
VCA0822	0.19	0.22	0.21	0.19	0.18	0.18	0.19
VCA0823	0.27	0.25	0.26	0.17	0.18	0.17	0.17
VCA0824	0.24	0.22	0.23	0.20	0.20	0.19	0.20
VCA0825	0.25	0.26	0.25	0.18	0.18	0.17	0.18
VCA0826	0.22	0.22	0.22	0.17	0.21		0.19
VCA0827	0.22	0.25	0.24	0.16	0.18	0.19	0.18
VCA0828	0.31	0.29	0.30	0.16	0.18	0.13	0.16
VCA0830	0.21	0.24	0.23	0.13	0.13	0.14	0.13
VCA0831	0.25	0.21	0.23	0.16	0.13		0.14
VCA0832	0.24	0.26	0.25	0.16	0.13		0.14
VCA0833	0.20	0.18	0.19	0.14	0.12		0.13
VCA0834	0.25	0.26	0.25	0.16	0.16		0.16
VCA0835	0.20	0.24	0.22	0.18	0.19		0.18
VCA0836	0.27	0.25	0.26	0.21	0.24	0.22	0.22
VCA0837	0.29	0.29	0.29	0.26	0.23		0.24
VCA0838	0.20	0.21	0.20	0.14	0.10		0.12
VCA0839	0.23	0.25	0.24	0.13	0.16		0.14
VCA0840	0.26	0.24	0.25	0.14	0.13		0.14
VCA0841	0.28	0.25	0.27	0.13	0.15		0.14
VCA0842	0.26	0.26	0.26	0.21	0.12	0.13	0.15
VCA0843	0.30	0.31	0.30	0.11	0.14		0.13
VCA0844	0.25	0.24	0.24	0.23	0.17	0.15	0.19
VCA0845	0.23	0.25	0.24	0.15	0.15		0.15
VCA0846	0.30	0.32	0.31	0.18	0.21		0.19
VCA0847	0.26	0.23	0.25	0.21	0.22		0.22
VCA0848	0.21	0.21	0.21	0.14	0.14		0.14
VCA0850	0.26	0.28	0.27	0.13	0.14		0.14
VCA0851	0.23	0.24	0.24	0.19	0.22		0.20
VCA0852	0.29	0.28	0.29	0.17	0.17		0.17
VCA0853	0.21	0.19	0.20	0.15	0.18		0.17
VCA0854	0.33	0.28	0.31	0.22	0.18		0.20
VCA0855	0.24	0.26	0.25	0.19	0.16		0.17
VCA0856	0.24	0.23	0.24	0.12	0.11		0.11

VCA0857	0.24	0.28		0.26	0.12	0.14		0.13
VCA0858	0.25	0.25		0.25	0.21	0.17		0.19
VCA0859	0.06	0.08		0.07	0.20	0.18		0.19
VCA0861	0.25	0.27		0.26	0.26	0.21	0.26	0.24
VCA0862	0.26	0.25	0.25	0.26	0.20	0.20		0.20
VCA0863	0.26	0.24		0.25	0.14	0.17		0.15
VCA0864	0.32	0.23		0.28	0.20	0.20		0.20
VCA0865	0.22	0.24		0.23	0.12	0.14		0.13
VCA0866	0.23	0.24		0.23	0.11	0.12		0.12
VCA0867	0.24	0.25	0.28	0.26	0.23	0.25		0.24
VCA0868	0.25	0.26		0.26	0.21	0.23	0.25	0.23
VCA0869	0.28	0.26		0.27	0.13	0.11		0.12
VCA0870	0.29	0.26	0.27	0.27	0.18	0.17		0.18
VCA0871	0.27	0.26		0.27	0.14	0.15		0.15
VCA0872	0.30	0.29		0.30	0.22	0.19		0.21
VCA0873	0.27	0.27	0.29	0.28	0.18	0.18		0.18
VCA0874	0.23	0.21		0.22	0.12	0.14		0.13
VCA0875	0.26	0.24		0.25	0.16	0.12		0.14
VCA0876	0.32	0.30	0.31	0.31	0.11	0.12		0.12
VCA0878	0.16	0.16		0.16	0.12	0.10		0.11
VCA0879	0.22	0.23		0.22	0.15	0.16		0.16
VCA0880	0.18	0.18	0.16	0.17	0.13	0.11		0.12
VCA0882	0.21	0.21		0.21	0.11	0.09		0.10
VCA0883	0.27	0.27		0.27	0.14	0.16		0.15
VCA0884	0.24	0.26		0.25	0.14	0.15		0.15
VCA0885	0.24	0.25		0.24	0.20	0.15		0.18
VCA0886	0.23	0.24		0.24	0.16	0.14		0.15
VCA0887	0.33	0.29		0.31	0.21	0.21		0.21
VCA0888	0.24	0.25		0.24	0.17	0.17		0.17
VCA0889	0.29	0.30		0.29	0.14	0.16		0.15
VCA0890	0.25	0.26		0.26	0.16	0.18		0.17
VCA0891	0.29	0.30		0.30	0.19	0.20		0.19
VCA0892					0.18	0.16	0.15	0.16
VCA0893	0.30	0.29		0.29	0.14	0.17		0.16
VCA0894	0.29	0.24		0.27	0.15	0.15		0.15
VCA0895	0.28	0.27		0.28	0.17	0.16	0.19	0.17
VCA0896	0.21	0.17		0.19	0.16	0.17		0.16
VCA0897					0.17	0.14	0.12	0.14
VCA0898	0.25	0.24		0.24	0.23	0.18		0.20
VCA0899					0.18	0.18	0.18	0.18
VCA0900	0.26	0.23		0.25	0.18	0.16		0.17
VCA0901	0.26	0.22		0.24	0.17	0.16		0.17
VCA0902	0.33	0.31		0.32	0.18	0.21		0.20

VCA0903	0.25	0.23		0.24	0.15	0.14		0.14
VCA0904	0.31	0.31		0.31	0.20	0.25		0.22
VCA0905	0.25	0.24		0.24	0.18	0.17		0.18
VCA0906	0.20	0.17		0.19	0.12	0.15		0.13
VCA0907	0.23	0.18		0.20	0.15	0.14		0.14
VCA0908	0.28	0.26		0.27	0.22	0.16		0.19
VCA0909	0.23	0.23		0.23	0.16	0.17		0.16
VCA0910	0.30	0.32		0.31	0.15	0.15		0.15
VCA0911					0.24	0.20	0.19	0.21
VCA0912	0.25	0.27		0.26	0.18	0.19		0.18
VCA0913	0.24	0.26		0.25	0.15	0.15		0.15
VCA0914	0.30	0.33		0.32	0.22	0.18		0.20
VCA0915	0.21	0.22		0.22	0.14	0.15		0.14
VCA0916	0.22	0.23		0.23	0.14	0.15		0.14
VCA0917	0.23	0.25		0.24	0.15	0.16		0.16
VCA0918	0.20	0.21		0.20	0.12	0.15	0.15	0.14
VCA0919	0.24	0.26		0.25	0.23	0.16		0.19
VCA0920	0.27	0.29		0.28	0.23	0.23		0.23
VCA0921	0.22	0.21	0.21	0.21	0.12	0.11		0.12
VCA0922	0.22	0.20		0.21	0.21	0.14		0.18
VCA0923	0.26	0.25	0.27	0.26	0.22	0.22		0.22
VCA0924	0.27	0.25	0.26	0.26	0.18	0.17		0.18
VCA0925	0.24	0.23		0.24	0.17	0.14		0.16
VCA0926	0.31	0.31		0.31	0.23	0.20		0.21
VCA0927	0.30	0.28	0.28	0.29	0.20	0.20		0.20
VCA0928	0.29	0.25	0.29	0.28	0.19	0.22		0.20
VCA0929	0.22	0.22		0.22	0.20	0.20		0.20
VCA0930	0.30	0.29	0.29	0.29	0.19	0.18		0.19
VCA0931	0.53	0.54		0.53	0.24	0.32		0.28
VCA0932	0.32	0.24		0.28	0.14	0.12		0.13
VCA0933	0.25	0.23		0.24	0.15	0.17		0.16
VCA0934	0.18	0.24		0.21	0.21	0.16	0.16	0.17
VCA0935	0.21	0.22		0.22	0.15	0.20		0.18
VCA0936	0.30	0.31		0.30	0.14	0.17		0.15
VCA0937	0.23	0.20	0.22	0.22	0.15	0.14		0.15
VCA0938	0.25	0.25		0.25	0.19	0.14	0.16	0.16
VCA0939	0.20	0.24		0.22	0.19	0.20		0.20
VCA0940	0.27	0.24		0.26	0.20	0.25		0.23
VCA0941	0.24	0.23	0.24	0.24	0.17	0.16		0.17
VCA0942	0.23	0.23		0.23	0.16	0.17		0.16
VCA0943	0.26	0.26		0.26	0.22	0.19		0.21
VCA0944	0.31	0.25		0.28	0.17	0.19		0.18
VCA0945	0.19	0.21		0.20	0.17	0.16		0.16

VCA0946	0.22	0.22		0.22	0.18	0.18		0.18
VCA0947	0.21	0.21		0.21	0.20	0.18		0.19
VCA0948	0.26	0.24		0.25	0.24	0.20		0.22
VCA0949	0.21	0.22		0.21	0.15	0.18		0.16
VCA0950	0.25	0.25		0.25	0.17	0.19		0.18
VCA0951	0.25	0.25		0.25	0.22	0.22		0.22
VCA0952	0.32	0.25		0.29	0.13	0.18		0.15
VCA0953	0.21	0.21		0.21	0.18	0.18		0.18
VCA0954	0.23	0.22		0.22	0.14	0.15		0.15
VCA0955	0.27	0.28		0.28	0.18	0.15		0.16
VCA0956	0.22	0.24		0.23	0.13	0.13		0.13
VCA0957	0.22	0.22	0.31	0.25	0.16	0.18		0.17
VCA0958	0.21	0.25		0.23	0.13	0.16		0.15
VCA0959	0.24	0.23		0.23	0.17	0.18		0.17
VCA0960	0.25	0.27		0.26	0.13	0.14		0.14
VCA0961	0.22	0.22	0.22	0.22	0.18	0.16		0.17
VCA0962	0.27	0.25		0.26	0.18	0.19		0.18
VCA0963	0.28	0.32	0.30	0.30	0.20	0.27		0.23
VCA0964	0.23	0.28	0.25	0.25	0.16	0.12		0.14
VCA0965	0.23	0.23		0.23	0.06	0.06		0.06
VCA0966	0.24	0.25		0.25	0.16	0.16		0.16
VCA0967	0.27	0.28		0.27	0.26	0.25	0.25	0.25
VCA0968	0.25	0.26		0.25	0.18	0.18		0.18
VCA0969	0.24	0.24		0.24	0.17	0.16	0.15	0.16
VCA0970	0.21	0.23		0.22	0.18	0.18		0.18
VCA0971	0.27	0.27		0.27	0.19	0.18		0.18
VCA0972	0.20	0.19		0.19	0.19	0.15	0.17	0.17
VCA0973	0.24	0.22		0.23	0.12	0.12		0.12
VCA0974	0.31	0.25		0.28	0.24	0.20	0.20	0.21
VCA0975	0.23	0.24		0.24	0.20	0.15		0.18
VCA0976	0.21	0.23		0.22	0.12	0.14		0.13
VCA0977	0.22	0.22		0.22	0.13	0.16	0.15	0.15
VCA0979	0.23	0.25	0.23	0.24	0.17	0.15		0.16
VCA0980	0.17	0.18		0.18	0.13	0.12		0.12
VCA0981	0.24	0.21		0.23	0.14	0.13	0.16	0.14
VCA0982	0.26	0.29	0.26	0.27	0.18	0.15		0.16
VCA0983	0.28	0.27		0.27	0.20	0.20		0.20
VCA0984	0.26	0.26		0.26	0.17	0.15		0.16
VCA0985	0.22	0.22		0.22	0.14	0.16		0.15
VCA0986	0.26	0.26	0.27	0.26	0.15	0.16		0.15
VCA0987	0.31	0.32		0.32	0.20	0.18		0.19
VCA0988	0.23	0.22		0.23	0.12	0.17	0.15	0.15
VCA0989	0.24	0.23		0.24	0.19	0.20	0.17	0.19

VCA0990	0.19	0.23		0.21	0.13	0.08		0.10
VCA0991	0.21	0.24		0.23	0.16	0.15		0.15
VCA0992	0.32	0.29		0.31	0.14	0.15		0.15
VCA0993	0.24	0.20		0.22	0.12	0.15		0.13
VCA0994	0.28	0.24		0.26	0.15	0.15		0.15
VCA0995	0.24	0.26		0.25	0.19	0.18		0.19
VCA0996	0.24	0.23		0.23	0.13	0.18		0.15
VCA0997	0.29	0.28		0.28	0.18	0.17		0.17
VCA0998	0.20	0.22		0.21	0.13	0.11		0.12
VCA0999	0.27	0.29		0.28	0.13	0.13		0.13
VCA1000	0.20	0.22		0.21	0.20	0.23		0.22
VCA1001	0.19	0.16		0.18	0.12	0.13		0.12
VCA1002	0.26	0.24		0.25	0.19	0.22		0.21
VCA1003	0.26	0.22		0.24	0.16	0.16		0.16
VCA1004	0.26	0.28		0.27	0.13	0.15		0.14
VCA1005	0.22	0.25		0.23	0.18	0.19		0.19
VCA1006	0.23	0.23		0.23	0.14	0.14		0.14
VCA1007	0.24	0.26		0.25	0.19	0.17		0.18
VCA1008	0.21	0.21		0.21	0.25	0.23		0.24
VCA1009	0.24	0.29		0.26	0.17	0.16		0.16
VCA1010	0.22	0.25		0.23	0.20	0.17		0.19
VCA1011	0.26	0.27		0.27	0.19	0.20		0.19
VCA1012	0.23	0.27		0.25	0.22	0.23		0.22
VCA1013	0.21	0.26		0.24	0.17	0.16		0.16
VCA1014	0.27	0.25		0.26	0.25	0.21	0.16	0.21
VCA1015	0.28	0.31		0.30	0.19	0.18		0.19
VCA1016	0.26	0.27		0.26	0.19	0.23		0.21
VCA1017	0.24	0.30		0.27	0.15	0.19		0.17
VCA1018	0.23	0.22		0.23	0.16	0.20		0.18
VCA1019	0.23	0.17		0.20	0.25	0.21		0.23
VCA1021	0.25	0.24		0.24	0.19	0.16		0.18
VCA1024	0.21	0.25		0.23	0.13	0.14		0.13
VCA1025	0.23	0.19		0.21	0.13	0.15		0.14
VCA1026	0.25	0.32		0.29	0.22	0.23		0.22
VCA1027	0.23	0.24		0.23	0.17	0.18		0.18
VCA1028	0.25	0.26		0.26	0.23	0.24		0.24
VCA1029	0.15	0.15		0.15	0.14	0.14		0.14
VCA1030	0.27	0.25		0.26	0.20	0.21	0.18	0.19
VCA1031	0.23	0.21		0.22	0.18	0.14	0.22	0.18
VCA1032	0.24	0.22	0.25	0.24	0.13	0.15		0.14
VCA1033	0.27	0.24	0.30	0.27	0.16	0.16		0.16
VCA1034	0.22	0.23		0.23	0.20	0.15		0.18
VCA1035	0.25	0.22	0.26	0.24	0.14	0.17		0.16

VCA1037	0.26	0.25	0.26	0.26	0.14	0.15		0.14
VCA1038	0.27	0.28	0.28	0.27	0.22	0.21		0.22
VCA1039	0.18	0.18	0.19	0.18	0.12	0.12		0.12
VCA1040	0.26	0.26		0.26	0.19	0.19		0.19
VCA1041	0.27	0.25		0.26	0.21	0.13		0.17
VCA1042	0.24	0.24	0.29	0.26	0.12	0.13		0.13
VCA1043	0.22	0.22		0.22	0.08	0.10		0.09
VCA1044	0.25	0.24		0.24	0.12	0.13	0.13	0.13
VCA1045	0.27	0.26		0.26	0.23	0.20		0.22
VCA1046	0.30	0.22	0.26	0.26	0.16	0.19		0.17
VCA1047	0.26	0.26	0.32	0.28	0.12	0.14		0.13
VCA1048	0.28	0.25		0.26	0.20	0.17		0.19
VCA1049	0.31	0.32		0.31	0.17	0.18		0.17
VCA1050	0.30	0.29	0.30	0.30	0.15	0.15		0.15
VCA1051	0.18	0.17	0.18	0.18	0.15	0.15		0.15
VCA1052	0.30	0.29	0.31	0.30	0.23	0.23		0.23
VCA1053	0.33	0.25	0.26	0.28	0.16	0.16		0.16
VCA1054	0.23	0.23	0.23	0.23	0.21	0.21		0.21
VCA1055	0.25	0.24		0.25	0.17	0.12		0.15
VCA1056	0.24	0.22		0.23	0.13	0.13		0.13
VCA1057	0.21	0.21		0.21	0.17	0.18	0.16	0.17
VCA1058	0.24	0.24	0.23	0.24	0.16	0.16		0.16
VCA1059	0.25	0.25		0.25	0.14	0.14		0.14
VCA1060	0.24	0.26		0.25	0.17	0.19	0.19	0.18
VCA1061	0.16	0.24		0.20	0.20	0.17	0.19	0.19
VCA1062	0.30	0.31	0.31	0.31	0.15	0.17		0.16
VCA1063	0.24	0.22		0.23	0.15	0.18		0.16
VCA1064	0.23	0.25		0.24	0.16	0.12	0.14	0.14
VCA1065	0.22	0.24		0.23	0.18	0.16	0.17	0.17
VCA1066	0.21	0.20		0.21	0.22	0.24	0.16	0.21
VCA1067	0.31	0.30		0.31	0.21	0.20		0.21
VCA1068	0.19	0.22		0.20	0.12	0.14		0.13
VCA1069	0.31	0.26		0.29	0.24	0.22		0.23
VCA1070	0.24	0.24	0.26	0.24	0.11	0.14		0.12
VCA1071	0.28	0.27	0.26	0.27	0.16	0.19		0.18
VCA1072	0.24	0.24		0.24	0.18	0.14		0.16
VCA1073	0.20	0.20		0.20	0.14	0.16		0.15
VCA1074	0.27	0.28		0.27	0.17	0.18		0.18
VCA1075	0.23	0.24	0.23	0.23	0.16	0.18		0.17
VCA1076	0.25	0.26		0.25	0.18	0.18		0.18
VCA1077	0.22	0.21		0.22	0.13	0.14		0.14
VCA1078	0.24	0.25	0.23	0.24	0.18	0.21		0.19
VCA1079	0.20	0.22		0.21	0.13	0.14		0.13

VCA1080	0.31	0.26	0.30	0.29	0.19	0.21		0.20
VCA1081	0.26	0.23		0.24	0.15	0.17		0.16
VCA1083	0.25	0.24		0.24	0.14	0.15		0.15
VCA1084	0.21	0.18		0.19	0.16	0.21		0.19
VCA1085	0.21	0.21		0.21	0.13	0.13		0.13
VCA1086	0.20	0.20		0.20	0.13	0.14		0.13
VCA1087	0.25	0.22		0.24	0.16	0.20		0.18
VCA1088	0.20	0.20	0.18	0.19	0.16	0.19		0.18
VCA1089	0.22	0.19		0.20	0.13	0.12	0.17	0.14
VCA1090	0.22	0.23		0.23	0.18	0.15		0.17
VCA1091	0.22	0.22		0.22	0.17	0.15		0.16
VCA1092	0.23	0.23		0.23	0.14	0.18		0.16
VCA1093	0.20	0.19		0.19	0.13	0.12		0.13
VCA1094	0.20	0.21		0.21	0.16	0.14		0.15
VCA1095	0.23	0.20		0.22	0.14	0.16		0.15
VCA1096	0.19	0.19	0.19	0.19	0.17	0.18		0.17
VCA1097	0.38	0.37		0.37	0.17	0.15		0.16
VCA1098	0.20	0.24	0.18	0.21	0.19	0.20		0.19
VCA1099	0.26	0.25	0.26	0.26	0.17	0.19		0.18
VCA1100	0.29	0.33		0.31	0.23	0.22		0.22
VCA1101	0.26	0.24	0.27	0.26	0.12	0.13		0.13
VCA1102	0.27	0.25		0.26	0.16	0.17		0.16
VCA1103	0.27	0.25	0.24	0.25	0.24	0.17		0.20
VCA1104	0.23	0.25		0.24	0.15	0.17	0.17	0.16
VCA1105	0.24	0.31		0.28	0.17	0.18		0.17
VCA1106	0.25	0.26		0.25	0.17	0.20	0.19	0.19
VCA1107	0.29	0.25		0.27	0.13	0.13		0.13
VCA1108	0.26	0.28		0.27	0.20	0.22		0.21
VCA1109	0.16	0.18		0.17	0.15	0.18		0.16
VCA1110	0.21	0.18		0.20	0.22	0.22		0.22
VCA1111	0.17	0.14		0.16	0.12	0.13		0.13
VCA1112	0.23	0.24		0.24	0.18	0.18		0.18
VCA1113	0.23	0.21		0.22	0.18	0.16		0.17
VCA1114	0.23	0.23	0.23	0.23	0.13	0.14		0.14
VCA1115	0.27	0.26		0.26	0.12	0.17		0.15
Average fraction bound of entire library				0.25				0.17
One standard deviation				0.04				0.04
Average + 3 standard deviations				0.36				0.28

*Fraction bounds were corrected for background binding by plate by subtracting the plate average fraction bound from each ORF and adjusted by setting the lowest fraction bound value to 0.

List of Abbreviations

ATP: adenosine triphosphate

c-di-AMP: bis-(3´-5´)-cyclic dimeric adenosine monophosphate

c-di-GMP: bis-(3´-5´)-cyclic dimeric guanosine monophosphate

cAG: 3´-5´, 5´-3´-cyclic adenosine monophosphate guanosine monophosphate

cAMP: cyclic adenosine monophosphate

cGMP: cyclic guanosine monophosphate

CTP: cytosine triphosphate

DGC: diguanylate cyclase

DHHA1: DHH-associated domain

DNA: deoxyribonucleic acid

DRaCALA: Differential Radial Capillary Action of Ligand Assay

EDTA: ethylenediaminetetraacetic acid

GDP: guanosine diphosphate

GMP: guanosine monophosphate

GTP: guanosine triphosphate

His-MBP-ORF: histidine-maltose binding protein fusion to an open reading frame

His-ORF: histidine fusion to an open reading frame

HPLC: high-performance liquid chromatography

IPTG: Isopropyl β-D-1-thiogalactopyranoside

k_{cat}: turnover number

K_d: dissociation constant

K_m: Michaelis constant

LB: Lysogeny Broth

LC-MS/MS: liquid chromatography-tandem mass spectrometry

MBP: maltose binding protein

nmer: an oligoribonucleotide n nucleotides in length

OD_{600}: optical density at 600 nm

ORF: open reading frame

ORFeome: ORF library containing a majority of ORFs from a genome

PAGE: polyacrylamide gel electrophoresis

PCR: polymerase chain reaction

PDE-A: phosphodiesterase A

PDE-B: phosphodiesterase B

PMSF: phenylmethane sulfonyl fluoride or phenylmethylsulfonyl fluoride

(p)ppGpp: guanosine pentaphosphate

pApA: 5´-phosphoadenylyl-(3´-5´)-adenosine

pApG: 5´-phosphoadenylyl-(3´-5´)- guanosine

pGpG: 5´-phosphoguanylyl-(3´-5´)-guanosine

poly(A): poly-adenosine RNA

poly(U): poly-uracil RNA

RNA: ribonucleic acid

SD: standard deviation

SDS: sodium dodecyl sulfate

SCV: small colony variant of *P. aeruginosa*

TLC: thin layer chromatography

UTP: uracil triphosphate

vol:vol: volume-to-volume ratio

Bibliography

1. Kolb A, Busby S, Buc H, Garges S, & Adhya S (1993) Transcriptional regulation by cAMP and its receptor protein. *Annu Rev Biochem* 62:749-795.
2. Emmer M, deCrombrugghe B, Pastan I, & Perlman R (1970) Cyclic AMP receptor protein of *E. coli*: its role in the synthesis of inducible enzymes. *Proc Natl Acad Sci U S A* 66(2):480-487.
3. Zubay G, Schwartz D, & Beckwith J (1970) Mechanism of activation of catabolite-sensitive genes: a positive control system. *Proc Natl Acad Sci U S A* 66(1):104-110.
4. Pesavento C & Hengge R (2009) Bacterial nucleotide-based second messengers. *Curr Opin Microbiol* 12(2):170-176.
5. Römling U, Galperin MY, & Gomelsky M (2013) Cyclic di-GMP: the first 25 years of a universal bacterial second messenger. *Microbiol Mol Biol Rev* 77(1):1-52.
6. Corrigan RM & Gründling A (2013) Cyclic di-AMP: another second messenger enters the fray. *Nat Rev Microbiol* 11(8):513-524.
7. Linder JU (2010) cGMP production in bacteria. *Mol Cell Biochem* 334(1-2):215-219.
8. Ross P*, et al.* (1987) Regulation of cellulose synthesis in *Acetobacter xylinum* by cyclic diguanylic acid. *Nature* 325(6101):279-281.
9. Tal R*, et al.* (1998) Three cdg operons control cellular turnover of cyclic di-GMP in *Acetobacter xylinum*: genetic organization and occurrence of conserved domains in isoenzymes. *J Bacteriol* 180(17):4416-4425.
10. Ryjenkov DA, Tarutina M, Moskvin OV, & Gomelsky M (2005) Cyclic diguanylate is a ubiquitous signaling molecule in bacteria: insights into biochemistry of the GGDEF protein domain. *J Bacteriol* 187(5):1792-1798.
11. Simm R, Morr M, Kader A, Nimtz M, & Römling U (2004) GGDEF and EAL domains inversely regulate cyclic di-GMP levels and transition from sessility to motility. *Mol Microbiol* 53(4):1123-1134.
12. Ausmees N*, et al.* (2001) Genetic data indicate that proteins containing the GGDEF domain possess diguanylate cyclase activity. *FEMS Microbiol Lett* 204(1):163-167.
13. Tamayo R, Tischler AD, & Camilli A (2005) The EAL domain protein VieA is a cyclic diguanylate phosphodiesterase. *J Biol Chem* 280(39):33324-33330.
14. Schmidt AJ, Ryjenkov DA, & Gomelsky M (2005) The ubiquitous protein domain EAL is a cyclic diguanylate-specific phosphodiesterase: enzymatically active and inactive EAL domains. *J Bacteriol* 187(14):4774-4781.
15. Ryan RP*, et al.* (2006) Cell-cell signaling in *Xanthomonas campestris* involves an HD-GYP domain protein that functions in cyclic di-GMP turnover. *Proc Natl Acad Sci U S A* 103(17):6712-6717.

16. Galperin MY, Nikolskaya AN, & Koonin EV (2001) Novel domains of the prokaryotic two-component signal transduction systems. *FEMS Microbiol Lett* 203(1):11-21.
17. Amikam D & Galperin MY (2006) PilZ domain is part of the bacterial c-di-GMP binding protein. *Bioinformatics* 22(1):3-6.
18. Ryjenkov DA, Simm R, Römling U, & Gomelsky M (2006) The PilZ domain is a receptor for the second messenger c-di-GMP: the PilZ domain protein YcgR controls motility in enterobacteria. *J Biol Chem* 281(41):30310-30314.
19. Hengge R (2009) Principles of c-di-GMP signalling in bacteria. *Nat Rev Microbiol* 7(4):263-273.
20. Schirmer T & Jenal U (2009) Structural and mechanistic determinants of c-di-GMP signalling. *Nat Rev Microbiol* 7(10):724-735.
21. Duerig A*, et al.* (2009) Second messenger-mediated spatiotemporal control of protein degradation regulates bacterial cell cycle progression. *Genes Dev* 23(1):93-104.
22. Newell PD, Monds RD, & O'Toole GA (2009) LapD is a bis-(3',5')-cyclic dimeric GMP-binding protein that regulates surface attachment by *Pseudomonas fluorescens* Pf0-1. *Proc Natl Acad Sci U S A* 106(9):3461-3466.
23. Qi Y*, et al.* (2011) Binding of cyclic diguanylate in the non-catalytic EAL domain of FimX induces a long-range conformational change. *J Biol Chem* 286(4):2910-2917.
24. Navarro MV, De N, Bae N, Wang Q, & Sondermann H (2009) Structural analysis of the GGDEF-EAL domain-containing c-di-GMP receptor FimX. *Structure* 17(8):1104-1116.
25. Lee VT*, et al.* (2007) A cyclic-di-GMP receptor required for bacterial exopolysaccharide production. *Mol Microbiol* 65(6):1474-1484.
26. Srivastava D, Hsieh ML, Khataokar A, Neiditch MB, & Waters CM (2013) Cyclic di-GMP inhibits *Vibrio cholerae* motility by repressing induction of transcription and inducing extracellular polysaccharide production. *Mol Microbiol* 90(6):1262-1276.
27. Hickman JW & Harwood CS (2008) Identification of FleQ from *Pseudomonas aeruginosa* as a c-di-GMP-responsive transcription factor. *Mol Microbiol* 69(2):376-389.
28. Baraquet C & Harwood CS (2013) Cyclic diguanosine monophosphate represses bacterial flagella synthesis by interacting with the Walker A motif of the enhancer-binding protein FleQ. *Proc Natl Acad Sci U S A* 110(46):18478-18483.
29. Tschowri N*, et al.* (2014) Tetrameric c-di-GMP mediates effective transcription factor dimerization to control *Streptomyces* development. *Cell* 158(5):1136-1147.
30. Leduc JL & Roberts GP (2009) Cyclic di-GMP allosterically inhibits the CRP-like protein (Clp) of *Xanthomonas axonopodis* pv. citri. *J Bacteriol* 191(22):7121-7122.
31. Chin KH*, et al.* (2010) The cAMP receptor-like protein Clp is a novel c-di-GMP receptor linking cell-cell signaling to virulence gene expression in *Xanthomonas campestris*. *J Mol Biol* 396(3):646-662.

32. Tao F, He YW, Wu DH, Swarup S, & Zhang LH (2010) The cyclic nucleotide monophosphate domain of *Xanthomonas campestris* global regulator Clp defines a new class of cyclic di-GMP effectors. *J Bacteriol* 192(4):1020-1029.
33. Krasteva PV*, et al.* (2010) *Vibrio cholerae* VpsT regulates matrix production and motility by directly sensing cyclic di-GMP. *Science* 327(5967):866-868.
34. Sudarsan N*, et al.* (2008) Riboswitches in eubacteria sense the second messenger cyclic di-GMP. *Science* 321(5887):411-413.
35. Lee ER, Baker JL, Weinberg Z, Sudarsan N, & Breaker RR (2010) An allosteric self-splicing ribozyme triggered by a bacterial second messenger. *Science* 329(5993):845-848.
36. Condon C (2007) Maturation and degradation of RNA in bacteria. *Curr Opin Microbiol* 10(3):271-278.
37. Goldman SR, Ebright RH, & Nickels BE (2009) Direct detection of abortive RNA transcripts in vivo. *Science* 324(5929):927-928.
38. Jenal U & Malone J (2006) Mechanisms of cyclic-di-GMP signaling in bacteria. *Annu Rev Genet* 40:385-407.
39. Goldman SR*, et al.* (2011) NanoRNAs prime transcription initiation in vivo. *Mol Cell* 42(6):817-825.
40. Vvedenskaya IO*, et al.* (2012) Growth phase-dependent control of transcription start site selection and gene expression by nanoRNAs. *Genes Dev* 26(13):1498-1507.
41. Druzhinin SY*, et al.* (2015) A conserved pattern of primer-dependent transcription initiation in *Escherichia coli* and *Vibrio cholerae* revealed by 5' RNA-Seq. *PLoS Genet* 11(7):e1005348.
42. Lacey MM, Partridge JD, & Green J (2010) *Escherichia coli* K-12 YfgF is an anaerobic cyclic di-GMP phosphodiesterase with roles in cell surface remodelling and the oxidative stress response. *Microbiology* 156(Pt 9):2873-2886.
43. Roelofs KG, Wang J, Sintim HO, & Lee VT (2011) Differential radial capillary action of ligand assay for high-throughput detection of protein-metabolite interactions. *Proc Natl Acad Sci U S A* 108(37):15528-15533.
44. Corrigan RM*, et al.* (2013) Systematic identification of conserved bacterial c-di-AMP receptor proteins. *Proc Natl Acad Sci U S A* 110(22):9084-9089.
45. Roelofs KG*, et al.* (2015) Systematic identification of cyclic-di-GMP binding proteins in *Vibrio cholerae* reveals a novel class of cyclic-di-GMP-binding ATPases associated with type II secretion systems. *PLoS pathogens* 11(10):e1005232.
46. Fang X*, et al.* (2014) GIL, a new c-di-GMP-binding protein domain involved in regulation of cellulose synthesis in enterobacteria. *Mol Microbiol* 93(3):439-452.
47. Beyhan S, Tischler AD, Camilli A, & Yildiz FH (2006) Transcriptome and phenotypic responses of *Vibrio cholerae* to increased cyclic di-GMP level. *J Bacteriol* 188(10):3600-3613.
48. Rolfs A*, et al.* (2008) Production and sequence validation of a complete full length ORF collection for the pathogenic bacterium *Vibrio cholerae*. *Proc Natl Acad Sci U S A* 105(11):4364-4369.

49. Datta AK & Niyogi K (1975) A novel oligoribonuclease of *Escherichia coli*. II. Mechanism of action. *J Biol Chem* 250(18):7313-7319.
50. Niyogi SK & Datta AK (1975) A novel oligoribonuclease of *Escherichia coli*. I. Isolation and properties. *J Biol Chem* 250(18):7307-7312.
51. Zhang X, Zhu L, & Deutscher MP (1998) Oligoribonuclease is encoded by a highly conserved gene in the 3'-5' exonuclease superfamily. *J Bacteriol* 180(10):2779-2781.
52. Ghosh S & Deutscher MP (1999) Oligoribonuclease is an essential component of the mRNA decay pathway. *Proc Natl Acad Sci U S A* 96(8):4372-4377.
53. Mechold U, Ogryzko V, Ngo S, & Danchin A (2006) Oligoribonuclease is a common downstream target of lithium-induced pAp accumulation in *Escherichia coli* and human cells. *Nucleic Acids Res* 34(8):2364-2373.
54. Mechold U, Fang G, Ngo S, Ogryzko V, & Danchin A (2007) YtqI from *Bacillus subtilis* has both oligoribonuclease and pAp-phosphatase activity. *Nucleic Acids Res* 35(13):4552-4561.
55. Lee RC & Ambros V (2001) An extensive class of small RNAs in *Caenorhabditis elegans*. *Science* 294(5543):862-864.
56. Lau NC, Lim LP, Weinstein EG, & Bartel DP (2001) An abundant class of tiny RNAs with probable regulatory roles in *Caenorhabditis elegans*. *Science* 294(5543):858-862.
57. Lagos-Quintana M, Rauhut R, Lendeckel W, & Tuschl T (2001) Identification of novel genes coding for small expressed RNAs. *Science* 294(5543):853-858.
58. Fang M*, et al.* (2009) Degradation of nanoRNA is performed by multiple redundant RNases in *Bacillus subtilis*. *Nucleic Acids Res* 37(15):5114-5125.
59. Liu MF*, et al.* (2012) Identification of a novel nanoRNase in *Bartonella*. *Microbiology* 158(Pt 4):886-895.
60. Aravind L & Koonin EV (1998) A novel family of predicted phosphoesterases includes *Drosophila* prune protein and bacterial RecJ exonuclease. *Trends Biochem Sci* 23(1):17-19.
61. Zuo Y & Deutscher MP (2001) Exoribonuclease superfamilies: structural analysis and phylogenetic distribution. *Nucleic Acids Res* 29(5):1017-1026.
62. Friedman L & Kolter R (2004) Genes involved in matrix formation in *Pseudomonas aeruginosa* PA14 biofilms. *Mol Microbiol* 51(3):675-690.
63. Cameron DE, Urbach JM, & Mekalanos JJ (2008) A defined transposon mutant library and its use in identifying motility genes in *Vibrio cholerae*. *Proc Natl Acad Sci U S A* 105(25):8736-8741.
64. Liberati NT*, et al.* (2006) An ordered, nonredundant library of *Pseudomonas aeruginosa* strain PA14 transposon insertion mutants. *Proc Natl Acad Sci U S A* 103(8):2833-2838.
65. Zhang XX, Lilley AK, Bailey MJ, & Rainey PB (2004) Functional and phylogenetic analysis of a plant-inducible oligoribonuclease (*orn*) gene from an indigenous *Pseudomonas* plasmid. *Microbiology* 150(Pt 9):2889-2898.
66. Tamayo R, Pratt JT, & Camilli A (2007) Roles of cyclic diguanylate in the regulation of bacterial pathogenesis. *Annu Rev Microbiol* 61:131-148.
67. Römling U & Simm R (2009) Prevailing concepts of c-di-GMP signaling. *Contrib Microbiol* 16:161-181.

68. Krasteva PV, Giglio KM, & Sondermann H (2012) Sensing the messenger: the diverse ways that bacteria signal through c-di-GMP. *Protein Sci* 21(7):929-948.
69. Aldridge P, Paul R, Goymer P, Rainey P, & Jenal U (2003) Role of the GGDEF regulator PleD in polar development of *Caulobacter crescentus*. *Mol Microbiol* 47(6):1695-1708.
70. Bobrov AG, Kirillina O, & Perry RD (2005) The phosphodiesterase activity of the HmsP EAL domain is required for negative regulation of biofilm formation in *Yersinia pestis*. *FEMS Microbiol Lett* 247(2):123-130.
71. Tischler AD & Camilli A (2004) Cyclic diguanylate (c-di-GMP) regulates *Vibrio cholerae* biofilm formation. *Mol Microbiol* 53(3):857-869.
72. Simm R, Fetherston JD, Kader A, Römling U, & Perry RD (2005) Phenotypic convergence mediated by GGDEF-domain-containing proteins. *J Bacteriol* 187(19):6816-6823.
73. Chan C*, et al.* (2004) Structural basis of activity and allosteric control of diguanylate cyclase. *Proc Natl Acad Sci U S A* 101(49):17084-17089.
74. De N, Navarro MV, Raghavan RV, & Sondermann H (2009) Determinants for the activation and autoinhibition of the diguanylate cyclase response regulator WspR. *J Mol Biol* 393(3):619-633.
75. Yang CY*, et al.* (2011) The structure and inhibition of a GGDEF diguanylate cyclase complexed with (c-di-GMP)(2) at the active site. *Acta Crystallogr D Biol Crystallogr* 67(Pt 12):997-1008.
76. Stelitano V*, et al.* (2013) C-di-GMP hydrolysis by *Pseudomonas aeruginosa* HD-GYP phosphodiesterases: analysis of the reaction mechanism and novel roles for pGpG. *PLoS One* 8(9):e74920.
77. Hickman JW, Tifrea DF, & Harwood CS (2005) A chemosensory system that regulates biofilm formation through modulation of cyclic diguanylate levels. *Proc Natl Acad Sci U S A* 102(40):14422-14427.
78. Ueda A & Wood TK (2009) Connecting quorum sensing, c-di-GMP, *pel* polysaccharide, and biofilm formation in *Pseudomonas aeruginosa* through tyrosine phosphatase TpbA (PA3885). *PLoS Pathog* 5(6):e1000483.
79. Robert-Paganin J, Nonin-Lecomte S, & Réty S (2012) Crystal structure of an EAL domain in complex with reaction product 5'-pGpG. *PLoS One* 7(12):e52424.
80. Irie Y*, et al.* (2012) Self-produced exopolysaccharide is a signal that stimulates biofilm formation in *Pseudomonas aeruginosa*. *Proc Natl Acad Sci U S A* 109(50):20632-20636.
81. Fong JC & Yildiz FH (2008) Interplay between cyclic AMP-cyclic AMP receptor protein and cyclic di-GMP signaling in *Vibrio cholerae* biofilm formation. *J Bacteriol* 190(20):6646-6659.
82. Pratt JT, McDonough E, & Camilli A (2009) PhoB regulates motility, biofilms, and cyclic di-GMP in *Vibrio cholerae*. *J Bacteriol* 191(21):6632-6642.
83. McKee RW, Kariisa A, Mudrak B, Whitaker C, & Tamayo R (2014) A systematic analysis of the in vitro and in vivo functions of the HD-GYP domain proteins of *Vibrio cholerae*. *BMC Microbiol* 14(1):272.

84. Pratt JT, Tamayo R, Tischler AD, & Camilli A (2007) PilZ domain proteins bind cyclic diguanylate and regulate diverse processes in *Vibrio cholerae*. *J Biol Chem* 282(17):12860-12870.
85. Srivastava D, Harris RC, & Waters CM (2011) Integration of cyclic di-GMP and quorum sensing in the control of *vpsT* and *aphA* in *Vibrio cholerae*. *J Bacteriol* 193(22):6331-6341.
86. Chin KH, Yang CY, Chou CC, Wang AH, & Chou SH (2006) The crystal structure of XC847 from *Xanthomonas campestris*: a 3'-5' oligoribonuclease of DnaQ fold family with a novel opposingly shifted helix. *Proteins* 65(4):1036-1040.
87. Zuo Y & Deutscher MP (2002) Mechanism of action of RNase T. I. Identification of residues required for catalysis, substrate binding, and dimerization. *J Biol Chem* 277(51):50155-50159.
88. Merritt JH, Kadouri DE, & O'Toole GA (2005) Growing and analyzing static biofilms. *Curr Protoc Microbiol* Chapter 1:Unit 1B.1.
89. Davies BW, Bogard RW, Young TS, & Mekalanos JJ (2012) Coordinated regulation of accessory genetic elements produces cyclic di-nucleotides for *V. cholerae* virulence. *Cell* 149(2):358-370.
90. Kellenberger CA*, et al.* (2015) GEMM-I riboswitches from *Geobacter* sense the bacterial second messenger cyclic AMP-GMP. *Proc Natl Acad Sci U S A* 112(17):5383-5388.
91. Huynh TN*, et al.* (2015) An HD-domain phosphodiesterase mediates cooperative hydrolysis of c-di-AMP to affect bacterial growth and virulence. *Proc Natl Acad Sci U S A* 112(7):E747-756.
92. Rao F*, et al.* (2010) YybT is a signaling protein that contains a cyclic dinucleotide phosphodiesterase domain and a GGDEF domain with ATPase activity. *J Biol Chem* 285(1):473-482.
93. Gao J*, et al.* (2015) Identification and characterization of phosphodiesterases that specifically degrade 3'3'-cyclic GMP-AMP. *Cell Res* 25(5):539-550.
94. Tatusov RL, Galperin MY, Natale DA, & Koonin EV (2000) The COG database: a tool for genome-scale analysis of protein functions and evolution. *Nucleic Acids Res* 28(1):33-36.
95. Gao X*, et al.* (2013) Functional characterization of core components of the *Bacillus subtilis* cyclic-di-GMP signaling pathway. *J Bacteriol* 195(21):4782-4792.
96. Oppenheimer-Shaanan Y, Wexselblatt E, Katzhendler J, Yavin E, & Ben-Yehuda S (2011) c-di-AMP reports DNA integrity during sporulation in *Bacillus subtilis*. *EMBO Rep* 12(6):594-601.
97. Witte G, Hartung S, Büttner K, & Hopfner KP (2008) Structural biochemistry of a bacterial checkpoint protein reveals diadenylate cyclase activity regulated by DNA recombination intermediates. *Mol Cell* 30(2):167-178.
98. Woolwine SC & Wozniak DJ (1999) Identification of an *Escherichia coli pepA* homolog and its involvement in suppression of the *algB* phenotype in mucoid *Pseudomonas aeruginosa*. *J Bacteriol* 181(1):107-116.

99. Even S, *et al.* (2005) Ribonucleases J1 and J2: two novel endoribonucleases in *B. subtilis* with functional homology to *E. coli* RNase E. *Nucleic Acids Res* 33(7):2141-2152.
100. Tock MR, Walsh AP, Carroll G, & McDowall KJ (2000) The CafA protein required for the 5′-maturation of 16 S rRNA is a 5′-end-dependent ribonuclease that has context-dependent broad sequence specificity. *J Biol Chem* 275(12):8726-8732.
101. Jiang X & Belasco JG (2004) Catalytic activation of multimeric RNase E and RNase G by 5'-monophosphorylated RNA. *Proc Natl Acad Sci U S A* 101(25):9211-9216.
102. Jourdan SS, Kime L, & McDowall KJ (2010) The sequence of sites recognised by a member of the RNase E/G family can control the maximal rate of cleavage, while a 5'-monophosphorylated end appears to function cooperatively in mediating RNA binding. *Biochem Biophys Res Commun* 391(1):879-883.
103. Jourdan SS & McDowall KJ (2008) Sensing of 5' monophosphate by *Escherichia coli* RNase G can significantly enhance association with RNA and stimulate the decay of functional mRNA transcripts in vivo. *Mol Microbiol* 67(1):102-115.
104. Callaghan AJ, *et al.* (2005) Structure of *Escherichia coli* RNase E catalytic domain and implications for RNA turnover. *Nature* 437(7062):1187-1191.
105. Nickels BE & Dove SL (2011) NanoRNAs: a class of small RNAs that can prime transcription initiation in bacteria. *J Mol Biol* 412(5):772-781.
106. Merighi M, Lee VT, Hyodo M, Hayakawa Y, & Lory S (2007) The second messenger bis-(3'-5')-cyclic-GMP and its PilZ domain-containing receptor Alg44 are required for alginate biosynthesis in *Pseudomonas aeruginosa*. *Mol Microbiol* 65(4):876-895.
107. Chen MW, *et al.* (2012) Structural insights into the regulatory mechanism of the response regulator RocR from *Pseudomonas aeruginosa* in cyclic di-GMP signaling. *J Bacteriol*.
108. Kulasekara HD, *et al.* (2005) A novel two-component system controls the expression of *Pseudomonas aeruginosa* fimbrial *cup* genes. *Mol Microbiol* 55(2):368-380.
109. May TB, *et al.* (1991) Alginate synthesis by *Pseudomonas aeruginosa*: a key pathogenic factor in chronic pulmonary infections of cystic fibrosis patients. *Clin Microbiol Rev* 4(2):191-206.
110. Chitnis CE & Ohman DE (1993) Genetic analysis of the alginate biosynthetic gene cluster of *Pseudomonas aeruginosa* shows evidence of an operonic structure. *Mol Microbiol* 8(3):583-593.
111. Goldberg JB & Ohman DE (1987) Construction and characterization of *Pseudomonas aeruginosa algB* mutants: role of *algB* in high-level production of alginate. *J Bacteriol* 169(4):1593-1602.
112. Hoang TT, Karkhoff-Schweizer RR, Kutchma AJ, & Schweizer HP (1998) A broad-host-range Flp-FRT recombination system for site-specific excision of chromosomally-located DNA sequences: application for isolation of unmarked *Pseudomonas aeruginosa* mutants. *Gene* 212(1):77-86.

113. Hoang TT, Kutchma AJ, Becher A, & Schweizer HP (2000) Integration-proficient plasmids for *Pseudomonas aeruginosa*: site-specific integration and use for engineering of reporter and expression strains. *Plasmid* 43(1):59-72.
114. Miller JH (1992) *A short course in bacterial genetics: a laboratory manual and handbook for* Escherichia coli *and related bacteria* (Cold Spring Harbor Laboratory Press, Plainview, N.Y.).
115. Massie JP*, et al.* (2012) Quantification of high-specificity cyclic diguanylate signaling. *Proc Natl Acad Sci U S A* 109(31):12746-12751.
116. Cole SJ, Records AR, Orr MW, Linden SB, & Lee VT (2014) Catheter-associated urinary tract infection by *Pseudomonas aeruginosa* is mediated by exopolysaccharide-independent biofilms. *Infect Immun* 82(5):2048-2058.
117. Oussenko IA, Sanchez R, & Bechhofer DH (2002) *Bacillus subtilis* YhaM, a member of a new family of 3'-to-5' exonucleases in gram-positive bacteria. *J Bacteriol* 184(22):6250-6259.
118. Mathy N*, et al.* (2007) 5'-to-3' exoribonuclease activity in bacteria: role of RNase J1 in rRNA. *Cell* 129(4):681-692.
119. Orr MW*, et al.* (2015) Oligoribonuclease is the primary degradative enzyme for pGpG in *Pseudomonas aeruginosa* that is required for cyclic-di-GMP turnover. *Proc Natl Acad Sci U S A* 112(36):E5048-5057.
120. Cheng ZF & Deutscher MP (2002) Purification and characterization of the *Escherichia coli* exoribonuclease RNase R. Comparison with RNase II. *J Biol Chem* 277(24):21624-21629.
121. Vincent HA & Deutscher MP (2006) Substrate recognition and catalysis by the exoribonuclease RNase R. *J Biol Chem* 281(40):29769-29775.
122. Amblar M, Barbas A, Fialho AM, & Arraiano CM (2006) Characterization of the functional domains of *Escherichia coli* RNase II. *J Mol Biol* 360(5):921-933.
123. Amblar M, Barbas A, Gomez-Puertas P, & Arraiano CM (2007) The role of the S1 domain in exoribonucleolytic activity: substrate specificity and multimerization. *RNA* 13(3):317-327.
124. Srivastav R*, et al.* (2014) Unique subunit packing in mycobacterial nanoRNase leads to alternate substrate recognitions in DHH phosphodiesterases. *Nucleic Acids Res* 42(12):7894-7910.
125. Sassetti CM, Boyd DH, & Rubin EJ (2003) Genes required for mycobacterial growth defined by high density mutagenesis. *Mol Microbiol* 48(1):77-84.
126. Griffin JE*, et al.* (2011) High-resolution phenotypic profiling defines genes essential for mycobacterial growth and cholesterol catabolism. *PLoS Pathog* 7(9):e1002251.
127. Christen B*, et al.* (2011) The essential genome of a bacterium. *Mol Syst Biol* 7:528.
128. Postic G, Danchin A, & Mechold U (2012) Characterization of NrnA homologs from *Mycobacterium tuberculosis* and *Mycoplasma pneumoniae*. *RNA* 18(1):155-165.
129. Taghbalout A, Yang Q, & Arluison V (2014) The *Escherichia coli* RNA processing and degradation machinery is compartmentalized within an organized cellular network. *Biochem J* 458(1):11-22.

130. Carpousis AJ (2007) The RNA degradosome of *Escherichia coli*: an mRNA-degrading machine assembled on RNase E. *Annu Rev Microbiol* 61:71-87.
131. Chandran V*, et al.* (2007) Recognition and cooperation between the ATP-dependent RNA helicase RhlB and ribonuclease RNase E. *J Mol Biol* 367(1):113-132.
132. Niyogi SK & Stevens A (1964) Studies on ribonucleic acid polymerase with synthetic polyribonucleotides as templates: effect of oligonucleotides on the reactions. *Biochem Biophys Res Commun* 16(3):272-277.
133. Niyogi SK & Stevens A (1965) Studies of the ribonucleic acid polymerase from *Escherichia coli* : IV. Effect of oligonucleotides on the ribonucleic acid polymerase reaction with synthetic polyribonucleotides as templates. *J Biol Chem* 240:2593-2598.
134. Hui MP, Foley PL, & Belasco JG (2014) Messenger RNA degradation in bacterial cells. *Annu Rev Genet* 48:537-559.
135. Mackie GA (1998) Ribonuclease E is a 5'-end-dependent endonuclease. *Nature* 395(6703):720-723.
136. Ruetsch N & Dennis D (1987) RNA polymerase. Limit cognate primer for initiation and stable ternary complex formation. *J Biol Chem* 262(4):1674-1679.
137. Guisbert E, Yura T, Rhodius VA, & Gross CA (2008) Convergence of molecular, modeling, and systems approaches for an understanding of the *Escherichia coli* heat shock response. *Microbiol Mol Biol Rev* 72(3):545-554.
138. Raivio TL (2014) Everything old is new again: an update on current research on the Cpx envelope stress response. *Biochim Biophys Acta* 1843(8):1529-1541.
139. Dalebroux ZD & Swanson MS (2012) ppGpp: magic beyond RNA polymerase. *Nat Rev Microbiol* 10(3):203-212.
140. McFarland KA*, et al.* (2015) A self-lysis pathway that enhances the virulence of a pathogenic bacterium. *Proc Natl Acad Sci U S A* 112(27):8433-8438.
141. Borlee BR*, et al.* (2010) *Pseudomonas aeruginosa* uses a cyclic-di-GMP-regulated adhesin to reinforce the biofilm extracellular matrix. *Mol Microbiol* 75(4):827-842.
142. Friedman L & Kolter R (2004) Two genetic loci produce distinct carbohydrate-rich structural components of the *Pseudomonas aeruginosa* biofilm matrix. *J Bacteriol* 186(14):4457-4465.
143. Mac Síomóin RA*, et al.* (1996) Identification and characterization of *ispA*, a *Shigella flexneri* chromosomal gene essential for normal in vivo cell division and intracellular spreading. *Mol Microbiol* 19(3):599-609.
144. Badaluddin NA & Kitakawa M (2015) *Escherichia coli* inner membrane protein YciB interacts with ZipA that is important for cell division. *Genes Cells* 20(11):956-965.
145. Li G, Badaluddin NA, & Kitakawa M (2015) Characterization of inner membrane protein YciB in *Escherichia coli*: YciB interacts with cell elongation and division proteins. *Microbiol Immunol* 59(11):700-704.

146. Niba ET, Naka Y, Nagase M, Mori H, & Kitakawa M (2007) A genome-wide approach to identify the genes involved in biofilm formation in *E. coli*. *DNA Res* 14(6):237-246.
147. Nixon BT, Ronson CW, & Ausubel FM (1986) Two-component regulatory systems responsive to environmental stimuli share strongly conserved domains with the nitrogen assimilation regulatory genes *ntrB* and *ntrC*. *Proc Natl Acad Sci U S A* 83(20):7850-7854.
148. Dong J, Iuchi S, Kwan HS, Lu Z, & Lin EC (1993) The deduced amino-acid sequence of the cloned *cpxR* gene suggests the protein is the cognate regulator for the membrane sensor, CpxA, in a two-component signal transduction system of *Escherichia coli*. *Gene* 136(1-2):227-230.
149. Raivio TL & Silhavy TJ (1997) Transduction of envelope stress in *Escherichia coli* by the Cpx two-component system. *J Bacteriol* 179(24):7724-7733.
150. Vogt SL & Raivio TL (2012) Just scratching the surface: an expanding view of the Cpx envelope stress response. *FEMS Microbiol Lett* 326(1):2-11.
151. Dorel C, Lejeune P, & Rodrigue A (2006) The Cpx system of *Escherichia coli*, a strategic signaling pathway for confronting adverse conditions and for settling biofilm communities? *Res Microbiol* 157(4):306-314.
152. Pogliano J*, et al.* (1998) Aberrant cell division and random FtsZ ring positioning in *Escherichia coli cpxA** mutants. *J Bacteriol* 180(13):3486-3490.
153. Yakhnina AA, McManus HR, & Bernhardt TG (2015) The cell wall amidase AmiB is essential for *Pseudomonas aeruginosa* cell division, drug resistance and viability. *Mol Microbiol* 97(5):957-973.
154. Hartmann RK, Toschka HY, Ulbrich N, & Erdmann VA (1986) Genomic organization of rDNA in *Pseudomonas aeruginosa*. *FEBS Lett* 195(1-2):187-193.
155. Asai T*, et al.* (1999) Construction and initial characterization of *Escherichia coli* strains with few or no intact chromosomal rRNA operons. *J Bacteriol* 181(12):3803-3809.
156. Yano K*, et al.* (2013) Multiple rRNA operons are essential for efficient cell growth and sporulation as well as outgrowth in *Bacillus subtilis*. *Microbiology* 159(Pt 11):2225-2236.
157. Klappenbach JA, Dunbar JM, & Schmidt TM (2000) rRNA operon copy number reflects ecological strategies of bacteria. *Appl Environ Microbiol* 66(4):1328-1333.
158. Shrestha PM, Noll M, & Liesack W (2007) Phylogenetic identity, growth-response time and rRNA operon copy number of soil bacteria indicate different stages of community succession. *Environ Microbiol* 9(10):2464-2474.
159. Arai H, Kodama T, & Igarashi Y (1999) Effect of nitrogen oxides on expression of the *nir* and *nor* genes for denitrification in *Pseudomonas aeruginosa*. *FEMS Microbiol Lett* 170(1):19-24.
160. Trunk K*, et al.* (2010) Anaerobic adaptation in *Pseudomonas aeruginosa*: definition of the Anr and Dnr regulons. *Environ Microbiol* 12(6):1719-1733.

161. Yoon MY, Lee KM, Park Y, & Yoon SS (2011) Contribution of cell elongation to the biofilm formation of *Pseudomonas aeruginosa* during anaerobic respiration. *PLoS One* 6(1):e16105.
162. Lapouge K, Schubert M, Allain FH, & Haas D (2008) Gac/Rsm signal transduction pathway of gamma-proteobacteria: from RNA recognition to regulation of social behaviour. *Mol Microbiol* 67(2):241-253.
163. Igarashi K & Kashiwagi K (1996) Polyamine transport in *Escherichia coli*. *Amino Acids* 10(1):83-97.
164. Bielaszewska M, Aldick T, Bauwens A, & Karch H (2014) Hemolysin of enterohemorrhagic *Escherichia coli*: structure, transport, biological activity and putative role in virulence. *Int J Med Microbiol* 304(5-6):521-529.
165. Kvist M, Hancock V, & Klemm P (2008) Inactivation of efflux pumps abolishes bacterial biofilm formation. *Appl Environ Microbiol* 74(23):7376-7382.
166. Matsumura K, Furukawa S, Ogihara H, & Morinaga Y (2011) Roles of multidrug efflux pumps on the biofilm formation of *Escherichia coli* K-12. *Biocontrol Sci* 16(2):69-72.
167. Baugh S, Ekanayaka AS, Piddock LJ, & Webber MA (2012) Loss of or inhibition of all multidrug resistance efflux pumps of *Salmonella enterica* serovar Typhimurium results in impaired ability to form a biofilm. *J Antimicrob Chemother* 67(10):2409-2417.
168. Baugh S, Phillips CR, Ekanayaka AS, Piddock LJ, & Webber MA (2014) Inhibition of multidrug efflux as a strategy to prevent biofilm formation. *J Antimicrob Chemother* 69(3):673-681.
169. Skurnik D*, et al.* (2013) A comprehensive analysis of in vitro and in vivo genetic fitness of *Pseudomonas aeruginosa* using high-throughput sequencing of transposon libraries. *PLoS Pathog* 9(9):e1003582.
170. van Opijnen T, Bodi KL, & Camilli A (2009) Tn-seq: high-throughput parallel sequencing for fitness and genetic interaction studies in microorganisms. *Nat Methods* 6(10):767-772.
171. van Opijnen T & Camilli A (2013) Transposon insertion sequencing: a new tool for systems-level analysis of microorganisms. *Nat Rev Microbiol* 11(7):435-442.
172. Cohen D*, et al.* (2015) Oligoribonuclease is a central feature of cyclic diguanylate signaling in *Pseudomonas aeruginosa*. *Proc Natl Acad Sci U S A* 112(36):11359-11364.
173. Imamura R*, et al.* (1996) Identification of the *cpdA* gene encoding cyclic 3',5'-adenosine monophosphate phosphodiesterase in *Escherichia coli*. *J Biol Chem* 271(41):25423-25429.
174. Keasling JD, Bertsch L, & Kornberg A (1993) Guanosine pentaphosphate phosphohydrolase of *Escherichia coli* is a long-chain exopolyphosphatase. *Proc Natl Acad Sci U S A* 90(15):7029-7033.
175. An G, Justesen J, Watson RJ, & Friesen JD (1979) Cloning the *spoT* gene of *Escherichia coli*: identification of the *spoT* gene product. *J Bacteriol* 137(3):1100-1110.

176. Xiao H*, et al.* (1991) Residual guanosine 3',5'-bispyrophosphate synthetic activity of *relA* null mutants can be eliminated by *spoT* null mutations. *J Biol Chem* 266(9):5980-5990.
177. Solovyev V & Salamov A (2011) Automatic annotation of microbial genomes and metagenomic sequences. *Metagenomics and its Applications in Agriculture, Biomedicine and Environmental Studies*, ed Li RW (Nova Science Publishers, New York City), pp 61-67.
178. Härtig E, Schiek U, Vollack KU, & Zumft WG (1999) Nitrate and nitrite control of respiratory nitrate reduction in denitrifying *Pseudomonas stutzeri* by a two-component regulatory system homologous to NarXL of *Escherichia coli*. *J Bacteriol* 181(12):3658-3665.
179. Schreiber K*, et al.* (2007) The anaerobic regulatory network required for *Pseudomonas aeruginosa* nitrate respiration. *J Bacteriol* 189(11):4310-4314.
180. Matsuyama BY*, et al.* (2016) Mechanistic insights into c-di-GMP-dependent control of the biofilm regulator FleQ from *Pseudomonas aeruginosa*. *Proc Natl Acad Sci U S A* 113(2):E209-218.
181. Jones CJ*, et al.* (2015) C-di-GMP regulates motile to sessile transition by modulating MshA pili biogenesis and near-surface motility behavior in *Vibrio cholerae*. *PLoS pathogens* 11(10):e1005068.
182. Okada Y*, et al.* (1994) Cytoplasmic axial filaments in *Escherichia coli* cells: possible function in the mechanism of chromosome segregation and cell division. *J Bacteriol* 176(3):917-922.
183. Krieger R, Rompf A, Schobert M, & Jahn D (2002) The *Pseudomonas aeruginosa hemA* promoter is regulated by Anr, Dnr, NarL and Integration Host Factor. *Mol Genet Genomics* 267(3):409-417.
184. Arai H, Mizutani M, & Igarashi Y (2003) Transcriptional regulation of the *nos* genes for nitrous oxide reductase in *Pseudomonas aeruginosa*. *Microbiology* 149(Pt 1):29-36.
185. Zierdt CH & Schmidt PJ (1964) Dissociation in *Pseudomonas aeruginosa*. *J Bacteriol* 87(5):1003-1010.
186. Thomassen MJ, Demko CA, Boxerbaum B, Stern RC, & Kuchenbrod PJ (1979) Multiple of isolates of *Pseudomonas aeruginosa* with differing antimicrobial susceptibility patterns from patients with cystic fibrosis. *J Infect Dis* 140(6):873-880.
187. Häussler S, Tümmler B, Weissbrodt H, Rohde M, & Steinmetz I (1999) Small-colony variants of *Pseudomonas aeruginosa* in cystic fibrosis. *Clin Infect Dis* 29(3):621-625.
188. Reinhardt A*, et al.* (2007) Development and persistence of antimicrobial resistance in *Pseudomonas aeruginosa*: a longitudinal observation in mechanically ventilated patients. *Antimicrob Agents Chemother* 51(4):1341-1350.
189. Kirisits MJ, Prost L, Starkey M, & Parsek MR (2005) Characterization of colony morphology variants isolated from *Pseudomonas aeruginosa* biofilms. *Appl Environ Microbiol* 71(8):4809-4821.

190. Malone JG (2015) Role of small colony variants in persistence of *Pseudomonas aeruginosa* infections in cystic fibrosis lungs. *Infect Drug Resist* 8:237-247.
191. Evans TJ (2015) Small colony variants of *Pseudomonas aeruginosa* in chronic bacterial infection of the lung in cystic fibrosis. *Future Microbiol* 10(2):231-239.
192. Tuckerman JR, Gonzalez G, & Gilles-Gonzalez MA (2011) Cyclic di-GMP activation of polynucleotide phosphorylase signal-dependent RNA processing. *J Mol Biol* 407(5):633-639.
193. Mohanty BK & Kushner SR (2006) The majority of *Escherichia coli* mRNAs undergo post-transcriptional modification in exponentially growing cells. *Nucleic Acids Res* 34(19):5695-5704.
194. Bralley P & Jones GH (2003) Overexpression of the polynucleotide phosphorylase gene (*pnp*) of *Streptomyces antibioticus* affects mRNA stability and poly(A) tail length but not ppGpp levels. *Microbiology* 149(Pt 8):2173-2182.
195. Pobre V & Arraiano CM (2015) Next generation sequencing analysis reveals that the ribonucleases RNase II, RNase R and PNPase affect bacterial motility and biofilm formation in *E. coli*. *BMC Genomics* 16:72.
196. Wang YC, Chin KH, Chuah ML, Liang ZX, & Chou SH (2012) Crystallization and preliminary X-ray diffraction studies of *Xanthomonas campestris* PNPase in the presence of c-di-GMP. *Acta Crystallogr Sect F Struct Biol Cryst Commun* 68(Pt 10):1247-1250.
197. Pfeiffer V, Papenfort K, Lucchini S, Hinton JC, & Vogel J (2009) Coding sequence targeting by MicC RNA reveals bacterial mRNA silencing downstream of translational initiation. *Nat Struct Mol Biol* 16(8):840-846.
198. Domingues S*, et al.* (2009) Biochemical characterization of the RNase II family of exoribonucleases from the human pathogens *Salmonella typhimurium* and *Streptococcus pneumoniae*. *Biochemistry* 48(50):11848-11857.
199. Zuo Y & Deutscher MP (2002) The physiological role of RNase T can be explained by its unusual substrate specificity. *J Biol Chem* 277(33):29654-29661.
200. Zuo Y*, et al.* (2007) Crystal structure of RNase T, an exoribonuclease involved in tRNA maturation and end turnover. *Structure* 15(4):417-428.
201. Zuo Y, Wang Y, & Malhotra A (2005) Crystal structure of *Escherichia coli* RNase D, an exoribonuclease involved in structured RNA processing. *Structure* 13(7):973-984.
202. Uemura Y*, et al.* (2013) Crystal structure of the ligand-binding form of nanoRNase from *Bacteroides fragilis*, a member of the DHH/DHHA1 phosphoesterase family of proteins. *FEBS Lett* 587(16):2669-2674.
203. Wakamatsu T*, et al.* (2010) Structure of RecJ exonuclease defines its specificity for single-stranded DNA. *J Biol Chem* 285(13):9762-9769.
204. Zuo Y*, et al.* (2006) Structural basis for processivity and single-strand specificity of RNase II. *Mol Cell* 24(1):149-156.

205. Frazão C*, et al.* (2006) Unravelling the dynamics of RNA degradation by ribonuclease II and its RNA-bound complex. *Nature* 443(7107):110-114.
206. Barbas A*, et al.* (2008) New insights into the mechanism of RNA degradation by ribonuclease II: identification of the residue responsible for setting the RNase II end product. *J Biol Chem* 283(19):13070-13076.
207. Matos RG, Barbas A, & Arraiano CM (2009) RNase R mutants elucidate the catalysis of structured RNA: RNA-binding domains select the RNAs targeted for degradation. *Biochem J* 423(2):291-301.
208. Fürste JP*, et al.* (1986) Molecular cloning of the plasmid RP4 primase region in a multi-host-range *ta20901cP* expression vector. *Gene* 48(1):119-131.
209. Rahme LG*, et al.* (1995) Common virulence factors for bacterial pathogenicity in plants and animals. *Science* 268(5219):1899-1902.
210. Kulasakara H*, et al.* (2006) Analysis of *Pseudomonas aeruginosa* diguanylate cyclases and phosphodiesterases reveals a role for bis-(3'-5')-cyclic-GMP in virulence. *Proc Natl Acad Sci U S A* 103(8):2839-2844.